DISS. ETH NO. 27541

Angiocrine control of tissue metabolism

A thesis submitted to attain the degree of DOCTOR OF SCIENCES of ETH ZURICH
(Dr. sc. ETH Zurich)

presented by

Abdiel Alvarado-Diaz

M. Sc. in Human Biology,

University of Copenhagen

born on 08.05.1988

citizen of Mexico

accepted on the recommendation of

Prof. Dr. Katrien De Bock

Prof. Dr. Christian Wolfrum

P.D. Dr. Jan Krützfeldt

Prof. Dr. Manfred Heller

2021

Acknowledgments

First and foremost, I would like to thank Katrien, to who I owe the deepest of my respect, consideration, and gratitude. Out of the many, the thing I am most grateful for is that she gave me a position where I felt privileged to have the chance of not only learning from her experience and using that knowledge into solving my research questions, but also incorporating into my own person the human values she holds as world-class group leader, researcher and human being. In retrospective, those human values were indeed instrumental in every single step along this academic experience.

I want to thank all the members, past and present, of the lab of Exercise and Health, for the enlightening discussions, suggestions and complementary perspectives that helped bringing my project forward. On a personal side, I feel fortunate and grateful for the times we had outside the lab sharing laughs, jokes and, overall, for all memorable moments. Specially, I want to thank Fateme for her unvaluable friendship and supporting my research with her sharp mind, extra hands and encouraging words. Without her continuous input, and all the things I learned from her, this project would not have been possible. Additionally, I want to thank Moheb for his support in the final moments of my project. I hold very dearly in my chest his friendship and help in those sleepless nights in the lab. I also want to thank the post-docs in the lab, Zheng, Ines, Gommaar and Tatiane for their practical input and suggestions for my project. Specially, I want to thank Gommaar, as he had to momentarily leave his family here in Zürich to get some cells in Denmark for my project amid the COVID-19 pandemic. Also, I want to thank Evi and Paola for their technical assistance and recommendations throughout.

Big thanks to all the people in SLA, specially to our animal care takers, Manuel and Conny for their practical teachings and experimental assistance.

I want to thank Prof. Dr. Christian Wolfrum, P.D. Dr. Jan Krützfeldt and Prof. Dr. Manfred Heller for being part of my doctoral committee and examining my doctoral defense. Also, to Prof. Dr. Peter Fischer for chairing the ceremony.

To my parents, Elsa and Abdiel, for teaching me resilience, how to recognize reality and for building a warm place where I can always go back to. To my sister, Elsa Gabriela, for always listening to my concerns and in general, for her spiritual counseling.

I also want to thank my Mexican friends here in Zürich, Aldo, Andrea, Damian, Miguel, Daniel, Karla and Marte for all the music we played together and lovable moments. Also to Chantal Brun for helping me in several matters on this project and emotional support.

Special mention goes to the Mexican Research Council for their financial support (CONACyT).

Finally, I'm very grateful with our collaborators that facilitated materials and overall for their input into this project. To group leader Dr. Sebastian Sebastian Beck Jørgensen, NovoNordisk, Denmark; Prof. Dr. Erik Richter and Dr. Kim Anker Sjøberg, University of Copenhagen, Denmark; Prof. Dr. Michael Potente and Dr. Kerstin Wilhelm, Max Planck Institute for Heart and Lung Research, Germany; Prof. Dr. Shahin Rafii, Weill Cornell Medicine, USA.

Abstract

Endothelial cells are important gatekeepers of organ homeostasis and metabolism. It has long been determined that impaired vascular function is associated with tissue dysregulation and metabolic disorders, but whether endothelial cells contribute to metabolic homeostasis beyond ensuring tissue perfusion is poorly described. Using an unbiased proteomics approach to analyze endothelial secretome, we identified GDF15 to be abundantly secreted. As GDF15 has been identified as an important modulator of metabolism through the control body weight, in this dissertation, the regulation of angiocrine GDF15 was explored and whether it influences other aspects of metabolism. It was determined that GDF15 expression is negatively controlled by FOXO1, master regulator of endothelial quiescence, but not NOTCH1, master regulator of endothelial specification. Inhibiting FOXO1 using the inhibitor AS1842856, increased GDF15 expression. *In vivo*, endothelial specific deletion of FOXO1 increased GDF15 expression (>4 fold) in endothelial cells isolated from different tissues and was associated with significant upregulation of GDF15 in urine and serum. Furthermore, endothelial specific deletion of FOXO1 provoked a significant decrease in food intake, suggesting that small changes in circulating GDF15 suffice to control food intake. Finally, it was determined that GDF15 has an acute insulin sensitizing effect, which is primary to the acute administration of GDF15 and independent of weight loss. This work identifies FOXO1 as a direct regulator of GDF15 in ECs and highlights the critical role of endothelial cells in whole body metabolic control.

Zusammenfassung

Endothelzellen sind wichtige Regulatoren der Organhomöostase und des Stoffwechsels. Es ist allgemein bekannt, dass eine gestörte Gefäßfunktion mit Gewebedysregulationen und Stoffwechselstörungen einhergeht. Jedoch ist bis heute nur unzureichend untersucht, ob und inwiefern Endothelzellen über die Sicherstellung der Gewebeperfusion hinaus zur metabolischen Homöostase beitragen. Unter Verwendung eines unvoreingenommenen Proteomik-Ansatzes zur Analyse des endothelialen Sekrets haben wir festgestellt, dass GDF15 reichlich sezerniert wird. Basierend auf der Feststellung, dass GDF15 mit Hilfe des Körpergewichts als wichtiger Regulator des Stoffwechsels fungiert, wurde in dieser Dissertation die Regulation von angiokrinem GDF15 untersucht und dessen Effekte auf den Stoffwechsel. Es wurde festgestellt, dass die GDF15-Expression durch FOXO1 (Hauptregulator der endothelialen Stilllegung) negativ reguliert wird, nicht aber durch NOTCH1 (Hauptregulator der endothelialen Spezifikation). Die Hemmung von FOXO1 mit dem Inhibitor AS1842856 erhöhte die GDF15-Expression. In vivo steigerte die endothelspezifische Deletion von FOXO1 die GDF15-Expression (>4fach) in den Endothelzellen, welche aus verschiedenen Geweben isoliert wurden. Zudem konnte eine signifikante Hochregulierung von GDF15 in Urin und Serum festgestellt werden. Darüber hinaus bewirkte die endothelspezifische Deletion von FOXO1 eine signifikante Abnahme der Nahrungsaufnahme, was darauf hindeutet, dass kleine Veränderungen im zirkulierenden GDF15 ausreichen, um die Nahrungsaufnahme zu kontrollieren. Schließlich konnte beobachtet werden, dass GDF15 einen akuten Insulin-sensibilisierenden Effekt hat, der primär auf die akute Verabreichung von GDF15 zurückzuführen ist und unabhängig vom Gewichtsverlust ist. Diese Arbeit konnte FOXO1 als einen direkten Regulator von GDF15 in Endothelzellen identifizieren und unterstreicht die entscheidende Rolle von Endothelzellen bei der Ganzkörper-Stoffwechselkontrolle.

Table of Contents

List of figures

skeletal muscle in control foxo1$^{fl/fl}$ (n=5) compared to foxo1$^{\Delta EC}$ mice (n=6).(Student-*t* test) **g.** *gdf15* mRNA expression in freshly isolated endothelial cells from heart tissue in control foxo1$^{fl/fl}$ (n= 4) compared to foxo1$^{\Delta EC}$ mice (n= 5). .(Student-*t* test) **h.** *foxo1* mRNA expression in freshly isolated endothelial cells from heart tissue in control foxo1$^{fl/fl}$ (n= 4) compared to foxo1$^{\Delta EC}$ mice (n= 5) .(Student-*t* test) **i.** *gdf15* mRNA expression in freshly isolated endothelial cells from white adipose tissue in control foxo1$^{fl/fl}$ (n= 4) compared to foxo1$^{\Delta EC}$ mice (n= 4). .(Student-*t* test) **j**. *foxo1* mRNA expression in freshly isolated endothelial cells from white adipose tissue in control foxo1$^{fl/fl}$ (n= 4) compared to foxo1$^{\Delta EC}$ mice (n= 4) .(Student-*t* test). **k.** *gdf15* mRNA expression in freshly isolated endothelial cells from kidney tissue in control foxo1$^{fl/fl}$ (n= 1) compared to foxo1$^{\Delta EC}$ mice (n= 1). **l.** *foxo1* mRNA expression in freshly isolated endothelial cells from kidney tissue in control foxo1$^{fl/fl}$ (n= 3) compared to foxo1$^{\Delta EC}$ mice (n=3). Housekeeping gene 18S was used as control for figure panels from **d** to **l**. **m.** Body mass of control foxo1$^{fl/fl}$ (n= 9) compared to foxo1$^{\Delta EC}$ mice (n= 14). Measurement was done 14 days after last tamoxifen administration and over 8 days (190 h). (Two-way ANOVA and Sidak's multiple comparison) was done **n.** energy expenditure against body weight is shown for *foxo1*$^{\Delta EC}$ mice (n= 14) or controls (n= 9). (One way ANCOVA). Significant values are represented in asterisks as follows *P<0.05, **P<0.01, ***P<0.001, and ****P<0.0001. 75

Figure 12 Endothelial cell secretome sensitizes skeletal muscle to the effects of insulin in vitro. **a**. Schematic of conditioned media generation from wild type HUVECs in the presence of serum and applied in a 3:7 ratio to human myotubes. **b**. Representative blot of insulin signaling from human myotubes that have been stimulated with CM or NC from WT HUVECs over 48 h **c**. CM treated myotubes increase responsiveness to insulin assessed by phosphorylation of AS160 T642 (n= 6) (Two-way ANOVA and Tukey's multiple comparison). **d**. CM treated myotubes increase responsiveness to insulin assessed by phosphorylation of AKT T308 (n= 6) **e**. CM treated myotubes does not respond differently to insulin when compared to control assessed by phosphorylation of AKT S473. (n= 6) (Two-way ANOVA and Tukey's multiple comparison) **f**. Schematic of CM generation from E4ORF1^{+} HUVECs in the absence of serum and applied in a 3:7 ratio to human myotubes. **g**. Representative blot of insulin signaling from human myotubes that have been stimulated with CM or NC from E4ORF1^{+} HUVECs over 48 h. **h**. CM generated in serum-free conditions increase responsiveness to insulin assessed by phosphorylation of AS160 T642 in human

from human myotubes that have been stimulated over 48 h with CM from E4ORF1 in serum free conditions or control. CM was either produced from sh-scrambled or sh-αGDF15 endothelial cells. (n= 3). **c.d.** Human myotubes treated with CM from sh-αGDF15 failed to increase insulin sensitivity as shown by quantification of downstream targets AKT T308 and AS160 T642 ((Two-way ANOVA and Tukey's multiple comparison). **e**. Representative blot from human Myotubes were treated for 48 h with rhGDF15 and then stimulated with insulin 100 nM. In figures **b** and **e**, the total load shows comparable amounts of protein loaded in the representative blot. **f. g**. **i**. rhGDF15 increases insulin sensitivity in human myotubes *in vitro* by increasing phosphorylation of downstream targets AS160 T642, AKT T308, IR-β Y1150/1151 upon maximal insulin stimulation 100 nM. (n= 6)((Two-way ANOVA and Tukey's multiple comparison). **h**. rhGDF15 stimulation of human myotubes does not increases ERK1/2 p42/44 as compared to other downstream targets (n= 6) (Two-way ANOVA and Tukey's multiple comparison). **j.** rhGDF15 stimulation in human myotubes increases glycolytic flux (n= 4)(Student-*t* test). **k.** rhGDF15 stimulation in human myotubes increases insulin mediated glucose uptake assessed by radioactive 2-deoxy glucose incorporation (n= 6) (Two-way ANOVA and Tukey's multiple comparison). **l.** 48 h stimulation of rhGDF15 (kindly donated by Group Leader Dr. Sebastian Jørgensen, Novonordisk) increases insulin-mediated GLUT4 translocation in rat L6-GLUT4-MYC myotubes (n= 10). (Two-way ANOVA and Tukey's multiple comparison). Significant values are represented in asterisks as follows *P<0.05, **P<0.01, ***P<0.001, and ****P<0.0001. 100

Figure 14 Administration of rhGDF15 promotes increased insulin sensitivity and greater glucose uptake in skeletal muscle in mice fed chow diet. Mice were administered 8 nmol of rhGDF15 at the beginning of their dark cycle. **a** There are no differences in changes in body weight after 5 days between controls (n= 6) and GDF15 treated animals (n= 6) (Two-way ANOVA with Sidak's multiple comparison). **b** GDF15 treated mice show an increased insulin signaling upon stimulated with 1 IU/kg body weight insulin for 15 min, the total load shows comparable amounts of protein loaded in the representative blot. **c. d**. Downstream insulin signaling was increased as measured by phosphorylation of AKT T308 and AS160 T642(Two-way ANOVA and Tukey's multiple comparison). **e**. rhGDF15 treatment improves insulin sensitivity as shown by ITT (vehicle, n= 4, rhGDF15, n= 3) (Two-way ANOVA and Sidak's multiple comparison) **f**. but treatment does not influence glucose handling as assessed in

Extended data figures

Supplementary tables

Abbreviations

AEC	Alveolar epithelial cell
2DG	2-Deoxy Glucose
3PO	3-(3-Pyridinyl)-1-(4-pyridinyl)-2-propen-1-one
6PG	6-phosphogluconate
6PGD	6-phosphogluconate dehydrogenase
ACAD	FAD-dependent acyl-CoA dehydrogenase
ACTB	Actin beta
AGO	Argonaute proteins
AKT	Protein kinase B
AMP	Adenosine monophosphate
AMPK	Adenosine monophosphate kinase
ANCOVA	Analysis of covariance
ANTP	Homeobox A7
AS160	Akt substrate 160
AS1842856	FOXO1 inhibitor
ATF4	Activating transcription factor 4
ATP	Adenosine triphosphate
BAT	brown adipose tissue
BCA	Bicinchoninic acid
BIP	Binding-Immunoglobulin Protein
BPTES	Bis-2-(5-phenylacetamido-1,2,4-thiadiazol-2-yl)ethyl sulfide

BSA	Bovine serum albumin
CD31	Cluster of differentiation 31
CD36	Cluster of differentiation 36
CD45	Cluster of differentiation 45
CHOP	C/EBP homologous protein
CM	Conditioned medium
CNS	Central nervous system
CONACyT	Mexican research council
CPT1	Carnitine palmitoyltransferase 1
CT	Cycle threshold
DAMP	Damage-associated molecular patterns
DAPT	N-[N-(3,5-Difluorphenacetyl)-L-alanyl]-S-phenylglycin-tert-butylester
DDA	Data-dependent mode
DHAP	Dihydroxyacetone phosphate
DLL4	Delta ligand-like 4
DMSO	Dimethyl sulfoxide
DNA	Deoxyribonucleic acid
DTT	Dithiothreitol
E4ORF1	E4 open reading frame 1
EC	Endothelial cell
ECM	Extra cellular matrix
EDL	Extensor digitorum longus
EDTA	Ethylenediamine tetra acetic acid
EGCS	Endothelial cell growth factor supplements

EGF	Epidermal growth factor
EGM2	Endothelial cell growth medium 2
EGTA	Ethylene Glycol Tetra acetic Acid
ELISA	Enzyme-linked immunosorbent assay
ER	Endoplasmic reticulum
ERC	European research council
ERK	Extracellular Signal-Regulated Kinase
ETC	electron transport chain
ETH	Swiss Federal Institute of Technology
FA	Fatty acids
FABP	Fatty acid binding protein
FACS	Fluorescence-activated cell sorting
FAD	Flavin adenine dinucleotide
FADH2	Flavin adenine dinucleotide (reduced)
FAO	Fatty acid oxidation
FATP	Long-chain fatty acid transport protein
FATP3	Long-chain fatty acid transport protein 3
FATP4	Long-chain fatty acid transport protein 4
FBS	Fetal bovine serum
FDR	False discovery rate
FELASA	Federation of European laboratory animal science associations
FGF	Fibroblast growth factor
FGF21	Fibroblast growth factor 21
FGFR	Fibroblast Growth Factor Receptor

FOXO	Forkhead Box O
FOXO1A3	Forkhead Box O1A3
FOXO1 CA	FOXO1 constitutively active
FOXO3	Forkhead Box O 3
FOXO4	Forkhead Box O 4
G3P	Glyceraldehyde-3-phosphate
G6P	Glucose-6-phosphate
G6PD	Glucose-6-phosphate dehydrogenase
GDF15	Growth differentiation facto 15
GDH	Glutamate dehydrogenase
GFP	Green fluorescent protein
GFRAL	GDNF family receptor alpha like
GLS1	Glutaminase 1
GLUT1	Glucose transporter 1
GLUT4	Glucose transporter 4
GPNA	L-γ-glutamyl-p-nitroanilide
GSEA	Gene set enrichment analysis
GTT	Glucose tolerance test
HADH	L-3-hydroxyacyl-CoA dehydrogenase
HEK	Human embryonic kidney
HES1	Hairy and enhancer of split 1
HEY1	Hes related family BHLH transcription factor with YRPW motif 1
HEY2	Hes related family BHLH transcription factor with YRPW motif 2
HGF	Hepatocyte growth factor

HIF	Hypoxia Inducible Factor
HIFU	High Intensity Focused Ultrasound
HIV	Human immunodeficiency virus
HK2	Hexokinase 2
HRP	Horseradish peroxide
HUVEC	Human umbilical cord vein endothelial cells
ICAM	Intercellular Adhesion Molecule
IDH	Isocitrate dehydrogenase
IGF1	Insulin Like Growth Factor 1
IR	Insulin receptor
ISR	Integrated stress response
ITT	Insulin tolerance test
IU	International units
IV	Intravenous
αKG	alpha ketoglutarate
KLF2	Kruppel like factor 2
LC	Liquid chromatography
LPS	Lipopolysaccharides
M199	Medium 199
ME	Malic enzyme
MEM	Minimal essential medium
MMP	Matrix metalloprotein protease
MMP2	Matrix metalloprotein protease 2
MOI	Multiplicity of infection

MS	Mass spectrometry
MXI1	MAX interactor 1, dimerization protein
MZ	Mass charge
NAD	Nicotinamide adenine dinucleotide
NADPH	Nicotinamide adenine dinucleotide phosphate
NC	Non-conditioned medium
NF	Nuclear factor
NO	Nitric oxide
NOS	Nitric oxide synthase
NRARP	NOTCH regulated ankyrin repeat protein
NRP1	Neuropilin 1
NTP	Nucleoside triphosphate
OAA	Oxaloacetic acid
OGDH	α-ketoglutarate dehydrogenase
OPD	o-Phenylenediamine
PAMP	Pathogen-associated molecular patterns
PAX2	Pair boxed 2
PBS	Phosphate buffer saline
PC	Pyruvate carboxylase
PCA	Perchloric acid
PCR	Polymerase chain reaction
PDH	Pyruvate carboxylase
PEP	Phosphoenolpyruvate
PFA	Paraformaldehyde

PFKFB3	6-phosphofructo-2-kinase/fructose-2,6-biphosphatase 3
PPAR	Peroxisome Proliferator Activated Receptor
PPP	Pentose phosphate pathway
PVDF	Polyvinylidene difluoride
RCF	Relative centrifugal force
RER	Respiratory exchange ratio
RLT	Lysis Buffer
RNA	Ribonucleic acid
ROCK1	Rho Associated Coiled-Coil Containing Protein Kinase 1
ROS	Reactive oxygen species
RT	Room temperature
Ru5P	Ribulose-5-phosphate
SEM	Standard error of mean
SGK	Serum/glucocorticoid –regulated kinase
SLC1A5	Solute Carrier Family 1 Member 5
SYBR Green	N',N'-dimethyl-N-[4-[(E)-(3-methyl-1,3-benzothiazol-2-ylidene)methyl]-1-phenylquinolin-1-ium-2-yl]-N-propylpropane-1,3-diamine
TA	Tibialis anterior
TBS	Tris buffer saline
TBX3	T-box transcription factor 3
TCA	Tricarboxylic acid cycle
TGF	Transforming growth factor
TLR	Toll-like receptors

TNF	Tumor necrotic factor
TSP1	Thrombospondin 1
UTR	Untranslated region
UV	Ultraviolet light
VCAM	Vascular Cell Adhesion Molecule
VEGF	Vascular endothelial growth factor
VEGFR1	Vascular endothelial growth factor receptor
VSMC	Vascular smooth muscle cells
VWF	Von Willebrand factor
WAT	white adipose tissue
WNT	Wingless-Type MMTV Integration Site Family
WT	Wild type

1. Introduction

The vascular endothelium is the organ system in charge of transporting oxygen and nutrients from the sites they are taken up towards the peripheral tissues, while at the same time, carrying by-products of metabolism for their disposal. Over the last decades, it has however become clear that the role of this widespread organ system goes far beyond, and that the endothelium plays an active role in the regulation of tissue homeostasis.

In this chapter, a short overview of vascular physiology will be given as an example of how the vascular endothelium regulates several important aspects of organ homeostasis. Furthermore, emphasis will be made on the emerging properties of vascular biology as a secretory organ and as a regulator of metabolic homeostasis, and how these two properties could be controlled by master regulators of endothelial cell specification.

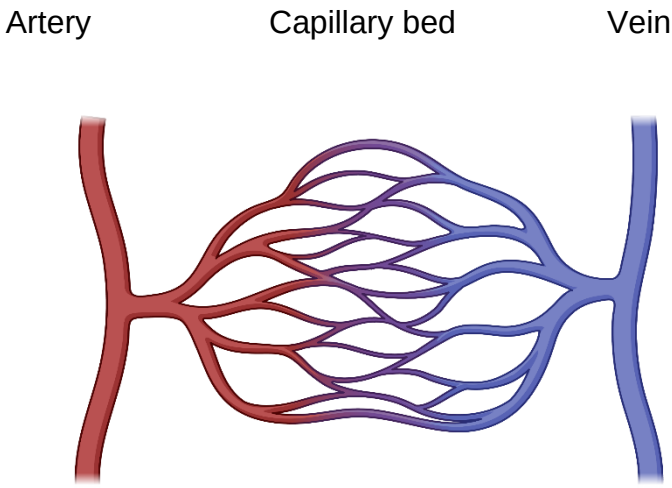

Figure 1 . Schematic representation of vascular tree. Three distinctive functional and morphological areas: arteries, veins, and capillaries. Arteries and veins are thick vessels composed of endothelial cells, perivascular cells, smooth muscle cells and elastic collagen fibers. On the other hand, capillaries are intricate vessel meshwork only formed by a single cell layer. This creates a large surface area through which it communicates with its surrounding tissue, and vice versa, for homeostatic communication and regulation.

1.1. Regulation of organ homeostasis through angiocrine signaling

1.1.1. Endothelial modulation of immune response.

The immunoregulatory role of endothelial cells is broad and fundamental to ensue a healthy immunogenic response (Jambusaria, Hong et al. 2020) and, ultimately, to resolve it (Kadl and Leitinger 2005). Upon inflammatory or necrotic stimulation, endothelial cells become active, they increase their leakiness, adhesiveness of leukocytes amplifies, platelet adhesion commences, and angiogenesis is triggered (Pober and Sessa 2007). Furthermore, endothelial cells participate in the innate immunity by reacting to pathogen-associated molecular patterns (PAMPs) (Pober and Sessa 2007) and damage-associated molecular patterns (DAMPs) (Vénéreau, Ceriotti et al. 2015). These molecular signatures interact with Toll-like receptors (TLRs) that trigger signals which lead to pro inflammatory cytokine expression, leukocyte recruitment, phagocytosis, and cytotoxicity (Maaser, Heidemann et al. 2006). However, during endothelial immunomodulatory events, endothelial cells are not only a recipient of inflammatory signals, but they also play a central role by directing the immune response by signaling immune cells contained in their milieu. This has been recently shown to occur through the secretion of metabolites. Zhang *et al* demonstrated that endothelial-derived lactate drives macrophage polarization to a regenerative M2-like phenotype, which ultimately is responsible of driving skeletal muscle regeneration in a hind limb ischemia model. (Zhang, Muri et al. 2020). Overall, it suggests that secretory capacity of endothelial cells cement their role in modulation of immune response and tissue regeneration

1.1.2. Endothelial modulation of vascular tone via nitric oxide production.

Blood vessels have the property of regulating blood pressure through the production of nitric oxide. Particularly, endothelial cells have a strong influence on vascular tone by releasing a battery of vasodilators like NO, prostacyclin and bradykinin, and vasoconstrictors such as endothelin and endothelium/derived constrictor factor (Andresen 2006).). Hypertension is the process in which the heart pumps to a greater resistance in peripheral tissues. Structural and functional modifications in arteries are the underlying mechanism to these changes (Andresen 2006). To counteract these effects, endothelial-derived vasoactive molecules take part in coordinating the

vasodilation of arterioles and in focalized adjustments of flow and shear stress in response to mechanical queues (Iadecola 2004). For instance, EC release nitric oxide to reestablish adequate vascular tone via signaling to vascular smooth muscle cells (VSMCs). Increased laminar shear stress stimulates production of nitric oxide by the enhanced expression of endothelial nitric oxide synthase (eNOS) and through increased activity via Kruppel-like factor 2 (Klf-2) and NF-kB. (Davis, Grumbach et al. 2004, Grumbach, Chen et al. 2005).

1.1.3. Angiocrine factors important in tissue regeneration.

It has been described that endothelial cells possess the capacity to regenerate their surrounding tissue upon injury. Beyond their known function to restore oxygen and nutrient supply through the formation of new blood vessels (angiogenesis), they have the capacity to mediate tissue regeneration and homeostasis through the secretion of angiocrine factors. These factors amongst others contribute to sustaining the clonal expansion of progenitor cells and to maintain an adequate vascular niche permissive for resident stem cells to return to their quiescent state, once they have been activated, and thus preventing stem cell exhaustion that could impair ulterior bouts of injury. The following cases are not meant to be an exhaustive revision of all regenerative properties of ECs described in literature, but rather to show case how the secretion of angiocrine factors take a central role in these processes.(Rafii, Butler et al. 2016).

Regeneration and fibrosis in liver. In basal conditions, angiocrine signals control the growth and expansion of hepatocytes by allowing the proliferation of diploid *AXIN*$2^{+/+}$ and T-box transcription factor $(TBX3)^{+/+}$ cells that replenish the liver (Wang, Zhao et al. 2015). These progenitors are located adjacent to EC in the central vein. These specialized EC produce WNT2 and WNT9b, which maintain a healthy population of an *AXIN*$2^{+/+}$and $TBX3^{+/+}$ double-positive cells. In other words, WNT2 and WNT9b are angiocrine factors. Tissue-specific deletion of endothelial Wntless in the adult mice exhausts these hepatic repopulating cells. Wntless is a specific transporter for WNT-ligands, which mechanistically explains the downregulation of these angiocrine factors in the extracellular space. Additionally, defined angiocrine expression of Rspondin3, a WNT agonist, by ECs in the central vein of the liver determines a β-catenin-dependent

metabolic zonation (Rocha, Vidal et al. 2015). Hence, both, repopulating potential and metabolic zonation of hepatocytes is determined by extrinsic, yet adjacent, angiocrine factors that arise from an instructive endothelial niche at the central vein of the liver.

Regeneration of lung epithelium. Lung capillary EC are instrumental in the regeneration of pulmonary epithelium. This has been demonstrated by removal of the left lung in mammals, procedure also known as pneumonectomy. This surgical ablation of the respiratory capacity leads to compensatory expansion of lung mass in the right lung, due to growth and further differentiation of alveolar epithelial stem and progenitor cells, in which alveolar type (AT) AT EC2 epithelial cells proliferate and regenerate lung epithelium. (Hogan, Barkauskas et al. 2014). This process is dependent of an intact angiogenic potential in ECs. Abrogation of the expression of FGFR-1 and VEGFR2 in adult ECs impairs this process (Ding, Nolan et al. 2011). Mechanistically, a growing vascular niche upregulates MMP-14, which later stimulates the epidermal growth factor (EGF) receptor on alveolar epithelial stem and progenitor cells via the cryptic EGF-like motif in HB-EGF and the gamma 2 chain of Laminin-5, and thus the proliferation of these cells leads to neo alveologenesis. Finally, endothelial cell specific knock out of MMP-14 in the adult blunts the regeneration capacity of alveolar epithelium with no repercussion on vascular perfusion. Taken altogether, endothelial-derived MMP-14 is an angiocrine signal that triggers the propagation of alveolar epithelial cells and basal cell progenitors.

1.1.4. Secretion of endothelial microRNA (miRNAs) in the modulation of cardiovascular biology.

Endothelial cells are capable of secreting microvessels containing micro RNAs. They have the main objective of silencing genes in distant tissues to modulate tissue homeostasis. Of note, MicroRNAs are short sequences of RNA, with an approximate length of 22 bp that bind to the untranslated region 3’ (3’ UTR) of their target messenger RNA to downregulate its expression. Mechanistically, Argonaute proteins (AGO) use these miRNAs as guide RNA to drive gene silencing, which may occur via 2 distinct processes, via a translation blockade and/or degradation of messenger RNA (mRNA)(Swarts, Makarova et al. 2014). miRNA can be assembled into a wide variety of membrane-derived vesicles for instance exosomes (30 to 150 nm), microvesicles (100 to 1000 nm) and apoptotic bodies (1 to 5 μm) to influence gene expression in

distant tissues and cells in a paracrine fashion (Rodrigues, Nimrichter et al. 2008). Due to the stability shown in the bloodstream, endothelial cells are thought to be an important contributor to the circulating pool of vesicle containing miRNA. Indeed, it has been shown that endothelial cells can secrete vesicle-containing miRNAs. To exemplify the extent of regulation endothelial cells, exert on tissues, the following EC-derived miRNAs are described. miR-222 is secreted by endothelial cells to reduce the tumor necrosis alpha (TNF-α) induced expression of intercellular adhesion molecule - 1 (ICAM-1), which recruits monocytes, in both, *in vivo* and *in vitro*. Importantly, in coronary artery disease (CAD), the relative abundance of miR-222 is reduced which may by partially responsible of an increased inflammatory state. (Jansen, Yang et al. 2015). Cardiac endothelial cells produce miR-126 and miR-210 to mediate survival of cardiac progenitor cells in transplanted cardiac cells in a myocardial infarction model. Mechanistically, miR-126 and miR-210 drive the upregulation of pro survival kinases and mediate a glycolytic switch in terminally differentiated cells cardiac which improves ejection fraction in mice. (Ong, Lee et al. 2014). Finally, endothelial-derived miRNAs can also be mediators of pathological states in target tissues. For instance, endothelial cells can produce miR-146a during peripartum cardiomyopathy. (Davis, Arany et al. 2020) a pregnancy-associated type of cardiomyopathy that could present itself as fatal condition, which contributes to an antimetabolic phenotype, impairing contractile and metabolic properties in cardiomyocytes (Halkein, Tabruyn et al. 2013). All in all, this exemplifies how endothelial cells are not only able to secrete metabolites, growth factors, hormones, and other archetypical molecules described during cell to cell communication, but also, as novel mechanisms of crosstalk are discovered, we see endothelial cells, and the whole vasculature in general, playing an important role and furthermore, assuming the central stage.

1.2. Regulation of organ homeostasis via controlling nutrient transport

1.2.1. Vascular endothelium as gatekeeper of substrate access.

Vascular endothelium, generally, can be rendered as a continuum lining of cells that barriers the contents present in the circulation (metabolites, nutrients, and growth factors) and the tissue they perfuse. However, ECs can form different types of capillary structures depending on the permeability needed in each capillary bed. They can be identified as continuous, fenestrated, and discontinuous. A continuous lining of

endothelial cells is characterized with tight junctions and a continuous basement membrane with the least permeability. Organs with continuous capillaries are skeletal muscle, lung, skin, central nervous system (CNS), heart, and adipose tissue (Bazzoni and Dejana 2004). Fenestrated capillaries are characterized by gaps, also referred as clefts, between adjacent ECs. Of note, despite these clefts, their basement membrane remains a continuum, therefore, they can be considered as the capillary structure with an intermediate permeability. Organs with these structures are typically endocrine organs which can secrete hormones more readily into circulation (Pavelka and Roth 2010). Finally, capillary structures with the highest permeability are discontinuous, also referred as sinusoids, where both endothelial cells and their basement membrane are discontinuous, which ensure maximal access of nutrient, metabolites, and factors to tissues (Buckley, Dickson et al. 1985, Braet and Wisse 2002, Shetty, Lalor et al. 2018). Organs with these vascular structures are liver, spleen, and bone marrow. Therefore, endothelial cells play different roles in modulating the access to different substrates in several organs, which ultimately furthers endothelial cell specificity as nutrient gatekeeper and modulator of metabolism.

Initially, it was believed that ECs were not able to actively modulate transport of glucose due to an allegedly inability to control expression of glucose transporter 1, GLUT1. A constitutive expression of GLUT1 would secure a continuous transendothelial transport and supply to tissues (Kaiser, Sasson et al. 1993). However, this view has been challenged by findings pointing that ECs downregulate expression of GLUT1 in CNS and heart when challenged for prolonged periods of time to high concentrations of glucose(Rajah, Olson et al. 2001, Alpert, Gruzman et al. 2005). Furthermore, it has been shown that when endothelial cells acquire a quiescent state, glycolysis is downregulated which leads to a GLUT1 upregulation in a NOTCH1-dependent manner. (Veys, Fan et al. 2020). Additionally, GLUT1 has been identified as a hypoxia inducible factor alpha (HIF1α) (Huang, Lei et al. 2012).), which improves endothelial cell survival in poorly irrigated and thus hypoxic zones, as endothelial cells heavily rely on glycolysis for ATP generation (De Bock, Georgiadou et al. 2013). As central glucose can be to cellular energy homeostasis, it is actively regulated in endothelial cells depending their physiological state.

To continue exemplifying the role of vascular endothelium to control the access to nutrients and metabolites in organ tissues, endothelial cells expresses a variety of fatty acid transporters (FA) in continuous capillaries which form a tight barrier to FA of a carbon chains equal or greater to 12 carbons. On the contrary, in the liver these tight junctions are not necessary as FA present in circulation are in direct contact with hepatocytes through liver sinusoids. Among the different FA transporters found in vascular tissue there are several worth to mention, for instance, fatty acid binding proteins (FABPs)(Antohe, Popov et al. 1998, Elmasri, Karaaslan et al. 2009) , which mediate their intracellular binding and mobility, fatty acid transport proteins (FATPs) which are transporters located at EC cell membrane that mediate FA uptake and CD36 which is a translocase, key in the transport of fatty acid in skeletal muscle and heart tissue (Greenwalt, Watt et al. 1990). Over expression of FATP3 and FATP4 in ECs synergistically enhance lipid accumulation, which highlight their role in the uptake of long-chain fatty acid in ECs. Importantly, their co expression is controlled by the stimulation of Vascular endothelial growth factor B(Hagberg, Falkevall et al. 2010)

1.3. Regulation of organ homeostasis through angiogenesis

Blood vessels are the functional unit of the vascular system. They are an assembly of endothelial cells, pericytes and smooth muscle cells that form the tubing fundamental in maintaining tissue homeostasis. In adults, around 95% of endothelial cells remain quiescent. However, ECs keep their capacity to respond to oxygen and nutrient shortage through the secretion of angiogenic growth factors from hypoxic and/or nutrient deprived cells which leads to the formation of new blood vessels in a process termed angiogenesis.(Wang Y. 2010). Among those angiogenic growth factors, VEGFA is the canonical molecule to signal towards vascular growth. It acts through the stimulation of VEGF receptor 2, VEGFR2, at the cell membrane of EC. Though the establishment of a VEGFA gradient in the capillary milieu and an intricate cell-to -cell signaling, three functionally distinct transient cell fates can be identified. These are: *tip cells* which are present at the forefront of sprouting region, they are distinguished by high migration capability but suppressed proliferation; *stalk cells,* on the contrary are highly proliferative with limited migratory capacity; and finally *phalanx cells*

characterized by their quiescent state (Zecchin, Kalucka et al. 2017). (De Bock, Georgiadou et al. 2013).

1.3.1. Tip cells

The main function of tip cells is to lead the angiogenic sprout upon stimulation with angiogenic factors. Tip cells are characterized by their high migratory capacity and decreased proliferative potential. They exhibit a unique morphology: highly elongated shape with multiple cell membrane projections like filopodia and lamellipodia. In addition, their cell membrane is abundant in receptors and molecules in charge of extracellular matrix remodeling, helping them to reach tissue not yet perfused. (De Bock, Georgiadou et al. 2013, Schoors, Bruning et al. 2015).

1.3.2. Stalk cells

The angiogenic stimuli at the tip cell is pivotal for the generation of proliferative stalk cells. Stimulation of VEGFR2 elicits a transcriptional program that results in the upregulation of delta-like ligand 4 (Dll4) in the tip cells. Dll4 activates NOTCH signaling in adjacent EC. This signal begins a transcriptional program that leads, among other expression changes, to the downregulation of several cognate receptors of angiogenic factors like VEGFR2, VEGFR3, and NRP1, while at the same time, upregulating VEGFR1, a decoy receptor that dampens VEGFA stimuli to inhibit tip cell formation and promote a rather proliferative phenotype (Blanco and Gerhardt 2013).

1.3.3. Quiescent phalanx cells

After a new blood vessel has formed, ECs become quiescent again. Under steady state conditions most of ECs, up to 95%, are quiescent(Ricard, Bailly et al. 2021). Despite being the prevailing vascular growth state in mammals, little is known about the physiological role it has in the body or the metabolic determinants of a *functionally quiescent endothelium.*

Upon exiting the proliferative stage into quiescence, endothelial cells undergo a dramatic metabolic change, reducing their glycolysis ~40% while increasing their relative ATP production from mitochondria. A similar phenotype, can be observed

when overexpressing the Kruppel like factor 2 (KLF2), a transcription factor induced by high laminar shear stress in EC. In the nuclei, KLF2 suppresses the expression of PFKFB3 . Interestingly, overexpressing PFKFB3 in EC resumes their glycolytic activity and overrides KLF2 inhibition of growth (Lin, Natesan et al. 2010, Doddaballapur, Michalik et al. 2015).

The transcription factor fork head box O 1 (FOXO1) is yet another driver of EC quiescence. Interestingly, activation of FOXO1 is dependent of concentration of growth factors exposed to the cell. In the lack of growth factors, FOXO1 is present in the nucleus where it drives a gene transcription program. When angiogenic factors are present, such as VEGFA, FOXO1 suffers phosphorylation by AKT or serum/glucocorticoid –regulated kinase (SGK) which promote their displacement outside from the nucleus where is degraded by ubiquitin-proteasome pathway. In EC, FOXO1, along with FOXO3 and FOXO4 control growth state, survival, cell progression, energy metabolism, differentiation, and oxidative stress resistance. Specifically, FOXO1 acts as a pivotal modulator of proliferation and metabolic output. Endothelial specific murine FOXO1 overexpression constrains vascular development, provokes reduction of branching points and reduction of capillary diameter. Furthermore, FOXO1 controls endothelial quiescence through the inhibition of metabolic activity, reducing glycolysis and oxidative phosphorylation via blocking MYC signaling(Paik, Kollipara et al. 2007, Roudier, Milkiewicz et al. 2013, Wilhelm, Happel et al. 2016).

Despite that transcriptional programs that are determinant in endothelial cell identity are well-characterized and their resulting metabolic output largely described , little is known regarding how the secretion of angiocrine factors is modulated by these states to ultimately control whole body metabolic control and energy homeostasis.

1.4. Aims of the thesis

The sections above give a brief overview of aspects in which vasculature plays a central real in maintaining whole body homeostasis. However, the mechanistic understanding of whether and how vascular growth controls skeletal muscle homeostasis is largely lacking. In this project, I focused to answer four major questions in EC-Skeletal Muscle crosstalk

1. Whether and how a metabolic cross talk between EC and skeletal muscle tissue occurs.
2. Characterization of endothelial cell specific secretome *in vitro* using an unbiased proteomic approach.
3. Validation of potential targets using differential vascular states such as FOXO1 or NOTCH1.
4. Metabolic characterization of a novel angiocrine able to control skeletal muscle metabolism.

Importantly, the initial aims put forth in the thesis proposal at the commencement of this doctoral project shifted to the ones presented on this dissertation, which should be considered a final version. This was caused by the fact that the onset of metabolic adaptations to exercise, specially to the ones corresponding to *ad libitum* running wheel, require several weeks of training. Therefore, it compromised the time allocated to finish this project.

2. Measuring glycolytic and mitochondrial fluxes in endothelial cells using radioactive tracers

Abdiel Alvarado-Diaz[1] , Koen Veys[2,3] , and Katrien De Bock[1]

Koen Veys and Abdiel Alvarado-Diaz contributed equally to this work

1. Laboratory of Exercise and Health, Department of Health Sciences and Technology, ETH Zürich, Zürich, Switzerland.

2. Laboratory of Angiogenesis and Vascular Metabolism, VIB Center for Cancer Biology, VIB, Leuven, Belgium.

3. Laboratory of Angiogenesis and Vascular Metabolism, Department of Oncology, KU Leuven, Leuven, Belgium.

Status: Published

DOI: https://doi.org/10.1007/978-1-4939-8769-6_9

2.1. Abstract

Endothelial cells (ECs) form the inner lining of the vascular network. Although they can remain quiescent for years, ECs exhibit high plasticity in both physiological and pathological conditions, when they need to rapidly form new blood vessels in a process called angiogenesis. EC metabolism recently emerged as an important driver of this angiogenic switch. The use of radioactive tracer substrates to assess metabolic flux rates in ECs has been essential for the discovery that fatty acid, glucose, and glutamine metabolism critically contribute to vessel sprouting. In the future, these assays will be useful as a tool for the characterization of pathological conditions in which deregulation of EC metabolism underlies and/or precedes the disease, but also for the identification of anti-angiogenic metabolic targets. This chapter describes in detail the radioactive tracer substrate assays that have been used for the determination of EC metabolic flux in vitro.

Key words. Endothelium, Metabolic flux rate, Radioactive tracer substrates, Glycolysis, Fatty acid oxidation, Glucose oxidation, Glutamine oxidation

2.2. Authors contributions

The general content and perspective of this chapter was proposed by Prof. Dr. Katrien De Bock. All the authors contributed to the technical expertise necessary to perform the experiments described in this protocol paper for the measurement of metabolic fluxes using radioactive tracers in endothelial cells. The design of the content, this is, the order and writing of each section of the manuscript, as well as the figure design was done by Abdiel Alvarado-Diaz and Dr. Koen Veys. The final figure formatting was carried out by Koen Veys. All authors reviewed and corrected the full contents of this manuscript chapter.

2.3. Introduction

Endothelial cells (ECs) line the inner surface of the vascular network and can stay quiescent for years. But in response to injury or during pathological conditions such as cancer, ECs are able to rapidly initiate the formation of new blood vessels in a tightly controlled but highly dynamic process termed sprouting angiogenesis. Sprouting angiogenesis is initiated by the secretion of pro-angiogenic factors from nearby cells into the microenvironment. Subsequently, one single EC is selected to become the leading “tip” cell and migrates toward the hypoxic and/or nutrient deprived area, while at the same time instructing its follower cells not to become tip cells. Instead, those “stalk” cells proliferate, extend the growing vascular sprout, and form a lumen. When two sprouts fuse, blood flow is reinitiated and ECs secrete a basement membrane while they return to their quiescent “phalanx” cell phenotype. Complex growth factor signaling networks and transcriptional signals control sprouting angiogenesis, but over the last few years it has become clear that these signals converge into metabolic changes that subsequently drive EC subtype (either tip, stalk, or phalanx cell) specification(Adams and Alitalo 2007, Carmeliet and Jain 2011).

ECs are glycolysis-addicted since the great majority of their ATP is produced by the glycolytic conversion of glucose to lactate, and only a limited number of glucose-derived pyruvate molecules are shunted into the TCA cycle for further oxidation(De Bock, Georgiadou et al. 2013). . Nonetheless, levels of glycolysis are strictly controlled in the quiescent endothelium(Doddaballapur, Michalik et al. 2015, Wilhelm, Happel et al. 2016) and reducing glycolysis suffices to promote a quiescent phenotype, even within the abnormal tumor environment (Schoors, De Bock et al. 2014, Cantelmo, Conradi et al. 2016). . During sprouting, glycolysis is upregulated in the migratory tip cells. In these cells, glycolytic enzymes, such as 6-phosphofructo-2-kinase/fructose-2,6-bisphosphatase 3 (PFKFB3) and hexokinase 2 (HK2), compartmentalize with F-actin at the so-called ATP hotspots of their membrane ruffles and thereby facilitate fast and local supply of ATP for migration (De Bock, Georgiadou et al. 2013, Yu, Wilhelm et al. 2017). Interestingly, proliferating stalk cells also require high glycolysis(De Bock, Georgiadou et al. 2013), but at the same time use fatty acid β-oxidation (FAO) for the synthesis of nucleotides for DNA replication. Fatty acid-derived carbons substantially

replenish the TCA cycle, and knock-down of carnitine palmitoyltransferase 1a (CPT1a), an enzyme involved in fatty acyl-CoA transport into the mitochondria and the rate-limiting enzyme for fatty acid β-oxidation, impairs EC proliferation in vitro (Schoors, Bruning et al. 2015, Wong, Wang et al. 2017), and reduces radial expansion and number of branch points of the retinal vascular network in vivo (Schoors, Bruning et al. 2015). Glutamine, however, is the main source of TCA cycle carbons(Kim, Li et al. 2017) and preventing glutamine anaplerotic via glutamine depletion or knock-down of glutaminase 1 (GLS1) reduced both nucleotide synthesis, protein synthesis, as well as lipid biosynthesis via reductive carboxylation (Huang, Vandekeere et al. 2017, Kim, Li et al. 2017). Interestingly, glutamine metabolism is also linked to asparagine metabolism, since angiogenic defects, observed upon inhibition of glutamine metabolism, could only be rescued by combined α-ketoglutarate and asparagine availability (Huang, Vandekeere et al. 2017). Other metabolic pathways have been studied in ECs but their role in EC specification in vivo is less clear. For instance, glucose flux into the oxidative pentose phosphate pathway (oxPPP) is required for EC proliferation and migration in vitro(Leopold, Walker et al. 2003). At the same time, oxPPP flux, via its rate-limiting enzyme glucose-6-phosphate dehydrogenase (G6PD), supports vascular redox homeostasis by limiting oxidative stress through the production of NADPH and the maintenance of sufficient nitric oxide levels(Leopold, Dam et al. 2007). For a detailed overview on EC metabolism, the reader is referred to elsewhere(Uebelhoer and Iruela-Arispe 2016, Sawada and Arany 2017, Eelen, de Zeeuw et al. 2018, Rohlenova, Veys et al. 2018).

The assessment of metabolic fluxes using radioactively labeled substrates has been fundamental to increase our understanding about EC metabolism. Here, we provide a detailed description on how to assess flux rate through several key EC metabolic pathways. The measurement of fatty acid β-oxidation (using palmitate as the lipid substrate) and glycolysis relies on the incorporation of ^{3}H into water, whereas the determination of glucose oxidation and oxPPP, as well as glutamine oxidation is dependent on the incorporation of ^{14}C into carbon dioxide.

2.3.1. Fatty Acid β-Oxidation Flux

Palmitate, the 16-carbon, saturated long chain fatty acid is the product of fatty acid synthesis and is a precursor for longer fatty acids as well as a substrate for oxidation through fatty acid β-oxidation (FAO). FAO progresses in four-step cycles, each time

cleaving two carbons that form acetyl-CoA at the end of every cycle. Subsequently, these acetyl-CoA units can be used for further oxidation in the TCA cycle.

The determination of FAO flux in ECs can be done using *[9,10-^{3}H(N)]-palmitic acid*. It is worth noting that the tritium atoms are chiral and that all four stereoisomers ((1) 9R-10R; (2) 9R-10S; (3) 9S-10R; (4) 9S-10S; see **Figure 2**). are present in equal amounts. The release of the hydrogen atoms is stereospecific and either in the form of [2-^{3} H]-acetyl-CoA units or as tritiated $FADH_2$ or NADH molecules, which eventually produce $^{3}H_2O$ in the electron transport chain (ETC) (see **Figure 2**) (Kler, Sherratt et al. 1992). This implies that for the β-oxidation of *[9,10-^{3} H(N)]-palmitic acid*, 75% of the ^{3} H atoms are indirectly released as $^{3}H_2O$ and 25% are released as [2-^{3} H]-acetyl-CoA. The fate of the ^{3} H-label derived from [2-^{3} H]- acetyl-CoA depends on the efficiency of its oxidation in the TCA cycle, and because TCA cycle flux is not always proportional to fatty acid β-oxidation (FAO) flux, the full recovery of the [2-^{3} H]-acetylCoA into $^{3}H_2O$ can thus be affected by changes in TCA cycle flux and lead to deviations in the experimental readout (Kler, Sherratt et al. 1992). Nonetheless, the utilization of *[9,10-^{3} H(N)]-palmitic acid* is considered more accurate than the utilization of ^{14}C-labeled palmitate tracers (Kler, Sherratt et al. 1992).

Fatty acids such as palmitate use the carnitine shuttle as a transport system for mitochondrial import. The first enzyme in the carnitine shuttle, CPT1, is rate-limiting for both fatty acylCoA transport and fatty acid β-oxidation (Drynan, Quant et al. 1996). Thus, pharmacological blockade of CPT1 using etomoxir can be used as a negative control for this assay

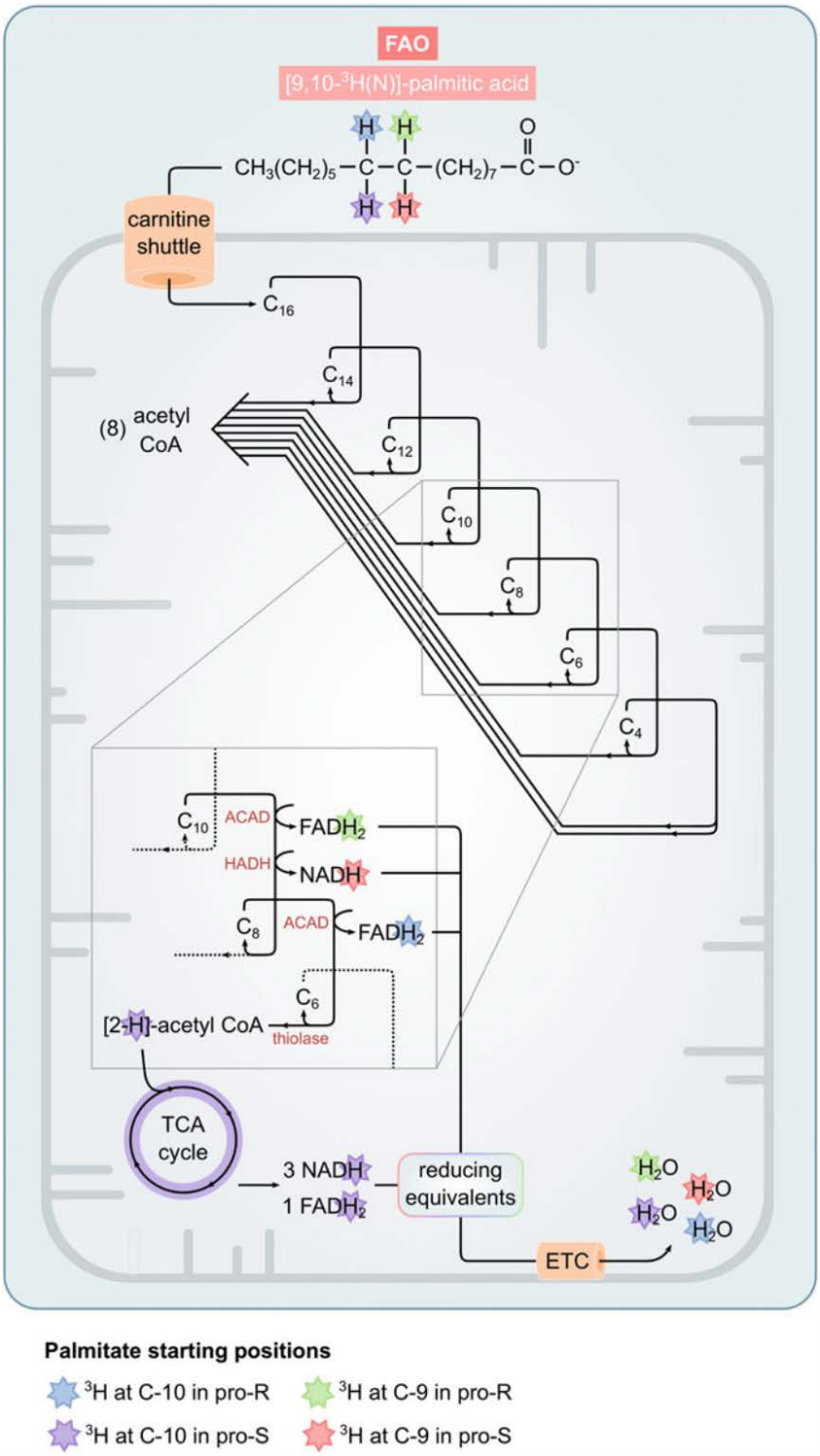

Figure 2. Schematic representation of FAO measurement using *[9,10-^{3} H(N)]-palmitic acid*. During the fourth cycle of FAO, palmitate is reduced to a 10-carbon molecule and the ^{3} H atom that started at position 9 is released as ^{3} H-labeled $FADH_2$ by the FAD-dependent acyl-CoA dehydrogenase (ACAD) from the pro-R form or released as ^{3} H-labeled NADH by the NAD^+ -dependent L-3-hydroxyacyl-CoA dehydrogenase (HADH) from the pro-S form. In the next cycle, the 8-carbon molecule releases the ^{3} H atom that started at position 10 by the ACAD enzyme as ^{3} H-labeled $FADH_2$ from the pro-R form, whereas the pro-S form releases it as [2-^{3} H]-acetyl-CoA, when its two carbons are removed by the thiolase enzyme. Further oxidation of [2-^{3} H]- acetyl-CoA in the TCA cycle yields labeled $FADH_2$ and NADH. In the ETC, ^{3} H2O is produced from labeled $FADH_2$ and NADH. *ACAD* FAD-dependent acyl-CoA dehydrogenase, *ETC* electron transport chain, *HADH* NAD^+ - dependent L-3-hydroxyacyl-CoA dehydrogenase.

2.3.2. Glycolytic Flux

To measure glycolytic flux, tritium labeled glucose is used as the substrate tracer. The tritium is positioned at the fifth glucose carbon which means that when glycolysis is active, the ^{3}H label from the *D-[5-^{3}H(N)]-glucose* tracer appears at the middle carbon of glyceraldehyde-3-phosphate (G3P). Subsequently, 2-phosphoglycerate (2PG) is converted to phosphoenolpyruvate (PEP) by the enolase enzyme, thereby producing tritium labeled H_2O (see **Figure 3**). Thus, flux rate through glycolysis is assessed by measuring the amount of tritium labeled water produced over time. Several inhibitors of glycolysis have been described in ECs. For instance, adding 2-deoxyglucose (2DG) to the assay medium in equal concentrations when compared to glucose rapidly reduces glycolytic flux (Schoors, De Bock et al. 2014). 2DG competes with glucose for uptake in the cell but cannot be further metabolized by glycolysis after its phosphorylation by hexokinase. Subsequently, the accumulation of the intracellularly trapped 2-deoxyglucose-6-phosphate leads to the inhibition of hexokinase activity and thus glycolytic flux. Also, pharmacological inhibition of the glycolytic regulator PFKFB3 using the small molecule 3-(3-pyridinyl)-1-(4-pyridinyl)-2-propen1-one (3PO) reduces endothelial glycolysis with approximately 30%.(Clem, Telang et al. 2008, Schoors, De Bock et al. 2014)

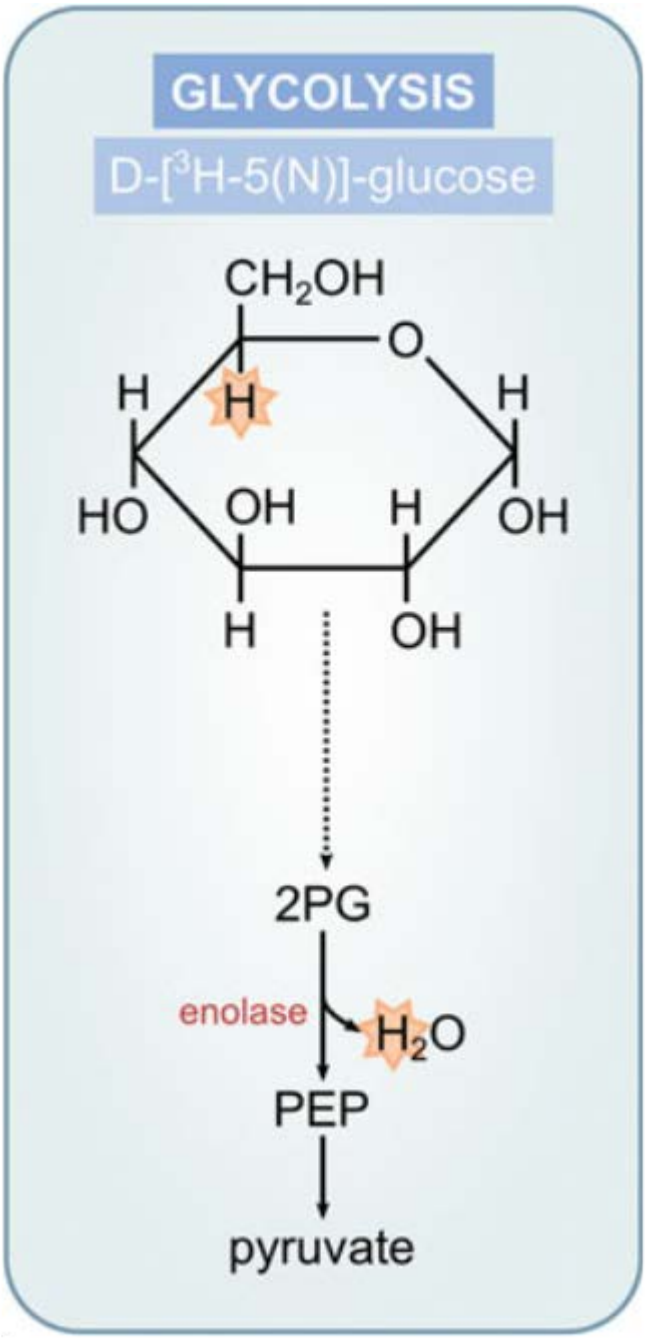

Figure 3. Schematic representation of glycolysis measurement using *D-[5-3 H(N)]- glucose*. *D-[5-3 H(N)]-glucose* produces $^{3}H_2O$ when 2PG is converted to PEP at the enolase-step of glycolysis. *2PG* 2-phosphoglycerate, *PEP* phosphoenolpyruvate

2.3.3. Glucose Oxidation and oxPPP Flux

To measure the oxidation of glucose, D-[6-^{14}C]-glucose is used as a tracer. The sixth carbon does not necessarily end up in dihydroxyacetone phosphate (DHAP) and rather travels through glycolysis as the third triose carbon from G3P to pyruvate. Next, pyruvate enters the TCA cycle after decarboxylation to acetyl-CoA and in the theoretical model, half of the D-[6-^{14}C]-glucose molecules lose their ^{14}C label in the form of ^{14}CO2 during the third TCA cycle. By the seventh cycle, more than 95% of the ^{14}C labels will have been released. Labeled carbons will arise as ^{14}CO2 during the conversion of isocitrate to α-ketoglutarate by isocitrate dehydrogenase (IDH) and during the conversion of α-ketoglutarate (α-KG) to succinyl-CoA by α-ketoglutarate dehydrogenase (OGDH), thereby being a measure of glucose oxidation **Figure 4a**Theoretically, pyruvate could also enter the TCA cycle as oxaloacetate (OAA) through pyruvate carboxylation(Lee, Kang et al. 2003). In that case, the ^{14}C label could already exit as ^{14}CO2 after the first TCA cycle. However, a significant contribution of pyruvate carboxylation flux in ECs remains largely unexplored.

Glucose oxidation flux in endothelial cells is detectable (De Bock, Georgiadou et al. 2013) , but under normal culture conditions it is only a small fraction of the glucose that went through glycolysis. To determine oxPPP flux, a combination of two tracers is used in parallel experiments: *D-[1-^{14}C]-glucose* and *D-[6-^{14}C]-glucose*. As mentioned above, the latter is an indicator of glucose oxidation in the TCA cycle, whereas the first one produces ^{14}CO2 as a result of both glucose oxidation and oxPPP activity. Indeed, the first carbon of G6P can be released in the oxPPP as ^{14}CO2 when 6-phosphogluconate (6PG) is converted to ribulose-5-phosphate (Ru5P). Ru5P formation is particularly relevant as a precursor for nucleotide biosynthesis (Pandolfi, Sonati et al. 1995). If *D-[1-^{14}C]-glucose* does not enter the oxPPP, it can run down the glycolytic pathway but unlike *D- [6-^{14}C]-glucose*, where the ^{14}C-labeled carbon bypasses DHAP, the labeled carbon needs to take a detour through DHAP before it ends up in G3P. At that point, both the *[1-^{14}C]* and the *[6-^{14}C]* end up at the same carbon position within G3P, making them indistinguishable. From there, both labeled carbons will follow the same route and therefore, their metabolic fate will be identical (see **Figure 4b**). To determine net oxPPP flux, two experiments – one using *D- [1-14C]-glucose* and one for *D-[6-14C]-glucose* – are run in parallel and $^{14}CO_2$ production from *D-[6-14C]-glucose* is subtracted from the $^{14}CO_2$ production from *D-[1-^{14}C]-glucose* (this is C1-$^{14}CO_2$ minus C6-$^{14}CO_2$).

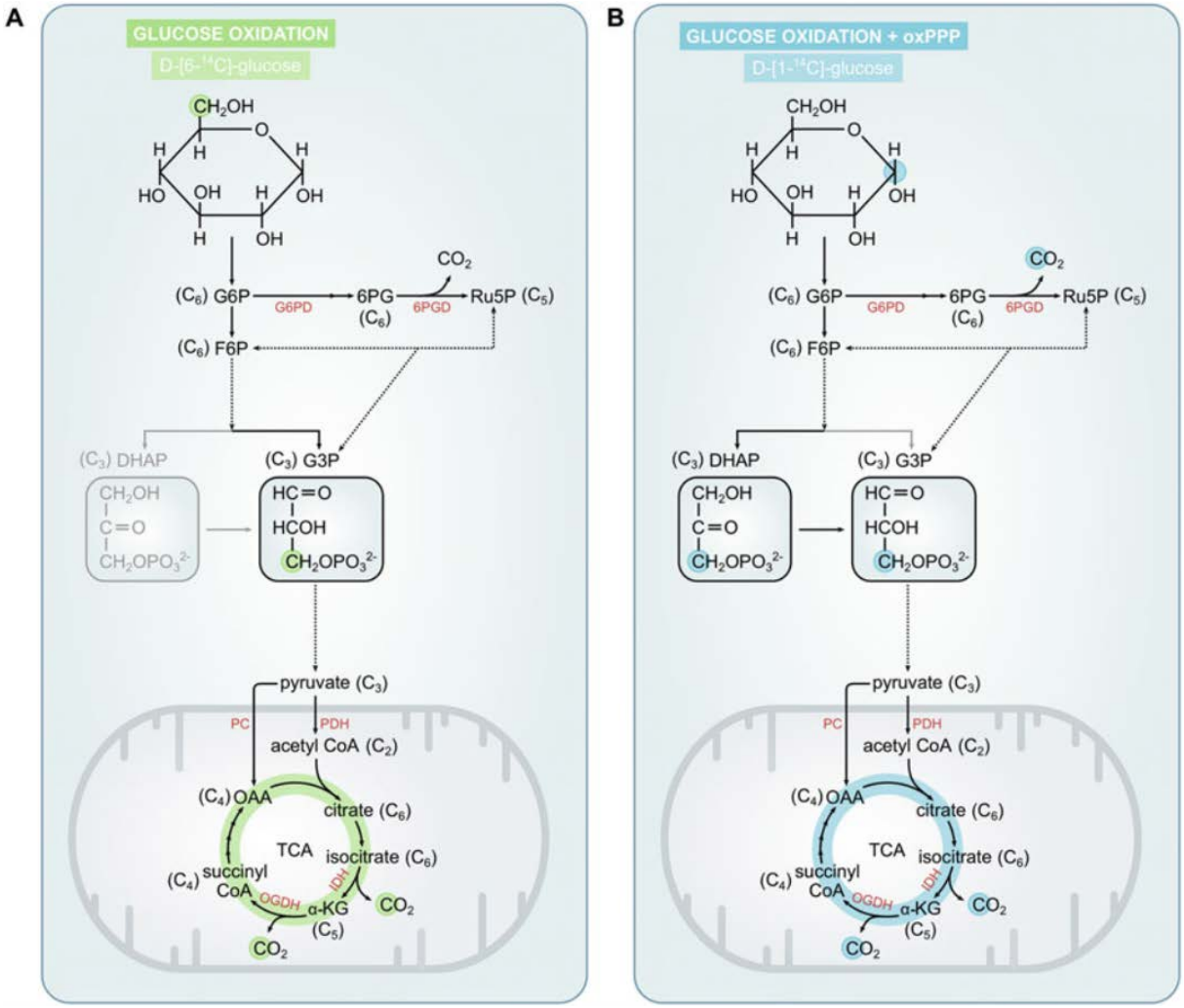

Figure 4.Schematic representation of glucose oxidation/oxPPP measurement using *D-[6-^{14}C]-glucose* and *D-[1-^{14}C]-glucose*. (a) Glucose oxidation: $^{14}CO_2$-production from the oxidation of *D-[6-^{14}C]-glucose* only starts during the third TCA cycle at the IDH- and OGDH-step. (b) Glucose oxidation + oxPPP: *D-[1-^{14}C]-glucose* releases CO_2 at the same steps of the TCA cycle, but can also release CO_2 at the 6PGD-step of the oxPPP. (a, b) Therefore, the subtraction of *D-[6-^{14}C]-glucose*-derived $^{14}CO_2$-production from *D-[1-^{14}C]-glucose*-derived $^{14}CO_2$-production yields a measure for the net oxPPP flux. 6PGD 6-phosphogluconate dehydrogenase, *G6PD* glucose-6-phosphate dehydrogenase, *IDH* isocitrate dehydrogenase, *OGDH* α-ketoglutarate dehydrogenase, *PC*, pyruvate carboxylase, *PDH* pyruvate dehydrogenase.

2.3.4. Glutamine Oxidation Flux

To assess glutamine oxidation flux, *L-[^{14}C(U)]-glutamine* has been used as a tracer. Glutamine is first converted to glutamate by GLS1(Leighton, Curi et al. 1987). , which in turn is metabolized to α-ketoglutarate before entering the TCA cycle. There, fully labeled α-ketoglutarate immediately releases a first $^{14}CO_2$ when converted into succinyl-CoA by OGDH and a second $^{14}CO_2$ when isocitrate is converted to α-ketoglutarate by IDH. In the second cycle of the theoretical model, OGDH releases a third $^{14}CO_2$ from α-ketoglutarate, but due to the symmetry of succinate, the remaining ^{14}C label is randomized and will gradually be released in the following cycles. It has recently been reported that about 10% of glutamine in ECs takes an alternative route via malic enzyme and pyruvate dehydrogenase in two subsequent decarboxylation steps before reentering in the TCA cycle (Huang, Vandekeere et al. 2017, Kim, Li et al. 2017). In this scenario, three $^{14}CO_2$ molecules are released in the first cycle but the start of the second cycle will not result in $^{14}CO_2$ release at OGDH. Thereafter, the metabolic fate of the label remains the same (see **Figure 5**). Although this alternative pathway only marginally affects the kinetics of 14CO2 production, it coincides with the production of NADPH for biomass generation or redox maintenance rather than the generation of NADH. In vitro pharmacological interventions have proven useful for the study of endothelial glutamine metabolism. To determine the role of exogenously administered glutamine in ECs, the use of the SLC1A5 transporter inhibitor L-γ-glutamyl-p-nitroanilide (GPNA) has been reported(Sanchez, Carroll et al. 2015). Furthermore, inhibitors of GLS1, such as CB-839 or bis-2-(5-phenylacetamido-1,3,4-thiadiazol-2-yl)ethyl sulfide (BPTES), have also been used to show that glutamine is required for tip cell competitiveness in vessel sprouting (Durante, Liu et al. 2017, Huang, Vandekeere et al. 2017).

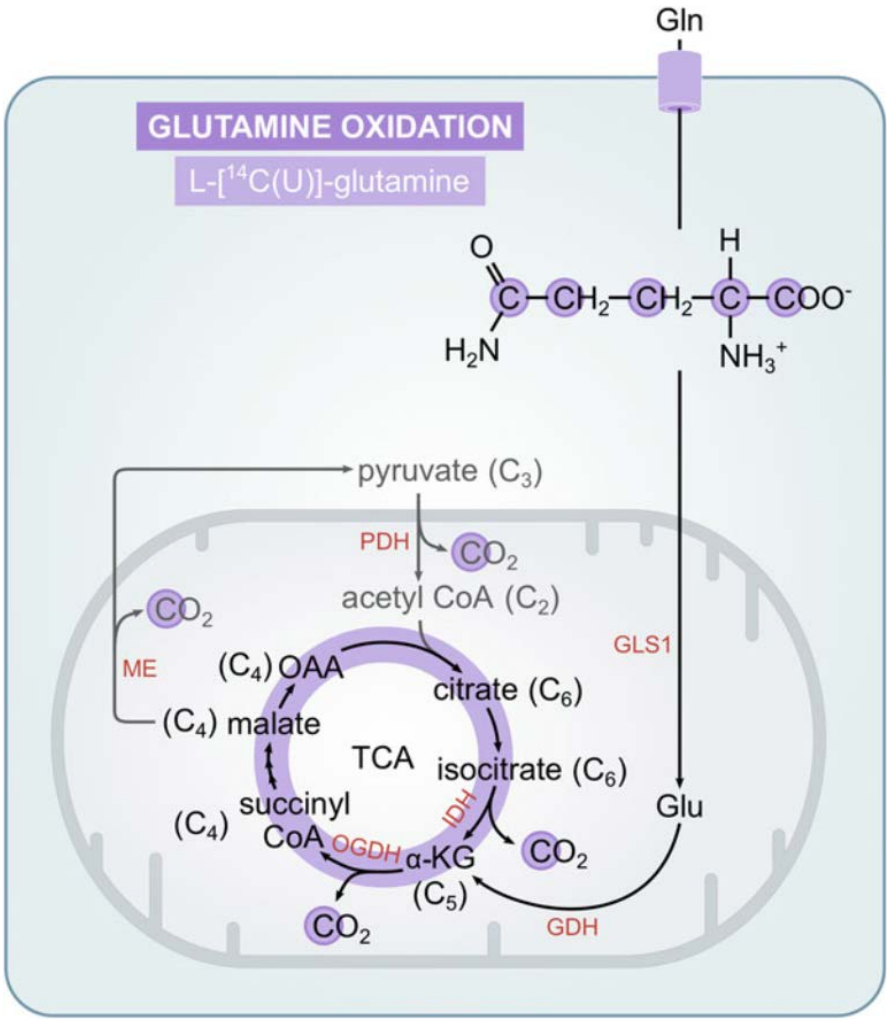

Figure 5. Schematic representation of glutamine oxidation measurement using *L-[^{14}C(U)]-glutamine*. Glutamine oxidation: *L-[^{14}C(U)]-glutamine* releases a first $^{14}CO_2$ when converted into succinyl-CoA by OGDH, and a second $^{14}CO_2$ when isocitrate is converted to α-ketoglutarate. In the second cycle of the theoretical model, α-ketoglutarate releases a third $^{14}CO_2$ by OGDH activity, but due to the symmetry of succinate, the remaining ^{14}C label is randomized and will gradually be released in the following cycles. About 10% of glutamine in ECs takes an alternative route via malic enzyme and pyruvate dehydrogenase in two subsequent decarboxylation steps before reentering in the TCA cycle. In this scenario, three $^{14}CO_2$ molecules are released in the first cycle but the start of the second cycle will not result in $^{14}CO_2$ release at OGDH. Thereafter, the metabolic fate of the label remains the same. *GDH* glutamate dehydrogenase, *GLS1* glutaminase 1, *IDH* isocitrate dehydrogenase, *ME* malic enzyme, *OGDH* α-ketoglutarate dehydrogenase.

2.4. Materials

2.4.1. General

1. β-counter.

2. Polyethylene hinge cap scintillation vials with 8 mL capacity.

3. Scintillation cocktail.

4. Regular endothelial cell culture medium such as EGM2 or M199 complete medium: 5.5 mM glucose, 2 mM glutamine, 20% FBS, supplemented with endothelial cell growth factors and heparin. Of note, the medium composition should be carefully considered depending on the specific research question. For instance, serum-free or fatty acid-free bovine serum albumin medium is required for the quantification of FAO flux because the precise fatty acid concentration should be known to calculate oxidation fluxes.

2.4.2. $^{3}H_2O$ Recovery for Fatty Acid β-Oxidation and Glycolysis Measurement

1. FAO tracer: *[9,10-^{3}H(N)]-palmitic acid* at a stock concentration of 1 mCi/0.2 mL EtOH; this is 5 µCi/µL. For the labeling solution, use 0.4 µL from the stock solution per mL culture medium. This results in a final concentration of 2 µCi/ mL medium. Use medium that is serum-deprived or supplemented with fatty acid-free bovine serum albumin. Add 100 µM palmitate (nonradioactive), 50 µM fatty acid-free bovine serum albumin and 50 µM carnitine.

2. 10 mM palmitate stock solution (nonradioactive) in absolute EtOH. Store at -20 C in a glass vial.

3. 50 mM carnitine stock solution in PBS.

4. Glycolysis tracer: *D-[5-^{3}H(N)]-glucose* at a stock concentration of 1 mCi/mL EtOH:Water (9:1); this is 1 µCi/µL. For the labeling solution, use 0.4 µL from the stock solution per mL culture medium. The final concentration will be 0.4 µCi/mL medium.

5. Glass vials.

6. Rubber stoppers.

7. Hanging wells.

8. Filter papers: 1 cm x 6 cm.

9. Ultrapure water.

2.4.3. $^{14}CO2$ Recovery for Glucose, Glutamine Oxidation and oxPPP Measurement.

1. Glucose oxidation tracer: *D-[6-^{14}C]-glucose* at a stock concentration of 50 µCi/0.5 mL EtOH:Water (9:1); this is 0.1 µCi/µ L. For the labeling solution, use 5.5 µL from the stock solution per mL culture medium. The final concentration therefore is 0.55 µCi/mL medium.

2. Glucose oxidation + oxPPP tracer: *D-[1-^{14}C]-glucose* at a stock concentration of 50 µCi/0.5 mL EtOH:Water (9:1); this is 0.1 µCi/µL. For the labeling solution, use 5.5 µL from the stock solution per mL culture medium. The final concentration is 0.55 µCi/mL medium.

3. Glutamine oxidation tracer: *L-[^{14}C(U)]-glutamine* at a stock concentration of 50 µCi/mL EtOH:Water (2:98); this is 0.05 µCi/µL. For the labeling solution, use 5.5 µL from the stock solution per mL culture medium. The final concentration is 0.275 µCi/mL medium.

4. 10X hyamine-hydroxide. Dilute to 1X hyamine solution in ultrapure water. Only use the hyamine solution under the hood. 5. 12% perchloric acid. 6. Filter papers: 2.6 cm x 2.6 cm. 7. Ultrapure water.

2.5. Methods

2.5.1. $^{3}H_2O$ Recovery for Fatty Acid β-Oxidation and Glycolysis Measurement

A schematic representation of this assay is depicted in **Figure 6**

1. Day 1: the day before the experiment, seed 150,000 endothelial cells per well in a gelatin-coated 12-well plate (see Note 1).

2. Day 2: replace the culture medium (see **Note 2**) with 500 µL labeling solution. For FAO, use 2 µCi/mL [9,10-^{3} H(N)]-palmitic acid supplemented with 100 µM palmitate (nonradioactive) (see **Note 3**) bound to 50 µM fatty acid-free bovine serum albumin and 50 µM carnitine. For glycolysis, use 0.4 µCi/mL D-[5-^{3} H(N)]-glucose). Incubate the cells with labeling solution at 37 C for 6 h (FAO) or 2 h (glycolysis). Likewise, add the same volume of labeling solution to empty wells of a 12-well plate for the determination of background signal. Make sure to keep a small fraction of labeling solution (>12 µL) to calculate the specific activity (see **Note 6**).

3. Prepare rubber stoppers with hanging wells. Roll the filter papers (1 cm x 6 cm) and insert one into each hanging well. Hydrate each filter paper with 200 µL ultrapure water.

4. After tracer incubation, transfer 400 µL out of 500 µL labeling solution from the 12-well plate to the glass vials. Aspirate the leftover tracer solution and prepare cell lysates for the determination of protein content. Close the glass vials with the rubber stoppers with hanging well and paper. If ECs attach poorly, add perchloric acid to stop any metabolic activity of unintentionally transferred cells.

5. Incubate the glass vials for at least 48 h at 37 C (see **Note 4**).

6. Prepare scintillation liquid vials containing 5 mL scintillation liquid and transfer each filter paper to its corresponding scintillation vial. Optional: wash the hanging well with 100 µL H_2O and transfer the water into the same scintillation vials.

7. Shake the vials thoroughly and allow the filter papers to disperse their radioactive material into the scintillation cocktail for at least 2 h and up to 16 h before counting.

8. Count the scintillation vials using the correct protocol, measuring the disintegrations per minute (dpm) of the ^{3}H label for at least 1 min per sample.

9. Rinse the equipment (glassware, rubber stoppers, and hanging wells) (**see Note 5**) to prevent the leftover radioactivity from adding noise to future experiments. 10. Typically, FAO or glycolytic flux is reported as nmol/hr/µg protein. See **Note 6** for calculations.

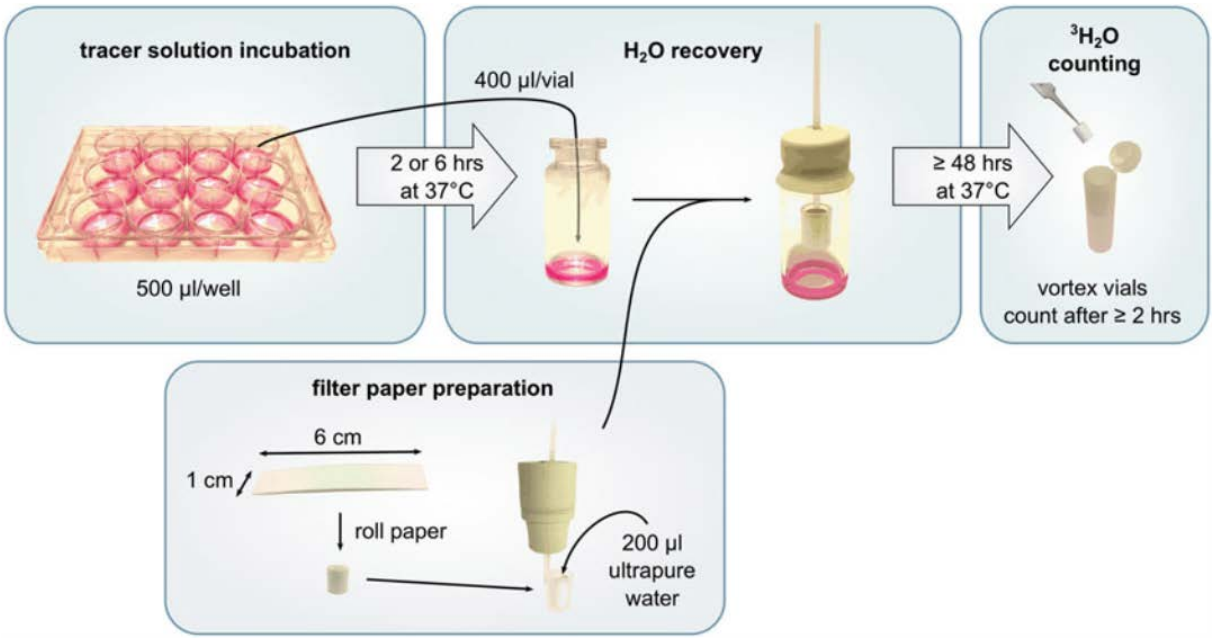

Figure 6. $^{3}H_2O$ recovery set-up (FAO/glycolysis). At the end of the tracer incubation period, 400 µL of 500 µL labeling solution is transferred from the 12-well plate to a glass vial. Once inserted inside the plastic hanging well, the filter paper is soaked with 200 µL ultrapure water. Next, the glass vial is closed with its rubber stopper and incubated at 37 C until equilibrium is reached (at least 48 h). Finally, the filter papers are transferred into scintillation vials containing scintillation cocktail and incubated at room temperature before counting

2.5.2. $^{14}CO_2$ Recovery for Glucose, Glutamine Oxidation, and oxPPP Measurement.

A schematic representation of this assay is depicted in **Figure 7**

1. Day 1: the day before the experiment, seed 150,000 endothelial cells per well in a staggered configuration (see **Note 7**) in a gelatin-coated 12-well plate.

2. Day 2: replace the culture medium with 500 µL labeling solution and incubate the cells for 6 h at 37 C. Likewise, add the same volume of labeling solution to empty wells of a 12-well plate for the determination of background signal.

3. Soak the filter papers (2.6 cm x 2.6 cm) in 1X hyamine solution.

4. At the end of the incubation period, add 100 µL of 12% perchloric acid to the labeling solution to lyse the cells, thereby releasing both labeled and unlabeled CO_2 (see **Note 8).** Close the well plate with the lid that contains hyamine-soaked papers on the inside to capture the CO_2. Alternatively, place the hyamine-soaked filter paper on the top of the well immediately after adding perchloric acid (**see Note 9**). Repeat this for each individual well. When all wells are covered with a filter paper, carefully put the lid on the top of the plate. Wrap the plate in parafilm to prevent the CO_2 from escaping from the wells and incubate overnight at room temperature (see **Note 10**).

5. Day 3: after overnight capturing of CO_2, transfer each filter paper to its corresponding scintillation vial containing 5 mL scintillation liquid.

6. Shake the vials thoroughly and allow the filter papers to disperse their radioactive material into the scintillation cocktail for at least 2 h and up to 16 h before counting.

7. Count the scintillation vials using the correct protocol, measuring the disintegrations per minute (dpm) of the ^{14}C label for at least 1 min per sample and calculate the flux rate after the necessary corrections (see **Note 11**).

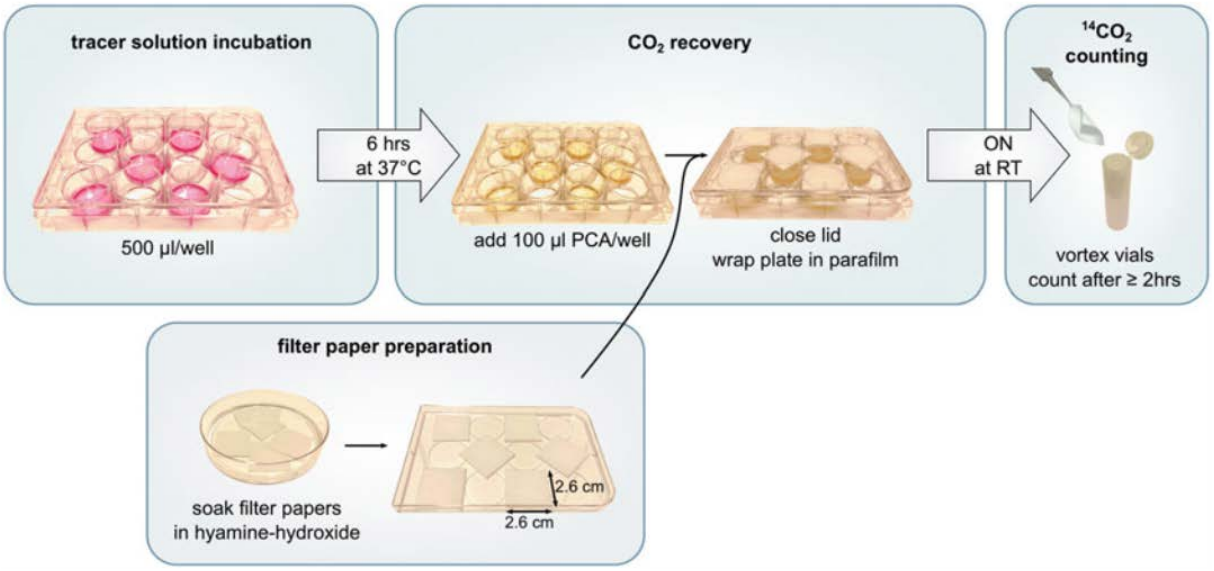

Figure 7. $^{14}CO_2$ recovery set-up (glucose oxidation/oxPPP/glutamine oxidation). Cells are seeded in a 12-well plate in a staggered configuration and are incubated with the labeling solution. After the addition of the strong acid, perchloric acid (PCA), every metabolic reaction is stopped and $^{14}CO_2$ is gradually released from the cells and medium. Thereafter, CO_2 is captured overnight by the hyamine-soaked papers upon closure of the well plate with its lid. These papers are either applied to the inside of the well plate lid as indicated here or are placed on the top of the well immediately after adding PCA. Finally, filter papers are transferred into scintillation vials containing scintillation cocktail and incubated at room temperature before counting

2.6. Notes

2.6.1. $^{3}H_2O$ Recovery for Fatty Acid β-Oxidation and Glycolysis Measurement

1. The assay can easily be scaled down to smaller well formats to lower cell numbers which allows the utilization of primary isolated ECs for flux assays. The volume of the labeling solution needs to be adjusted to the size of the well. When using lower cell numbers, researchers should consider increasing the labeling time to get more reliable results.

2. For FAO: in order to be able to calculate the FAO flux, the exact concentration of nonradioactive fatty acids (palmitate) has to be known. Since the precise concentration of fatty acids in the serum is usually not known, either serum-free or fatty acid-free medium has to be used.

3. Nonradioactive palmitate precipitates upon long-term storage in - 20 C. Make sure it is completely solubilized before adding it to the labeling solution.

4. Handle the glass vials gently, as any spillover of labeling solution onto the filter paper will lead to contamination of the ^{3}H2O signal with the labeled substrate tracer signal. For the same reason, avoid contact between the glass vial and the hanging well. Contamination with labeling medium is apparent by the presence of erroneously high values in the dataset.

5. Check national biosafety regulations concerning the proper disposal of radioactive waste. To remove any leftover radioactivity from the glass vials, aspirate the labeling solution and wash 3 times with tap water, before autoclaving the glass vials. Wash the rubber stoppers and hanging wells with a detergent and wash two times in tap water before leaving them out to air dry. It is important that the medium inside the glass vials is free of bacterial and fungal contaminations, to prevent organisms from metabolizing the substrate tracers to ^{3}H2O, which would give rise to flux overestimation.

6. Calculations: To report FAO or glycolytic flux as nmol/h/µg protein, we suggest running a BCA assay to determine protein content or correct the measurement by the number of cells. Also, since only a part of the total ^{3}H2O produced by the cells is captured in the filter paper, the measured dpm values only represent partial ^{3}H2O recovery and not the total ^{3}H2O-production. Therefore, a correction factor has to be applied in order to calculate total ^{3}H2O production. The percentage of ^{3}H2O-recovery can be easily determined through the use of a known amount of commercially available

^{3} H2O (e.g., 2 µCi/ mL culture medium). As long as all experimental conditions are kept identical, it is sufficient to calculate one correction factor for all future FAO or glycolysis experiments. However, since this factor is influenced by the amount of radioactive metabolite, equilibration time, incubation temperature, volume of the glass vial, and volume of the medium, a new correction factor needs to be developed and applied every time specific conditions are changed. Lastly, background signal is subtracted from corrected dpm values and the resulting net dpm values are converted to nmol substrate. Once the substrate concentration (nmol glucose or palmitate per µL) and the radioactivity concentration are known (dpm per µL; typically, duplicates of 2 µL and 4 µL from the labeling solution are measured by liquid scintillation counting), the specific activity (dpm/nmol) can be calculated for its use as a conversion factor.

2.6.2. $^{14}CO_2$ Recovery for Glucose, Glutamine Oxidation, and oxPPP Measurement

7. Cells are seeded in a staggered configuration to prevent possible cross-contamination of label from neighboring wells during the CO_2 capturing process.

8. Do not inhale radioactive $^{14}CO_2$; therefore, always work under the hood while performing $^{14}CO_2$ recovery experiments.

9. Because CO_2 rapidly dissipates when plates are removed from the incubator, both the addition of the strong acid and the placement of the hyamine-soaked paper on the top of the well have to be done fast. It is strongly advised to work plate by plate; this will minimize CO_2 loss and variability within the technical replicates.

10. Gently handle the plates, since direct contact between the radioactive medium and filter paper will contaminate the $^{14}CO_2$ signal with the labeled substrate tracer signal and will give rise to erroneous data.

11. Calculations: Experimentally, corrections factors have not been determined for $^{14}CO_2$ recovery. Therefore, this method is always a semiquantitative measure in which absolute oxidation rates (e.g., nmol/h) cannot be calculated. However, the dpm-values should be comparable between replicates, and relative between treatments, within an experiment. A parallel experiment should be run to correct for protein or DNA content; alternatively, number of cells can also be used.

3. Endothelial cells secrete GDF15 in a FOXO1 dependent manner

Running title: Vascular control of GDF15.

Abdiel Alvarado-Diaz[1], Moheb Ghobrial[1], Fateme Jaleh[3], Zheng Fan[1], Adhideb Ghosh[2], Guillermo Turiel[1], Evi Masschelein[1], Tatiane Gorski[1], Paola Gilardoni[1], and Katrien De Bock[1]

(1) Laboratory of Exercise and Health, Department Health Sciences and Technology, Swiss Federal Institute of Technology (ETH) Zürich, Zürich, 8603, Switzerland.; (2); Functional Genomics Center Zürich, Swiss Federal Institute of Technology, ETH/University of Zürich, Zürich, 8057, Switzerland.(3) ETH Alumni

Status: In preparation

Corresponding author:

Katrien De Bock

Laboratory of Exercise and Health

Institute of Movement Sciences (D-HEST)

ETH Zürich - Swiss Federal Institute of Technology

ETH Zürich, SLA C7

Schorenstrasse 16

CH-8603 Schwerzenbach

Switzerland

Tel. +41 44 655 7389

Email: Katrien-debock@ethz.ch

3.1. Abstract

Endothelial cells are important gatekeepers of organ homeostasis and metabolism. It has long been determined that impaired vascular function is associated with tissue dysregulation and metabolic disorders, but whether endothelial cells contribute to metabolic homeostasis beyond ensuring tissue perfusion is poorly described. Vascular expression of FOXO1, master regulator of endothelial quiescence, is often found to be upregulated in such pathological conditions. Using an unbiased proteomics approach to analyze the endothelial secretome, we found that endothelial cells secrete growth differentiation factor (GDF15). Moreover, FOXO1 activation reduced while inhibiting FOXO1 increased gdf15 expression. In vivo, endothelial specific deletion of GDF15 did not reduce circulating GDF15 levels. However, deletion of FOXO1 (Foxo1ΔEC) increased gdf15 expression (>4 fold) in endothelial cells isolated from different tissues and upregulated GDF15 in urine and serum. Furthermore, Foxo1ΔEC mice showed a significant decrease in food intake, suggesting that physiological changes in circulating GDF15 suffice to control food intake. This work identifies FOXO1 as a direct regulator of GDF15 in ECs and highlights the critical role of endothelial cells in whole body metabolic control

3.2. Authors contributions

The general content, perspective and supervision of this manuscript chapter was proposed by Prof. Dr. Katrien De Bock. The design, execution, and analysis of all the experiments, writing the full manuscript content, and creation of all figures was carried out by Abdiel Alvarado Diaz. Over the course of this project, several contributors have significantly supported its realization in forms of assistance during the execution and/or analysis of some experiments or figures. Moheb Ghobrial supported the isolation of primary mouse endothelial cells associated with figures 9 and 11, furthermore, he assisted in the design and formatting of all figures, and correction of manuscript. Dr. Fateme Jaleh supported the methodological approach, design, execution, and analysis of proteomic characterization of endothelial cell secretome associated with figure 8, additionally, she supported the qPCR screening that revealed GDF15 as a candidate of interest for this project and technically assisted with experiments associated with figure 10. Dr. Zheng Fan supported with valuable input in the design of the all the experiment, donated material such as lentiviral construct for ATF4 knockdown experiments associated with extended data figure 2 and proved valuable throughout the duration of this chapter. Dr. Adhideb Ghosh supported the bioinformatic proteomic analysis associated with figure 8 and extended data figure 1. Guillermo Turiel also supported the bioinformatic analysis associated with figure 8. Dr. Evi Masschelein, as our animal experimental specialist gave technical assistance to all the *in vivo* experiments associated to figures 9 and 11. Dr. Tatiane Gorski assisted technical support manipulating the cell sorter associated to figures 9 and 11. Dr. Paola Gilardoni provided technical assistance in the conduct of all experiments. The general supervision and correction of this manuscript was done by Abdiel Alvarado Diaz and Prof. Dr. Katrien De Bock.

3.3. Introduction

The physiological role of blood vessels goes beyond acting as simple blood conduits that passively regulate the distribution of blood throughout the entire organism. The endothelium can control tissue function and organ homeostasis, and this is particularly true for the regulation of tissue metabolic control (Graupera and Claret 2018, Pi, Xie et al. 2018, Hasan and Fischer 2021): blood vessels adapt oxygen and nutrient delivery to the metabolic requirements of the tissue by regulating of tissue perfusion via altering capillary recruitment or by forming of new blood vessels through angiogenesis. Moreover, endothelial cells can actively control the transport of nutrients, particularly lipids, from the blood to the parenchymal tissues. The signals that mediate this crosstalk between endothelial cells and their microenvironment are increasingly be studied but still remain poorly understood. For instance, the release of 3-hydroxybutyrate from skeletal muscle enhances endothelial lipid transport (Jang, Oh et al. 2016). On the other hand, endothelial cells also release angiocrine factors, such as nitric oxide (NO), which determines amongst others vascular tone (Pi, Xie et al. 2018). Another example is the secretion and deposition of laminins by islet ECs in the pancreas to stimulate β-cell proliferation and insulin production (Nikolova, Jabs et al. 2006).

Metabolic homeostasis and energy balance are dependent on a tightly orchestrated crosstalk between different highly vascularized metabolic tissues such as muscle, liver, adipose tissue and pancreas on one side, and nutrient intake on the other side. It is therefore not surprising that pathological processes in many of these tissues critically contribute to the development of metabolic disorders such as obesity. Endothelial dysfunction has been linked to metabolic diseases, and vascular complications are a major cause of morbidity and mortality in obese and diabetic patients (King, Aubert et al. 1998). Hyperlipidemia, hyperglycemia and other metabolic stressors result into endothelial dysfunction. However, emerging evidence indicates that endothelial cells do not solely act as passive responders to metabolic stress, but directly contribute to the development of metabolic disorders. For instance, obesity in high-fat diet fed mice (Nwadozi, Roudier et al. 2016) as well as in humans (Karki, Farb et al. 2015) has been associated with increased endothelial expression and activity of the transcription factor forkhead box O-1 (FOXO1), a master regulator of both quiescence and metabolism in endothelial cells (Wilhelm, Happel et al. 2016). Also, endothelial FOXO1 levels are higher in a mouse model of type I diabetes characterized by high glucose levels (Shi,

Fan et al. 2018). Interestingly, reducing endothelial FOXO1 can alleviate metabolic dysfunction and vascular dysfunction caused by obesity. Loss of endothelial FOXO1 reduced weight gain upon the intake of a high-fat diet and improved metabolic control (Rudnicki, Abdifarkosh et al. 2018). These metabolic alterations were attributed to enhanced vascular density in white adipose tissue combined with increased glycolytic activity of the endothelial cells. Moreover, FOXO1 inhibition improved impaired revascularization and wound closure in a mouse model for type 1 diabetes by improving endothelial function (Shi, Fan et al. 2018). However, whether FOXO1 also controls the expression of angiocrine signals that can modulate systemic metabolism and energy balance was not investigated.

Here, we used unbiased proteomics to identify angiocrine factors. We identify the growth and differentiation factor 15 (GDF15; also known as macrophage inhibitory cytokine-1) as one of the most abundantly secreted angiocrine factors. Administration of GDF15 has recently been proposed as an anti-obesity drug due to its ability to suppress appetite in mice and non-human primates (Mullican, Lin-Schmidt et al. 2017, Xiong, Walker et al. 2017). We show that endothelial deletion of *gdf15* does not affect circulating GDF15 levels and food intake under physiological conditions. However, we found that endothelial *gdf15* expression in a quiescent endothelium is repressed by FOXO1. Finally, deletion of FOXO1 in the endothelium enhances circulating GDF15 and reduces food intake. Our data suggest that the endothelium can control systemic metabolism through the modulation of food intake.

3.4. Results

3.4.1. Proteomic characterization of the endothelial secretome

To identify which proteins are secreted by ECs proteins, we decided to use E4ORF1$^+$ HUVECs (Seandel, Butler et al. 2008). Lentiviral introduction of *E4ORF1* in ECs allows the long-term survival and growth of ECs under serum free conditions, which allows the analysis of the secretome in the absence of cellular stress induced by serum starvation. We thus generated conditioned medium (CM) from E4ORF1$^+$ HUVECs cultured under serum free conditions and subjected it to proteomic analysis (**Figure 8A**). Non-conditioned (NC) medium was used as a control, this is, fresh medium that has not been in cultured in the presence of cells. Protein identification and quantification were performed using MaxQuant and Andromeda search engine (Cox and Mann 2008, Cox and Mann 2011, Cox, Neuhauser et al. 2011). In total, 818 proteins were detected during the analysis. Sample clustering clearly differentiated between CM and NC, implying a high correlation between the samples which enables the identification of relevant protein targets for further screening (**Figure 8B**). Furthermore, we found that 227 proteins were significantly upregulated and abundant in CM whereas 20 proteins were more abundant in NC (**Figure 8C**, **Supplemental table 1**). Out of the 227 proteins upregulated in CM, 116 proteins were uniquely found in CM (**Figure 8C**, black rectangle), which means that they were secreted by ECs and not detected in NC medium. Taking into consideration uniquely identified proteins, top 40 most abundant proteins are shown (**Extended data figure 1A**). Subsequently, we used the bioinformatic tools SignalP5 (http://www.cbs.dtu.dk/services/SignalP/), which identifies proteins with a signal peptide, and Secretome 2.0 (http://www.cbs.dtu.dk/services/SecretomeP/) which predicts non-classical protein secretion, to assemble a *bona fide* endothelial cell-secreted protein repository containing 113 proteins (**Figure 8D**). The remaining 114 proteins were mapped against the databases ExoCarta (Keerthikumar, Chisanga et al. 2016) and Vesiclepedia (Kalra, Simpson et al. 2012) to determine whether they have been reported as being secreted through non-classical pathways such as microvesicles and exosomes. Indeed, 105 proteins were overlapping with ExoCarta and 110 against vesiclepedia (**Figure 8D**). Finally, we performed cellular component categorization analysis using GSEA on all 227 proteins, yielding a total of 229 identifiers from which 226 were unambiguously mapped, which showed that main categories were related to vesicle, extracellular

space, membrane, and membrane enclosed lumen, confirming their secretory nature (**Figure 8E**).

Finally, to determine which proteins could exert angiocrine signaling to surrounding tissues, we focused on the proteins that were previously identified as ligands. We used the Cellphone DB repository of curated receptors, ligands, and their interactions to delimitate cell-to-cell interactions via factor secretion. From 227 predicted to have a signal peptide or undergo non-classical secretion, the list was reduced to 29 proteins that were identified either as ligands, extracellular matrix (ECM) proteins or receptors (**Figure 8F**). Of them, 16 proteins were known curated ligands (**Figure 8G**). Many of those have a known role in endothelial biology: For instance, thrombospondin 1 (TSP1) is a negative regulator of angiogenesis (Lawler and Lawler 2012) which is also involved platelet adherence to vasculature (Bonnefoy, Daenens et al. 2006). The secretion of matrix metalloproteases (MMPs) such as MMP2 by EC occurs via vesicle packaging and is stimulated by VEGFA (Taraboletti, D'Ascenzo et al. 2002). Also, Von Willebrand factor (VWF) plays a crucial role in hemostasis, inflammation, permeability and angiogenesis both inside and outside the EC (Jaffe, Hoyer et al. 1974, Randi, Smith et al. 2018). Activated ECs also release intercellular adhesion molecules (Videm and Albrigtsen 2008) which normally play a crucial role in leukocyte transendothelial migration. Finally, we decided to focus on growth and differentiation factor 15 (GDF15; also known as macrophage inhibitory cytokine-1).

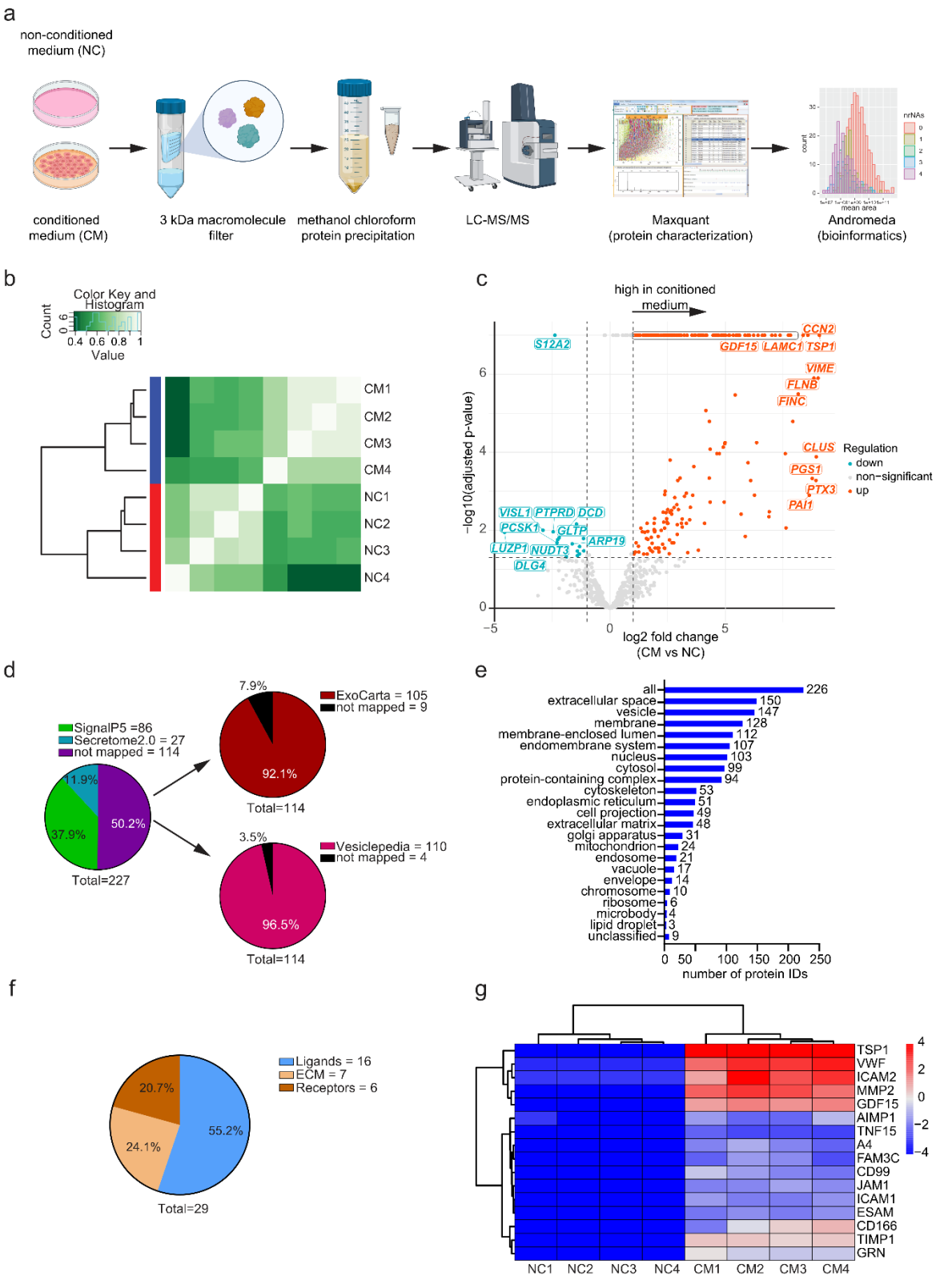
a
non-conditioned medium (NC)
conditioned medium (CM)
3 kDa macromolecule filter
methanol chloroform protein precipitation
LC-MS/MS
Maxquant (protein characterization)
Andromeda (bioinformatics)
b
Color Key and Histogram
Count
Value
CM1
CM2
CM3
CM4
NC1
NC2
NC3
NC4
c
high in conitioned medium
−log10(adjusted p-value)
log2 fold change (CM vs NC)
Regulation
down
non−significant
up
S12A2
CCN2
GDF15
LAMC1
TSP1
VIME
FLNB
FINC
CLUS
PGS1
PTX3
PAI1
VISL1
PTPRD
DCD
PCSK1
GLTP
ARP19
LUZP1
NUDT3
DLG4
d
SignalP5 =86
Secretome2.0 = 27
not mapped = 114
Total=227
ExoCarta = 105
not mapped = 9
Total=114
Vesiclepedia = 110
not mapped = 4
Total=114
e
all 226
extracellular space 150
vesicle 147
membrane 128
membrane-enclosed lumen 112
endomembrane system 107
nucleus 103
cytosol 99
protein-containing complex 94
cytoskeleton 53
endoplasmic reticulum 51
cell projection 49
extracellular matrix 48
golgi apparatus 31
mitochondrion 24
endosome 21
vacuole 17
envelope 14
chromosome 10
ribosome 6
microbody 4
lipid droplet 3
unclassified 9
number of protein IDs
f
Ligands = 16
ECM = 7
Receptors = 6
Total=29
g
TSP1
VWF
ICAM2
MMP2
GDF15
AIMP1
TNF15
A4
FAM3C
CD99
JAM1
ICAM1
ESAM
CD166
TIMP1
GRN
NC1 NC2 NC3 NC4 CM1 CM2 CM3 CM4

Figure 8. Workflow of generation and quantification of secretome of HUVECs produced in serum-free conditions **a.** Culturing conditions of E4ORF1 HUVECs, conditioned medium processing and LC-MS/MS workflow. **b.** Clustering depending on sample correlation and protein expression profile. Side colors on the left side of the heatmap indicate groupings. **c.** Volcano plot showing adjusted p- values computed from moderated t-test between all quantified proteins in conditioned media and non-conditioned control in endothelial secretome. Noted in a rectangle, all uniquely identified proteins in CM. **d.** Pie chart (left) shows overlap between proteins found in CM and proteins to be predicted for secretion either by the predicted presence of signal peptides or to undergo non-classical secretion. Pie charts (right) shows overlap between proteins not mapped to be secreted in endothelial secretome and proteins that have been identified in isolated vesicles (top) and exosomes (bottom), in the vesiclepedia and exocarta datasets respectively. **e.** Categorization of identified EC secreted proteins according to their cellular localization. **f**. Distribution of protein classes among those that have an interactor role according to Cellphone DB in endothelial secreted proteins. **g.** Heatmap of relative abundance determined by escalated expression in identified secreted ligand proteins according to Cellphone DB

3.4.2. Endothelial deletion of GDF15 does not contribute to circulating GDF15 under physiological conditions.

GDF15 is a stress responsive cytokine and a distant member of the transforming growth factor β superfamily (Bootcov, Bauskin et al. 1997, Tsai, Husaini et al. 2018). GDF15 signals through its receptor glial-derived neurotrophic factor receptor alpha-like (GFRAL), which is highly localized in brain areas which are involved in appetite control (Emmerson, Wang et al. 2017, Hsu, Crawley et al. 2017, Mullican, Lin-Schmidt et al. 2017, Yang, Chang et al. 2017). Due to its ability to suppress appetite in mice and non-human primates, pharmacological administration of GDF15 has been proposed as an anti-obesity drug (Mullican, Lin-Schmidt et al. 2017, Xiong, Walker et al. 2017). Under physiological conditions, *gdf15* is modestly expressed in many tissues and fairly high baseline circulating levels have been detected (Fairlie, Moore et al. 1999, Tsai, Husaini et al. 2018). In addition, *gdf15* can be induced in many tissues in response to specific stressors. Interestingly, some *in vitro* studies have suggested that ECs also efficiently upregulate *gdf15* in response to stressors such as high glucose (Li, Yang et al. 2013) or during senescence (Ha, De Torres et al. 2019), but a contribution of ECs to GDF15 physiology *in vivo* has not been shown. We first confirmed using an ELISA that on low passage WT HUVECs cultured under angiogenic conditions secrete GDF15 (**Extended data figure 1B**). To investigate the *in vivo* relevance of endothelial GDF15 secretion, we subsequently decided to generate endothelial specific *gdf15* knock-out mice. To do so, we intercrossed *gdf15*$^{Lox/Lox}$ mice with a tamoxifen-inducible endothelial specific *pdgfb-Cre*^{ERT2} (Claxton, Kostourou et al. 2008), leading to the generation of *gdf15*$^{\Delta EC}$ mice (**Figure 9A**). Despite efficient deletion of *gdf15* mRNA levels in ECs isolated from different organs (muscle, white adipose tissue, heart), with an average approximate efficiency of 80% (**Figure 9E, F, G**), we did not observe altered GDF15 levels in the blood of *gdf15*$^{\Delta EC}$ mice (**Figure 9B**). Moreover, food intake was not affected by loss of endothelial *gdf15* (**Figure 9C**). Interestingly, upon lipopolysaccharide stimulation, but not metformin, circulating GDF15 is decreased in *gdf15*$^{\Delta EC}$ mice compared to controls (**Figure 9D**) Altogether, this data indicates that under basal physiological conditions, endothelial cells do not contribute to the maintenance of basal circulating GDF15 levels, but rather contribute in LPS inflammatory response (Luan, Wang et al. 2019).

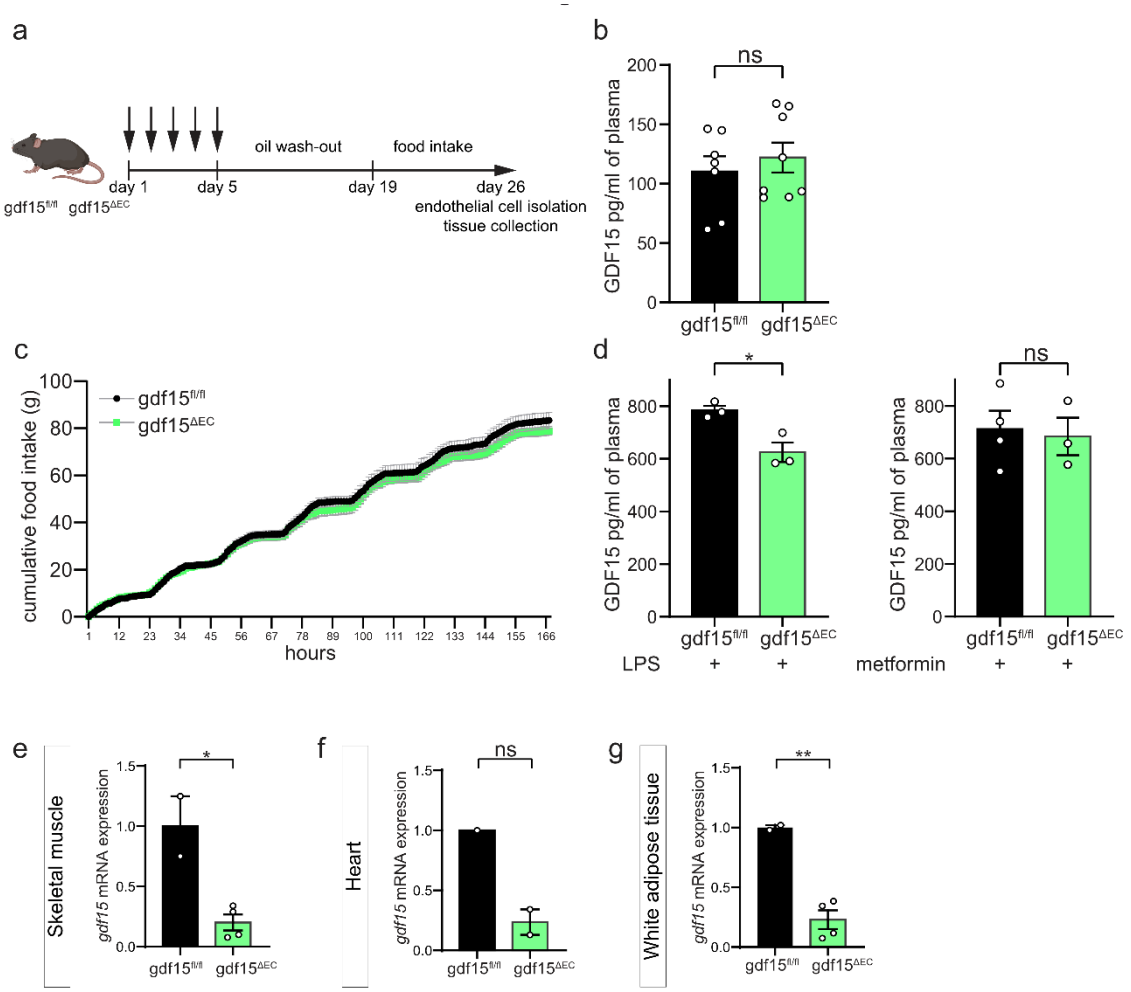

Figure 9. Angiocrine GDF15 does not significantly contribute to circulating levels in basal conditions, only contributes in inflammatory response**. a.** Schematic of tamoxifen injection in *gdf15$^{\Delta EC}$*. **b.** GDF15 ELISA from plasma in *gdf15$^{\Delta EC}$* (n= 8) mice or controls (n= 7) (Student-*t* test). **c.** Cumulative food intake over 7 days, 167 h, in *gdf15$^{\Delta EC}$* (n= 7) mice or controls (n= 6). (Two-way ANOVA and Sidak's multiple comparison). **d.** GDF15 ELISA after inflammatory challenge with LPS, blood was sampled 2 h after in in *gdf15$^{\Delta EC}$* (n= 3) mice or controls (n= 3) (Student-*t* test). and GDF15 ELISA after metformin administration 600 mg/kg body weight, blood was sampled 6 h after in *gdf15$^{\Delta EC}$* (n= 3) mice or controls (n= 4) (Student-*t* test). Knockdown efficiency in *gdf15$^{\Delta EC}$* compared to controls in freshly isolated endothelial cells from **e** skeletal muscle (controls, n= 2; *gdf15$^{\Delta EC}$* n= 4), **f** heart (controls, n= 1; *gdf15$^{\Delta EC}$* n= 2), **g**, or white adipose tissue (controls, n= 2; *gdf15$^{\Delta EC}$* n= 4). Housekeeping gene 18S was used as control for figure panels **e**, **f**, **g**. Significant values are represented in asterisks as follows *P<0.05, **P<0.01, ***P<0.001, and ****P<0.0001.

3.4.3. Endothelial cells control GDF15 in a FOXO1 dependent manner

To further understand the mechanisms that might control GDF15 release from ECs, we decided to evaluate whether GDF15 is controlled by NOTCH1 and/or Forkhead Box O1 (FOXO1). Both FOXO1 as well as NOTCH are essential regulators of endothelial quiescence and vascular homeostasis (Wilhelm, Happel et al. 2016, Kalucka, Bierhansl et al. 2018). Moreover, increasing evidence also suggests that deregulated FOXO1 and NOTCH1 contribute to endothelial dysfunction during obesity. FOXO1 protein levels are increased in capillary ECs from mice on a high-fat diet (Nwadozi, Roudier et al. 2016) and removing FOXO1 from ECs during high-fat diet prevents the development of insulin resistance (Rudnicki, Abdifarkosh et al. 2018). NOTCH1 activity is also increased in diabetic vessels (Miloudi, Oubaha et al. 2019) and sustained genetic activation of Notch signaling lowers insulin sensitivity (Hasan, Jabs et al. 2020). On the other hand, inhibiting NOTCH1 impairs fatty acid transport into the heart (Jabs, Rose et al. 2018) Whether endothelial FOXO1 or NOTCH1 can control the release of angiocrine factors involved in metabolic control, such as GDF15, is not known.

To address whether NOTCH1 controls *GDF15* expression, we activated NOTCH1 by culturing HUVECs in the presence of the Notch ligand DLL4. DLL4 treatment activated NOTCH1, since the expression of canonical downstream targets such as *HES1, HEY1/2,* and *NRARP* was increased, but NOTCH1 activation did not affect *GDF15* expression (**Figure 10A**). Also, inhibition of NOTCH signaling using the gamma-secretase inhibitor DAPT reduced the expression of NOTCH1 targets but did not affect *GDF15* (**Figure 10B**). Second, we also tested whether FOXO1 controls *GDF15*. To do so, we transduced ECs with a Tet-On constitutively active FOXO1A3 expression construct ($FOXO1^{CA}$)(Potente, Urbich et al. 2005). RT-qPCR quantification of FOXO1 downstream genes *MXI1*, *PDK1*, *PDK4*, *CD36* and *ANG2* confirmed activation of FOXO1 in ECs upon doxycycline treatment (**Figure 10C**). Furthermore, we found that $FOXO1^{CA}$ lowered *GDF15* mRNA content in ECs (**Figure 10C**). As a result, $FOXO1^{CA}$ also lowered the secretion of GDF15 into the cell culture medium (**Figure 10D**). We confirmed the regulation of *GDF15* gene expression in $E4ORF1^{+}$ HUVECs (**Figure 10E**). The decrease in *GDF15* in those cells was dose-dependent since increasing doxycycline concentrations further lowered *GDF15* (**Extended data figure 2A**). Subsequently, we also assessed whether inhibition of FOXO1 in ECs would lead to an increased expression and release of GDF15. Inhibition of FOXO1 using the specific

inhibitor AS1842856 (Nagashima, Shigematsu et al. 2010) increased *GDF15* expression (**Figure 10F**) and increased the accumulation of GDF15 in cell culture media (**Figure 10G**). The altered secretion of GDF15 was not secondary to alterations in EC proliferation in response to FOXO1 modulation since treatment with the proliferation inhibitor mitomycin C also resulted into reduced GDF15 secretion upon $FOXO1^{CA}$ versus increased GDF15 upon FOXO1 pharmacological inhibition (**Extended data figure 3A B**).. Recently it has shown been shown that FOXO1 inhibition increases ATF4 expression in immune cells (Vallejo-Gracia, Chen et al. 2020). In turn, ATF4 has been reported to be a metabolic rheostat of nutritional stress that ultimately drives the expression of GDF15 in mice and humans (Patel, Alvarez-Guaita et al. 2019). Therefore, we tested whether GDF15 upregulation upon FOXO1 pharmacological inhibition is dependent on ATF4 and thus indirect. Despite that treatment with AS1842856 increased ATF4 expression as previously reported **Extended data figure 2B**). Efficient knockdown of ATF4 did not blunt GDF15 upregulation upon FOXO1 blockade (**Extended data figure 2CD**). Thus, ECs control GDF15 secretion in a FOXO1 dependent manner and independent of ATF4.

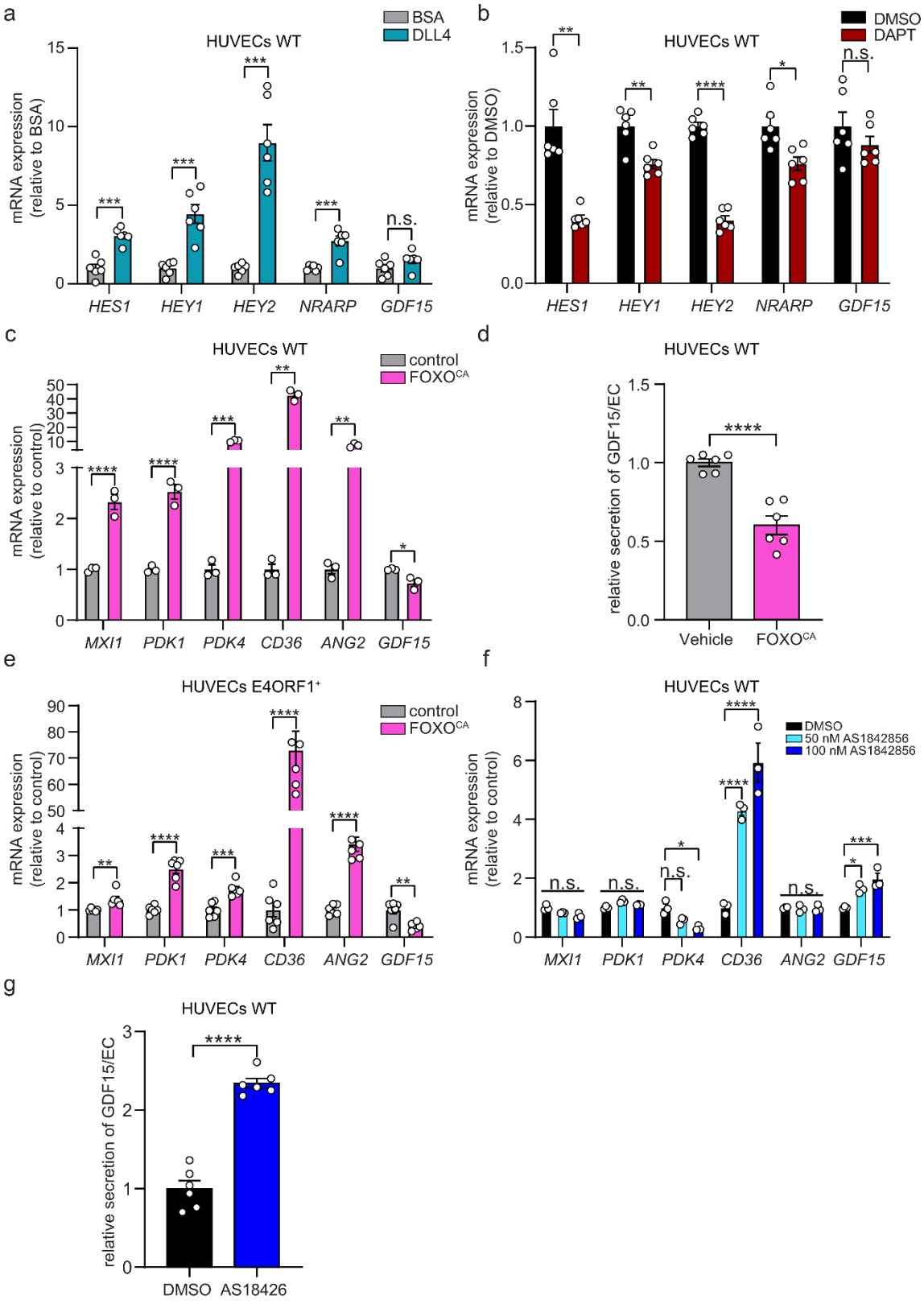
a
HUVECs WT
BSA
DLL4
mRNA expression (relative to BSA)
HES1
HEY1
HEY2
NRARP
GDF15
n.s.
b
HUVECs WT
DMSO
DAPT
mRNA expression (relative to DMSO)
n.s.
c
HUVECs WT
control
FOXOCA
mRNA expression (relative to control)
MXI1
PDK1
PDK4
CD36
ANG2
GDF15
d
HUVECs WT
relative secretion of GDF15/EC
Vehicle
FOXOCA
e
HUVECs E4ORF1+
control
FOXOCA
mRNA expression (relative to control)
f
HUVECs WT
DMSO
50 nM AS1842856
100 nM AS1842856
mRNA expression (relative to control)
n.s.
g
HUVECs WT
relative secretion of GDF15/EC
DMSO
AS18426

Figure 10 FOXO1 negatively regulates GDF15 expression in E4ORF1^{+} and WT HUVECs**. a.** Gene expression analysis of NOTCH1 target genes (*HES1, HEY1, HEY2* and *NRARP*) and *GDF15* upon stimulation with notch ligand, DLL4 or vehicle (0.02% BSA), over 24 h in HUVECs. DLL4 did not regulate *GDF15* expression (n= 6) (Student-t test). **b.** Gene expression analysis of NOTCH1 target genes (*HES1, HEY1, HEY2* and *NRARP)* and *GDF15* upon treatment with gamma-secretase inhibitor, DAPT 10 µM, over 24 h in HUVECs (n= 6). DAPT did not regulate *GDF15* expression (Student-t test). **c.** Gene expression analysis of FOXO1 target genes (*MXI1,PDK1, PDK4, CD36, ANG2*) and *GDF15*, 3hrs after induction of FOXO1^{CA} with 200 ng/ml doxycycline in Tet-On FOXO1^{CA} HUVECs (n=3).(Student-t test) **d.** Secretion of GDF15 in cell culture supernatants 48h after induction of FOXO1^{CA} with 200 ng/ml doxycycline in Tet-On FOXO1^{CA} HUVECs (n=6) (Student-t test). **e.** Gene expression analysis of FOXO1 target genes (*MXI1, PDK1, PDK4, CD36, ANG2*) and *GDF15* 24 h after induction of FOXO1^{CA} with 200 ng/ml doxycycline in Tet-On FOXO1^{CA} E4ORF1^{+} HUVECs in serum free conditions (n=6) (Student-t test). **f.** Gene expression analysis of FOXO1 target genes (*MXI1, PDK1, PDK4, CD36, ANG2*) and *GDF15*, 24 hrs. after treatment with pharmacological FOXO1 inhibitor, AS1842856 in HUVECs (n=3) (Two-way ANOVA and Dunnet multiple comparison. **g.** Secretion of GDF15 in cell culture supernatants 48h after treatment with pharmacological FOXO1 inhibitor, AS1842856 in HUVECs (n=6) (Student-t test). Housekeeping gene *ACTB* was used as control for figure panels **a**, **b**, **c**, **e**, **f**. Significant values are represented in asterisks as follows *P<0.05, **P<0.01, ***P<0.001, and ****P<0.0001

3.4.4. Endothelial deletion of FOXO1 leads to increased circulating GDF15

Since FOXO1 is active in a quiescent endothelium, the expression and release of GDF15 under homeostatic conditions is expected to be low. To study whether endothelial FOXO1 contributes to the regulation of circulating GDF15, we subsequently decided to use an inducible endothelial-specific FOXO1 knock-out mice *foxo1*$^{\Delta EC}$ which have been generated previously (Wilhelm, Happel et al. 2016)(**Figure 11A**). Three weeks after the tamoxifen treatment, whole tissue expression analysis of *GDF15* reveled a significant upregulation in skeletal muscle, white adipose tissue and heart. To elucidate EC contribution in those capillary beds, ECs from different tissue beds were isolated for analysis, including the kidney, this to understand whether this is a regional or rather a general regulation. Consistent with previous observations (Rudnicki, Abdifarkosh et al. 2018), we found that *foxo1* mRNA levels were efficiently downregulated in ECs isolated from skeletal muscle, white adipose tissue, kidney and heart (**Figure 11F H J L**). Reduction of *foxo1* coincided with an approximate 4-fold increase in *gdf15* expression in those ECs **Figure 11E G I K**). To test whether increased endothelial *gdf15* expression could affect circulating GDF15 levels, we analyzed serum as well as urine GDF15 which confirmed that circulating GDF15 levels were increased upon endothelial *foxo1* deletion (**Figure 11B**).

Since pharmacological GDF15 delivery, leading to higher increases in GDF15 levels, has been shown to reduce food intake (Emmerson, Wang et al. 2017, Mullican, Lin-Schmidt et al. 2017), we subsequently wondered whether small increments in circulating GDF15 are able to repress food intake in *foxo1*$^{\Delta EC}$ mice. Indeed, we found that endothelial deletion of *gdf15* sufficed to reduce food intake by approximately 22.7% **(Figure 11C)** without affecting body weight **(Figure 11M)** nor energy expenditure **(Figure 11N)**

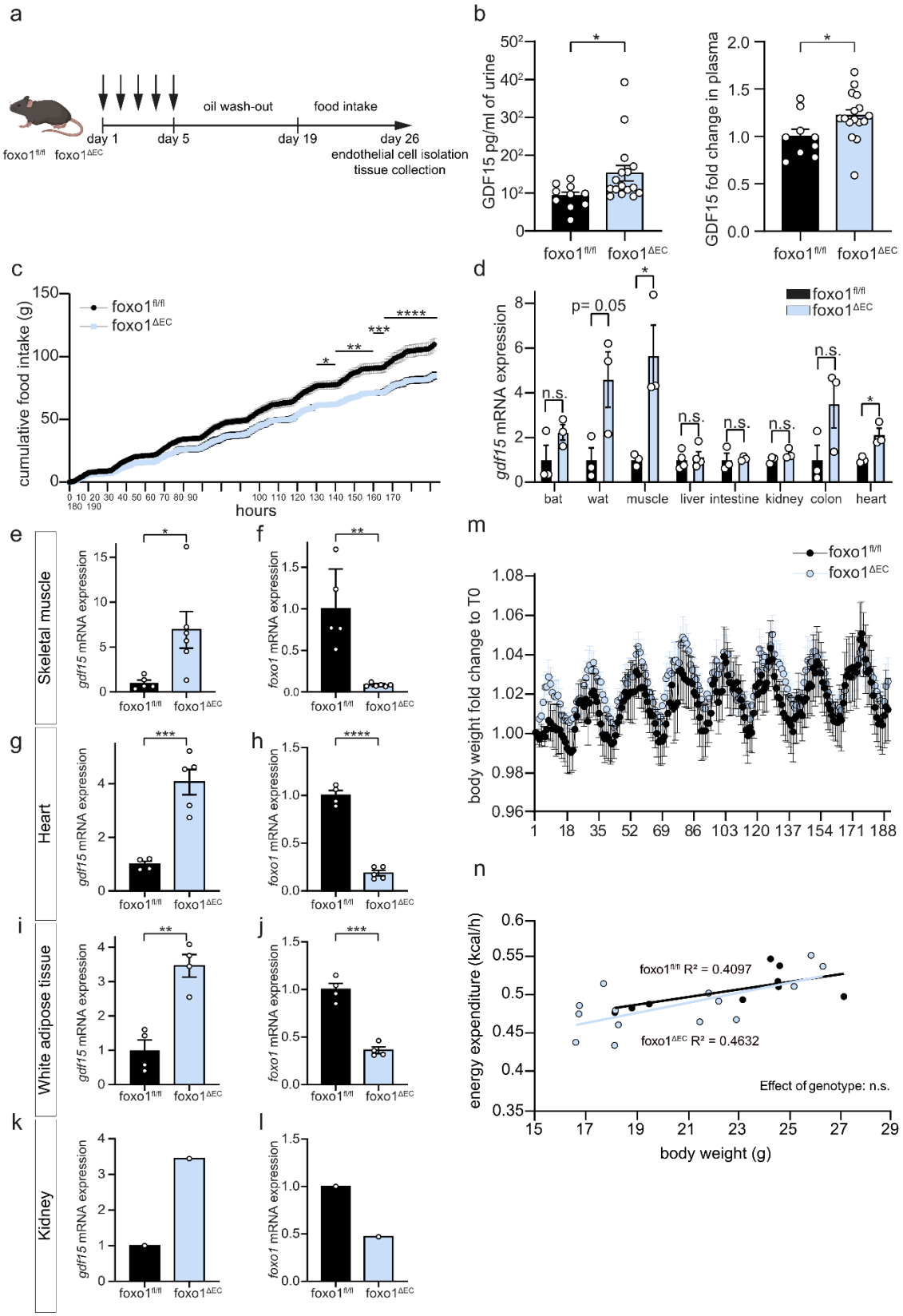
a
oil wash-out
food intake
day 1
day 5
day 19
day 26
endothelial cell isolation
tissue collection
foxo1fl/fl
foxo1ΔEC
b
GDF15 pg/ml of urine
GDF15 fold change in plasma
c
cumulative food intake (g)
hours
d
gdf15 mRNA expression
p= 0.05
n.s.
bat
wat
muscle
liver
intestine
kidney
colon
heart
e
Skeletal muscle
f
g
Heart
h
i
White adipose tissue
j
k
Kidney
l
gdf15 mRNA expression
foxo1 mRNA expression
m
body weight fold change to T0
n
energy expenditure (kcal/h)
body weight (g)
foxo1fl/fl R² = 0.4097
foxo1ΔEC R² = 0.4632
Effect of genotype: n.s.

Figure 11 GDF15 is upregulated in foxo1$^{\Delta EC}$ mice and is associated with a decrease in food intake. **a.** Schematic of conditional deletion of FOXO1 in vascular endothelium, foxo1$^{fl/fl}$ mice were crossed with tamoxifen-inducible endothelial specific pdgfb-CreERT2 mice. Tamoxifen was administered once daily for 5 consecutive days. Tissues and/or endothelial cell isolation occurred at least 14 days after last tamoxifen dose. **b.** Urine concentrations of GDF15 in control foxo1$^{fl/fl}$ (n= 10) compared to foxo1$^{\Delta EC}$ mice (n= 16). Urine was collected at the beginning of dark cycle. Plasma concentrations of GDF15 in control foxo1$^{fl/fl}$ (n=9) compared to foxo1$^{\Delta EC}$ mice (n=16). .(Student-*t* test). **c.** Cumulative food intake in chow fed of control foxo1$^{fl/fl}$ (n= 9) compared to foxo1$^{\Delta EC}$ mice (n= 14). Measurement was done 14 days after last tamoxifen administration and over 8 days (190 h)(Two-way ANOVA and Sidak's multiple comparison). **d**. *gdf15* mRNA expression was measured in whole tissue lysates in brown adipose tissue (BAT), white adipose tissue (WAT), skeletal muscle, liver, intestine, kidney, colon and heart in control foxo1$^{fl/fl}$ (n= 3) compared to foxo1$^{\Delta EC}$ mice (n= 3).(Student-*t* test). **e.** *gdf15* mRNA expression in freshly isolated endothelial cells from skeletal muscle in control foxo1$^{fl/fl}$ (n=5) compared to foxo1$^{\Delta EC}$ mice (n=6). .(Student-*t* test) **f.** *foxo1* mRNA expression in freshly isolated endothelial cells from skeletal muscle in control foxo1$^{fl/fl}$ (n=5) compared to foxo1$^{\Delta EC}$ mice (n=6).(Student-*t* test) **g.** *gdf15* mRNA expression in freshly isolated endothelial cells from heart tissue in control foxo1$^{fl/fl}$ (n= 4) compared to foxo1$^{\Delta EC}$ mice (n= 5). .(Student-*t* test) **h.** *foxo1* mRNA expression in freshly isolated endothelial cells from heart tissue in control foxo1$^{fl/fl}$ (n= 4) compared to foxo1$^{\Delta EC}$ mice (n= 5) .(Student-*t* test) **i.** *gdf15* mRNA expression in freshly isolated endothelial cells from white adipose tissue in control foxo1$^{fl/fl}$ (n= 4) compared to foxo1$^{\Delta EC}$ mice (n= 4). .(Student-*t* test) **j**. *foxo1* mRNA expression in freshly isolated endothelial cells from white adipose tissue in control foxo1$^{fl/fl}$ (n= 4) compared to foxo1$^{\Delta EC}$ mice (n= 4) .(Student-*t* test). **k.** *gdf15* mRNA expression in freshly isolated endothelial cells from kidney tissue in control foxo1$^{fl/fl}$ (n= 1) compared to foxo1$^{\Delta EC}$ mice (n= 1). **l.** *foxo1* mRNA expression in freshly isolated endothelial cells from kidney tissue in control foxo1$^{fl/fl}$ (n= 3) compared to foxo1$^{\Delta EC}$ mice (n=3). Housekeeping gene 18S was used as control for figure panels from **d** to **l**. **m.** Body mass of control foxo1$^{fl/fl}$ (n= 9) compared to foxo1$^{\Delta EC}$ mice (n= 14). Measurement was done 14 days after last tamoxifen administration and over 8 days (190 h). (Two-way ANOVA and Sidak's multiple comparison) was done **n.** energy expenditure against body weight is shown for *foxo1*$^{\Delta EC}$ mice (n= 14) or controls (n= 9). (One way ANCOVA). Significant values are represented in asterisks as follows *P<0.05, **P<0.01, ***P<0.001, and ****P<0.0001.

3.5. Discussion.

In this paper, we performed unbiased proteomic characterization to identify angiocrine factors that might be involved in tissue metabolic control. To do so, we decided to analyze the secretome of HUVECs expressing the adenoviral protein E4ORF1, which enables EC growth and survival in the absence of serum, growth factors and cytokines (Seandel, Butler et al. 2008). Using this approach, we identified 227 secreted proteins, many of which have previously been validated to be secreted by endothelial cells. Moreover, there was significant overlap between our data and a previously published one where a labeled amino acid approach was used (Burghoff and Schrader 2011). The latter approach revealed 78 secreted proteins, more than half of them, including GDF15, also showed up in our analysis.

We found that ECs secrete significant amounts of GDF15 under proliferating conditions. Moreover, *GDF15* expression was negatively controlled by FOXO1, a known negative regulator of endothelial proliferation through the repression of c-Myc (Wilhelm, Happel et al. 2016). Activation of FOXO1 reduced GDF15 whereas inhibition of FOXO1 increased GDF15. This effect was not caused by changes in proliferation since treating HUVECs with mitomycin C did not affect FOXO1 mediated alterations in GDF15. Furthermore, we assessed the *in vivo* effect of FOXO1 deletion on GDF15 levels less than two weeks after inducing *foxo1* gene deletion. It is unlikely that significant endothelial proliferation occurred at that point. In fact, despite the critical role for FOXO1 in controlling endothelial proliferation during developmental angiogenesis, endothelial specific deletion of FOXO1 does not induce widespread endothelial proliferation (Rudnicki, Abdifarkosh et al. 2018), likely due to redundancy with other FOXO family members (Paik, Kollipara et al. 2007). An increase in vascular density in *foxo1*$^{\Delta EC}$ mice has only been observed in white adipose tissue 16 weeks after recombination. Thus, FOXO1-mediated regulation of GDF15 is proliferation-independent.

It is unclear how FOXO1 controls *gdf15* expression. Among other alternative regulatory pathways, the integrated stress response instructs the upregulation of GDF15 in response to nutritional stress via ATF4/CHOP signaling upon an obesogenic diet (Patel, Alvarez-Guaita et al. 2019). This cellular stress response is replicated upon metformin stimulation (Day, Ford et al. 2019, Coll, Chen et al. 2020). FOXO1 has also been recognized as nutrient sensor (Dong, Copps et al. 2008, Banks, Kim-Muller et al.

2011, Barbato, Tatulli et al. 2013), in which decreased transcriptional activity promotes energy balance and nutrient homeostasis, while increased activity drives maladjustments to nutrient intake and endocrine regulation. The fact that FOXO1 inhibition secretes a nutritional signal to drive energy balance extends the idea that secreted proteins and cytokines, such as GDF15, will continue driving these beneficial effects to whole body through paracrine secretion. We evaluated whether the activity of these aforementioned nutrient sensors were intertwined to mechanistically drive the expression of GDF15 in FOXO1-abrogated endothelial cells, as both, their synergistic interaction (Rached, Kode et al. 2010, Kode, Mosialou et al. 2012, Kode, Mosialou et al. 2012), and negative regulation has been previously described (Wang, Zhou et al. 2014, Chen, Gong et al. 2019, Ma, Su et al. 2020, Vallejo-Gracia, Chen et al. 2020). Despite that pharmacological blockade of FOXO1 upregulates the expression of ATF4, an instructing signal in integrated stress response, ISR, an ATF4 knockdown with a short hairpin did not blunted the upregulation of *GDF15* upon FOXO1 inhibition, which further sustains ATF4 independent mechanisms. Finally, whether the repressor activity is driven by previously described nuclear proteins remains to be elucidated (Nakae, Cao et al. 2012, Langlet, Haeusler et al. 2017). All in all, this evidence suggests that FOXO1 represses expression of GDF15 by directly binding to FOXO1 binding elements in GDF15 promoter and its interaction is independent of ATF4 activity/ signaling.

To address the *in vivo* relevance of GDF15 secretion by ECs, we generated endothelial specific *gdf15* knock out mice. Removing *gdf15* from the endothelium however did not affect GDF15 levels. This is not surprising, since FOXO1 is active in a quiescent endothelium and thus should keep *gdf15* expression relatively low under physiological conditions. In contrast, deleting endothelial FOXO1 unleashed *gdf15* resulting into a more than 4-fold upregulation of its gene expression in ECs which sufficed to induce a modest but significant increase in circulating GDF15. Even more, the increase in GDF15 decreased food intake in these mice, underscoring the physiological relevance of our observations. There has been considerable debate about the physiological role of endogenous GDF15 on energy homeostasis in response to different stressors. For instance, vigorous endurance exercise leads to a 4-5 fold increase GDF15 without affecting food intake (Klein, Nicolaisen et al. 2021). On the other hand, similar increases in GDF15 induced by metformin treatment sufficed to reduce food intake and affect energy balance (Day, Ford et al. 2019, Coll, Chen et al. 2020). We found that

upon endothelial deletion, small changes in GDF15 suffice to affect food intake. Our genetic data suggest that even small differences in GDF15 production are enough to sustain a measurable amount of food aversion.

To the best of our knowledge, we could not find any reference discussing the potential contribution of the endothelium to circulating GDF15 levels. In many tissues, the endothelial volume only is a fraction of the total tissue volume. Nonetheless, the total mass of endothelial cells in an adult human body is significant and the localization of the endothelium, as the direct interface between nutrient delivery and nutrient consumption, render it perfectly suited to play a significant role in the regulation of energy balance. Future research needs to unravel the contribution of endothelial cells to whole body metabolic control and energy balance.

In conclusion, we found that endothelial cells are a significant source of GDF15, a main regulator of energy balance and food intake. While endothelial GDF15 does not contribute to circulating GDF15 under physiological conditions, deleting FOXO1 unleashes endothelial *gdf15* expression, leading to increased circulating GDF15 levels and reduced food intake. Our data suggest that endothelial cells can contribute to the control of energy balance.

3.6. Acknowledgments

We thank the Functional Genomics Center Zürich for technical support. This project was funded by the European Research Council (ERC) Starting Grant (716140) to KDB. AAD is supported by a PhD fellowship from the National Research and Technology Council of Mexico (CONACyT). KDB is endowed by the Schulthess Foundation.

3.7. Methods

Mice

Wildtype C57BL/6J mice were obtained from The Jackson Laboratory (000664 | B6). Endothelial specific GDF15$^{\Delta EC}$ mice were generated by crossing *gdf15$^{loxP/loxP}$* mice (obtained from Randy Seeley, University of Michigan, USA) with *pdgfb-Cre^{ERT2}* mice, an EC-selective tamoxifen inducible Cre-driver line (Claxton, Kostourou et al. 2008). *Foxo1*$^{\Delta EC}$ mice were generated by crossing *foxo1$^{loxP/loxP}$* mice (*Foxo1$^{tm1Rdp/J}$),* with *pdgfb-Cre^{ERT2}* mice. *Foxo1*$^{\Delta EC}$ and *gdf15*$^{\Delta EC}$ were used in C57BL/6 background. Recombination was induced in 8-12 weeks old mice by daily intraperitoneal administration of 1mg tamoxifen (T5648, Sigma-Aldrich) dissolved in 1:10 ethanol: corn oil solution for 5 consecutive days. A wash out period of at least 14 days was allowed before starting the experiments. Tamoxifen-treated Cre-negative littermates were used as control for all experiments. GDF15 blocking antibody and IgG control (against the non-mammalian protein ANTP) were a kind gift from Sebastian Beck Jørgensen (NovoNordisk A/S). Mice were injected intraperitoneally with 10 mg/ kg of body weight at the beginning of dark cycle every 7 days. Metformin (D150959, Sigma Aldrich) was administered diluted in water with a dosing of 600 mg/kg body weight via oral gavage. Thereafter, food was removed for 6h until blood sampling through a small cut in tail vein. Lipopolysaccharides (LPS - 10 mg/ kg of body weight) from *E. coli* O55:B5 (L6529, Sigma-Aldrich) administered intraperitoneally as described previously (Luan, Wang et al. 2019) and mice were euthanized 2 h later. Blood was sampled by cardiac puncture in heparinized tubes.

For metabolic measurements, *foxo1$^{\Delta EC}$* and *gdf15$^{\Delta EC}$* mice were acclimatized to single caging over 24h and put in metabolic cages thereafter (Promethion Cages, Sable Systems International). Food intake, water intake, spontaneous locomotor activity, oxygen (VO_2) consumption and carbon dioxide production (VCO_2), respiratory exchange ratio (RER) and energy expenditure were measured over 7 days.

Mice were randomly allocated to different treatment groups, and the investigator was blinded to the group allocation during the experiment as well as during the analysis. All mice were housed at standard housing conditions (22 °C, 12 h inverted light/dark cycle), with ad libitum access to chow diet (18 % proteins, 4.5 % fibers, 4.5 % fat, 6.3

% ashes, Provimi Kliba SA) and water. Health status of all mouse lines was regularly monitored according to FELASA guidelines. Animal experiments were approved by the local animal ethics committee (Kantonales Veterinärsamt Zürich, licenses ZH014/2016 and ZH211/2019), and performed according to local guidelines (TschV, Zurich) and the Swiss animal protection law (TschG). All mice used in this study were between 8-12 weeks old. Both male and female mice were included in the study.

Isolation of primary mouse endothelial cells (ECs)

Primary ECs from skeletal muscle, white adipose tissue, heart and kidney were isolated from adult *foxo1*$^{\Delta EC}$ mice as well as from *gdf15*$^{\Delta EC}$ and their respective WT littermates 14 days after the first tamoxifen injection. Mice were anesthetized using 117 mg/kg body weight ketamine and 13 mg/kg body weight xylazine. Skeletal muscle from both hind limbs, white adipose tissue, heart and kidney were dissected and put immediately on a dish at 4ºC and finely minced with surgical scalpels. Thereafter, the mashed muscle was enzymatically digested in digestion buffer containing 2 mg/ml Dispase II (D4693, Sigma-Aldrich, Steinheim, Germany), 2 mg/ml Collagenase IV (17104019, Thermo Fisher Scientific, Zurich, Switzerland), 2 mM $CaCl_2$ and 2% BSA in PBS at 37°C for 20 min under continuous gentle shaking. The digestion reaction was stopped by mixing with an equal volume of cold Hank's Balanced Salt Solution (Thermo Fisher 14025-050) containing 10% FBS. The suspension was filtered through a 70 µm cell strainer (#431751, Corning, New York, USA) to remove large cell debris. Cells were centrifuged 500 RCF for 5 min at 4º C. Supernatant was subsequently discarded, while the cell pellets were resuspended in 1 ml hemolytic buffer (NH_4Cl 154 mM, $KHCO_3$ 10 mM and EDTA 0.1 mM pH 7.35) at room temperature for 3 minutes. To stop the reaction, 30 mL of ice-cold PBS was added to the mixture and centrifuged at 500 RCF for 5 min at 4ºC. The cell pellets were resuspended in FACS buffer (PBS + 1% Bovine Serum Albumin) containing anti-CD31 PE conjugated antibody in a concentration of 1:200 (BD Pharmigen 553373) and anti-CD45 PerCP conjugated antibody in a concentration of 1:200 (BD Pharmigen 557235) for 30 min at 4º C, protected from light. Thereafter the cells were washed with 1ml of FACS buffer, centrifuged in a tabletop centrifuge (CAT number) at 500 RCF at 4º C for 5 min. Finally, the cell pellets were resuspend in 1 ml of FACS buffer (PBS + 1% Bovine Serum Albumin) and the suspension was passed through a 35 µm cell strainer of a FACS

sorting tube (352235, Corning). Immediately before sorting, SYTOX^{TM} blue was added in 1:1000 (Thermo Fisher, S34857) to exclude dead cells from further analysis. Viable endothelial cells (CD31^{+}, CD45^{-}, SYTOX^{TM} blue^{-}) were sorted by a FACS Aria III (BD Bioscience) sorter directly into RLT plus RNeasy plus lysis buffer and RNA was extracted using RNeasy Plus Micro Kit (Cat No. 74034, Qiagen, Hilden, Germany). The FACS plots were analyzed with Flowjo (version 10.4.2).

Cell culture.

Human umbilical vein endothelial cells (HUVECs) from pooled donors (C-12203, PromoCell, Heidelberg, Germany) were cultured in M199 ((11150059, Thermo Fisher Scientific) supplemented with 20% fetal bovine serum (FBS) (10270-106, Thermo Fisher Scientific), 30 mg/L endothelial cell growth factor supplements (EGCS) (E2759, Sigma-Aldrich), 10 U/mL heparin (H3149 Sigma-Aldrich) and 1% Penicillin-Streptomycin (10,000 U/mL) (15140122, Thermo Fisher Scientific). Cells were routinely maintained in 5% CO2 and 95% air at 37 ºC and medium was changed every 48 h**.** HUVECs overexpressing E4ORF1 and E4ORF1 lentiviral particles (Seandel, Butler et al. 2008) were a kind donation of Prof. Shahin Rafii (Weill Cornell School of Medical Science, New York).

***In vitro* analysis**

For DLL4 stimulation**,** culture plates were coated with 1 µg/mL recombinant human Delta-like ligand 4 (rhDLL4, cat.1506-D4 R&D Systems) in 0.1% gelatin/PBS. The control plates were coated with 0.1% gelatin supplemented with 0.02% BSA. Prior to EC seeding, excess coating solution was removed by aspiration and ECs were seeded at a density of 30,000 cells/cm^2. Cells were harvested 24 h after seeding. For NOTCH inhibition, cells were treated with the γ-secretase inhibitor N-[N-(3,5-Difluorophenacetyl)-L-alanyl]-S-phenylglycine t-butyl ester (DAPT; 10 µM, 5657702, Calbiochem) for 24 h. For proliferation blocking, Mitomycin C (cat 4150. Carl Roth) was added at a final concentration of 1µg/ml in cell culture media for 72 h. Subsequently, cell culture supernatants were taken for GDF15 quantification and cells were stained with Hoechst 33342 (H3570, Invitrogen) to allow normalization for cell numbers using a plate reader (Tecan, Spark). The FOXO1 inhibitor AS1842856 (4265, TOCRIS) was

resuspended in DMSO at a concentration of 50 µM and kept -20℃. For FOXO1 inhibition, readily attached HUVECs were treated with either 50 or 100 nM for the indicated duration. An equivalent volume of DMSO was used as control.

Sample preparation for proteomic analysis

Conditioned media was generated from E4ORF1 HUVECs seeded at a cell density of 15,000 cells/cm^2, grown in serum-free M199 (2mM L-glutamine, 30 mg/l endothelial cell growth factor supplements (Sigma E2759), 10 units/ml heparin (Sigma H3149), 50 IU/ml penicillin and 50 µg/ml) for 48 hours. The media were collected and centrifuged for 10 min at 500 RCF to precipitate cell debris. To facilitate volume handling during protein precipitation and further LC-MS/MS analysis, the conditioned media was subsequently concentrated using Amicon Ultra filters with a molecular weight cut-off value of 3 kDa (Merck-Millipore UFC900296). Proteins in the conditioned media were then precipitated using the chloroform methanol method according to Wessel and Flügge (Wessel and Flugge 1984) to prepare for label free quantification proteomic analysis. Briefly, a mixture of conditioned media, methanol, chloroform, and distilled water was prepared in a ratio of 1:4:1:3, respectively. The mixture was thoroughly vortexed and centrifuged for 10 min, 5,000 RCF at 4°C. The aqueous (upper) phase was removed and the remaining interphase/organic phase was further mixed with 3 parts of methanol. After centrifugation, the supernatant was removed and the resulting pellet was vacuum (5305000304, Eppendorf) dried for 5 min. Dried protein pellets were kept at -80 ºC until further processing.

Knock down and overexpression plasmid constructions and lentiviral particle production.

Lentiviral particles were generated by transfection of HEK 293 cells (Cat.# ACC635; EGF, Braunschweig, Germany) with Pmd2 (AddGene, Plasmid #12259), lentiviral envelope plasmid psPAX2 (AddGene, Plasmid #12260) and the plasmids. The pLVX-TetOn-Puro-FLAG-FOXO1A3 (FOXO1^{CA}) plasmid was a kind gift of Michael Potente (Max Planck Institute for Heart and Lung Research, Bad Nauheim, Germany). Additionally, GIPZ lentiviral shRNA targeting *atf4* (V2LHS272113; V3LHS302002; V3LHS302003) were purchased from Dharmacon (Horizon Discovery; Waterbeach,

United Kingdom). A nonsense scrambled shRNA sequence was used as control. Lentiviral particles were generated by transfection of HEK 293 cells with the respective plasmid and pLenti-C-mGFP- PEP-Puro Lentiviral Gene Expression Vector (Cat. #PS100093, Origene). Lipofectamine 2000 (Cat.# 11668030; Thermo Fisher Scientific) was used for transfection. Viral particles were collected at least 48 hours after incubation. Subsequently, HUVECs were transduced with particle containing supernatant (passed through a 0.45 µm filter) for 72 hours in the presence of 8 µg/ml polybrene and re-fed with fresh medium the next day. Transduced HUVECs were subsequently selected with 2 µg/ml of puromycin over 3 days. Puromycin containing medium was changed every 24 h. To induce expression of pLVX-TetOn-Puro-FLAG-FOXO1A3 ($FOXO1^{CA}$), transfected endothelial cells were treated with the noted concentration of doxycycline for 24 h E4ORF1 HUVECs and 3 h in wild type HUVECs . To generate E4ORF1 expressing HUVECs, we transduced a 30% confluent T75 flask with15 µl of E4ORF1 lentiviral particles (Seandel, Butler et al. 2008) reaching an approximate MOI of 3. After 48hours, the medium was removed and cells were selected by culturing them in serum deprived medium for 4 days.

GDF15 enzyme-linked immunosorbent assay ELISA

For determination of GDF15, urine was acquired at the beginning of dark cycle by placing a plastic film under an animal while it was being restrained. Urine (approximately 10 µl) was taken and diluted in 490 µl of calibrator diluent. Blood samples were taken from the tail vein according to approved ethical procedures. Blood was acquired in heparinized tubes (Microvette CB 300 K2E) which were centrifuged at 4℃ for 20 min at 2000 RCF to acquire the plasma. If ELISA was not carried out immediately after, plasma was stored at -80℃. Cell culture supernatants were centrifuged for 10 min at 500 RCF to eliminate cell debris. 50 µl of diluted urine, serum or cell culture supernatants were used to quantify GDF15 concentrations according to manufacturer instructions (R&D systems, Quantikine Mouse/Rat GDF15 ELISA, MGD150).

RNA extraction and quantitative RT-PCR

RNA of directly FACS sorted mEC was extracted using an RNeasy Plus Micro Kit according to the manufacturer's instructions (QIAGEN, 74034). RNA of cultured HUVECs was extracted using PureLink™ RNA Mini Kit (12183020, Thermo Fischer Scientific). RNA purity and concentration were assed via a spectrophotometer (Tecan, Spark). RNA was reverse-transcribed to cDNA by High Capacity cDNA Reverse Transcription Kit (Thermo Fisher, 43-688-13). A SYBR Green-based master mix (ThermoFisher Scientific, A25778) was used for real-time qPCR analysis with primers listed in Table 1. To compensate for variations in RNA input and efficiency of reverse-transcription, 18S was used as a housekeeping gene for primary isolated EC and Actin Beta for HUVECs. The delta-delta CT method was used to normalize the data**.**

Proteomic analysis.

Sample preparation

Samples were prepared by using a commercial iST Kit (PreOmics, Germany) with an updated version of the protocol. Briefly, 50 ug of the samples were solubilized in 'Lyse' buffer, boiled at 95°C for 10 minutes and processed with High Intensity Focused Ultrasound (HIFU) for 30s setting the ultrasonic amplitude to 85%. Then the samples were transferred to the cartridge and digested by adding 50ul of the 'Digest' solution. After 60min of incubation at 37°C the digestion was stopped with 100ul of Stop solution. The solutions in the cartridge were removed by centrifugation at 3800g, while the peptides were retained by the iST-filter. Finally the peptides were washed, eluted, dried and re-solubilized in 20ul 'LC-Load' buffer for MS-Analysis.

Liquid chromatography-mass spectrometry analysis

Mass spectrometry analysis was performed on an Orbitrap Fusion Lumos (Thermo Scientific) equipped with a Digital PicoView source (New Objective) and coupled to a M-Class UPLC (Waters). Solvent composition at the two channels was 0.1% formic acid for channel A and 0.1% formic acid, 99.9% acetonitrile for channel B. For each sample 2 µL of peptides were loaded on a commercial MZ Symmetry C18 Trap Column (100Å, 5 µm, 180 µm x 20 mm, Waters) followed by nanoEase MZ C18 HSS T3 Column (100Å, 1.8 µm, 75 µm x 250 mm, Waters). The peptides were eluted at a flow rate of 300 nL/min by a gradient from 5 to 22% B in 80 min, 32% B in 10 min and 95% B in 1 min. Samples were acquired in a randomized order. The mass spectrometer

was operated in data-dependent mode (DDA) acquiring a full-scan MS spectra (300−1’500 m/z) at a resolution of 120’000 at 200 m/z after accumulation to a target value of 500’000. Data-dependent MS/MS were recorded in the linear ion trap using quadrupole isolation with a window of 0.8 Da and HCD fragmentation with 35% fragmentation energy. The ion trap was operated in rapid scan mode with a target value of 10’000 and a maximum injection time of 50 ms. Only precursors with intensity above 5’000 were selected for MS/MS and the maximum cycle time was set to 3 s. Charge state screening was enabled. Singly, unassigned, and charge states higher than seven were rejected. Precursor masses previously selected for MS/MS measurement were excluded from further selection for 30 s, and the exclusion window was set at 10 ppm. The samples were acquired using internal lock mass calibration on m/z 371.1012 and 445.1200. The mass spectrometry proteomics data were handled using the local laboratory information management system (LIMS) (Türker, Akal et al. 2010).

Protein identification and label free protein quantification

The acquired raw MS data were processed by MaxQuant (version 1.6.2.3), followed by protein identification using the integrated Andromeda search engine(Cox and Mann 2008). Spectra were searched against a Swissprot Homo sapiens reference proteome (taxonomy 9606, version from 2019-07-09), concatenated to its reversed decoyed fasta database and common protein contaminants. Carbamidomethylation of cysteine was set as fixed modification, while methionine oxidation and N-terminal protein acetylation were set as variable. Enzyme specificity was set to trypsin/P allowing a minimal peptide length of 7 amino acids and a maximum of two missed-cleavages. MaxQuant Orbitrap default search settings were used. The maximum false discovery rate (FDR) was set to 0.01 for peptides and 0.05 for proteins. Label free quantification was enabled and a 2 minutes window for match between runs was applied. In the MaxQuant experimental design template, each file is kept separate in the experimental design to obtain individual quantitative values. Protein fold changes were computed based on Intensity values reported in the proteinGroups.txt file. A set of functions implemented in the R package SRMService (Wolski, Grossmann et al. 2018) was used to filter for proteins with 2 or more peptides allowing for a maximum of 4 missing values, and to normalize the data with a modified robust z-score transformation and to compute

p-values using the t-test with pooled variance. If all measurements of a protein are missing in one of the conditions, a pseudo fold change was computed replacing the missing group average by the mean of 10% smallest protein intensities in that condition.

Figures and diagrams

Figures in this manuscript were created with BioRender.com. or R studio.

Quantification and statistical analysis

All data represent mean ± SEM. GraphPhad Prism software (version 8.0.0) was used for statistical analyses. Investigators were always blinded to group allocation. Unless otherwise indicated, when comparing two group means, Student's *t*-test was used in an unpaired two-tailed fashion. For more than two groups, one-way ANOVA with Tukey's multiple comparisons test was used and for experimental set-ups with a second variable, two-way ANOVA with Sidak's multiple comparisons test was used. The statistical method used for each experiment is indicated in each figure legend. Asterisks in figure legends denote statistical significance. No experiment-wide multiple test correction was applied. $P>0.05$ is considered non-significant (ns). $P<0.05$ is considered significant (*).

Table 1. Sequences of primers used for RT-PCR

gene	Forward	Reverse
18s (m.& h.)	AGTCCCTGCCCTTTGTACACA	CGATCCGAGGGCCTCACTA
ATF4 (h.)	GTTCTCCAGCGACAAGGCTA	ATCCTGCTTGCTGTTGTTGG
BIP (h.)	TGTTCAACCAATTATCAGCAAACTC	TTCTGCTGTATCCTCTTCACCAGT
CHOP (h.)	AGAACCAGGAAACGGAAACAGA	TCTCCTTCATGCGCTGCTTT
HEY1 (h.)	TGGATCACCTGAAAATGCTGC	CGAAATCCCAAACTCCGATAGT
HEY2 (h.)	TGGGGAGCGAGAACAATTAC	TCAAAAGCAGTTGGCACAAG
HES1 (h.)	TGAAGAAAGATAGCTCGCGGC	GGTACTTCCCCAGCACACTT
NRARP (h.)	CGCTGTTGCTGGTGTTCTAAA	CATTGACCACGCAGTGTTTTC
foxo1 (m.)	AGTTAGTGAGCAGGCTACATTT	TTGGACTGCTCCTCAGTTCC
CD36 (h)	GCTGTTGATTTGTGAATAAGAACCA	GCACCTGTTTCTTGCAAACTCC
MXI1 (*h*.)	GCCAAAGCACACATCAAGAAACT	GCTGTTCCAGTCGCCACTTT
PDK1 (h.)	TCTCAGGACACCATCCGTTCA	ACCATGTTCTTCTAGGCCTTTCAT
ANG2 (h.)	TGCCACGGTGAATAATTCAG	TTCTTCTTTAGCAACAGTGGG
PDK4 (h.)	GTAGCAGTGGTCCAAGATGCC	ACACGATGTGAATTGGTTGGTCT
GDF15 (h.)	ATACTCACGCCAGAAGTGCGG	GAACAGAGCCCGGTGAAGGC
gdf15 (m.)	GAGCCGAGAGGACTCGAACT	CCCCAATCTCACCTCTGGACT
ACTB(m. h.)	GCTCCTCCTGAGCGCAAG	CATCTGCTGGAAGGTGGACA

4. Angiocrine GDF15 improves glucose homeostasis by direct effects on insulin sensitivity in skeletal muscle and is independent of weight loss.

Running title: GDF15 is a *bonafide* insulin sensitizer.

Abdiel Alvarado-Diaz[1], Fatemeh Jaleh[2], Gommaar D'Hulst[1], Moheb Ghobrial[1], Paola Gilardoni[1] and Katrien De Bock[1].

(1) Laboratory of Exercise and Health, Department Health Sciences and Technology, Swiss Federal Institute of Technology (ETH) Zurich, Zurich, 8603, Switzerland.; (2) ETH Alumni

Status: In preparation

Corresponding author:

Katrien De Bock

Laboratory of Exercise and Health

Institute of Movement Sciences (D-HEST)

ETH Zürich - Swiss Federal Institute of Technology

ETH Zürich, SLA C7

Schorenstrasse 16

CH-8603 Schwerzenbach

Switzerland

Tel. +41 44 655 7389

Email: Katrien-debock@ethz.ch

4.1. Abstract.

Endothelial cell form the inner lining of blood vessels. Yet, the function of blood vessels lies beyond simple conduits that exchange oxygen and nutrients between blood and the tissues they irrigate. It has been recently suggested that endothelial cell can control the function of metabolic organs and, with this, whole energy homeostasis. Indeed, it has become increasingly clear that endothelial cell dysfunction precedes metabolic disease and diabetes type II. On the other hand, increasing their responsiveness to growth factors, metabolic adaptation to nutrient insults, nitric oxide (NO) and reactive oxygen species signaling (ROS) improves glucose handling and insulin sensitivity. Along with these evidences, in this study we hypothesized that endothelial cells are capable of sensitizing skeletal muscle to the effect of insulin via the secretion of soluble factors. Furthermore, in a previous study we identified GDF15 to be abundantly secreted by endothelial cells *in vivo*. Therefore, we explored whether GDF15 could be a *bonafide* insulin sensitizer by direct actions to skeletal muscle and whole body glucose homeostasis. First, *in vitro*, we found that endothelial cell conditioned media increases insulin sensitivity in human myotubes and that GDF15 plays a significant role in this observation. Furthermore, GDF15 alone increases insulin sensitivity shown by both, insulin signaling and GLUT4 translocation in myotubes. Finally, *in vivo,* mice that were administrated GDF15 display an improved glucose handling in an insulin tolerance test (ITT), increased glucose uptake, and insulin signaling in skeletal muscle. Importantly, these effects were found to be acute and independent of well-established anorectic effects on weight loss.

4.2. Authors contributions

The general content, perspective and supervision of this chapter was proposed by Prof. Dr. Katrien De Bock. The design, execution, and analysis of all the experiments, writing the full manuscript content, and creation of all figures was carried out by Abdiel Alvarado Diaz. Over the course of this project, several contributors have significantly supported its realization in forms of assistance during the execution and/or analysis of some experiments or figures. Dr. Fateme Jaleh supported the design and execution of experiment associated with figures 12, 13 and 14. She also gave valuable input to the design of manuscript. Finally, she helped me solve fundamental technical issues assessing *in vivo* glucose homeostasis experiments. Dr. Gommaar D'Hulst technically supported the execution of experiments associated to figure 13. Moheb Ghobrial assisted with significant input regarding the design of figures 12, 13, 14. Dr. Paola Gilardoni provided technical assistance in the conduct of all experiments. The general supervision and correction of this manuscript was done by Abdiel Alvarado Diaz and Prof. Dr. Katrien De Bock.

4.3. Introduction.

By mass, skeletal muscle harbors the largest amount of vascular endothelial cells (Egginton 2011). The skeletal muscle vasculature consists of an intricated meshwork of endothelial cells in charge of sustaining the high metabolic demands of oxygen and nutrients while enduring the high mechanical stress of its surrounding tissue(Olfert and Birot 2011). However, the importance of adequate vascular function and structure lies beyond this primary function as the balance between perfusion and metabolic demands also needs to match the emerging properties of vascular endothelium. Among these emerging regulatory roles of these muscle-associated vascular endothelial cells, we find that ECs can modulate skeletal muscle regeneration. ECs reside in close proximity to satellite cells ($Pax7^+$ and $Myf5^+$ expressing muscle progenitor cells) (Christov, Chrétien et al. 2007) , this close association suggests that crosstalk may occur via direct or indirect mechanisms, this is, through cell-to-cell contact or through paracrine communication via the secretion of angiocrine factors into interstitial space of musculoskeletal tissue(Verma, Asakura et al. 2018). ECs control skeletal muscle stem cells and its progenitor clonal expansion and differentiation through the secretion of angiocrine IGF1, HGF, FGF-2, VEGFA and homodimers of platelet-derived growth factor β (Arsic, Zacchigna et al. 2004, Bryan, Walshe et al. 2008, Borselli, Storrie et al. 2010). Interestingly, vascular endothelial cells have also been demonstrated to undergo myogenic differentiation *in vivo (Zheng, Cao et al. 2007)*, which suggest that skeletal muscle cells and its supplying vasculature, in permissive conditions, have overlapping physiological properties. Furthermore, a reciprocal synergistical contribution between myogenesis and angiogenesis has been previously reported to occur through the secretion of soluble factors *in vitro(Osaki, Sivathanu et al. 2018)*. However, whether EC can modulate the other aspects of skeletal muscle biology such as metabolism has not been addressed in proper depth.

There are preliminary indications that indeed EC can control skeletal muscle metabolism, specifically in the context of insulin-mediated control of glucose homeostasis. It has been shown that a dampened insulin signaling in EC leads to a decreased glucose uptake in skeletal muscle (Kubota, Kubota et al. 2011) . Additionally, caveolin-1, insulin-receptor and insulin-like growth factor receptor-1 have been identified to be important players in the transendothelial transport of insulin

towards the skeletal muscle (Wang, Liu et al. 2006). This via formation of caveolae, which are membrane invaginations involved in the transport of large macromolecules to interstitial compartment (Schubert, Frank et al. 2001). Furthermore, during exercise, skeletal muscle goes from a basal insulin sensitivity to high insulin sensitivity (Richter, Garetto et al. 1982, Reynolds IV, Brozinick Jr et al. 2000). However, before these metabolic changes happen, a significant increase of skeletal muscle capillarity occurs (Waters, Rotevatn et al. 2004). Furthermore, it has been shown that upon VEGFB stimulation an increase of capillarity in adipose tissue leads to improved glucose metabolism, for which an improved insulin supply is shown to be partially responsible; these changes are also accompanied by weight loss in mice under obesogenic diet (Robciuc, Kivelä et al. 2016). Additionally, it has been previously suggested that endothelial cells present in the skeletal muscle are the primary source for NO and ROS regulation of glucose homeostasis(Sansbury and Hill 2014, Paneni, Costantino et al. 2015, Watt, Gage et al. 2017). Yet, the regulation of skeletal muscle glucose homeostasis by direct secretion of angiocrine factors is not yet established, despite growing evidence that crosstalk between endothelial cells and other metabolic organs plays a fundamental role in metabolic organs homeostasis and ultimately whole energy control (Nolan, Ginsberg et al. 2013, Robciuc, Kivelä et al. 2016, Potente and Mäkinen 2017).

Under the light that endothelial cells control tissue homeostasis through the secretion of angiocrine factors, the closely related physical and physiological relationship between endothelial cells and skeletal muscle cells and the importance of endothelial cells in muscle adaptations exercise, the aim of the present work is to identify whether soluble factors secreted by endothelial cells improve insulin sensitivity and glucose homeostasis in skeletal muscle. Previously, we identified GDF15 to be abundantly secreted by endothelial cells. GDF15 is a distant member of the transforming growth factor B family (TGF-β), which has been shown to modulate food intake via interaction with its receptor, GFRAL, in the area postrema of the hindbrain (Emmerson, Wang et al. 2017, Hsu, Crawley et al. 2017, Mullican, Lin-Schmidt et al. 2017, Yang, Chang et al. 2017). Besides the well-established central nervous system (CNS) anorectic effects in food intake and the consequential metabolic benefits of a reducing adipose mass in the body such as improved insulin sensitivity and overall glucose homeostasis, it has

been suggested that GDF15 could also act locally to reduce cytokine-induced β-cell apoptosis and resolve endoplasmic reticulum (ER) stress in diabetes type I model of human pancreata (Nakayasu, Syed et al. 2020) or to modulate the macrophage metabolism to drive systemic insulin actions (Jung, Choi et al. 2018). Altogether this suggest that GDF15 may have a rather pleiotropic influence in the control of glucose homeostasis in mammals. The identification of secreted GDF15 in culturing media from EC, led us to hypothesize that GDF15 could be a potential angiocrine factor that can be considered as *bonafide* insulin sensitizer to the skeletal muscle and thus improving whole body glucose homeostasis.

4.4. Results

4.4.1. Endothelial cell conditioned medium sensitizes human myotubes to insulin.

Recent studies have pointed out that improving endothelial function has a positive impact in insulin sensitivity and glucose homeostasis (Robciuc, Kivelä et al. 2016) . Yet, mechanistic approaches are largely lacking. To explore the hypothesis that ECs control muscle insulin sensitivity via secretion of soluble factors, also known as angiocrine factors, rather than cell-to-cell contact, we stimulated human myotubes with endothelial cell conditioned medium (CM), and then assessed their insulin responsiveness. We first generated CM from HUVECs in standard culturing conditions, this is, with medium supplemented with fetal bovine serum and endothelial growth factors. As non-conditioned (NC) control, we used fresh media incubated at 5% of CO_2 in without cells for the same amount of time. Fully differentiated human myotubes (HSkM) were stimulated in a CM or NC / differentiation medium ratio of 3:7 for 48 h (**Figure 12A**). Subsequently, myotubes were stimulated with 100 nM of insulin, and tissues were harvested 30 min later. We observed that myotubes stimulated with endothelial CM, but NC control, upregulated targets of the insulin signaling cascade (**Figure 12B**) such as increased phosphorylation in AS160 T642 (**Figure 12C**), AKT T308 (**Figure 12D**) and AKT S473 (**Figure 12E**).

However, some of the limitations of addition of fetal serum in standard culturing conditions is the presence of overt amounts of growth factors and cytokines that are exogenous to ones produced by ECs (Hannoun, Fletcher et al. 2010, Jeon, Lim et al. 2010, Karnieli, Friedner et al. 2017). To exclude a potential interference from the serum-associated cytokines and growth factors in media, we subsequently used $E4ORF1^+$ ECs, which were a kind donation from Prof. Shahin Raffi (Butler, Nolan et al. 2010). E4ORF1 is an adenoviral protein that keeps AKT constitutively active in cells expressing it, thus ensuring survival in the absence of serum, which allow for a long term culture. CM was produced from $E4ORF1^+$ HUVECs serum-free , again a ratio 3:7 in differentiation media was applied on human myotubes, as shown before (**Figure 12F**).CM stimulation in serum-free conditions also proved to increase insulin signaling (**Figure 12G**) as shown by increased phosphorylation of AS160 T642 (**Figure 12H**), AKT T308 (**Figure 12I**) and AKT S473 (**Figure 12J**) compared to controls.

Finally, we excluded that increased insulin sensitivity responses in myotubes stimulated with CM compared to control are caused by differences in relative concentration of nutrients. To do so, we used serum-free conditioned medium taken from E4ORF1^{+} HUVECs and concentrated it 40x by filtering it through a filter with cut-off value of 3 kDa, which means that only macromolecules with a molecular weight value superior of 3kDa were taken to stimulate human myotubes with an approximate ratio of 1:9 in skeletal muscle differentiation media (**Figure 12K**). Concentrated CM provoked an increased in insulin cascade (**Figure 12L**) as shown by increased phosphorylation of AS160 T642 (**Figure 12M**), AKT T308 (**Figure 12N**), AKT S473 (**Figure 12O**), ERK 1/2 p42/44 (**Figure 12P**). This upregulation of insulin sensitivity was not caused by energy stress as assessed by phosphorylation of AMPK T172 (**Figure 12Q**). Furthermore, increased insulin sensitivity in human myotubes was accompanied by enhanced glycolytic flux (**Figure 12R**) and insulin dependent glucose translocation of glucose transporter 4 (GLUT4) (**Figure 12S**)

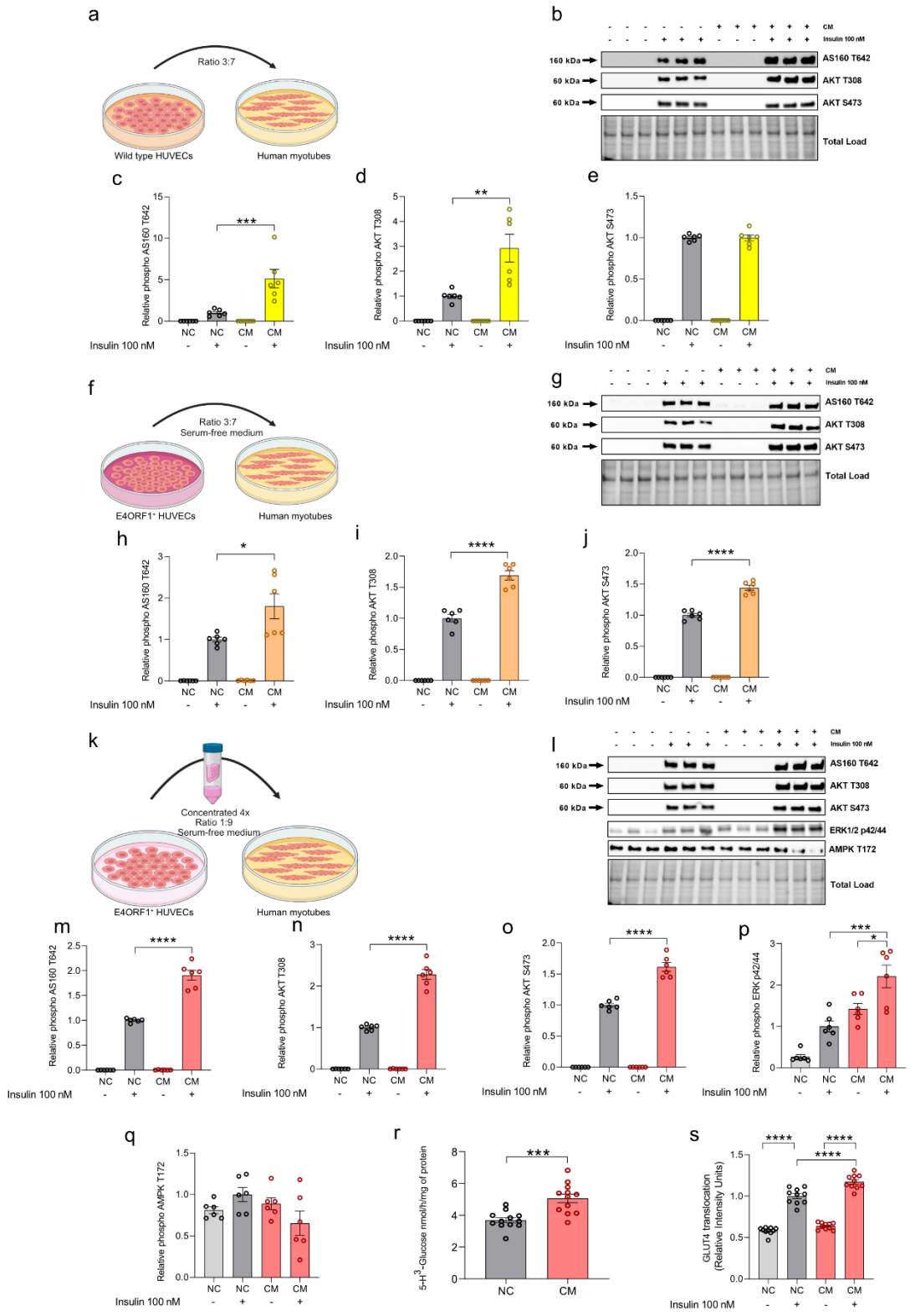
a
Ratio 3:7
Wild type HUVECs
Human myotubes
b
CM
Insulin 100 nM
160 kDa
60 kDa
60 kDa
AS160 T642
AKT T308
AKT S473
Total Load
c
Relative phospho AS160 T642
d
Relative phospho AKT T308
e
Relative phospho AKT S473
NC NC CM CM
Insulin 100 nM - + - +
f
Ratio 3:7
Serum-free medium
E4ORF1+ HUVECs
Human myotubes
g
h
i
j
k
Concentrated 4x
Ratio 1:9
Serum-free medium
E4ORF1+ HUVECs
Human myotubes
l
ERK1/2 p42/44
AMPK T172
m
n
o
p
Relative phospho ERK p42/44
q
Relative phospho AMPK T172
r
5-H3-Glucose nmol/h/mg of protein
s
GLUT4 translocation (Relative Intensity Units)

Figure 12 Endothelial cell secretome sensitizes skeletal muscle to the effects of insulin in vitro. **a**. Schematic of conditioned media generation from wild type HUVECs in the presence of serum and applied in a 3:7 ratio to human myotubes. **b**. Representative blot of insulin signaling from human myotubes that have been stimulated with CM or NC from WT HUVECs over 48 h **c**. CM treated myotubes increase responsiveness to insulin assessed by phosphorylation of AS160 T642 (n= 6) (Two-way ANOVA and Tukey's multiple comparison). **d**. CM treated myotubes increase responsiveness to insulin assessed by phosphorylation of AKT T308 (n= 6) **e**. CM treated myotubes does not respond differently to insulin when compared to control assessed by phosphorylation of AKT S473. (n= 6) (Two-way ANOVA and Tukey's multiple comparison) **f**. Schematic of CM generation from E4ORF1^{+} HUVECs in the absence of serum and applied in a 3:7 ratio to human myotubes. **g**. Representative blot of insulin signaling from human myotubes that have been stimulated with CM or NC from E4ORF1^{+} HUVECs over 48 h. **h**. CM generated in serum-free conditions increase responsiveness to insulin assessed by phosphorylation of AS160 T642 in human myotubes (n= 6) (Two-way ANOVA and Tukey's multiple comparison). **i.** CM generated in serum-free conditions increase responsiveness to insulin assessed by phosphorylation of AKT T308 in human myotubes (n= 6) (Two-way ANOVA and Tukey's multiple comparison). **j**. CM generated in serum-free conditions increase responsiveness to insulin assessed by phosphorylation of AKT S473 in human myotubes (n= 6) (Two-way ANOVA and Tukey's multiple comparison). **k**. Schematic of 40x concentrated CM generation from E4ORF1^{+} HUVECs in the absence of serum and applied in a 1:10 ratio to human myotubes. **l**. Representative blot of insulin signaling from human myotubes that have been stimulated with 4x CM or NC from E4ORF1^{+} HUVECs over 48 h. **m**. 4x concentrated CM generated in serum-free conditions increase responsiveness to insulin assessed by phosphorylation of AS160 T642 in human myotubes (n= 6) (Two-way ANOVA and Tukey's multiple comparison). **n**. 4x concentrated CM generated in serum-free conditions increase responsiveness to insulin assessed by phosphorylation of AKT T308 in human myotubes (n= 6) (Two-way ANOVA and Tukey's multiple comparison). **o**. 4x concentrated CM generated in serum-free conditions increase responsiveness to insulin assessed by phosphorylation of AKT S473 in human myotubes (n= 6) (Two-way ANOVA and Tukey's multiple comparison). **p**. 4x concentrated CM generated in serum-free conditions increase responsiveness to insulin assessed by phosphorylation of ERK1/2 p42/44 in human myotubes (n= 6) (Two-way ANOVA and Tukey's multiple comparison). **q**. Insulin sensitizing effects of conditioned media are not mediated by differences in energy stress as assessed by AMPK T172 in human myotubes stimulates with 4x concentrated CM produced in serum-free conditions (n= 6) (Two-way ANOVA and Tukey's multiple comparison). **r**. Human myotubes treated with 4x concentrated CM generated in serum-free conditions have increased glycolytic flux (n= 12) (Student-t test). **s**. Rat L6 myotubes treated with 4x concentrated CM generated in serum-free conditions display a greater GLUT4 translocation upon insulin stimulation (n= 10) (Two-way ANOVA and Tukey's multiple comparison). In figures **b**, **g** and **l,** the total load shows comparable amounts of protein loaded in the representative blot. Significant values are represented in asterisks as follows *P<0.05, **P<0.01, ***P<0.001, and ****P<0.0001.

4.4.2. GDF15 significantly contributes to insulin sensitizing effects of conditioned media

From a previous study where we analyzed endothelial secretome *in vitro*, we identified GDF15 to be highly abundant and upregulated in endothelial cell secretome. GDF15 is a distant member of the TGF-β family. Upon binding to its receptor, GFRAL, in the area postrema of the hind brain, it mediates aversion to food intake, and thus ultimately leads to reduction of body mass (Emmerson, Wang et al. 2017, Hsu, Crawley et al. 2017, Mullican, Lin-Schmidt et al. 2017, Yang, Chang et al. 2017). . Despite that it has been suggested that GDF15 acts locally in peripheral tissue, no receptor outside CNS has been identified so far. Along with findings that GDF15 has a holistic influence on glucose homeostasis, we evaluated whether its able to synergistically act with insulin. To assess whether angiocrine GDF15 plays a significant role in the insulin sensitizing effects of endothelial CM, GDF15 was knocked down in E4ORF1 ECs, and CM was produced culturing these cells in in serum free conditions over 48 h as shown previously. with an efficiency of 78% (**Figure 13A**). CM from α-GDF15 E4ORF1 failed to increase insulin sensitivity as compared to sh-scrambled control (**Figure 13B**) as phosphorylated AKT308 (**Figure. 13C**) and AS160 T642 (**Figure 13D**) were not significantly different from scrambled control. Altogether this suggests that GDF15 alone could be a *bonafide* insulin sensitizer. To further test this proposition *in vitro*, we stimulated fully differentiated human myotubes with GDF15 from commercial suppliers. Treatment increased insulin signaling (**Figure 13E**), as shown by increased phosphorylation AS160 T642 (**Figure 13F**), AKT T308 (**Figure 13G**) insulin receptor β Y1150/1151 (**Figure 13I**), but not ERK 1/2 p42/44 (**Figure 13H**). Furthermore, GDF15 treatment also increases glycolytic flux (**Figure 13J**), glucose uptake (**Figure 13K**) and insulin mediated GLUT4 translocation (**Figure 13L**). Altogether this suggests that GDF15 could directly act on skeletal muscle.

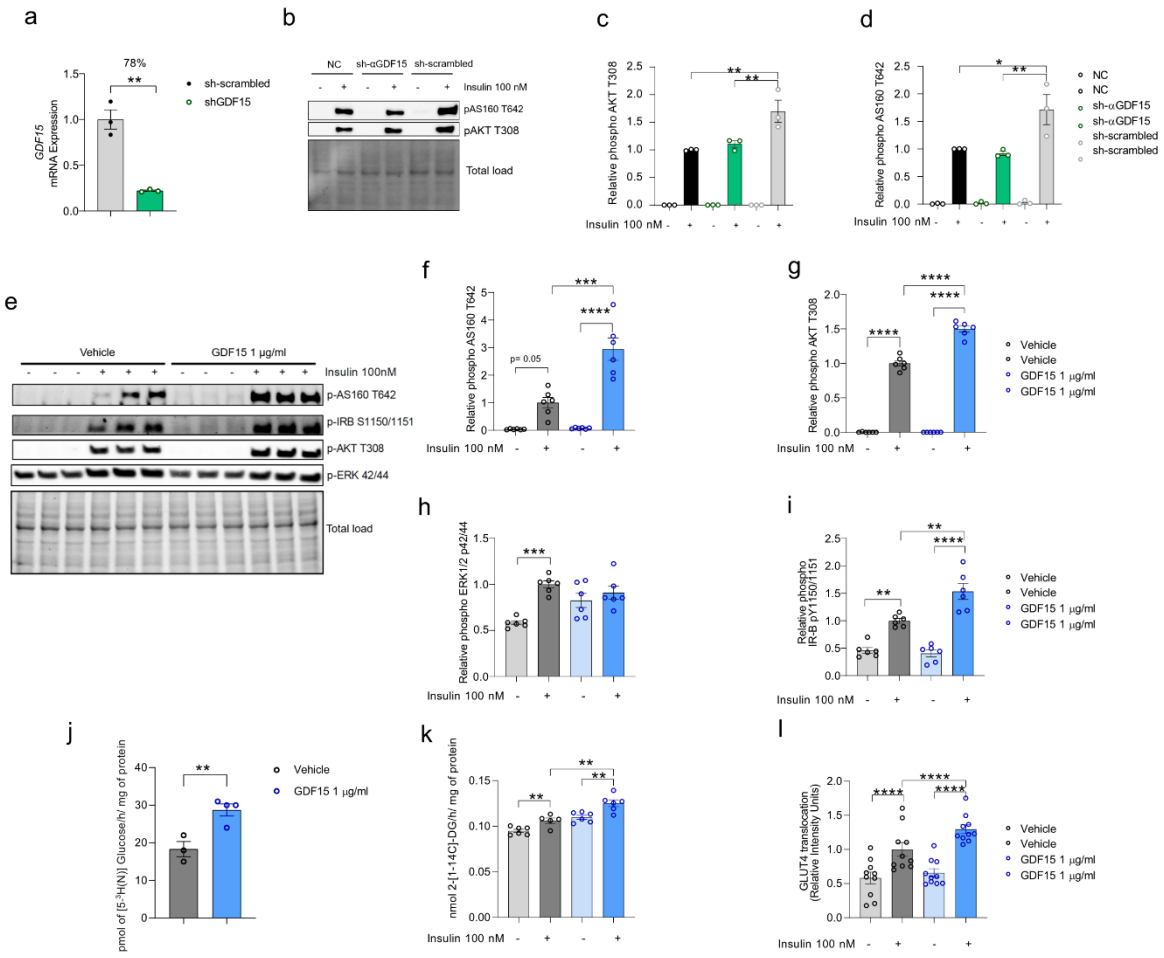

Figure 13 GDF15 stimulation increases insulin sensitivity and glucose handling in human myotubes. **a**. *GDF15* knockdown efficiency in E4ORF1 HUVECs using sh-αGDF15 lentiviral viral particles. (n= 3)(Student-*t* test). **b**. Insulin signaling cascade from human myotubes that have been stimulated over 48 h with CM from E4ORF1 in serum free conditions or control. CM was either produced from sh-scrambled or sh-αGDF15 endothelial cells. (n= 3). **c.d.** Human myotubes treated with CM from sh-αGDF15 failed to increase insulin sensitivity as shown by quantification of downstream targets AKT T308 and AS160 T642 ((Two-way ANOVA and Tukey's multiple comparison). **e**. Representative blot from human Myotubes were treated for 48 h with rhGDF15 and then stimulated with insulin 100 nM. In figures **b** and **e**, the total load shows comparable amounts of protein loaded in the representative blot. **f. g**. **i**. rhGDF15 increases insulin sensitivity in human myotubes *in vitro* by increasing phosphorylation of downstream targets AS160 T642, AKT T308, IR-β Y1150/1151 upon maximal insulin stimulation 100 nM. (n= 6)((Two-way ANOVA and Tukey's multiple comparison). **h**. rhGDF15 stimulation of human myotubes does not increases ERK1/2 p42/44 as compared to other downstream targets (n= 6) (Two-way ANOVA and Tukey's multiple comparison). **j.** rhGDF15 stimulation in human myotubes increases glycolytic flux (n= 4)(Student-*t* test). **k.** rhGDF15 stimulation in human myotubes increases insulin mediated glucose uptake assessed by radioactive 2-deoxy glucose incorporation (n= 6) (Two-way ANOVA and Tukey's multiple comparison). **l.** 48 h stimulation of rhGDF15 (kindly donated by Group Leader Dr. Sebastian Jørgensen, Novonordisk) increases insulin-mediated GLUT4 translocation in rat L6-GLUT4-MYC myotubes (n= 10). (Two-way ANOVA and Tukey's multiple comparison). Significant values are represented in asterisks as follows *P<0.05, **P<0.01, ***P<0.001, and ****P<0.0001.

4.4.3. GDF15 administration improves glucose homeostasis and insulin response *in vivo*.

Despite the growing evidence suggesting that GDF15 could also act locally(Chung, Ryu et al. 2017, Jung, Choi et al. 2018, Nakayasu, Syed et al. 2020), the expression of the only known receptor, GFRAL, can be found exclusively in the area postrema of the hindbrain (Emmerson, Wang et al. 2017, Hsu, Crawley et al. 2017, Mullican, Lin-Schmidt et al. 2017, Yang, Chang et al. 2017). and other areas of the central nervous system (CNS), however, is absent in peripheral tissues (Li, Wang et al. 2005, Hsu, Crawley et al. 2017, Emmerson, Duffin et al. 2018, Nakayasu, Syed et al. 2020) Nonetheless these observations may be contradictory, a plausible scenario is that GDF15 acts through a yet unknown receptor that has not been described in periphery. The *in vitro* data in this work, so far suggests that this unknown mechanism or receptor could be present in skeletal muscle to partially mediate insulin sensitivity and improved glucose homeostasis.

Insulin sensitivity and improved glucose homeostasis have been described in literature upon administration of GDF15 *in vivo*. However, they are often referred as to be secondary to the effects of reduced body weight in animals fed an obesogenic diet. Therefore, to test whether GDF15 has insulin sensitizing properties that are primary to its stimulation and not secondary to weight loss, we decided to administer GDF15 acutely 3 times every other day. Assessment of their body weight indicated that there were no significant differences between treated rhGDF15 animals and controls after 5 days **(Figure 14A).** Furthermore, insulin signaling in skeletal muscle showed increased phosphorylation in insulin signaling cascade (**Figure 14B**) as shown by AKT T308 (**Figure 14C**) and AS160 T642 (**Figure 14D**). Yet, when assessing insulin responsiveness in an insulin tolerance test (ITT), GDF15 treated mice showed lower glucose levels in different time points compared to control mice (**Figure 14E**). However, no differences were found in a glucose tolerance test (GTT) **(Figure 14F),** which suggest that endogenous levels of insulin release are not sufficient to elicit changes in glucose levels in chow fed mice. Finally, when assessing glucose uptake in a radioactive assay *in* vivo we observe that different muscle like tibialis anterior (Ta), extensor digitorum longus (Edl), soleus and oxidative gastrocnemius (Rgas)(**Figure 14G**). Despite these interesting findings, further experiments are still necessary to

elucidate the molecular mechanisms in charge of GDF15 insulin sensitizing effects on skeletal muscle *in vivo* and *in vitro.*

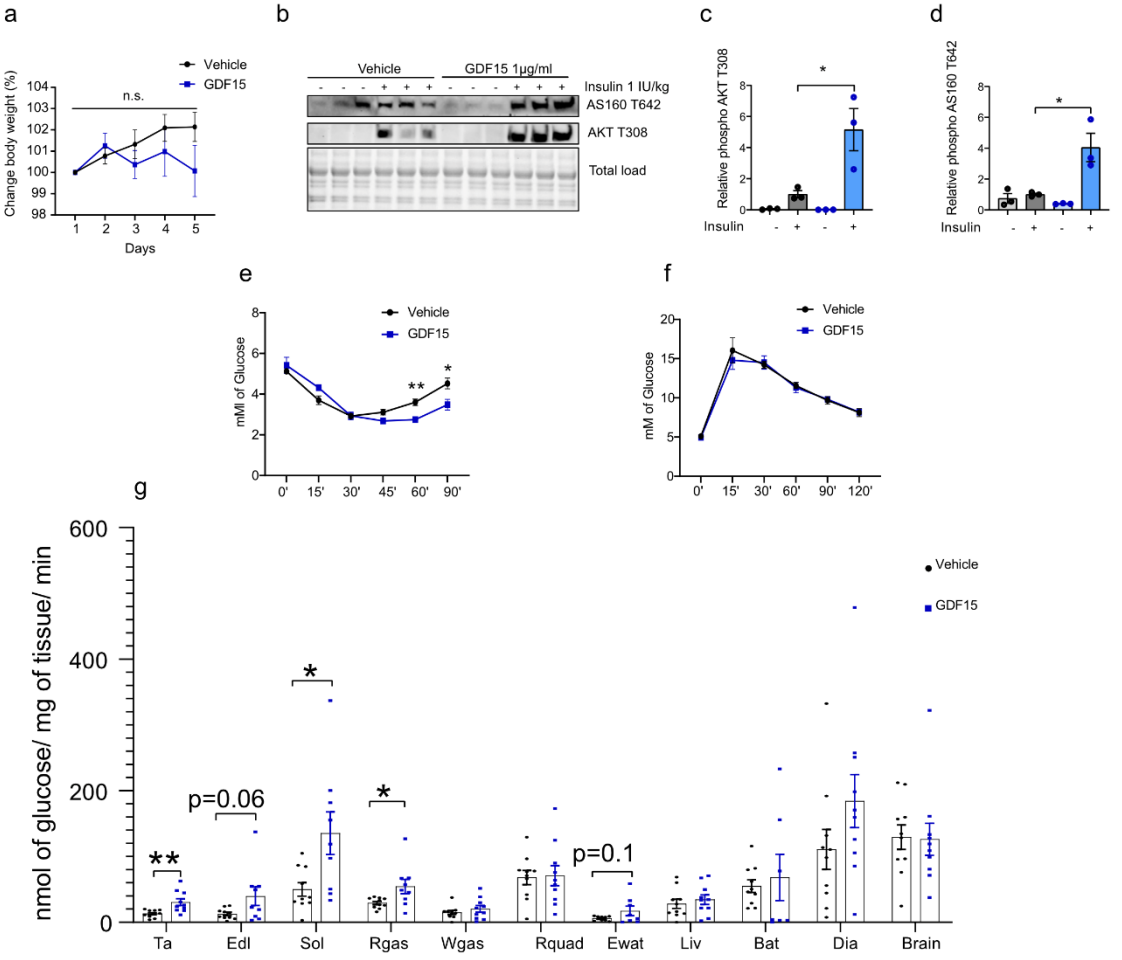

Figure 14 Administration of rhGDF15 promotes increased insulin sensitivity and greater glucose uptake in skeletal muscle in mice fed chow diet. Mice were administered 8 nmol of rhGDF15 at the beginning of their dark cycle. **a** There are no differences in changes in body weight after 5 days between controls (n= 6) and GDF15 treated animals (n= 6) (Two-way ANOVA with Sidak's multiple comparison). **b** GDF15 treated mice show an increased insulin signaling upon stimulated with 1 IU/kg body weight insulin for 15 min, the total load shows comparable amounts of protein loaded in the representative blot. **c. d**. Downstream insulin signaling was increased as measured by phosphorylation of AKT T308 and AS160 T642(Two-way ANOVA and Tukey's multiple comparison). **e**. rhGDF15 treatment improves insulin sensitivity as shown by ITT (vehicle, n= 4, rhGDF15, n= 3) (Two-way ANOVA and Sidak's multiple comparison) **f**. but treatment does not influence glucose handling as assessed in ipGTT (n= 4) (Two-way ANOVA and Sidak's multiple comparison). **g**. *In vivo* insulin-stimulated radioactive 2-Deoxy glucose uptake of several tissue (Student-t test). *Ta*, tibialis anterior; *Edl*, extensor digitorum longus; *Sol*, soleus; *Rgas*, red gastrocnemius; *Wgas*, white gastrocnemius; *Rquad*, red quadriceps; *Ewat*, epididymal white adipose tissue; *Liv*, liver; *Bat*, brown adipose tissue; *Dia*, diaphragm. Significant values are represented in asterisks as follows *P<0.05, **P<0.01, ***P<0.001, and ****P<0.0001

4.5. Discussion

Skeletal muscle constitutes approximately 45% of total body mass in humans(Spargo, Pratt et al. 1979), which makes it the largest metabolic organ in the adult and a major site of glucose uptake (Kim and Kim 2020) . Indeed, skeletal muscle is recipient of up to 80% glucose uptake postprandially (Thiebaud, Jacot et al. 1982), which makes it a central component in whole body energy homeostasis and its dysregulation leads to metabolic disease and diabetes. However, the extent to which it responds to insulin greatly varies depending on the health status (Wu and Ballantyne 2017, Schwartsburd 2019), age (Gupte, Bomhoff et al. 2008), and physical activity of an individual(Richter and Hargreaves 2013). Hence, skeletal muscle shows metabolic plasticity that is adapted to meet physiological demands of the body. Importantly, this metabolic plasticity also shows circadian rhythmicity, during active cycle skeletal muscle is more responsive to the effects of insulin, in both, signaling and glucose clearance potential; while in the inactive cycle the signaling induction is dampened(Basse, Dalbram et al. 2018). Furthermore, skeletal muscle insulin sensitivity can be modulated by the stimulation of several growth factors, cytokines, hormones and metabolites. In this work, we present angiocrine GDF15 as a *bonafide* insulin sensitizer in skeletal muscle, which independent of weight loss.

Previously, published literature suggests that an increased in muscle capillarization enhances insulin sensitivity after exercise and detraining in senile human subjects independently from known exercise-induced benefits to glucose handling(Prior, Goldberg et al. 2015), this vascular control of glucose homeostasis has also been replicated in other target organs such as adipose tissue (Robciuc, Kivelä et al. 2016), pancreas (Duvillié 2013, El-Gohary and Gittes 2018, Obata, Kimura et al. 2019) and liver(Tsuchiya and Accili 2013). We show that vascular derived secreted factors can modulate skeletal muscle insulin sensitivity. In an *in vitro* model system, we stimulated human skeletal muscle myotubes with conditioned media from HUVECs in serum free conditions, ultimately allowing us to delimit endothelial cell secretome insulin sensitizing capabilities in human skeletal muscle myotubes. Indeed, we found that CM from endothelial cells promotes increase insulin signaling by the increased phosphorylation of AKT, AS160 and ERK1, and increased GLUT4 translocation in rat L6 myotubes.

We explored whether the consequential enhanced glucose handling *in vivo* is independent of anorectic effects arising from the central nervous system (CNS). We found that human recombinant stimulation of GDF15 on human myotubes *in vitro* mimic the improved metabolic properties of endothelial CM, which leads to an increased insulin signaling increased phosphorylation, increased GLUT4 translocation to cell membrane. Thus, suggesting that GDF15 stimulation in skeletal muscle could go via an independent mechanism of GFRAL

Skeletal muscle is subject to the action of different cytokines that modulate its insulin sensitivity and glucose handling potential. To exemplify this, adipose tissue has been identified to be a metabolic organ with secretory capacity that signals to muscle. It modulates the expression of positive and negative signaling molecules. Fibroblast Growth Factor 21 (FGF 21) is among the molecules that exert an improved glucose handling phenotype. It acts on skeletal muscle by preventing insulin resistance upon high fat diet though peripheral and CNS (BonDurant, Ameka et al. 2017) , mediated effects in preclinical models of diabetes in rats (Sarruf, Thaler et al. 2010) and rhesus monkeys (Kharitonenkov, Wroblewski et al. 2007). Closely associated to FGF21, adiponectin is yet another adipokine that improves GLUT4 translocation in muscle through the activation of its receptor adiponectin receptor 1 (AdipoR1) and adiponectin receptor 2 (AdipoR2) (Ceddia, Somwar et al. 2005). Importantly, signaling via adiponectin receptor is blunted upon overexpression of a dominant negative AMP kinase (AMPK), which supports the notion that an adequate response against energy stress is fundamental in regulation of glucose homeostasis(Yamauchi, Kamon et al. 2002). Furthermore, skeletal muscle stimulation with adiponectin increases fatty acid uptake and oxidation via mitochondrial biogenesis and suppresses fatty acid synthesis through the actions of AMPK, p38 and PPARα (Fruebis, Tsao et al. 2001, Yamauchi, Kamon et al. 2002, Yoon, Lee et al. 2006, Ritchie and Dyck 2012).

We identified that GDF15 interacts directly with skeletal muscle. Seminal publications identified the direct relationship between GDF15 and skeletal muscle metabolic benefits by improving lipid mobilization and oxidative metabolism (Chung, Ryu et al. 2017). Beyond the skeletal muscle, GDF15 has been demonstrated to have metabolic benefits in liver(Kim, Kim et al. 2018), adipose tissue (Chrysovergis, Wang et al. 2014), macrophages(Jung, Choi et al. 2018) and pancreas (Nakayasu, Syed et al. 2020). We showed increased insulin signaling and increased glucose uptake in several muscle

like TA, EDL, RGAS and soleus. These improved glucose handling was accompanied by an increased insulin sensitivity as shown by ITT.

In conclusion, we present evidence that endothelial cell secretome is able to stimulate skeletal muscle to have a greater responsiveness to insulin. Furthermore, that endothelial cells secrete GDF15 in pharmacologically relevant concentrations. *In vitro*, GDF15 was able to increase insulin signaling and GLUT4 translocation. I*n vivo* GDF15 was able to induce an increase insulin sensitivity, an increased skeletal muscle insulin sensitivity and glucose uptake in muscle like TA, EDL, RGAS and soleus. Importantly, these insulin sensitizing effects are independent of weight loss, which furthers GDF15 as a pleiotropic metabolic regulator against deleterious effects of obesity and diabetes.

4.6. Methods

Cell culture.

HUVECs and E4ORF1 HUVECs were cultured on gelatin coated plates and M199 medium (1 mg/ml D-glucose) supplemented with 20% fetal bovine serum (FBS), 2mM L-glutamine, 30 mg/l endothelial cell growth factor supplements (Sigma E2759), 10 units/ml heparin (Sigma H3149), 50 IU/ml penicillin and 50 µg/ml streptomycin. Cells were routinely maintained in 5% CO2 and 95% air at 37 ºC and medium changed every 48 h. E4ORF1 HUVECs were a kind donation from the lab Prof. Shahin Rafii at the Weill Cornell School of Medical Science, New York. CM was produced culturing EC over 48 h in the aforementioned conditions. CM was subsequently concentrated using Amicon Ultra filters with a molecular weight cut-off value of 3 kDa (Merck-Millipore UFC900396).

Culture and differentiation of human myoblasts

Human myoblasts from healthy donors were obtained from Cook Myosite. Myoblasts were cultured in proliferation media (Cook Myosite MB-2222) avoiding confluence greater than 60% to ensure cell-cell contact and thus spontaneous differentiation. For differentiation, human myoblasts were seeded in collagen coated well-plates and medias was replaced for differentiation media (Cook Myosite MD-5555). Briefly, for the collagen coating, 10% v/v of collagen solution (Gibco A10483-01) was prepared in PBS. Coating solution was incubated on plates at 37℃ for 4 h or overnight at 4℃. Solution was discarded, and plates dried for 2 h. Myoblasts differentiated for 7 days before using in assays. *In vitro*, human myoblasts were stimulated with rhGDF15 (R&D Systems, 957-GD-025, source unless otherwise noted) for 48 h at a concentration of 1 µg/ml in differentiation media (Cook Myosite MD-5555).

Glycolysis Flux

Determination of glycolytic flux was performed as described before (Veys, Alvarado-Diaz et al. 2019). Briefly, cells were incubated for 2 h in culture medium containing D-[5-3H(N)]-glucose (NET53100, PerkinElmer,) at a final concentration of 0.4 µCi/mL medium. The supernatant was then transferred into glass vials sealed with rubber stoppers, and 3H2O was captured in hanging wells using a H2O-soaked Whatman paper for 48 h at 37°C to reach saturation. Radioactivity in 3H-labeled paper was

determined by liquid scintillation counting (LSC) and the glycolytic flux was measured by the rate of 3H2O production

Radioactive Glucose Uptake *in vitro*.

Fully differentiated human myotubes were incubated for 3 h in no glucose Krebs-Ringer-Buffer for 3 h to starve them. Myotubes were incubated for 30 min in 100 nM insulin (Actrapid, Novonordisk) in Krebs-Ringer-Bicarbonate buffer. Myotubes were washed quickly with clean Krebs-Ringer-Bicarbonate buffer. Tracer was added 1 µCi 2-[1-^{14}C]-Deoxy Glucose/ml (Perkin Elmer NEC495A001MC) in Krebs Ringer Buffer. Labeling occurred over 1 h. Immediately after, cells were wash twice with ice cold PBS. Then, they were lysed with 1 000 µl of1 M NaOH at room temperature for 30 min.

Colorimetric GLUT4 translocation assay.

L6-GLUT4-MYC rat myoblasts were a kind donation from Prof. Amira Klip, University of Toronto, Hospital for Sick Children, Toronto, Canada. L6-Glut4-Myc cells were grown in α-Minimal Essential Medium (α-MEM) (Gibco, 12571-06) supplemented with 10% FBS 50 IU/ml penicillin and 50 µg/ml streptomycin until confluency and differentiated in α-MEM supplemented with 2% horse serum (HS) 50 IU/ml penicillin and 50 µg/ml streptomycin over 5 days. For insulin stimulation, serum-starve cells (3 hours, 37˚C) prior to experimentation. Insulin (Actrapid, Novonordisk) was added at a concentration of 100 nM for 20 minutes and incubated at 37˚C. Some cells were left untreated for measurements of basal GLUT4-MYC density and background immunoreactivity, which was used to further calculate relative intensity units, basal GLUT4-MYC background was considered with a relative intensity unit of 1. To end the incubation, place cells were placed on ice and quickly washed twice with ice-cold PBS (1 mL per wash). Cells were incubated with cold 3% paraformaldehyde (PFA) in PBS for 15 min at 4°C. PFA was aspirated, cells were washed twice with PBS and incubated with 0.1 M glycine in PBS at 4˚C for 10 min to quench trace formaldehyde. Cells were blocked with 5% goat serum in PBS for 15 min at 4˚C, approx. 1 ml per well). Cells were incubated with 1 mg/ml anti-MYC polyclonal antibody containing 5% goat serum for 60 min at 4˚C, 250 µl approximately. For background staining, two wells were left untreated without the primary antibody per plate. Absorbance determinations give the

background and should be subtracted from each condition. Cells were washed six times with PBS at 4˚C with aspiration, avoid disturbing attached cells between washes. Cells were incubated with a 1:1000 dilution of HRP-conjugated goat anti-rabbit IgG in PBS containing 5% goat serum for 45 min at 4˚C. Incubation can also be performed for 30 min at room temperature. Cells were washed six times with PBS. Cells were incubated with 1 ml per well of OPD peroxidase reagent (Sigma, P9187) at room temperature for up to 30 min protected from light. Stop the reaction with the addition of 250 µl of 3M HCl per well and gentle mixing. Absorbance was read at 492 nm in a multiplate reader (Tecan, Spark)

Mice

Wildtype C57BL/6J mice were obtained from The Jackson Laboratory (000664 | B6). Mice were randomly allocated to different treatment groups, and the investigator was blinded to the group allocation during the experiment as well as during the analysis. All mice were housed at standard housing conditions (22 °C, 12 h inverted light/dark cycle), with ad libitum access to chow diet (18 % proteins, 4.5 % fibers, 4.5 % fat, 6.3 % ashes, Provimi Kliba SA) and water. Health status of all mouse lines was regularly monitored according to FELASA guidelines. Animal experiments were approved by the local animal ethics committee (Kantonales Veterinärsamt Zürich, licenses ZH014/2016 and ZH211/2019), and performed according to local guidelines (TschV, Zurich) and the Swiss animal protection law (TschG). All mice used in this study were between 8-12 weeks old. Both male and female mice were included in the study. rhGDF15 (R&D Systems, 957-GD-025; or donated by Group Leader Dr. Sebastian Jørgensen, Novonordisk) was administered intravenously

Insulin Tolerance Test (ITT)

Mice were food starved during 6 h at the beginning of the dark cycle. Mice body mass was determined prior the beginning of the assay. Insulin (Actrapid, Novonordisk) was diluted in saline and administered intraperitoneally at dose of 0.65 IU/ kg of body weight for females and 0.75 IU/kg body weight for males. Blood was samples by a small cut in the tail vein in the following timepoints: 0 min, 15 min, 30 min, 45 min, 60 min and 90 min with a portable glucose meter.

Glucose Tolerance Test (GTT)

Mice were food starved during 6 h at the beginning of the dark cycle. Mice body mass was determined prior the beginning of the assay. D-Glucose (Sigma G8270) was diluted 10% w/v in saline. Mice body mass was determined prior the beginning of the assay. Dose of glucose was 1 g/ kg of body weight and administered intraperitoneally. Blood was samples by a small cut in the tail vein in the following timepoints: 0 min, 15 min, 30 min, 60 min, 90 min and 120 with a portable glucose meter (AccuCheck AVIVA, 06870317001).

Skeletal muscle *in vivo* insulin stimulation.

Mice were food starved during 6 h at the beginning of the dark cycle, while in starvation they had free access to water. Mice body mass was determined prior the beginning of the assay. Insulin (Actrapid, Novonordisk) was diluted in saline and administered intraperitoneally at dose 1 IU/kg of body weight and skeletal muscle was taken 15 min later. Animals were anesthetized 5 min before muscle was dissected with pentobarbital. Muscle samples were snap frozen and stored at -80℃ until further processing.

***In vivo* radioactive glucose uptake.**

Determination of radioactive glucose uptake in vivo has been described before (10.1038/s41598-017-15548-6). Briefly, mice were food starved during 6 h at the beginning of the dark cycle, while in starvation they had free access to water. Mice body mass was determined prior the beginning of the assay. Mice were injected 5 µCi of 2-[1-^{14}C]-Deoxy Glucose intravenously (Perkin Elmer NEC495A001MC). After 5 min, mice were administered 1 IU/kg body weight of insulin (Actrapid, Novonordisk) intraperitoneally and tissues were taken 15 min later. Of note, mice were euthanized while in anesthesia with pentobarbital 5 min before tissue harvesting. Glucose levels were measured by a small cut in the tail vein in the following timepoints considering insulin administration as zero: -5, 0, 7.5 and 15 min with a portable glucose meter (AccuCheck AVIVA, 06870317001) and blood was sampled to calculate circulating specific activity from plasma. Tissues were quickly dissected, weighted, and digested overnight with 0.5 ml of 1 M NaOH at 65℃. Next day, reaction was neutralized by adding 0.5 ml of 1M HCl. Each sample was split in two parts: 200 µL of lysate should

be mixed with 0.5 ml $ZnSO_4$ and 0.5 ml Ba $(OH)_2$; while another 200 µL of lysate with 1 ml of 6% perchloric acid. (Sigma 244252). Both samples groups were vortexed thoroughly and centrifuged 13 000 RCF for 2 min. A volume of 800 µl supernatants were transferred to 5 ml of scintillation liquid (Perkin Elmer Ultima Gold 6013329) and counted with liquid scintillator (Tri-Carb 2000CA). The subtraction of values of $Ba(OH)_2$ + $ZnSO_4$ from perchloric acid gives a quantitative value of phosphorylated 2DG and thus glucose uptake.

Transfection of packaging cells and lentiviral transduction of HUVEC's.

Briefly, on the first, 2 x 106 HEK 293T cells were plated on 10 cm dishes. On the second day, HEK293T cells were transfected with 3.4 µg of pMD2.G (AddGene, Plasmid #12259),3.4 µg of psPAX2 (AddGene, Plasmid #12260) and 5.4 µg of GIPZ lentiviral shRNA to target *gdf15* (RHS4531) were acquired from Dharmacon (Horizon Discovery; Waterbeach, United Kingdom). A nonsense scrambled shRNA sequence was used as control. Plasmids used for transfection were use with Lipofectamine 2000 (Thermo Fisher 11668019) according to instructions of manufacturer in Opti-MEM (Thermo Fisher 31985070) and incubated for 4h, cell medium was changed to medium containing 10% serum. E4ORF1 HUVEC's or WT HUVEC's were used for lentiviral transduction, they were seeded one day before at a confluence of 8 x 105 cells in a 10 cm dish. Viral particle- containing supernatant were filtered through a 0.45 µm filter mounter syringe. Polybrene was used at a concentration of 8 µg/ml for three consecutive days with viral particle containing supernatants. Transduced HUVEC's were selected with 2 µg/ml of puromycin over 3 days. Puromycin containing medium was changed every 24 h.

RNA extraction and quantitative RT-PCR

RNA isolate from cell cultured HUVECs was extracted using PureLink™ RNA Mini Kit (12183020, Thermo Fischer). RNA purity and concentration were assed via a spectrophotometer (Tecan, Spark). RNA was reverse-transcribed to cDNA by High Capacity cDNA Reverse Transcription Kit (Thermo Fisher, 43-688-13). A SYBR Green-based master mix (Thermo Fisher Scientific, A25778) was used for real-time qPCR analysis with primers listed in Table 1. To compensate for variations in RNA input and

efficiency of reverse-transcription, beta actin was used as a housekeeping gene. The delta-delta CT method was used to normalize the data.

Immunoblotting.

Cells were collected and lysed with [50 mM Tris–HCl pH 7.0, 270 mM sucrose, 5 mM EGTA, 1 mM EDTA, 1 mM sodium orthovanadate, 50 mM glycerophosphate, 5 mM sodium pyrophosphate, 50 mM sodium fluoride, 1 mM DTT, 0.1% Triton-X 100 and a complete protease inhibitor tablet (Roche Applied Science)]. Lysates were centrifuged at 10, 000 RCF for 10 min at 4°C. Supernatant was collected and protein concentration was measured using the DC protein assay kit (5000116, Bio-rad). 5-10 µg of total protein was loaded in a 10-well pre-casted gradient gel (456-8086, Bio-Rad). After electrophoresis, a picture of the gel was taken under UV-light to determine protein loading using strain-free technology. Proteins were transferred onto a PVDF membrane (Bio-rad, 170-4156) with a semi-dry system and subsequently blocked for 1 h at room temperature with 5% milk in 0.1% TBS-Tween. Membranes were incubated overnight at 4 °C with primary antibodies see table below. The appropriate HRP-linked secondary antibodies were used for chemiluminescent detection of proteins. Membranes were scanned with a Chemidoc imaging system (Bio-rad) and quantified using Image Lab 6 software (Bio-rad). Normalization of data was carried out dividing chemiluminescent intensity of a given band by the one of their respective total protein load.

Figures and Diagrams

Figures in this manuscript were created with BioRender.com.

Quantification and statistical analysis

The images presented in the manuscript are representative of the data (quantification of image is approximately the group average) and the image/staining quality. All data represent mean ± SEM. GraphPhad Prism software (version 8.0.0) was used for statistical analyses. Investigators were always blinded to group allocation. Unless otherwise indicated, when comparing two group means, Student’s t-test was used in an unpaired two-tailed fashion. For more than two groups, one-way ANOVA with

Tukey's multiple comparisons test was used and for experimental set-ups with a second variable, two-way ANOVA with Sidak's multiple comparisons test was used. The statistical method used for each experiment is indicated in each figure legend. Asterisks in figure legends denote statistical significance. No experiment-wide multiple test correction was applied. $P>0.05$ is considered non-significant (ns). $P<0.05$ is considered significant (*).

List of primers

GDF15 (h.)	ATACTCACGCCAGAAGTGCGG	GAACAGAGCCCGGTGAAGGC
ACTB(m. h.)	GCTCCTCCTGAGCGCAAG	CATCTGCTGGAAGGTGGACA

List of antibodies

p-AKT (Thr 308)	13038S	Cell signaling
p-AKT (Ser 473)	4060S	Cell signaling
p-AS160 (Thr 642)	8881S	Cell signaling
p-ERK1/2 (p42/44)	9101S	Cell signaling
pAMPK (T172)	2531L	Cell signaling
pIR-β (Tyr 1150/1151)	3024L	Cell signaling

5. Concluding remarks

The secretory properties of ECs in modulation of tissue metabolism is still a developing area. The prevailing view is that metabolism is mostly controlled unidirectionally from signals arising in tissues towards vascular endothelium. While this has been long validated, seminal work has suggested that ECs, as well, exert an influence on their surrounding tissue that may counteract the commencement, progression and even reversal of metabolic disease. In other words, they suggest that the metabolic communication between endothelial cells and tissues is bidirectional instead. However, mechanistic approaches are lacking that may shed light on the molecules, receptors and signaling driving these findings.

In this project, through an unbiased approach, we have revealed the identity of novel angiocrine protein, GDF15. Furthermore, we identified a previously unrecognized property on glucose homeostasis. GDF15 has insulin sensitizing properties, which are acute and independent of body weight loss. Interestingly, by modulating the activity of transcriptional master regulators in ECs, we showed that FOXO1 negatively controls GDF15 expression. This is, FOXO1 activity decreases, while FOXO1 abrogation increase expression of GDF15. This opens a new paradigm in the angiocrine control of tissue metabolism, as angiocrine expression of GDF15 potentially links immunity, inflammation response, regulation of food intake and body mass, adaptations to exercise, glucose handling and insulin sensitivity to vascular biology. Nonetheless, proper experimental examination are necessary to test the limits of these new propositions.

One of the questions that remain to be answered is whether a reduction of food intake is the main purpose of angiocrine GDF15 upon exiting quiescence transcriptional program when FOXO1 is abrogated. This, due to the small yet significant increase in circulating GDF15. It is unlikely there is a non-pathological condition which would lead to a general vascular exit of quiescence that would parallel the genetic model we have used in this project. Rather, the integration of all this knowledge would point towards a

local influence on cells and tissue in close vicinity to endothelial cells secreting GDF15. Along the same train of thought, another question that remains to be answered is whether angiocrine GDF15 would also promote metabolic beneficial effects over longer periods of time, for instance during aging or to even extend life span of an organism.

This project has contributed to the exciting new avenues of research and potential treatments that are being explored where angiocrine secretion of proteins/metabolites produced in different stages of vascular development are taking the central stage.

6. Extended data figures

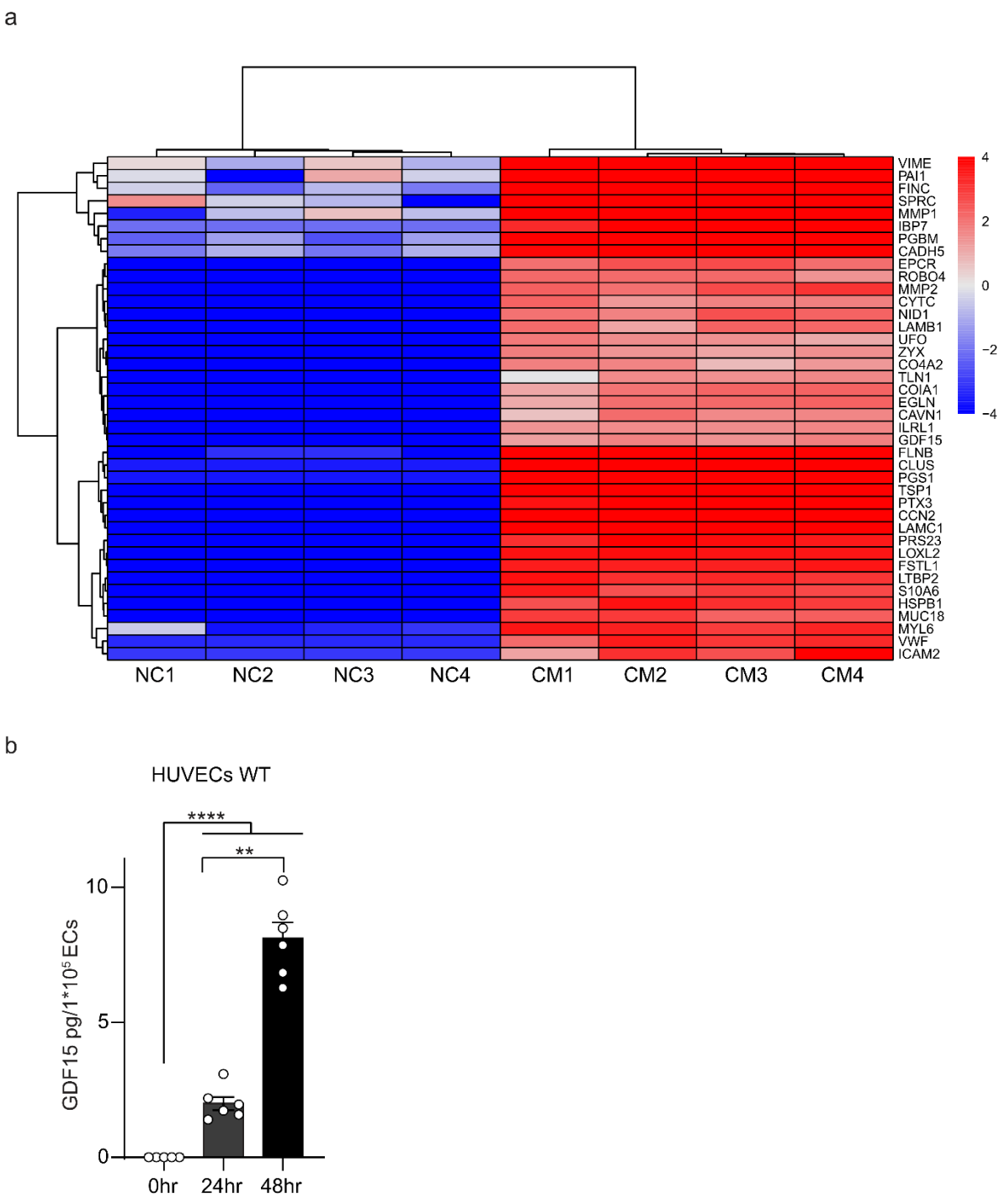

Extended data figure 1 Workflow of generation and quantification of secretome of HUVECs produced in serum-free conditions. **a.** Heatmap of the top 40 most upregulated proteins present in CM. Uniquely identified proteins were included in the analysis, relative abundance is shown as escalated expression compared to control. **b** GDF15 accumulates in HUVECs culture supernatants in standard culturing conditions over time (0 h, 24 and 48 h), GDF15 ELISA. (Student-*t* test) *P<0.05, **P<0.01, ***P<0.001, and ****P<0.0001

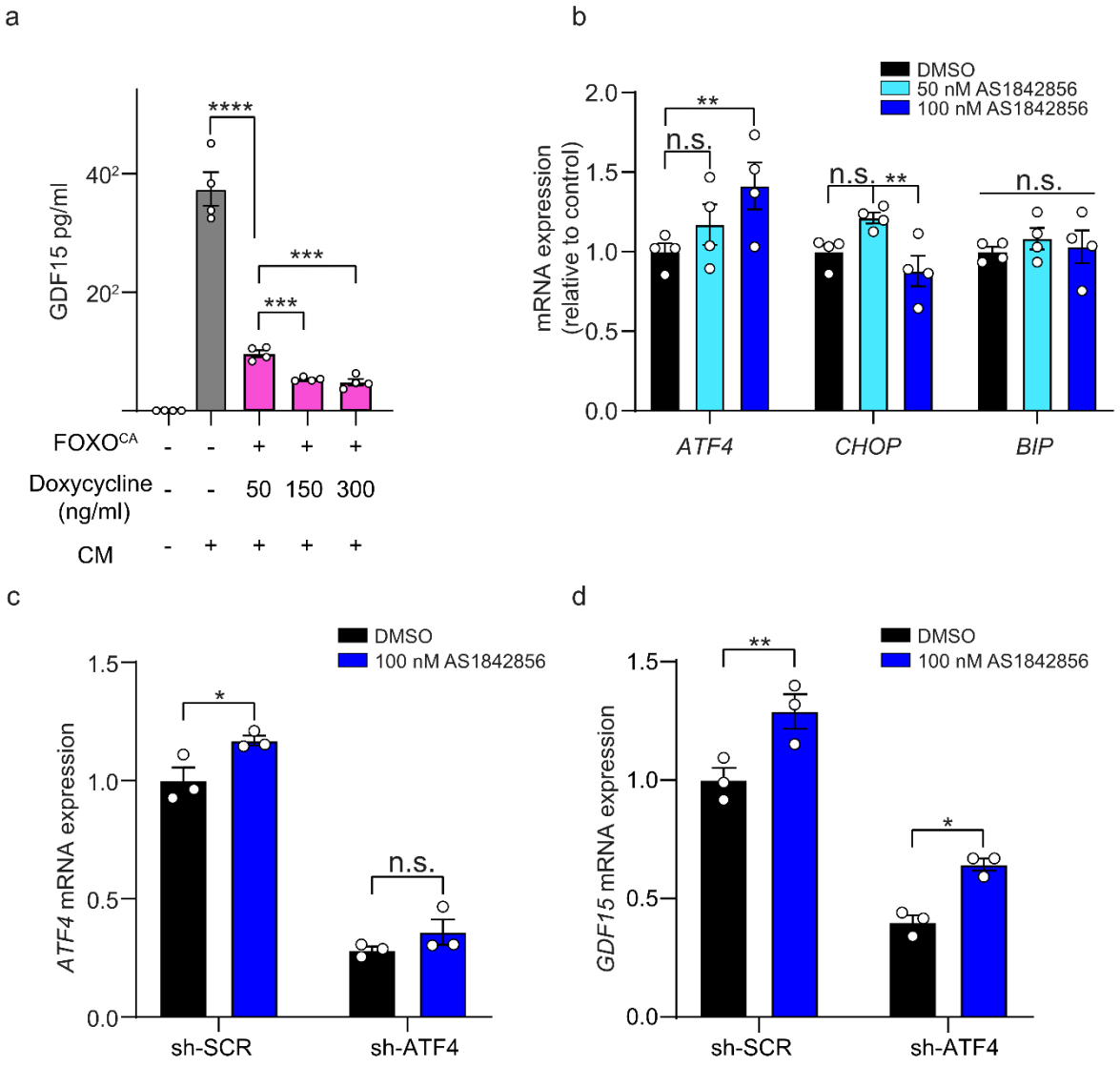

Extended data figure 2 FOXO1, but not NOTCH1, regulates expression of GDF15 in E4ORF1 and WT HUVECs**. a.** Dose response secretion of GDF15, 48 hrs. after induction of FOXO1CA with 50, 150 and 300 ng/ml doxycycline in Tet-On FOXO1CA E4ORF1 HUVECs in serum free conditions (n=4) (Two-way ANOVA and Tukey's multiple comparison). **b** FOXO1 inhibition, AS1842856, increases in a dose response expression of *ATF4* but not *CHOP* (*CHOP* was upregulated with 50 nM but not 100 nM AS1842856 treatment) or *BIP* (Two-way ANOVA with Tukey's multiple comparison). **c.** Knockdown of *ATF4* in HUVECs (n=3) **d** did not blunt *GDF15* upregulation upon FOXO1 pharmacological blockade (n=3) (Student-*t* test). Housekeeping gene *ACTB* was used as control for figure panels **b**, **c**, **d.** Significant values are represented in asterisks as follows *P<0.05, **P<0.01, ***P<0.001, and ****P<0.0001

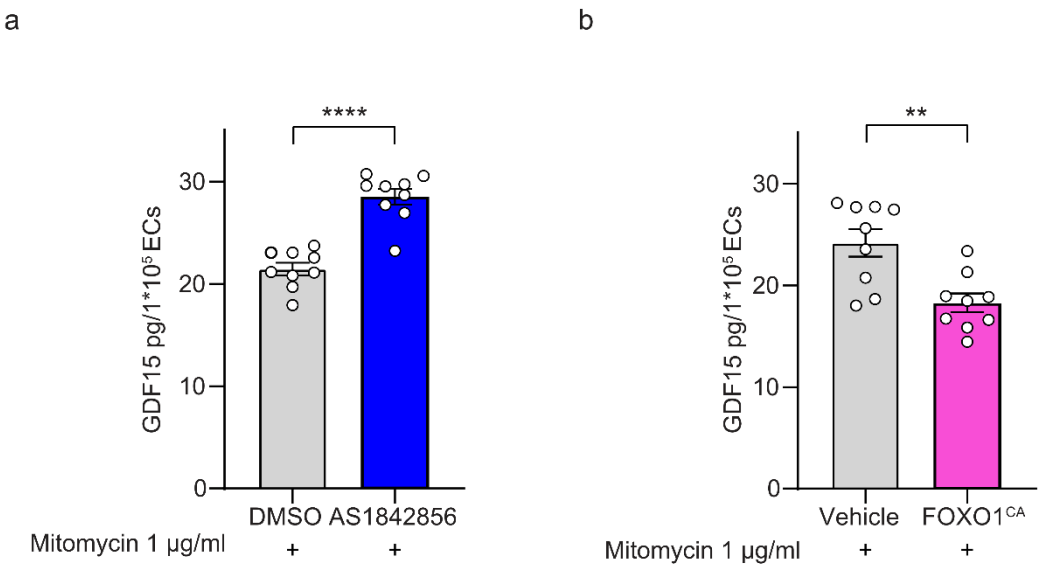

Extended data figure 3 A block of proliferation by Mitomycin C treatment does not blunt FOXO1 negative regulation on GDF15 in vitro. **a**. GDF15 secretion of HUVECs that were treated with FOXO1 inhibitor, AS1842856,100 nM (n= 9), or an equivalent volume of vehicle, DMSO (n= 9), both in the presence of Mitomycin C 1 µg/ml. Cell culture supernatants were collected after 72 hours.(Student-t test) **b**. GDF15 secretion of FOXO1CA HUVECs (n= 9) or controls cells (n= 9) that were treated with Mitomycin C 1 µg/ml. Cell culture supernatants were collected after 72 hours .(Student-t test). Significant values are represented in asterisks as follows *P<0.05, **P<0.01, ***P<0.001, and ****P<0.0001

7. Supplemental Tables.

Supplemental table 1. Full list of identified proteins in proteomic analysis. In yellow are highlighted uniquely identified proteins.

	ProteinName	# Peptides	Ctrl	Group1	log2FC	CI.L	CI.R	Ave Expr	t	P.Value	adj.P.Val	B	nrNAs	M.3_Control.raw	M.2_Control.raw	M.4_Control.raw	M.1_Control.raw	E4.2_Group_1.raw	E4.4_Group_1.raw	E4.3_Group_1.raw	E4.1_Group_1.raw	M.3_Control.transf	M.2_Control.transf	M.4_Control.transf	M.1_Control.transf	E4.2_Group_1.transf	E4.4_Group_1.transf	E4.3_Group_1.transf	E4.1_Group_1.transf	pseudo.Ctrl	pseudo.Group1	pseudo.log2FC	pseudo.P.Value	pseudo.adj.P.Val
2	O75369|FLNB	77	-3.72	5.12	8.84	7.93	9.75	0.70	21.83	2.70E-09	1.25E-06	11.29	0	3.07E+06	2.58E+06	2.20E+06	3.68E+06	3.98E+09	3.26E+09	3.67E+09	9.07E+08	-3.906	-3.175	-4.640	-3.158	5.228	5.395	5.309	4.541	-3.720	5.118	8.838	2.70E-09	1.25E-06
3	P08670|VIME	42	-0.29	8.73	9.02	8.06	9.98	4.22	21.11	3.67E-09	1.25E-06	11.06	0	2.62E+07	1.21E+07	6.43E+07	5.93E+07	3.32E+10	2.79E+10	3.46E+10	2.07E+10	-0.937	-1.052	0.245	0.589	8.394	8.732	8.712	9.086	-0.289	8.731	9.020	3.67E-09	1.25E-06
4	P02751|FINC	46	-1.33	6.83	8.16	7.15	9.17	2.75	18.19	1.42E-08	3.21E-06	10.03	0	1.33E+07	5.01E+06	4.18E+07	2.14E+07	1.20E+10	9.04E+09	1.18E+10	3.25E+09	-1.878	-2.263	-0.379	-0.788	6.871	6.981	7.081	6.397	-1.327	6.832	8.159	1.42E-08	3.21E-06
5	P21333|FLNA	61	-0.27	5.16	5.43	4.73	6.12	2.45	17.52	1.99E-08	3.39E-06	9.75	0	3.96E+07	3.09E+07	3.85E+07	2.78E+07	3.84E+09	3.19E+09	3.96E+09	9.97E+08	-0.366	0.237	-0.499	-0.436	5.177	5.363	5.425	4.679	-0.266	5.161	5.427	1.99E-08	3.39E-06
6	Q02818|NUCB1	23	1.10	5.25	4.16	3.55	4.76	3.18	15.44	6.22E-08	8.46E-06	8.79	0	1.46E+08	4.50E+07	1.17E+08	8.63E+07	4.07E+09	2.80E+09	3.69E+09	1.51E+09	1.444	0.752	1.104	1.093	5.262	5.158	5.318	5.281	1.098	5.255	4.156	6.22E-08	8.46E-06
7	P98160|PGBM	56	-2.47	5.45	7.92	6.96	8.88	2.81	19.41	1.54E-07	1.62E-05	7.32	2	NA	NA	1.08E+07	5.58E+06	5.24E+09	3.56E+09	4.99E+09	1.13E+09	NA	NA	-2.341	-2.598	5.639	5.534	5.775	4.863	-2.469	5.453	7.922	1.54E-07	1.62E-05
8	Q9UBP4|DKK3	5	-1.38	2.93	4.31	3.61	5.01	0.78	13.82	1.67E-07	1.62E-05	7.92	0	1.42E+07	1.00E+07	2.13E+07	1.74E+07	7.51E+08	5.31E+08	7.70E+08	4.31E+08	-1.784	-1.310	-1.358	-1.064	2.743	2.575	2.941	3.460	-1.379	2.930	4.309	1.67E-07	1.62E-05
9	P33151|CADH5	14	-1.92	4.44	6.36	5.40	7.31	2.32	15.55	7.48E-07	5.65E-05	6.24	2	NA	NA	1.49E+07	8.92E+06	2.51E+09	2.34E+09	2.08E+09	5.72E+08	NA	NA	-1.875	-1.965	4.545	4.878	4.447	3.872	-1.920	4.436	6.356	7.48E-07	5.65E-05
10	Q8NBS9|TXND5	7	-1.37	3.62	4.99	4.13	5.84	1.48	13.39	6.70E-07	5.65E-05	6.60	1	2.26E+07	7.70E+06	2.23E+07	NA	1.72E+09	1.18E+09	1.35E+09	2.91E+08	-1.143	-1.673	-1.290	NA	3.980	3.817	3.791	2.891	-1.369	3.620	4.989	6.70E-07	5.65E-05
11	P02545|LMNA	21	-1.52	3.46	4.98	4.09	5.86	1.33	12.92	8.88E-07	6.04E-05	6.36	1	1.72E+07	NA	1.21E+07	2.03E+07	1.09E+09	1.05E+09	9.39E+08	4.96E+08	-1.516	NA	-2.179	-0.859	3.302	3.628	3.241	3.663	-1.518	3.458	4.976	8.88E-07	6.04E-05
12	Q5VTE0|EF1A3	7	-3.01	1.90	4.91	4.00	5.81	-0.21	12.44	1.20E-06	7.42E-05	6.09	1	4.94E+06	3.09E+06	NA	4.59E+06	4.47E+08	4.80E+08	4.53E+08	8.28E+07	-3.246	-2.928	NA	-2.860	1.969	2.419	2.137	1.062	-3.011	1.897	4.908	1.20E-06	7.42E-05
13	P07737|PROF1	6	-0.02	4.32	4.34	3.44	5.25	2.15	10.79	1.47E-06	8.33E-05	5.89	0	2.79E+07	3.29E+07	9.59E+07	2.88E+07	2.27E+09	1.90E+09	2.10E+09	5.75E+08	-0.848	0.319	0.822	-0.384	4.392	4.556	4.459	3.879	-0.023	4.321	4.344	1.47E-06	8.33E-05
14	P19022|CADH2	11	-3.96	0.78	4.74	3.91	5.57	-0.80	13.32	2.23E-06	1.08E-04	5.39	2	2.82E+06	NA	3.66E+06	NA	1.95E+08	1.81E+08	2.10E+08	5.64E+07	-4.023	NA	-3.903	NA	0.733	0.902	0.970	0.504	-3.963	0.777	4.740	2.23E-06	1.08E-04
15	P62857|RS28	2	-2.52	2.12	4.64	3.82	5.45	0.57	13.34	2.22E-06	1.08E-04	5.40	2	9.54E+06	NA	8.36E+06	NA	4.78E+08	3.94E+08	4.34E+08	1.82E+08	-2.335	NA	-2.708	NA	2.071	2.110	2.073	2.207	-2.521	2.115	4.637	2.22E-06	1.08E-04
16	Q12841|FSTL1	4	-4.10	3.49	7.60	6.46	8.74	1.97	16.12	2.39E-06	1.08E-04	4.60	3	NA	NA	NA	1.82E+06	1.18E+09	9.34E+08	1.21E+09	4.40E+08	NA	NA	NA	-4.105	3.412	3.452	3.621	3.489	-4.105	3.494	7.599	2.39E-06	1.08E-04
17	P10909|CLUS	12	-3.51	5.43	8.94	7.54	10.33	3.64	15.48	3.07E-06	1.30E-04	4.46	3	NA	NA	4.80E+06	NA	3.97E+09	4.45E+09	4.72E+09	1.17E+09	NA	NA	-3.511	NA	5.226	5.879	5.690	4.907	-3.511	5.425	8.937	3.07E-06	1.30E-04
18	P09382|LEG1	4	2.55	5.15	2.61	2.00	3.22	3.85	9.62	3.95E-06	1.58E-04	4.93	0	2.90E+08	1.37E+08	3.33E+08	3.27E+08	3.38E+09	2.73E+09	3.41E+09	1.54E+09	2.390	2.285	2.625	2.888	4.985	5.121	5.198	5.312	2.547	5.154	2.607	3.95E-06	1.58E-04
19	P60660|MYL6	5	-2.65	3.33	5.98	4.54	7.42	0.34	9.35	5.00E-06	1.86E-04	4.69	0	5.62E+06	1.78E+06	3.80E+07	3.21E+06	8.59E+08	9.11E+08	1.02E+09	4.68E+08	-3.067	-3.685	-0.517	-3.345	2.943	3.414	3.373	3.580	-2.653	3.327	5.981	5.00E-06	1.86E-04
20	zz|Y-FGC2Cont00440|	26	-2.43	4.82	7.25	5.64	8.87	1.71	10.32	5.18E-06	1.86E-04	4.73	1	6.53E+06	NA	3.73E+07	2.15E+06	2.78E+09	2.48E+09	2.87E+09	1.01E+09	-2.860	NA	-0.545	-3.886	4.696	4.970	4.936	4.694	-2.430	4.824	7.254	5.18E-06	1.86E-04
21	Q14118|DAG1	10	-2.26	1.37	3.63	2.80	4.47	-0.19	9.96	6.83E-06	2.32E-04	4.47	1	7.68E+06	3.89E+06	1.87E+07	NA	2.99E+08	2.41E+08	2.92E+08	9.69E+07	-2.635	-2.610	-1.541	NA	1.372	1.349	1.469	1.291	-2.262	1.370	3.632	6.83E-06	2.32E-04
22	P68371|TBB4B	8	-4.09	0.22	4.30	3.31	5.30	-1.22	10.16	1.47E-05	4.59E-04	3.76	2	2.12E+06	NA	NA	2.35E+06	1.02E+08	1.13E+08	1.30E+08	6.42E+07	-4.416	NA	NA	-3.762	-0.239	0.166	0.241	0.692	-4.089	0.215	4.304	1.47E-05	4.59E-04
23	P80404|GABT	2	-2.73	0.31	3.04	2.26	3.81	-1.00	9.00	1.49E-05	4.59E-04	3.71	1	6.44E+06	2.84E+06	1.13E+07	NA	1.36E+08	1.01E+08	1.58E+08	5.59E+07	-2.880	-3.044	-2.271	NA	0.193	0.000	0.537	0.492	-2.731	0.305	3.037	1.49E-05	4.59E-04
24	P21810|PGS1	10	-3.57	5.20	8.76	6.97	10.56	3.45	11.83	1.58E-05	4.66E-04	3.40	3	NA	NA	4.62E+06	NA	5.32E+09	3.52E+09	4.25E+09	6.63E+08	NA	NA	-3.566	NA	5.664	5.515	5.530	4.085	-3.566	5.199	8.765	1.58E-05	4.66E-04
25	P26022|PTX3	11	-4.13	4.80	8.93	7.02	10.83	3.01	11.36	2.02E-05	5.28E-04	3.22	3	NA	NA	NA	1.79E+06	3.52E+09	3.74E+09	2.78E+09	4.96E+08	NA	NA	NA	-4.127	5.045	5.607	4.886	3.662	-4.127	4.800	8.927	2.02E-05	5.28E-04
26	P29401|TKT	9	-1.71	1.23	2.94	2.16	3.71	-0.03	8.65	2.00E-05	5.28E-04	3.42	1	NA	8.84E+06	1.82E+07	8.39E+06	2.50E+08	2.00E+08	2.16E+08	1.33E+08	NA	-1.484	-1.584	-2.048	1.102	1.056	1.014	1.748	-1.705	1.230	2.935	2.00E-05	5.28E-04
27	P30530|UFO	3	-4.61	1.49	6.10	4.80	7.39	0.27	11.39	1.99E-05	5.28E-04	3.23	3	NA	NA	NA	1.26E+06	3.22E+08	2.72E+08	2.22E+08	1.46E+08	NA	NA	NA	-4.606	1.482	1.538	1.057	1.889	-4.606	1.492	6.098	1.99E-05	5.28E-04
28	zz|Y-FGC2Cont00087|	15	-3.09	4.00	7.08	5.22	8.95	1.64	8.91	3.58E-05	9.01E-04	2.93	2	NA	NA	2.15E+06	1.26E+07	1.60E+09	1.33E+09	1.68E+09	6.20E+08	NA	NA	-4.671	-1.503	3.874	4.007	4.121	3.987	-3.087	3.997	7.084	3.58E-05	9.01E-04
29	O14979|HNRDL	3	-2.33	0.06	2.39	1.69	3.09	-0.96	7.86	4.09E-05	9.94E-04	2.70	1	NA	4.27E+06	1.10E+07	7.59E+06	1.55E+08	1.09E+08	1.01E+08	3.70E+07	NA	-2.484	-2.314	-2.183	0.386	0.109	-0.137	-0.107	-2.327	0.063	2.390	4.09E-05	9.94E-04
30	Q15904|VAS1	4	-1.10	2.22	3.31	2.26	4.36	0.56	7.11	4.76E-05	1.12E-03	2.42	0	4.87E+07	1.69E+07	2.12E+07	6.74E+06	5.01E+08	4.61E+08	4.85E+08	1.74E+08	-0.080	-0.598	-1.360	-2.343	2.139	2.357	2.238	2.139	-1.095	2.218	3.313	4.76E-05	1.12E-03
31	P31948|STIP1	14	1.45	3.83	2.38	1.61	3.14	2.64	7.01	5.36E-05	1.22E-03	2.30	0	1.77E+08	4.93E+07	2.07E+08	9.86E+07	1.16E+09	1.35E+09	1.27E+09	7.13E+08	1.709	0.876	1.936	1.273	3.388	4.028	3.701	4.190	1.449	3.827	2.378	5.36E-05	1.22E-03
32	zz|Y-FGC2Cont00316|	6	-2.82	0.04	2.86	1.94	3.79	-1.39	6.97	5.58E-05	1.22E-03	2.26	0	5.22E+06	2.80E+06	1.78E+07	3.02E+06	1.24E+08	1.03E+08	1.22E+08	3.80E+07	-3.171	-3.062	-1.612	-3.427	0.060	0.031	0.150	-0.068	-2.818	0.043	2.861	5.58E-05	1.22E-03
33	P04275|VWF	12	-3.28	2.98	6.26	4.66	7.86	1.73	9.48	5.94E-05	1.26E-03	2.38	3	NA	NA	NA	3.36E+06	8.98E+08	9.79E+08	9.51E+08	1.73E+08	NA	NA	NA	-3.281	3.010	3.527	3.260	2.130	-3.281	2.982	6.262	5.94E-05	1.26E-03
34	P05121|PAI1	21	-1.18	7.45	8.63	5.96	11.31	3.75	7.41	6.32E-05	1.26E-03	2.27	1	NA	1.06E+06	4.71E+07	8.45E+07	2.14E+10	1.62E+10	2.04E+10	3.01E+09	NA	-4.402	-0.206	1.065	7.735	7.883	7.910	6.284	-1.181	7.453	8.634	6.32E-05	1.26E-03
35	Q09028|RBBP4	3	-5.26	-1.67	3.59	2.56	4.62	-2.87	8.21	6.21E-05	1.26E-03	2.40	2	1.52E+06	NA	1.10E+06	NA	5.02E+07	4.03E+07	3.43E+07	8.87E+06	-4.880	NA	-5.640	NA	-1.290	-1.433	-1.776	-2.184	-5.260	-1.671	3.589	6.21E-05	1.26E-03
36	P21291|CSRP1	3	-1.10	2.13	3.23	2.29	4.17	1.05	8.07	6.92E-05	1.35E-03	2.30	2	2.00E+07	NA	NA	1.97E+07	5.14E+08	5.18E+08	3.33E+08	1.71E+08	-1.309	NA	NA	-0.897	2.177	2.536	1.672	2.120	-1.103	2.126	3.230	6.92E-05	1.35E-03
37	Q96HC4|PDLI5	4	-1.81	1.00	2.81	1.86	3.75	-0.40	6.70	7.66E-05	1.45E-03	1.94	0	9.32E+06	4.48E+06	1.53E+07	2.42E+07	2.50E+08	1.70E+08	2.06E+08	8.73E+07	-2.368	-2.417	-1.829	-0.618	1.105	0.810	0.944	1.140	-1.808	1.000	2.808	7.66E-05	1.45E-03
38	P07437|TBB5	10	-2.23	2.11	4.34	3.12	5.56	1.24	8.60	0.000106	1.89E-03	1.89	3	NA	NA	1.16E+07	NA	4.34E+08	4.25E+08	3.83E+08	2.09E+08	NA	NA	-2.229	NA	1.927	2.229	1.884	2.410	-2.229	2.112	4.341	1.06E-04	1.89E-03
39	P48681|NEST	11	-5.52	-0.57	4.95	3.56	6.34	-1.56	8.60	0.000105	1.89E-03	1.89	3	NA	NA	NA	6.38E+05	6.12E+07	5.87E+07	1.08E+08	3.02E+07	NA	NA	NA	-5.521	-0.994	-0.849	-0.034	-0.402	-5.521	-0.570	4.951	1.05E-04	1.89E-03
40	P52943|CRIP2	3	-1.48	1.42	2.90	1.86	3.94	-0.03	6.28	0.000126	2.20E-03	1.42	0	1.81E+07	1.90E+07	2.26E+07	5.01E+06	3.45E+08	2.30E+08	2.47E+08	1.21E+08	-1.451	-0.436	-1.272	-2.744	1.583	1.275	1.214	1.617	-1.476	1.422	2.898	1.26E-04	2.20E-03
41	P09651|ROA1	4	-3.74	-0.25	3.48	2.34	4.63	-2.00	7.16	0.000152	2.58E-03	1.51	2	3.63E+06	NA	7.23E+06	1.24E+06	9.62E+07	9.50E+07	8.85E+07	NA	-3.671	NA	-2.919	-4.623	-0.321	-0.100	-0.341	NA	-3.738	-0.254	3.484	1.52E-04	2.58E-03
42	Q96GK7|FAH2A	4	-3.03	-0.25	2.78	1.86	3.69	-1.18	7.12	0.000157	2.61E-03	1.49	2	5.69E+06	NA	6.76E+06	NA	7.07E+07	9.08E+07	1.04E+08	4.04E+07	-3.050	NA	-3.017	NA	-0.779	-0.170	-0.091	0.020	-3.033	-0.255	2.778	1.57E-04	2.61E-03
43	P11021|BIP	13	-1.52	0.98	2.50	1.56	3.45	-0.27	5.97	0.000186	2.95E-03	1.02	0	1.16E+07	5.87E+06	2.22E+07	2.32E+07	1.76E+08	2.29E+08	1.53E+08	1.19E+08	-2.061	-2.046	-1.296	-0.679	0.579	1.271	0.494	1.583	-1.521	0.982	2.502	1.86E-04	2.95E-03
44	Q99714|HCD2	4	-3.89	-0.92	2.97	1.90	4.03	-2.19	6.38	0.000183	2.95E-03	1.18	1	NA	3.18E+06	3.62E+06	1.05E+06	6.08E+07	5.61E+07	6.81E+07	1.97E+07	NA	-2.889	-3.921	-4.849	-1.005	-0.917	-0.737	-1.021	-3.886	-0.920	2.967	1.83E-04	2.95E-03
45	P09496|CLCA	3	-3.28	-0.61	2.67	1.70	3.64	-1.76	6.30	0.0002	3.09E-03	1.09	1	4.60E+06	3.25E+06	4.40E+06	NA	5.31E+07	5.09E+07	1.13E+08	3.47E+07	-3.344	-2.859	-3.637	NA	-1.206	-1.068	0.030	-0.203	-3.280	-0.612	2.668	2.00E-04	3.09E-03
46	P03956|MMP1	16	-1.38	5.52	6.90	4.50	9.30	3.22	6.75	0.000221	3.35E-03	1.15	2	NA	NA	5.16E+06	6.21E+07	6.07E+09	2.36E+09	5.92E+09	1.54E+09	NA	NA	-3.408	0.650	5.860	4.892	6.035	5.308	-1.379	5.524	6.902	2.21E-04	3.35E-03
47	Q43396|TXNL1	7	-1.51	0.80	2.31	1.41	3.20	-0.36	5.78	0.000237	3.46E-03	0.77	0	1.17E+07	7.77E+06	3.85E+07	9.97E+06	1.50E+08	1.95E+08	2.41E+08	6.24E+07	-2.058	-1.661	-0.498	-1.816	0.342	1.016	1.179	0.652	-1.508	0.797	2.306	2.37E-04	3.46E-03
48	P63261|ACTG	16	4.50	7.10	2.60	1.58	3.61	5.80	5.77	0.000239	3.46E-03	0.76	0	1.86E+09	3.51E+08	2.48E+09	7.11E+08	1.35E+10	1.04E+10	1.44E+10	4.18E+09	4.964	3.573	5.531	3.935	7.046	7.201	7.382	6.760	4.501	7.097	2.597	2.39E-04	3.46E-03

	ProteinName	# Peptides	Ctrl	Group1	log2FC	CI.L	CI.R	Ave Expr	t	P.Value	adj.P.Val	B	nrNAs	M.3_Control.raw	M.2_Control.raw	M.4_Control.raw	M.1_Control.raw	E4.2_Group1.raw	E4.4_Group1.raw	E4.3_Group1.raw	E4.1_Group1.raw	M.3_Control.transf	M.2_Control.transf	M.4_Control.transf	M.1_Control.transf	E4.2_Group_1.transf	E4.4_Group_1.transf	E4.3_Group_1.transf	E4.1_Group_1.transf	pseudo.Ctrl	pseudo.Group1	pseudo.log2FC	pseudo.P.Value	pseudo.adj.P.Val
49	P35241|RADI	8	-3.74	-1.31	2.43	1.52	3.34	-2.35	6.11	0.000247	3.50E-03	0.87	1	3.28E+06	1.31E+06	NA	3.33E+06	4.36E+07	3.13E+07	4.66E+07	2.63E+07	-3.813	-4.105	NA	-3.292	-1.499	-1.827	-1.312	-0.602	-3.737	-1.310	2.427	2.47E-04	3.50E-03
50	P61081|UBC12	4	-3.06	-0.39	2.68	1.61	3.74	-1.73	5.66	0.000277	3.84E-03	0.61	0	2.94E+06	2.06E+06	1.70E+07	3.77E+06	8.79E+07	7.89E+07	7.29E+07	3.79E+07	-3.962	-3.483	-1.682	-3.126	-0.455	-0.388	-0.635	-0.074	-3.063	-0.388	2.676	2.77E-04	3.84E-03
51	Q9Y490|TLN1	13	-4.52	1.16	5.68	3.79	7.58	0.02	7.25	0.000283	3.85E-03	1.01	3	NA	NA	NA	1.34E+06	3.24E+08	2.79E+08	3.26E+08	3.82E+07	NA	NA	NA	-4.523	1.489	1.578	1.637	-0.060	-4.523	1.161	5.684	2.83E-04	3.85E-03
52	P09486|SPRC	6	-1.13	5.76	6.89	4.19	9.59	2.81	5.85	0.000336	4.48E-03	0.56	1	2.61E+06	NA	1.60E+08	2.09E+07	7.37E+09	5.57E+09	6.61E+09	8.57E+08	-4.130	NA	1.562	-0.819	6.149	6.228	6.201	4.459	-1.129	5.759	6.888	3.36E-04	4.48E-03
53	P61978|HNRPK	9	-0.01	1.92	1.93	1.16	2.70	1.09	5.74	0.00038	4.97E-03	0.43	1	4.15E+07	3.07E+07	5.58E+07	NA	4.16E+08	4.12E+08	4.69E+08	1.08E+08	-0.302	0.226	0.038	NA	1.862	2.182	2.188	1.444	-0.013	1.919	1.932	3.80E-04	4.97E-03
54	Q9Y220|SGT1	2	-2.40	0.06	2.46	1.47	3.44	-0.99	5.71	0.000394	5.05E-03	0.39	1	8.22E+06	3.77E+06	1.37E+07	NA	1.07E+08	7.63E+07	9.83E+07	8.07E+07	-2.541	-2.654	-1.992	NA	-0.158	-0.440	-0.181	1.024	-2.396	0.062	2.457	3.94E-04	5.05E-03
55	O94985|CSTN1	7	-1.32	1.81	3.13	1.87	4.39	0.47	5.69	0.000406	5.11E-03	0.36	1	3.49E+07	8.88E+06	1.42E+07	NA	5.66E+08	4.27E+08	4.55E+08	5.75E+07	-0.541	-1.478	-1.945	NA	2.323	2.237	2.143	0.533	-1.321	1.809	3.130	4.06E-04	5.11E-03
56	Q9BQE3|TBA1C	6	-0.59	2.86	3.45	1.99	4.91	1.13	5.32	0.000435	5.38E-03	0.14	0	5.58E+07	2.35E+07	5.80E+07	6.30E+06	9.85E+08	8.06E+08	1.08E+09	1.20E+08	0.110	-0.139	0.095	-2.435	3.148	3.224	3.460	1.601	-0.592	2.858	3.450	4.35E-04	5.38E-03
57	Q06124|PTN11	5	-2.00	0.47	2.47	1.40	3.54	-0.77	5.20	0.000508	6.16E-03	-0.02	0	1.26E+07	4.32E+06	2.22E+07	6.99E+06	2.58E+08	2.30E+08	1.02E+08	2.96E+07	-1.955	-2.467	-1.296	-2.295	1.150	1.273	-0.131	-0.432	-2.003	0.465	2.468	5.08E-04	6.16E-03
58	Q9Y3F4|STRAP	5	-3.67	-1.34	2.33	1.35	3.30	-2.34	5.49	0.000518	6.17E-03	0.11	1	2.53E+06	1.51E+06	7.17E+06	NA	6.19E+07	4.34E+07	5.39E+07	1.02E+07	-4.172	-3.908	-2.931	NA	-0.977	-1.315	-1.092	-1.985	-3.670	-1.342	2.328	5.18E-04	6.17E-03
59	O43852|CALU	8	0.13	1.74	1.61	0.89	2.32	0.94	5.06	0.000615	6.66E-03	-0.21	0	7.97E+07	2.16E+07	6.74E+07	3.48E+07	2.80E+08	3.37E+08	4.10E+08	1.40E+08	0.603	-0.257	0.312	-0.130	1.274	1.870	1.984	1.828	0.132	1.739	1.607	6.15E-04	6.66E-03
60	P14618|KPYM	14	2.09	4.00	1.91	1.07	2.76	3.04	5.08	0.000598	6.66E-03	-0.19	0	1.74E+08	1.21E+08	4.28E+08	1.23E+08	1.39E+09	1.18E+09	1.91E+09	7.25E+08	1.685	2.111	2.986	1.569	3.662	3.810	4.316	4.215	2.088	4.001	1.913	5.98E-04	6.66E-03
61	P22626|ROA2	6	-2.25	0.26	2.51	1.39	3.63	-0.99	5.06	0.000617	6.66E-03	-0.22	0	1.64E+07	3.28E+06	2.24E+07	3.38E+06	1.68E+08	1.64E+08	1.22E+08	3.12E+07	-1.588	-2.848	-1.282	-3.275	0.509	0.746	0.146	-0.355	-2.248	0.262	2.510	6.17E-04	6.66E-03
62	P30101|PDIA3	6	-3.95	-0.63	3.31	1.91	4.72	-2.05	5.40	0.000576	6.66E-03	0.00	1	1.52E+06	1.74E+06	5.79E+06	NA	1.18E+08	9.93E+07	8.34E+07	9.63E+06	-4.881	-3.720	-3.240	NA	-0.014	-0.031	-0.430	-2.064	-3.947	-0.635	3.312	5.76E-04	6.66E-03
63	Q96AE4|FUBP1	7	-4.00	0.10	4.10	2.43	5.77	-1.26	5.75	0.000608	6.66E-03	0.12	2	6.74E+06	6.00E+05	NA	NA	1.16E+08	1.65E+08	1.38E+08	2.56E+07	-2.816	-5.179	NA	NA	-0.038	0.759	0.329	-0.644	-3.998	0.102	4.099	6.08E-04	6.66E-03
64	Q99798|ACON	12	1.89	4.99	3.10	1.73	4.47	3.44	5.09	0.000591	6.66E-03	-0.17	0	2.64E+08	1.15E+08	5.16E+08	3.83E+07	3.05E+09	2.88E+09	3.38E+09	1.03E+09	2.262	2.036	3.258	0.000	4.834	5.205	5.184	4.728	1.889	4.988	3.099	5.91E-04	6.66E-03
65	Q12904|AIMP1	3	-4.14	-1.65	2.49	1.38	3.60	-2.89	5.05	0.000628	6.68E-03	-0.24	0	2.25E+06	7.18E+05	2.83E+06	4.10E+06	2.72E+07	6.02E+07	2.52E+07	1.59E+07	-4.336	-4.932	-4.276	-3.014	-2.206	-0.810	-2.247	-1.336	-4.140	-1.650	2.490	6.28E-04	6.68E-03
66	Q15811|ITSN1	5	-0.48	-1.93	-1.45	-2.11	-0.80	-1.20	-5.01	0.000665	6.96E-03	-0.30	0	2.79E+07	1.81E+07	3.76E+07	3.79E+07	2.73E+07	3.13E+07	3.47E+07	1.06E+07	-0.849	-0.503	-0.534	-0.015	-2.200	-1.824	-1.759	-1.928	-0.475	-1.928	-1.452	6.65E-04	6.96E-03
67	Q9BRK5|CAB45	10	-0.81	2.11	2.92	1.77	4.06	1.53	6.17	0.000697	7.18E-03	0.17	3	NA	1.44E+07	NA	NA	4.95E+08	4.04E+08	4.73E+08	1.54E+08	NA	-0.810	NA	NA	2.122	2.152	2.201	1.963	-0.810	2.109	2.919	6.97E-04	7.18E-03
68	P56945|BCAR1	2	-5.47	-2.34	3.13	1.87	4.40	-2.96	6.00	0.000815	8.27E-03	0.01	3	NA	NA	1.24E+06	NA	2.81E+07	1.70E+07	2.39E+07	9.42E+06	NA	NA	-5.469	NA	-2.157	-2.770	-2.324	-2.096	-5.469	-2.337	3.132	8.15E-04	8.27E-03
69	Q16270|IBP7	6	-2.08	5.55	7.63	4.51	10.74	4.02	5.93	0.000868	8.68E-03	-0.05	3	NA	NA	NA	8.20E+06	8.25E+09	6.41E+09	6.65E+09	3.67E+08	NA	NA	NA	-2.080	6.317	6.445	6.210	3.225	-2.080	5.549	7.629	8.68E-04	8.68E-03
70	P10809|CH60	14	3.00	4.34	1.34	0.71	1.97	3.67	4.79	0.000908	8.82E-03	-0.62	0	4.02E+08	1.95E+08	5.90E+08	3.38E+08	1.89E+09	1.70E+09	1.97E+09	8.67E+08	2.844	2.766	3.452	2.934	4.123	4.381	4.364	4.475	2.999	4.336	1.337	9.08E-04	8.82E-03
71	P28838|AMPL	5	-2.84	-0.48	2.37	1.29	3.44	-1.49	5.04	0.000906	8.82E-03	-0.47	1	7.81E+06	1.70E+06	1.21E+07	NA	7.03E+07	6.87E+07	1.30E+08	2.35E+07	-2.612	-3.746	-2.170	NA	-0.788	-0.602	0.247	-0.767	-2.843	-0.477	2.365	9.06E-04	8.82E-03
72	P38646|GRP75	24	2.74	4.65	1.91	1.00	2.82	3.70	4.72	0.001004	9.62E-03	-0.72	0	5.05E+08	1.03E+08	6.26E+08	2.24E+08	2.76E+09	2.58E+09	2.30E+09	7.60E+08	3.156	1.884	3.538	2.379	4.683	5.034	4.603	4.284	2.739	4.651	1.912	1.00E-03	9.62E-03
73	P62760|VISL1	3	-1.22	-4.12	-2.90	-4.20	-1.60	-2.67	-5.23	0.00107	9.97E-03	-0.49	2	2.18E+07	1.27E+07	1.98E+07	NA	1.32E+07	8.85E+06	3.40E+06	NA	-1.195	-0.991	-1.463	NA	-3.285	-3.788	-5.284	NA	-1.216	-4.119	-2.902	1.07E-03	9.97E-03
74	Q93052|LPP	2	-0.82	-2.26	-1.44	-2.11	-0.77	-1.44	-4.91	0.001069	9.97E-03	-0.64	1	3.08E+07	1.56E+07	2.54E+07	2.17E+07	2.77E+07	2.19E+07	2.55E+07	NA	-0.715	-0.703	-1.099	-0.766	-2.174	-2.377	-2.226	NA	-0.821	-2.259	-1.439	1.07E-03	9.97E-03
75	O43399|TPD54	6	-1.98	-0.06	1.91	0.99	2.84	-1.02	4.66	0.001094	1.01E-02	-0.81	0	1.98E+07	6.92E+06	1.48E+07	4.51E+06	9.27E+07	1.32E+08	7.44E+07	4.95E+07	-1.325	-1.821	-1.877	-2.886	-0.376	0.411	-0.604	0.315	-1.977	-0.063	1.914	1.09E-03	1.01E-02
76	P20908|CO5A1	12	0.25	2.47	2.22	1.22	3.22	1.73	5.19	0.001115	1.01E-02	-0.50	2	NA	NA	5.14E+07	5.88E+07	6.78E+08	6.28E+08	5.90E+08	1.48E+08	NA	NA	-0.080	0.577	2.591	2.835	2.538	1.909	0.248	2.468	2.220	1.12E-03	1.01E-02
77	Q9Y524|HEBP2	5	-3.59	-1.64	1.95	1.06	2.83	-2.29	5.16	0.001154	1.03E-02	-0.54	2	4.50E+06	NA	NA	2.27E+06	3.86E+07	3.57E+07	3.07E+07	1.60E+07	-3.375	NA	NA	-3.808	-1.682	-1.618	-1.948	-1.322	-3.592	-1.643	1.949	1.15E-03	1.03E-02
78	O14737|PDCD5	7	0.35	1.99	1.64	0.83	2.44	1.17	4.59	0.001208	1.07E-02	-0.91	0	5.04E+07	2.06E+07	1.02E+08	7.18E+07	4.86E+08	3.92E+08	3.42E+08	1.63E+08	-0.031	-0.325	0.916	0.846	2.095	2.105	1.711	2.050	0.352	1.990	1.638	1.21E-03	1.07E-02
79	O75874|IDHC	7	0.36	1.76	1.40	0.71	2.09	1.06	4.55	0.001282	1.09E-02	-0.97	0	5.29E+07	3.12E+07	1.09E+08	4.20E+07	3.67E+08	2.98E+08	4.10E+08	1.27E+08	0.036	0.247	1.014	0.124	1.676	1.679	1.983	1.687	0.355	1.757	1.401	1.28E-03	1.09E-02
80	P23468|PTPRD	2	-0.99	-3.45	-2.46	-3.60	-1.33	-2.22	-5.09	0.001255	1.09E-02	-0.66	2	3.07E+07	1.23E+07	2.35E+07	NA	1.77E+07	1.36E+07	6.18E+06	NA	-0.716	-1.028	-1.212	NA	-2.841	-3.121	-4.376	NA	-0.985	-3.446	-2.461	1.26E-03	1.09E-02
81	P26368|U2AF2	5	-3.30	-1.36	1.94	1.00	2.87	-2.19	4.77	0.001287	1.09E-02	-0.83	1	6.91E+06	1.95E+06	4.67E+06	NA	7.62E+07	3.49E+07	4.89E+07	1.09E+07	-2.782	-3.558	-3.551	NA	-0.667	-1.657	-1.238	-1.881	-3.297	-1.361	1.936	1.29E-03	1.09E-02
82	P35080|PROF2	4	-0.48	1.03	1.51	0.76	2.26	0.27	4.51	0.001353	1.12E-02	-1.03	0	3.05E+07	3.33E+07	3.22E+07	2.15E+07	2.22E+08	1.91E+08	2.03E+08	9.59E+07	-0.728	0.336	-0.755	-0.779	0.924	0.986	0.917	1.276	-0.481	1.026	1.507	1.35E-03	1.12E-02
83	Q86V48|LUZP1	2	-1.65	-6.22	-4.57	-6.44	-2.69	-5.08	-6.16	0.001345	1.12E-02	-0.35	4	1.56E+07	NA	NA	NA	NA	1.24E+06	1.62E+06	9.66E+05	-1.651	NA	NA	NA	NA	-6.844	-6.404	-5.406	-1.651	-6.218	-4.568	1.35E-03	1.12E-02
84	Q9NR12|PDLI7	3	-3.18	-0.27	2.92	1.52	4.31	-1.24	4.91	0.00155	1.27E-02	-0.84	2	NA	5.08E+06	NA	1.80E+06	8.60E+07	1.19E+08	6.78E+07	3.72E+07	NA	-2.246	NA	-4.123	-0.488	0.252	-0.743	-0.098	-3.185	-0.269	2.915	1.55E-03	1.27E-02
85	P0DMV9|HS71B	15	1.33	3.42	2.09	1.00	3.17	2.38	4.33	0.001784	1.44E-02	-1.31	0	1.67E+08	6.67E+07	2.71E+08	4.09E+07	1.15E+09	1.34E+09	1.02E+09	2.96E+08	1.625	1.292	2.324	0.086	3.383	4.010	3.372	2.913	1.332	3.419	2.087	1.78E-03	1.44E-02
86	P13598|ICAM2	3	-3.03	2.84	5.87	3.12	8.61	1.67	5.17	0.001798	1.44E-02	-0.76	3	NA	NA	NA	4.06E+06	6.89E+08	7.66E+08	2.03E+09	8.99E+07	NA	NA	NA	-3.026	2.614	3.144	4.414	1.182	-3.026	2.839	5.865	1.80E-03	1.44E-02
87	Q15366|PCBP2	6	-0.57	1.22	1.79	0.87	2.71	0.45	4.46	0.001929	1.53E-02	-1.25	1	4.22E+07	1.89E+07	2.73E+07	NA	3.59E+08	2.01E+08	3.32E+08	5.65E+07	-0.276	-0.440	-0.997	NA	1.641	1.063	1.666	0.508	-0.571	1.220	1.791	1.93E-03	1.53E-02
88	Q9N2D2|GLTP	4	0.25	-1.96	-2.21	-3.38	-1.04	-0.86	-4.25	0.001992	1.56E-02	-1.43	0	4.96E+07	3.90E+07	8.09E+07	3.58E+07	1.34E+07	2.28E+07	4.04E+07	2.40E+07	-0.053	0.555	0.577	-0.093	-3.262	-2.316	-1.530	-0.736	0.246	-1.961	-2.208	1.99E-03	1.56E-02
89	O60664|PLIN3	6	-1.26	0.32	1.58	0.76	2.40	-0.36	4.40	0.002116	1.62E-02	-1.35	1	1.81E+07	1.56E+07	1.77E+07	NA	1.45E+08	1.00E+08	1.77E+08	4.87E+07	-1.448	-0.707	-1.626	NA	0.292	-0.014	0.712	0.290	-1.260	0.320	1.580	2.12E-03	1.62E-02
90	P48539|PCP4	3	3.43	2.28	-1.15	-1.76	-0.53	2.85	-4.21	0.002109	1.62E-02	-1.49	0	4.85E+08	2.91E+08	7.30E+08	5.29E+08	5.32E+08	4.88E+08	4.97E+08	1.78E+08	3.101	3.314	3.760	3.536	2.230	2.444	2.278	2.171	3.428	2.281	-1.147	2.11E-03	1.62E-02
91	P11142|HSP7C	26	5.67	7.31	1.64	0.75	2.52	6.49	4.17	0.002264	1.71E-02	-1.56	0	3.88E+09	1.18E+09	4.89E+09	1.53E+09	1.66E+10	1.43E+10	1.32E+10	4.74E+09	5.981	5.236	6.513	4.968	7.357	7.698	7.255	6.943	5.674	7.313	1.639	2.26E-03	1.71E-02
92	P81605|DCD	2	1.51	-0.76	-2.27	-3.47	-1.07	0.22	-4.32	0.00234	1.75E-02	-1.45	1	NA	7.60E+07	8.80E+07	2.23E+08	4.18E+07	5.02E+07	9.68E+07	3.56E+07	NA	1.471	0.699	2.371	-1.564	-1.091	-0.204	-0.163	1.514	-0.756	-2.270	2.34E-03	1.75E-02
93	Q9NYL9|TMOD3	2	-4.69	-2.11	2.58	1.25	3.91	-2.97	4.55	0.002377	1.76E-02	-1.28	2	1.82E+06	NA	NA	1.12E+06	1.28E+07	3.71E+07	3.32E+07	1.21E+07	-4.626	NA	NA	-4.759	-3.332	-1.560	-1.826	-1.736	-4.693	-2.113	2.579	2.38E-03	1.76E-02
94	P80303|NUCB2	7	-3.12	-0.43	2.69	1.31	4.07	-0.97	4.72	0.002874	2.09E-02	-1.23	3	NA	2.69E+06	NA	NA	1.00E+08	9.98E+07	8.31E+07	1.98E+07	NA	-3.120	NA	NA	-0.256	-0.022	-0.435	-1.013	-3.120	-0.432	2.688	2.87E-03	2.09E-02
95	Q92804|RBP56	3	-3.90	-1.13	2.76	1.21	4.32	-2.52	4.01	0.002894	2.09E-02	-1.81	0	1.68E+06	1.08E+06	1.91E+06	1.14E+07	5.18E+07	5.90E+07	7.23E+07	1.15E+07	-4.738	-4.375	-4.847	-1.632	-1.243	-0.840	-0.648	-1.803	-3.898	-1.133	2.765	2.89E-03	2.09E-02

1	ProteinName	# Peptides	Ctrl	Group1	log2FC	CI.L	CI.R	Ave Expr	t	P.Value	adj.P.Val	B	nrNAs	M.3_Control.raw	M.2_Control.raw	M.4_Control.raw	M.1_Control.raw	E.4.2_Group_1.raw	E.4.4_Group_1.raw	E.4.3_Group_1.raw	E.4.1_Group_1.raw	M.3_Control.transf	M.2_Control.transf	M.4_Control.transf	M.1_Control.transf	E4.2_Group_1.transf	E4.4_Group_1.transf	E4.3_Group_1.transf	E4.1_Group_1.transf	pseudo.Ctrl	pseudo.Group1	pseudo.log2FC	pseudo.P.Value	pseudo.adj.P.Val
96	P28072|PSB6	2	-0.91	0.23	1.14	0.50	1.78	-0.34	4.00	0.00293	2.10E-02	-1.83	0	2.30E+07	1.24E+07	2.66E+07	2.73E+07	1.19E+08	1.12E+08	1.33E+08	5.60E+07	-1.118	-1.017	-1.032	-0.456	-0.001	0.150	0.278	0.494	-0.906	0.230	1.136	2.93E-03	2.10E-02
97	Q9UHG2|PCSK1	2	-4.29	-6.59	-2.30	-3.48	-1.11	-5.21	-4.69	0.002965	2.10E-02	-1.36	3	1.49E+06	NA	3.85E+06	1.78E+06	1.68E+06	NA	1.24E+06	NA	-4.902	NA	-3.829	-4.138	-6.359	NA	-6.817	NA	-4.290	-6.588	-2.298	2.96E-03	2.10E-02
98	Q15717|ELAV1	3	-4.43	-2.60	1.83	0.84	2.81	-3.21	4.35	0.003068	2.15E-02	-1.55	2	2.64E+06	NA	2.05E+06	NA	2.76E+07	2.14E+07	1.51E+07	5.86E+06	-4.112	NA	-4.744	NA	-2.184	-2.415	-3.024	-2.785	-4.428	-2.602	1.826	3.07E-03	2.15E-02
99	P56211|ARP19	3	2.21	0.57	-1.64	-2.57	-0.70	1.39	-3.94	0.003211	2.23E-02	-1.92	0	2.68E+08	8.04E+07	3.13E+08	2.38E+08	1.17E+08	9.96E+07	2.14E+08	1.00E+08	2.279	1.548	2.533	2.461	-0.035	-0.026	1.001	1.339	2.205	0.570	-1.636	3.21E-03	2.23E-02
100	P06733|ENOA	15	2.68	4.97	2.28	0.97	3.60	3.82	3.92	0.003314	2.28E-02	-1.95	0	3.84E+08	1.95E+08	9.66E+08	8.15E+07	3.65E+09	2.16E+09	3.62E+09	1.03E+09	2.780	2.764	4.165	1.017	5.099	4.756	5.290	4.719	2.682	4.966	2.284	3.31E-03	2.28E-02
101	zz|Y-FGC2Cont00285|	21	2.95	0.68	-2.27	-3.58	-0.95	1.82	-3.89	0.003485	2.37E-02	-2.00	0	2.87E+08	2.71E+08	6.25E+08	2.79E+08	1.02E+08	7.57E+07	4.22E+08	1.03E+08	2.375	3.217	3.535	2.675	-0.230	-0.452	2.028	1.380	2.950	0.682	-2.269	3.49E-03	2.37E-02
102	P37802|TAGL2	9	3.89	5.13	1.23	0.51	1.96	4.51	3.83	0.003815	2.57E-02	-2.10	0	9.59E+08	4.96E+08	1.09E+09	3.95E+08	3.71E+09	3.00E+09	3.16E+09	1.27E+09	4.046	4.047	4.338	3.145	5.126	5.269	5.084	5.031	3.894	5.128	1.234	3.82E-03	2.57E-02
103	O75044|SRGP2	2	-1.69	-3.01	-1.32	-2.08	-0.55	-2.44	-3.96	0.003907	2.60E-02	-1.98	1	1.69E+07	6.50E+06	1.77E+07	NA	1.38E+07	1.13E+07	1.74E+07	6.65E+06	-1.542	-1.906	-1.621	NA	-3.212	-3.403	-2.803	-2.603	-1.690	-3.005	-1.316	3.91E-03	2.60E-02
104	REV__Q8TCU4|ALMS1	2	-1.84	-3.87	-2.04	-3.25	-0.83	-2.71	-3.86	0.004529	2.86E-02	-2.14	1	2.17E+07	3.21E+06	1.79E+07	1.11E+07	NA	5.38E+06	7.52E+06	5.12E+06	-1.199	-2.874	-1.609	-1.666	NA	-4.562	-4.079	-2.983	-1.837	-3.874	-2.037	4.53E-03	2.86E-02
105	Q14019|COTL1	4	0.12	2.18	2.05	0.81	3.30	1.15	3.73	0.004446	2.86E-02	-2.25	0	1.97E+07	4.82E+07	1.41E+08	2.82E+07	4.78E+08	4.12E+08	4.57E+08	1.94E+08	-1.333	0.847	1.381	-0.413	2.071	2.182	2.148	2.300	0.120	2.175	2.055	4.45E-03	2.86E-02
106	Q16775|GLCI2	3	-0.77	0.94	1.71	0.67	2.75	0.08	3.72	0.004534	2.86E-02	-2.27	0	4.79E+07	7.95E+06	5.32E+07	1.43E+07	2.09E+08	3.01E+08	1.72E+08	5.85E+07	-0.102	-1.629	-0.030	-1.325	0.840	1.693	0.666	0.557	-0.771	0.939	1.710	4.53E-03	2.86E-02
107	Q92747|ARC1A	2	-2.92	-0.56	2.35	1.04	3.67	-1.03	4.33	0.004438	2.86E-02	-1.67	3	NA	3.12E+06	NA	NA	7.03E+07	6.16E+07	1.09E+08	2.52E+07	NA	-2.915	NA	NA	-0.788	-0.772	-0.025	-0.664	-2.915	-0.562	2.353	4.44E-03	2.86E-02
108	Q92777|SYN2	3	-3.83	-1.71	2.12	0.89	3.35	-2.77	4.05	0.00446	2.86E-02	-1.98	2	1.77E+06	1.36E+06	7.99E+06	NA	3.71E+07	3.13E+07	3.94E+07	NA	-4.667	-4.056	-2.774	NA	-1.741	-1.823	-1.569	NA	-3.832	-1.711	2.121	4.46E-03	2.86E-02
109	Q92945|FUBP2	9	-2.17	-0.22	1.95	0.78	3.13	-1.19	3.75	0.004343	2.86E-02	-2.23	0	2.46E+07	2.43E+06	7.68E+06	1.20E+07	8.80E+07	7.98E+07	7.80E+07	5.59E+07	-1.026	-3.257	-2.831	-1.570	-0.453	-0.371	-0.531	0.491	-2.171	-0.216	1.955	4.34E-03	2.86E-02
110	Q9Y2D5|AKAP2	5	-4.04	-1.67	2.38	1.04	3.72	-2.14	4.29	0.004632	2.89E-02	-1.71	3	NA	NA	3.33E+06	NA	3.08E+07	3.17E+07	5.31E+07	1.22E+07	NA	NA	-4.041	NA	-2.017	-1.807	-1.115	-1.721	-4.041	-1.665	2.376	4.63E-03	2.89E-02
111	P62820|RAB1A	2	-3.28	-1.18	2.09	0.90	3.29	-2.02	4.25	0.004822	2.98E-02	-1.87	3	NA	2.29E+06	NA	3.53E+06	6.15E+07	NA	6.98E+07	1.11E+07	NA	-3.341	NA	-3.215	-0.988	NA	-0.701	-1.860	-3.278	-1.183	2.095	4.82E-03	2.98E-02
112	P30046|DOPD	4	-4.86	-1.03	3.83	1.60	6.06	-1.80	4.17	0.005339	3.24E-02	-1.85	3	NA	NA	1.89E+06	NA	8.02E+07	8.86E+07	6.56E+07	7.02E+06	NA	NA	-4.859	NA	-0.591	-0.207	-0.793	-2.524	-4.859	-1.029	3.830	5.34E-03	3.24E-02
113	Q13153|PAK1	13	0.84	2.60	1.76	0.67	2.86	1.72	3.62	0.005298	3.24E-02	-2.43	0	1.20E+08	4.78E+07	3.81E+07	1.54E+08	6.54E+08	7.08E+08	4.85E+08	2.42E+08	1.165	0.833	-0.512	1.876	2.538	3.022	2.239	2.621	0.841	2.605	1.764	5.30E-03	3.24E-02
114	zz|Y-FGC2Cont00466|	5	-1.83	-3.67	-1.83	-2.94	-0.73	-2.75	-3.91	0.005419	3.26E-02	-2.18	2	1.33E+07	5.35E+06	1.99E+07	NA	1.29E+07	5.58E+06	1.35E+07	NA	-1.873	-2.174	-1.455	NA	-3.310	-4.506	-3.190	NA	-1.834	-3.669	-1.835	5.42E-03	3.26E-02
115	zz|Y-FGC2Cont00037|	9	2.38	3.72	1.33	0.50	2.17	3.05	3.59	0.005561	3.29E-02	-2.48	0	3.36E+09	9.66E+07	4.46E+08	1.81E+08	1.99E+09	1.20E+09	1.25E+09	3.49E+08	2.594	1.801	3.048	2.095	4.195	3.845	3.680	3.154	2.385	3.718	1.334	5.56E-03	3.29E-02
116	zz|Y-FGC2Cont00365|	15	-0.37	0.99	1.36	0.51	2.22	0.31	3.59	0.005545	3.29E-02	-2.48	0	5.43E+07	2.50E+07	3.95E+07	1.76E+07	3.01E+08	1.17E+08	2.24E+08	9.71E+07	0.072	-0.056	-0.460	-1.046	1.380	0.229	1.066	1.294	-0.372	0.992	1.364	5.55E-03	3.29E-02
117	P78352|DLG4	2	-0.12	-2.84	-2.72	-4.33	-1.12	-1.21	-4.10	0.00574	3.36E-02	-2.05	3	7.83E+07	1.00E+07	7.11E+07	NA	1.99E+07	NA	1.52E+07	NA	0.578	-1.315	0.389	NA	-2.670	NA	-3.012	NA	-0.116	-2.841	-2.725	5.74E-03	3.36E-02
118	Q2M2I8|AAK1	9	2.35	1.21	-1.14	-1.85	-0.42	1.78	-3.56	0.005797	3.37E-02	-2.52	0	4.26E+08	1.12E+08	2.32E+08	2.23E+08	2.09E+08	2.06E+08	3.03E+08	1.04E+08	2.923	2.004	2.102	2.371	0.839	1.102	1.527	1.390	2.350	1.214	-1.135	5.80E-03	3.37E-02
119	Q15746|MYLK	4	0.02	-1.39	-1.41	-2.29	-0.53	-0.79	-3.68	0.005893	3.40E-02	-2.41	1	5.25E+07	2.65E+07	NA	3.86E+07	2.77E+07	5.62E+07	4.16E+07	2.01E+07	0.024	0.024	NA	0.008	-2.176	-0.916	-1.487	-0.998	0.019	-1.394	-1.413	5.89E-03	3.40E-02
120	P18065|IBP2	2	-1.42	0.71	2.13	0.81	3.44	0.00	3.80	0.006199	3.53E-02	-2.28	2	NA	NA	1.06E+07	2.69E+07	2.11E+08	1.46E+08	1.50E+08	7.69E+07	NA	NA	-2.360	-0.475	0.853	0.564	0.461	0.956	-1.417	0.708	2.126	6.20E-03	3.53E-02
121	Q9BPX5|ARPC5L	3	-1.74	0.11	1.84	0.68	3.00	-0.68	3.64	0.00623	3.53E-02	-2.46	1	1.67E+07	NA	1.07E+07	1.47E+07	1.72E+08	1.95E+08	7.85E+07	2.61E+07	-1.558	NA	-2.356	-1.296	0.547	1.016	-0.522	-0.617	-1.736	0.106	1.842	6.23E-03	3.53E-02
122	P14550|AK1A1	3	-3.72	-1.60	2.12	0.84	3.41	-2.02	3.99	0.006546	3.62E-02	-2.06	3	NA	NA	NA	NA	4.90E+07	3.91E+07	4.10E+07	9.50E+06	NA	NA	-3.724	NA	-1.327	-1.480	-1.505	-2.084	-3.724	-1.599	2.125	6.55E-03	3.62E-02
123	Q14195|DPYL3	19	2.78	4.03	1.25	0.44	2.06	3.40	3.49	0.006551	3.62E-02	-2.65	0	4.57E+08	1.56E+08	6.00E+08	1.90E+08	2.08E+09	1.44E+09	1.68E+09	4.74E+08	3.020	2.462	3.477	2.154	4.259	4.128	4.127	3.599	2.778	4.028	1.250	6.55E-03	3.62E-02
124	Q16643|DREB	3	-2.17	-1.08	1.10	0.40	1.80	-1.55	3.60	0.006548	3.62E-02	-2.52	1	1.11E+07	6.23E+06	1.01E+07	NA	4.80E+07	5.53E+07	5.60E+07	2.03E+07	-2.124	-1.964	-2.437	NA	-1.356	-0.939	-1.035	-0.980	-2.175	-1.078	1.097	6.55E-03	3.62E-02
125	P31939|PUR9	5	-4.91	-1.54	3.37	1.25	5.49	-2.66	3.73	0.006819	3.74E-02	-2.37	2	NA	NA	4.00E+06	4.31E+05	5.91E+07	5.49E+07	6.34E+07	4.06E+06	NA	NA	-3.774	-6.050	-1.046	-0.952	-0.846	-3.319	-4.912	-1.541	3.371	6.82E-03	3.74E-02
126	P67936|TPM4	5	-2.88	-0.31	2.57	0.97	4.17	-0.82	3.90	0.007326	3.99E-02	-2.18	3	NA	NA	7.45E+06	NA	5.84E+07	1.26E+08	1.09E+08	2.88E+07	NA	NA	-2.876	NA	-1.064	0.335	-0.022	-0.473	-2.876	-0.306	2.570	7.33E-03	3.99E-02
127	P25705|ATPA	5	-0.44	-1.76	-1.32	-2.19	-0.45	-1.10	-3.40	0.007513	4.04E-02	-2.79	0	2.87E+07	2.38E+07	5.40E+07	2.09E+07	2.92E+07	2.73E+07	2.84E+07	2.24E+07	-0.809	-0.125	-0.010	-0.819	-2.096	-2.040	-2.066	-0.838	-0.441	-1.760	-1.319	7.51E-03	4.04E-02
128	Q14103|HNRPD	2	-1.70	-0.65	1.05	0.35	1.74	-1.17	3.40	0.007554	4.04E-02	-2.79	0	1.52E+07	5.10E+06	1.88E+07	1.44E+07	7.89E+07	8.13E+07	7.15E+07	2.04E+07	-1.692	-2.239	-1.534	-1.316	-0.617	-0.342	-0.663	-0.974	-1.695	-0.649	1.046	7.55E-03	4.04E-02
129	P04075|ALDOA	18	2.99	4.45	1.46	0.49	2.44	3.72	3.38	0.007718	4.06E-02	-2.82	0	3.84E+08	1.57E+08	1.03E+09	2.33E+08	2.22E+09	1.51E+09	2.19E+09	1.02E+09	2.779	2.472	4.258	2.433	4.361	4.194	4.528	4.710	2.985	4.448	1.463	7.72E-03	4.06E-02
130	P62942|FKB1A	2	-0.20	1.42	1.62	0.54	2.69	0.61	3.38	0.007735	4.06E-02	-2.82	0	1.89E+07	2.46E+07	7.32E+07	4.59E+07	4.79E+08	2.59E+08	1.64E+08	1.16E+08	-1.391	-0.081	0.431	0.243	2.071	1.460	0.593	1.551	-0.199	1.419	1.618	7.73E-03	4.06E-02
131	Q99497|PARK7	5	4.66	5.57	0.92	0.31	1.52	5.11	3.38	0.00777	4.06E-02	-2.82	0	1.28E+09	8.19E+08	1.64E+09	1.09E+09	4.22E+09	4.15E+09	4.20E+09	1.99E+09	4.440	4.737	4.933	4.515	5.319	5.770	5.515	5.682	4.656	5.571	0.915	7.77E-03	4.06E-02
132	O43768|ENSA	7	4.79	3.89	-0.89	-1.50	-0.29	4.34	-3.34	0.008259	4.29E-02	-2.88	0	1.56E+09	7.06E+08	1.67E+09	1.49E+09	1.67E+09	1.05E+09	1.45E+09	6.71E+08	4.722	4.532	4.957	4.934	3.935	3.629	3.902	4.103	4.786	3.892	-0.894	8.26E-03	4.29E-02
133	O14594|NCAN	2	-0.40	-1.81	-1.41	-2.36	-0.46	-1.20	-3.42	0.008676	4.47E-02	-2.80	1	4.57E+07	1.71E+07	3.99E+07	NA	4.61E+07	3.58E+07	4.31E+07	5.95E+06	-0.167	-0.574	-0.447	NA	-1.418	-1.618	-1.430	-2.763	-0.396	-1.807	-1.411	8.68E-03	4.47E-02
134	O14745|NHRF1	2	0.53	-0.46	-0.99	-1.67	-0.31	0.03	-3.29	0.008942	4.57E-02	-2.96	0	8.24E+07	3.87E+07	6.91E+07	5.87E+07	7.71E+07	7.29E+07	6.37E+07	4.40E+07	0.648	0.546	0.349	0.573	-0.650	-0.510	-0.838	0.143	0.529	-0.464	-0.993	8.94E-03	4.57E-02
135	O95989|NUDT3	2	-1.73	-3.62	-1.89	-3.16	-0.62	-2.68	-3.49	0.00951	4.83E-02	-2.76	2	1.18E+07	4.09E+06	3.57E+07	NA	1.21E+07	8.50E+06	1.03E+07	NA	-2.038	-2.544	-0.609	NA	-3.409	-3.850	-3.602	NA	-1.730	-3.621	-1.890	9.51E-03	4.83E-02
136	O00151|PDLI1	7	-2.18	0.00	2.18	0.73	3.63	-0.44	3.64	0.009937	5.01E-02	-2.49	3	NA	NA	NA	7.59E+06	1.09E+08	6.87E+07	1.27E+08	5.76E+07	NA	NA	NA	-2.184	-0.136	-0.604	0.203	0.535	-2.184	0.000	2.183	9.94E-03	5.01E-02
137	Q9UPX8|SHAN2	3	-1.29	-3.39	-2.09	-3.57	-0.62	-2.34	-3.21	0.010302	5.15E-02	-3.11	0	3.07E+07	1.78E+07	2.27E+07	5.33E+06	8.71E+06	5.36E+06	3.27E+07	4.33E+06	-0.719	-0.524	-1.263	-2.660	-3.902	-4.566	-1.852	-3.224	-1.292	-3.386	-2.094	1.03E-02	5.15E-02
138	P38117|ETFB	3	-2.03	-1.02	1.01	0.29	1.73	-1.53	3.17	0.010852	5.38E-02	-3.16	0	9.80E+06	4.72E+06	1.90E+07	8.97E+06	5.70E+07	3.93E+07	6.49E+07	2.46E+07	-2.298	-2.347	-1.522	-1.959	-1.101	-1.470	-0.810	-0.699	-2.032	-1.020	1.012	1.09E-02	5.38E-02
139	Q9NQ48|LZTL1	2	-3.41	-1.77	1.64	0.50	2.77	-2.32	3.39	0.010922	5.38E-02	-2.86	2	5.05E+06	NA	4.50E+06	NA	3.61E+07	5.55E+07	2.90E+07	7.93E+06	-3.216	NA	-3.606	NA	-1.783	-0.934	-2.031	-2.346	-3.411	-1.773	1.638	1.09E-02	5.38E-02
140	P04406|G3P	11	-0.19	2.81	3.00	0.88	5.12	1.52	3.25	0.011232	5.50E-02	-3.07	1	NA	4.79E+06	2.34E+08	2.91E+07	1.03E+09	5.81E+08	9.87E+08	1.54E+08	NA	-2.327	2.112	-0.370	3.221	2.716	3.317	1.968	-0.195	2.806	3.001	1.12E-02	5.50E-02
141	Q15293|RCN1	7	-2.00	0.09	2.10	0.61	3.58	-0.80	3.23	0.011536	5.60E-02	-3.10	1	1.52E+07	3.74E+06	1.74E+07	NA	2.29E+08	1.79E+08	1.19E+08	1.33E+07	-1.692	-2.666	-1.650	NA	0.970	0.883	0.113	-1.592	-2.002	0.094	2.096	1.15E-02	5.60E-02
142	Q92598|HS105	8	-0.58	0.68	1.26	0.35	2.17	0.05	3.13	0.011734	5.66E-02	-3.24	0	3.72E+07	8.69E+06	5.93E+07	2.67E+07	1.25E+08	1.59E+08	2.13E+08	7.61E+07	-0.451	-1.508	0.127	-0.490	0.075	0.706	0.993	0.940	-0.581	0.679	1.259	1.17E-02	5.66E-02

1	ProteinName	# Peptides	Ctrl	Group1	log2FC	CI.L	CI.R	Ave Expr	t	P.Value	adj.P.Val	B	nrNAs	M.3_Control.raw	M.2_Control.raw	M.4_Control.raw	M.1_Control.raw	E4.2_Group1.raw	E4.4_Group1.raw	E4.3_Group1.raw	E4.1_Group1.raw	M.3_Control.transf	M.2_Control.transf	M.4_Control.transf	M.1_Control.transf	E4.2_Group_1.transf	E4.4_Group_1.transf	E4.3_Group_1.transf	E4.1_Group_1.transf	pseudo.Ctrl	pseudo.Group1	pseudo.log2FC	pseudo.P.Value	pseudo.adj.P.Val
143	Q9P265|DIP2B	2	-1.08	-3.04	-1.96	-3.35	-0.58	-1.73	-3.33	0.011886	5.69E-02	-2.95	2	2.89E+07	1.41E+07	4.34E+07	6.77E+06	NA	1.45E+07	1.47E+07	NA	-0.801	-0.844	-0.325	-2.337	NA	-3.023	-3.058	NA	-1.077	-3.041	-1.964	1.19E-02	5.69E-02
144	Q96GW7|PGCB	3	-0.28	-2.01	-1.73	-2.96	-0.51	-1.15	-3.32	0.01213	5.77E-02	-3.02	2	5.35E+07	1.58E+07	4.71E+07	NA	6.16E+07	2.12E+07	1.96E+07	NA	0.051	-0.689	-0.207	NA	-0.985	-2.429	-2.625	NA	-0.282	-2.013	-1.731	1.21E-02	5.77E-02
145	P0DP25|CALM3	5	2.24	0.61	-1.64	-2.84	-0.44	1.42	-3.07	0.012911	6.05E-02	-3.34	0	3.20E+08	5.95E+07	5.58E+08	1.62E+08	1.40E+08	1.11E+08	1.41E+08	1.25E+08	2.526	1.134	3.371	1.941	0.239	0.145	0.371	1.665	2.243	0.605	-1.638	1.29E-02	6.05E-02
146	Q9BYH1|SE6L1	3	-0.02	-1.48	-1.46	-2.51	-0.41	-0.75	-3.27	0.012867	6.05E-02	-3.08	2	5.33E+07	2.30E+07	5.65E+07	NA	7.21E+07	3.87E+07	2.60E+07	NA	0.045	-0.168	0.057	NA	-0.751	-1.495	-2.199	NA	-0.022	-1.482	-1.460	1.29E-02	6.05E-02
147	Q96QV1|IHHIP	8	-1.94	0.28	2.21	0.60	3.82	-0.67	3.15	0.01303	6.07E-02	-3.22	1	3.15E+07	NA	2.13E+07	2.33E+06	1.56E+08	1.33E+08	8.59E+07	6.29E+07	-0.683	NA	-1.353	-3.776	0.400	0.423	-0.385	0.663	-1.937	0.275	2.213	1.30E-02	6.07E-02
148	Q9BRT3|MIEN1	2	1.60	0.61	-0.98	-1.71	-0.26	1.11	-3.04	0.013461	6.10E-02	-3.38	0	1.46E+08	8.28E+07	1.57E+08	1.48E+08	1.43E+08	1.15E+08	1.74E+08	9.78E+07	1.444	1.588	1.537	1.824	0.273	0.200	0.682	1.304	1.598	0.615	-0.983	1.35E-02	6.10E-02
149	Q9BUJ8|DOHH	2	-1.13	-2.31	-1.18	-2.03	-0.33	-1.72	-3.24	0.013398	6.10E-02	-3.12	2	3.11E+07	8.77E+06	2.39E+07	NA	2.58E+07	2.13E+07	2.58E+07	NA	-0.701	-1.495	-1.190	NA	-2.285	-2.424	-2.209	NA	-1.129	-2.306	-1.177	1.34E-02	6.10E-02
150	Q9UHD9|UBQL2	8	-0.13	-1.94	-1.81	-3.14	-0.49	-1.17	-3.13	0.013414	6.10E-02	-3.25	1	5.50E+07	2.67E+07	3.79E+07	NA	4.53E+07	3.63E+07	4.99E+07	3.50E+06	0.089	0.035	-0.522	NA	-1.442	-1.593	-1.210	-3.533	-0.133	-1.945	-1.812	1.34E-02	6.10E-02
151	zz|Y-FGCZCont00485|	13	1.76	3.88	2.12	0.55	3.68	2.82	3.04	0.013428	6.10E-02	-3.38	0	7.26E+07	2.65E+08	2.67E+08	8.59E+07	2.76E+09	1.40E+09	5.10E+08	8.43E+08	0.474	3.185	2.305	1.087	4.681	4.078	2.317	4.435	1.763	3.878	2.115	1.34E-02	6.10E-02
152	zz|Y-FGCZCont00256|	5	3.12	4.09	0.97	0.25	1.69	3.61	3.04	0.013612	6.13E-02	-3.39	0	5.33E+08	3.61E+08	4.94E+08	2.36E+08	1.57E+09	1.58E+09	1.70E+09	6.77E+08	3.232	3.613	3.195	2.452	3.844	4.270	4.145	4.116	3.123	4.094	0.971	1.36E-02	6.13E-02
153	Q14011|CIRBP	2	-2.41	-0.90	1.51	0.43	2.59	-1.50	3.38	0.013807	6.18E-02	-2.97	3	6.74E+06	NA	1.36E+07	NA	6.84E+07	6.28E+07	5.28E+07	NA	-2.817	NA	-2.002	NA	-0.830	-0.743	-1.124	NA	-2.409	-0.899	1.511	1.38E-02	6.18E-02
154	Q9UKX9|NUDT5	3	-4.43	-3.12	1.31	0.34	2.28	-3.68	3.10	0.01404	6.24E-02	-3.30	1	2.58E+06	1.12E+06	1.93E+06	NA	2.63E+07	1.04E+07	1.01E+07	4.86E+06	-4.145	-4.320	-4.828	NA	-2.253	-3.531	-3.639	-3.057	-4.431	-3.120	1.311	1.40E-02	6.24E-02
155	O75083|WDR1	4	-3.59	-1.34	2.25	0.57	3.92	-2.31	3.08	0.014544	6.34E-02	-3.33	1	2.25E+06	1.59E+06	9.03E+06	NA	9.87E+07	2.00E+07	9.76E+07	7.79E+06	-4.336	-3.838	-2.597	NA	-0.283	-2.517	-0.192	-2.373	-3.591	-1.341	2.249	1.45E-02	6.34E-02
156	P05997|COL5A2	10	-0.53	1.47	2.00	0.55	3.44	1.07	3.34	0.014618	6.34E-02	-2.88	3	NA	NA	3.77E+07	NA	2.67E+08	3.24E+08	2.04E+08	1.52E+08	NA	NA	-0.527	NA	1.204	1.805	0.923	1.942	-0.527	1.468	1.996	1.46E-02	6.34E-02
157	P22314|UBA1	9	-1.16	2.05	3.22	0.80	5.63	0.44	2.99	0.014595	6.34E-02	-3.46	0	1.70E+07	3.14E+07	1.28E+08	1.24E+06	4.42E+08	3.02E+08	5.92E+08	1.59E+08	-1.537	0.259	1.246	-4.626	1.953	1.701	2.541	2.011	-1.165	2.051	3.216	1.46E-02	6.34E-02
158	Q9UPP5|K1107	3	1.94	-0.25	-2.19	-3.75	-0.64	0.84	-3.57	0.014645	6.34E-02	-2.84	4	1.32E+08	1.70E+08	NA	NA	8.77E+07	9.83E+07	NA	NA	1.300	2.578	NA	NA	-0.458	-0.047	NA	NA	1.939	-0.253	-2.191	1.46E-02	6.34E-02
159	Q16352|AINX	4	-1.62	-3.09	-1.46	-2.55	-0.37	-2.46	-3.06	0.014887	6.41E-02	-3.35	1	1.89E+07	3.94E+06	NA	1.98E+07	1.41E+07	1.19E+07	1.17E+07	7.52E+06	-1.388	-2.593	NA	-0.893	-3.186	-3.328	-3.403	-2.424	-1.625	-3.085	-1.460	1.49E-02	6.41E-02
160	Q6NXS1|IPP2B	2	0.48	-0.56	-1.04	-1.85	-0.24	-0.04	-2.92	0.016445	6.99E-02	-3.58	0	6.75E+07	2.76E+07	6.76E+07	8.98E+07	6.33E+07	6.37E+07	7.03E+07	4.27E+07	0.373	0.081	0.317	1.148	-0.944	-0.720	-0.690	0.101	0.479	-0.563	-1.042	1.64E-02	6.99E-02
161	zz|Y-FGCZCont00195|	5	1.03	2.36	1.33	0.31	2.35	1.70	2.93	0.016355	6.99E-02	-3.57	0	1.27E+08	7.38E+07	1.78E+08	3.16E+07	6.75E+08	5.34E+08	5.50E+08	1.41E+08	1.246	1.431	1.720	-0.260	2.584	2.584	2.430	1.841	1.034	2.360	1.326	1.64E-02	6.99E-02
162	P02686|MBP	3	2.25	1.28	-0.97	-1.71	-0.22	1.77	-2.91	0.016661	7.04E-02	-3.59	0	2.44E+08	1.01E+08	3.21E+08	2.29E+08	2.11E+08	2.32E+08	2.23E+08	1.51E+08	2.150	1.866	2.573	2.411	0.854	1.288	1.060	1.935	2.250	1.284	-0.966	1.67E-02	7.04E-02
163	zz|Y-FGCZCont00307|	2	-0.49	-2.21	-1.72	-3.02	-0.41	-1.35	-3.09	0.016801	7.05E-02	-3.35	2	1.92E+07	1.62E+07	7.95E+07	NA	2.33E+07	2.02E+07	3.64E+07	NA	-1.369	-0.656	0.551	NA	-2.434	-2.504	-1.690	NA	-0.492	-2.209	-1.718	1.68E-02	7.05E-02
164	P08123|CO1A2	15	6.79	5.74	-1.04	-1.85	-0.23	6.26	-2.90	0.016973	7.06E-02	-3.61	0	7.01E+09	2.63E+09	7.19E+09	6.59E+09	3.83E+09	3.58E+09	4.80E+09	3.59E+09	6.798	6.339	7.070	6.937	5.173	5.542	5.716	6.541	6.786	5.743	-1.043	1.70E-02	7.06E-02
165	P46821|MAP1B	14	3.78	3.00	-0.79	-1.40	-0.18	3.39	-2.90	0.017028	7.06E-02	-3.61	0	8.91E+08	4.36E+08	6.24E+08	6.37E+08	7.07E+08	7.42E+08	9.24E+08	3.19E+08	3.944	3.870	3.533	3.787	2.652	3.096	3.217	3.022	3.784	2.997	-0.787	1.70E-02	7.06E-02
166	O94760|DDAH1	10	4.26	5.15	0.89	0.20	1.59	4.70	2.88	0.017516	7.22E-02	-3.64	0	1.13E+09	3.98E+08	1.47E+09	8.94E+08	3.63E+09	3.45E+09	3.12E+09	1.21E+09	4.270	3.744	4.771	4.245	5.094	5.484	5.063	4.960	4.258	5.150	0.892	1.75E-02	7.22E-02
167	P00558|PGK1	14	3.24	4.41	1.17	0.25	2.09	3.82	2.86	0.018202	7.37E-02	-3.68	0	5.27E+08	2.38E+08	1.05E+09	2.30E+08	2.23E+09	1.59E+09	2.58E+09	7.17E+08	3.216	3.042	4.280	2.416	4.366	4.279	4.776	4.200	3.238	4.405	1.167	1.82E-02	7.37E-02
168	Q96JE9|MAP6	7	2.19	1.17	-1.02	-1.83	-0.22	1.68	-2.86	0.018108	7.37E-02	-3.68	0	1.95E+08	1.09E+08	2.44E+08	3.02E+08	2.52E+08	1.46E+08	2.40E+08	1.38E+08	1.842	1.969	2.175	2.782	1.118	0.570	1.176	1.805	2.192	1.167	-1.025	1.81E-02	7.37E-02
169	Q9Y2T3|GUAD	4	-0.24	0.69	0.94	0.20	1.67	0.23	2.86	0.018069	7.37E-02	-3.67	0	4.26E+07	1.56E+07	7.12E+07	2.87E+07	1.90E+08	1.29E+08	2.25E+08	6.16E+07	-0.264	-0.701	0.391	-0.391	0.691	0.376	1.077	0.632	-0.241	0.694	0.935	1.81E-02	7.37E-02
170	O75061|AUXI	6	0.46	-0.45	-0.90	-1.62	-0.19	0.01	-2.84	0.018921	7.61E-02	-3.72	0	6.84E+07	2.24E+07	8.60E+07	7.96E+07	8.29E+07	8.16E+07	8.38E+07	2.86E+07	0.392	-0.209	0.665	0.985	-0.542	-0.336	-0.423	-0.483	0.458	-0.446	-0.904	1.89E-02	7.61E-02
171	P09972|ALDOC	16	4.91	5.72	0.81	0.16	1.46	5.31	2.79	0.020535	8.12E-02	-3.80	0	2.07E+09	7.18E+08	2.07E+09	1.25E+09	4.49E+09	4.29E+09	4.95E+09	2.27E+09	5.109	4.557	5.269	4.701	5.410	5.823	5.763	5.873	4.909	5.717	0.808	2.05E-02	8.12E-02
172	P52907|CAZA1	7	-1.55	1.29	2.84	0.55	5.13	-0.13	2.79	0.020497	8.12E-02	-3.80	0	3.08E+07	2.84E+06	3.47E+07	1.02E+07	6.57E+08	4.53E+08	4.97E+08	1.02E+07	-0.713	-3.043	-0.649	-1.784	2.545	2.329	2.276	-1.985	-1.547	1.291	2.838	2.05E-02	8.12E-02
173	Q13561|DCTN2	12	1.84	2.91	1.08	0.21	1.94	2.37	2.79	0.020521	8.12E-02	-3.80	0	3.58E+08	1.19E+08	1.56E+08	8.38E+07	9.71E+08	7.34E+08	7.31E+08	2.35E+08	2.680	2.083	1.526	1.055	3.127	3.078	2.861	2.577	1.836	2.911	1.075	2.05E-02	8.12E-02
174	P38159|RBMX	5	-3.50	-0.53	2.97	0.59	5.34	-1.52	2.93	0.021122	8.30E-02	-3.54	2	4.21E+06	NA	4.76E+06	NA	2.24E+08	1.81E+08	4.06E+07	7.40E+06	-3.469	NA	-3.525	NA	0.943	0.900	-1.521	-2.446	-3.497	-0.531	2.966	2.11E-02	8.30E-02
175	Q14315|FLNC	23	-0.68	1.17	1.85	0.36	3.34	0.55	2.91	0.021637	8.41E-02	-3.56	2	3.16E+07	NA	3.40E+07	NA	3.89E+08	3.08E+08	2.89E+08	3.31E+07	-0.679	NA	-0.679	NA	1.763	1.728	1.455	-0.271	-0.679	1.169	1.848	2.16E-02	8.41E-02
176	zz|Y-FGCZCont00371|	17	7.44	6.54	-0.91	-1.65	-0.17	6.99	-2.76	0.021527	8.41E-02	-3.85	0	9.34E+09	6.22E+09	1.01E+10	1.00E+10	6.24E+09	7.26E+09	7.73E+09	5.55E+09	7.196	7.521	7.563	7.500	5.899	6.640	6.438	7.173	7.445	6.538	-0.907	2.15E-02	8.41E-02
177	P15848|ARSB	4	-1.37	-0.06	1.31	0.23	2.39	-0.72	2.73	0.022714	8.78E-02	-3.90	0	9.91E+06	1.79E+07	3.98E+07	7.35E+06	1.08E+08	9.35E+07	1.05E+08	4.27E+07	-2.282	-0.518	-0.451	-2.226	-0.141	-0.125	-0.085	0.102	-1.369	-0.062	1.307	2.27E-02	8.78E-02
178	P35998|PRS7	2	-5.45	-3.54	1.92	0.36	3.47	-4.30	2.98	0.023169	8.90E-02	-3.50	3	6.94E+05	NA	NA	9.79E+05	NA	7.03E+06	8.37E+06	6.92E+06	-5.962	NA	NA	-4.944	NA	-4.146	-3.918	-2.544	-5.453	-3.536	1.917	2.32E-02	8.90E-02
179	P21695|GPDA	4	0.87	0.08	-0.79	-1.45	-0.13	0.48	-2.71	0.023352	8.92E-02	-3.93	0	9.86E+07	3.87E+07	1.31E+08	6.83E+07	1.62E+08	8.93E+07	1.11E+08	4.11E+07	0.897	0.544	1.270	0.778	0.457	-0.195	0.009	0.046	0.872	0.079	-0.794	2.34E-02	8.92E-02
180	Q9NWV4|C2LB	4	-0.18	0.66	0.84	0.14	1.55	0.24	2.69	0.024093	9.15E-02	-3.96	0	5.34E+07	1.68E+07	4.62E+07	3.98E+07	2.00E+08	1.87E+08	1.91E+08	4.24E+07	0.048	-0.600	-0.234	0.049	0.772	0.954	0.824	0.090	-0.184	0.660	0.844	2.41E-02	9.15E-02
181	Q8IXS6|PALM2	2	-1.03	-2.07	-1.04	-1.92	-0.17	-1.55	-2.68	0.024634	9.31E-02	-3.98	0	5.14E+07	7.08E+06	2.34E+07	1.71E+07	2.84E+07	2.43E+07	2.92E+07	1.08E+07	-0.005	-1.790	-1.220	-1.088	-2.137	-2.217	-2.022	-1.898	-1.026	-2.069	-1.043	2.46E-02	9.31E-02
182	P07602|SAP	6	2.34	3.16	0.82	0.12	1.52	2.75	2.64	0.026214	9.85E-02	-4.04	0	3.21E+08	1.59E+08	3.30E+08	1.39E+08	9.77E+08	8.09E+08	1.08E+09	2.79E+08	2.530	2.483	2.612	1.734	3.136	3.229	3.449	2.825	2.340	3.160	0.820	2.62E-02	9.85E-02
183	O75506|HSBP1	3	1.49	0.50	-0.99	-1.83	-0.14	1.00	-2.63	0.026618	9.95E-02	-4.06	0	1.55E+08	6.71E+07	1.78E+08	1.10E+08	1.29E+08	1.15E+08	1.24E+08	1.15E+08	1.520	1.300	1.719	1.416	0.113	0.191	0.167	1.534	1.489	0.501	-0.987	2.66E-02	9.95E-02
184	P55263|ADK	3	-3.35	-1.87	1.48	0.22	2.74	-2.37	2.75	0.027381	1.02E-01	-3.80	2	NA	NA	5.81E+06	2.92E+06	3.17E+07	3.09E+07	6.03E+07	5.99E+06	NA	NA	-3.235	-3.471	-1.974	-1.843	-0.922	-2.753	-3.353	-1.873	1.480	2.74E-02	1.02E-01
185	P49418|AMPH	5	3.19	2.23	-0.96	-1.79	-0.13	2.71	-2.60	0.027981	1.03E-01	-4.11	0	6.40E+08	2.26E+08	6.75E+08	2.73E+08	3.57E+08	3.61E+08	6.80E+08	2.29E+08	3.485	2.966	3.646	2.646	1.635	1.976	2.753	2.542	3.186	2.227	-0.959	2.80E-02	1.03E-01
186	P35612|ADDB	4	1.22	-0.11	-1.33	-2.49	-0.18	0.55	-2.60	0.02818	1.04E-01	-4.11	0	1.99E+08	5.97E+07	4.74E+07	1.78E+08	8.85E+07	1.33E+08	7.67E+07	4.34E+07	1.867	1.140	-0.196	2.070	-0.444	0.424	-0.556	0.123	1.220	-0.113	-1.334	2.82E-02	1.04E-01
187	Q13177|PAK2	13	-2.77	-0.81	1.96	0.26	3.66	-1.65	2.64	0.028846	1.05E-01	-4.02	1	2.81E+06	NA	1.55E+07	6.15E+06	6.54E+07	1.14E+08	1.04E+08	7.45E+06	-4.027	NA	-1.818	-2.467	-0.896	0.185	-0.090	-2.438	-2.771	-0.809	1.961	2.88E-02	1.05E-01
188	P07195|LDHB	8	0.25	1.98	1.73	0.22	3.24	1.11	2.57	0.029284	1.06E-01	-4.15	0	3.45E+07	3.58E+07	2.28E+08	1.88E+07	3.88E+08	1.91E+08	5.63E+08	2.57E+08	-0.556	0.438	2.075	-0.957	1.758	0.984	2.466	2.707	0.250	1.979	1.728	2.93E-02	1.06E-01
189	P20339|RAB5A	3	-2.05	-3.70	-1.64	-3.06	-0.23	-3.29	-2.94	0.030098	1.07E-01	-3.49	4	NA	NA	1.31E+07	NA	NA	8.29E+06	1.19E+07	2.89E+06	NA	NA	-2.053	NA	NA	-3.890	-3.389	-3.813	-2.053	-3.697	-1.644	3.01E-02	1.07E-01

1	ProteinName	# Peptides	Ctrl	Group1	log2FC	CI.L	CI.R	Ave Expr	t	P.Value	adj.P.Val	B	nrNAs	M.3_Control.raw	M.2_Control.raw	M.4_Control.raw	M.1_Control.raw	E4.2_Group_1.raw	E4.4_Group_1.raw	E4.3_Group_1.raw	E4.1_Group_1.raw	M.3_Control.transf	M.2_Control.transf	M.4_Control.transf	M.1_Control.transf	E4.2_Group_1.transf	E4.4_Group_1.transf	E4.3_Group_1.transf	E4.1_Group_1.transf	pseudo.Ctrl	pseudo.Group1	pseudo.log2FC	pseudo.P.Value	pseudo.adj.P.Val
190	P49903|SPS1	4	-2.25	-0.92	1.33	0.18	2.49	-1.45	2.79	0.030089	1.07E-01	-3.77	3	1.44E+07	NA	8.15E+06	NA	6.35E+07	6.72E+07	5.07E+07	NA	-1.764	NA	-2.745	NA	-0.940	-0.638	-1.185	NA	-2.255	-0.921	1.334	3.01E-02	1.07E-01
191	P54578|UBP14	3	-1.58	-0.81	0.77	0.09	1.45	-1.20	2.56	0.029967	1.07E-01	-4.17	0	1.48E+07	7.73E+06	1.80E+07	1.42E+07	5.71E+07	4.91E+07	6.59E+07	3.38E+07	-1.732	-1.668	-1.602	-1.336	-1.098	-1.124	-0.787	-0.241	-1.585	-0.812	0.772	3.00E-02	1.07E-01
192	Q01518|CAP1	5	2.67	-0.02	-2.69	-5.01	-0.36	0.52	-2.80	0.029862	1.07E-01	-3.60	3	NA	NA	NA	2.78E+08	1.11E+08	2.53E+08	9.99E+07	1.72E+07	NA	NA	NA	2.671	-0.113	1.423	-0.156	-1.222	2.671	-0.017	-2.687	2.99E-02	1.07E-01
193	P19021|AMD	3	-1.26	-3.48	-2.22	-4.18	-0.26	-2.37	-2.55	0.030414	1.08E-01	-4.19	0	1.09E+08	2.45E+07	7.38E+06	3.80E+06	1.44E+07	9.74E+06	9.78E+06	3.70E+06	1.038	-0.086	-2.889	-3.117	-3.149	-3.638	-3.681	-3.456	-1.264	-3.481	-2.218	3.04E-02	1.08E-01
194	Q14247|SRC8	5	0.01	-1.09	-1.10	-2.08	-0.13	-0.54	-2.55	0.030695	1.08E-01	-4.20	0	1.03E+08	1.71E+07	6.64E+07	2.45E+07	4.74E+07	7.85E+07	5.32E+07	1.45E+07	0.952	-0.578	0.290	-0.605	-1.377	-0.397	-1.111	-1.469	0.015	-1.088	-1.103	3.07E-02	1.08E-01
195	Q99627|CSN8	2	-1.39	-0.23	1.16	0.14	2.17	-0.62	2.67	0.03063	1.08E-01	-3.91	2	1.43E+07	1.25E+07	NA	NA	1.19E+08	9.40E+07	6.55E+07	3.93E+07	-1.772	-1.009	NA	NA	-0.008	-0.115	-0.797	-0.020	-1.390	-0.235	1.165	3.06E-02	1.08E-01
196	Q727J9|CK2N1	2	-1.74	-3.19	-1.45	-2.73	-0.17	-2.46	-2.66	0.03115	1.08E-01	-3.98	2	2.07E+07	3.47E+06	NA	1.60E+07	1.07E+07	1.15E+07	2.00E+07	NA	-1.261	-2.767	NA	-1.182	-3.590	-3.378	-2.594	NA	-1.737	-3.187	-1.451	3.11E-02	1.08E-01
197	Q96FW1|OTUB1	3	-1.43	-0.51	0.92	0.10	1.73	-0.97	2.54	0.031034	1.08E-01	-4.21	0	2.62E+07	8.31E+06	2.50E+07	8.22E+06	1.01E+08	9.13E+07	7.88E+07	1.85E+07	-0.937	-1.569	-1.124	-2.076	-0.244	-0.161	-0.517	-1.115	-1.427	-0.509	0.917	3.10E-02	1.08E-01
198	O15400|STX7	5	2.14	1.13	-1.01	-1.91	-0.11	1.64	-2.52	0.032004	1.10E-01	-4.24	0	2.28E+08	8.98E+07	2.48E+08	2.65E+08	1.62E+08	2.66E+08	1.69E+08	1.50E+08	2.060	1.700	2.198	2.607	0.459	1.500	0.640	1.928	2.141	1.132	-1.009	3.20E-02	1.10E-01
199	P49419|AL7A1	7	-1.43	0.11	1.54	0.17	2.92	-0.55	2.58	0.031875	1.10E-01	-4.12	1	6.04E+06	1.35E+07	4.08E+07	NA	1.53E+08	8.55E+07	1.45E+08	3.81E+07	-2.968	-0.907	-0.414	NA	0.370	-0.263	0.413	-0.066	-1.430	0.114	1.543	3.19E-02	1.10E-01
200	P11137|MTAP2	26	6.01	5.28	-0.73	-1.39	-0.07	5.65	-2.49	0.03348	1.14E-01	-4.28	0	4.44E+09	1.69E+09	4.58E+09	2.71E+09	3.40E+09	2.85E+09	4.11E+09	1.72E+09	6.167	5.735	6.416	5.741	4.995	5.187	5.481	5.471	6.015	5.283	-0.731	3.35E-02	1.14E-01
201	Q14194|DPYL1	12	-0.43	1.58	2.01	0.19	3.83	0.57	2.48	0.033989	1.16E-01	-4.30	0	5.41E+07	3.22E+07	1.17E+08	3.61E+06	3.94E+08	2.74E+08	3.79E+08	8.60E+07	0.067	0.290	1.105	-3.183	1.782	1.546	1.866	1.118	-0.430	1.578	2.008	3.40E-02	1.16E-01
202	P61970|NTF2	3	1.37	2.06	0.69	0.06	1.32	1.71	2.48	0.034459	1.17E-01	-4.31	0	1.50E+08	5.53E+07	1.43E+08	1.21E+08	5.10E+08	4.60E+08	3.92E+08	1.36E+08	1.482	1.035	1.402	1.547	2.167	2.354	1.919	1.786	1.366	2.056	0.690	3.45E-02	1.17E-01
203	P51149|RAB7A	7	-1.14	-0.06	1.07	0.09	2.06	-0.52	2.51	0.03531	1.18E-01	-4.22	1	2.18E+07	7.86E+06	3.65E+07	NA	8.39E+07	1.25E+08	1.55E+08	2.72E+07	-1.190	-1.646	-0.574	NA	-0.524	0.322	0.507	-0.555	-1.137	-0.062	1.075	3.53E-02	1.18E-01
204	Q9NVS9|PNPO	2	-2.89	-2.20	0.69	0.06	1.32	-2.54	2.46	0.035222	1.18E-01	-4.33	0	6.49E+06	2.88E+06	8.67E+06	4.12E+06	3.13E+07	2.97E+07	2.35E+07	6.92E+06	-2.869	-3.023	-2.655	-3.006	-1.996	-1.908	-2.351	-2.545	-2.888	-2.200	0.688	3.52E-02	1.18E-01
205	Q01082|SPTB2	13	-0.86	0.06	0.92	0.08	1.76	-0.40	2.46	0.035688	1.19E-01	-4.35	0	4.76E+07	9.73E+06	2.82E+07	1.76E+07	1.63E+08	1.31E+08	7.70E+07	3.76E+07	-0.112	-1.353	-0.947	-1.048	0.467	0.394	-0.552	-0.086	-0.865	0.056	0.921	3.57E-02	1.19E-01
206	Q15907|RB11B	5	-1.59	0.85	2.45	0.22	4.68	-0.13	2.66	0.035786	1.19E-01	-3.95	3	5.14E+06	NA	5.44E+07	NA	1.78E+08	2.19E+08	1.84E+08	NA	-3.191	NA	0.001	NA	0.598	1.196	0.767	NA	-1.595	0.854	2.449	3.58E-02	1.19E-01
207	P05387|RLA2	3	-0.66	0.59	1.25	0.10	2.40	-0.04	2.44	0.036779	1.20E-01	-4.37	0	3.02E+07	6.65E+06	3.68E+07	5.67E+07	1.44E+08	2.48E+08	1.48E+08	4.70E+07	-0.741	-1.876	-0.563	0.527	0.276	1.391	0.441	0.239	-0.663	0.587	1.250	3.68E-02	1.20E-01
208	P17066|HSP76	6	3.76	5.25	1.49	0.12	2.86	4.61	2.49	0.036732	1.20E-01	-4.26	1	1.23E+09	1.27E+08	1.40E+09	NA	3.57E+09	2.48E+09	3.97E+09	1.78E+09	4.384	2.179	4.707	NA	5.069	4.969	5.427	5.519	3.757	5.246	1.489	3.67E-02	1.20E-01
209	Q16890|TPD53	2	-1.61	-2.55	-0.95	-1.82	-0.08	-2.08	-2.55	0.03682	1.20E-01	-4.15	2	1.64E+07	9.35E+06	1.54E+07	NA	1.92E+07	1.63E+07	2.79E+07	NA	-1.598	-1.407	-1.821	NA	-2.727	-2.842	-2.089	NA	-1.605	-2.553	-0.948	3.68E-02	1.20E-01
210	Q9UPA5|BSN	3	-1.56	-2.64	-1.08	-2.08	-0.08	-2.10	-2.42	0.037781	1.23E-01	-4.40	0	1.64E+07	1.22E+07	1.25E+07	1.27E+07	1.19E+07	1.34E+07	2.33E+07	1.31E+07	-1.585	-1.045	-2.122	-1.488	-3.432	-3.141	-2.364	-1.616	-1.560	-2.638	-1.078	3.78E-02	1.23E-01
211	P35611|ADDA	5	1.63	0.17	-1.46	-2.83	-0.09	0.90	-2.40	0.039199	1.26E-01	-4.44	0	1.25E+08	7.24E+07	1.40E+08	2.46E+08	1.76E+08	1.64E+08	2.19E+08	1.24E+07	1.225	1.404	1.369	2.504	0.578	0.746	1.036	-1.699	1.626	0.165	-1.460	3.92E-02	1.26E-01
212	P61106|RAB14	6	-2.69	-0.54	2.14	0.14	4.14	-1.26	2.51	0.038902	1.26E-01	-4.15	2	NA	5.68E+06	5.61E+06	NA	1.33E+08	1.19E+08	1.05E+08	7.04E+06	NA	-2.092	-3.285	NA	0.162	0.256	-0.076	-2.519	-2.688	-0.544	2.144	3.89E-02	1.26E-01
213	P82979|SARNP	2	-1.91	-3.40	-1.49	-2.87	-0.10	-2.81	-2.60	0.039208	1.26E-01	-4.04	3	8.54E+06	NA	2.15E+07	NA	7.66E+06	1.46E+07	1.43E+07	NA	-2.489	NA	-1.341	NA	-4.093	-3.011	-3.100	NA	-1.915	-3.401	-1.487	3.92E-02	1.26E-01
214	P30084|ECHM	2	-3.56	-1.71	1.85	0.12	3.57	-2.08	2.59	0.039512	1.26E-01	-3.88	3	3.94E+06	NA	NA	NA	3.33E+07	2.38E+07	2.95E+07	2.48E+07	-3.558	NA	NA	NA	-1.903	-2.249	-2.006	-0.687	-3.558	-1.711	1.846	3.95E-02	1.26E-01
215	O75475|PSIP1	2	-2.80	-4.05	-1.25	-2.42	-0.08	-3.42	-2.50	0.039947	1.27E-01	-4.23	2	7.39E+06	2.02E+06	NA	7.54E+06	4.92E+06	9.35E+06	9.76E+06	NA	-2.689	-3.514	NA	-2.192	-4.752	-3.702	-3.685	NA	-2.798	-4.046	-1.248	3.99E-02	1.27E-01
216	P47755|CAZA2	6	-1.59	0.01	1.60	0.08	3.11	-0.68	2.42	0.040803	1.29E-01	-4.36	1	1.61E+07	3.39E+06	4.26E+07	NA	1.52E+08	1.45E+08	1.39E+08	1.71E+07	-1.612	-2.800	-0.351	NA	0.359	0.563	0.348	-1.233	-1.588	0.009	1.597	4.08E-02	1.29E-01
217	P30049|ATPD	3	3.01	2.16	-0.84	-1.65	-0.04	2.59	-2.37	0.041331	1.30E-01	-4.49	0	4.21E+08	1.98E+08	4.29E+08	4.60E+08	6.10E+08	2.34E+08	4.85E+08	2.52E+08	2.907	2.784	2.991	3.349	2.434	1.303	2.240	2.682	3.008	2.165	-0.843	4.13E-02	1.30E-01
218	O95817|BAG3	3	-0.47	0.21	0.68	0.03	1.32	-0.13	2.35	0.042611	1.33E-01	-4.52	0	3.64E+07	1.33E+07	3.96E+07	3.76E+07	1.26E+08	1.13E+08	1.25E+08	5.16E+07	-0.481	-0.921	-0.456	-0.025	0.085	0.172	0.189	0.375	-0.471	0.205	0.676	4.26E-02	1.33E-01
219	P51693|APLP1	3	0.89	-0.07	-0.95	-1.87	-0.04	0.41	-2.35	0.04243	1.33E-01	-4.51	0	7.82E+07	3.75E+07	8.74E+07	1.44E+08	7.60E+07	1.24E+08	8.72E+07	5.43E+07	0.576	0.502	0.688	1.783	-0.671	0.321	-0.363	0.450	0.887	-0.066	-0.953	4.24E-02	1.33E-01
220	P06576|ATPB	17	1.48	2.80	1.32	0.04	2.60	2.24	2.37	0.044509	1.38E-01	-4.45	1	1.06E+08	5.71E+07	2.80E+08	NA	1.04E+09	8.43E+08	8.89E+08	1.15E+08	1.003	1.079	2.372	NA	3.223	3.293	3.159	1.540	1.485	2.804	1.319	4.45E-02	1.38E-01
221	Q15121|PEA15	6	5.33	4.57	-0.76	-1.51	-0.02	4.95	-2.30	0.045958	1.42E-01	-4.59	0	3.09E+09	1.13E+09	2.59E+09	1.43E+09	1.88E+09	2.36E+09	2.92E+09	7.68E+08	5.665	5.183	5.594	4.882	4.112	4.897	4.962	4.300	5.331	4.568	-0.763	4.60E-02	1.42E-01
222	zz|Y-FGC2Cont00172|	14	7.09	6.45	-0.64	-1.26	-0.01	6.77	-2.30	0.046086	1.42E-01	-4.59	0	7.78E+09	4.95E+09	9.50E+09	5.67E+09	8.33E+09	6.66E+09	7.92E+09	3.49E+09	6.943	7.209	7.473	6.734	6.331	6.505	6.477	6.499	7.090	6.453	-0.637	4.61E-02	1.42E-01
223	P15291|B4GT1	2	-1.86	-3.76	-1.90	-3.75	-0.04	-3.29	-2.59	0.046475	1.42E-01	-3.93	4	NA	6.71E+06	NA	NA	1.67E+07	6.98E+06	6.97E+06	NA	NA	-1.862	NA	NA	-2.928	-4.157	-4.195	NA	-1.862	-3.760	-1.898	4.65E-02	1.42E-01
224	P49721|PSB2	3	-2.68	-1.56	1.11	0.01	2.21	-1.93	2.38	0.047703	1.45E-01	-4.35	2	5.33E+06	NA	1.18E+07	NA	4.13E+07	2.56E+07	5.55E+07	1.43E+07	-3.140	NA	-2.213	NA	-1.582	-2.138	-1.047	-1.489	-2.676	-1.564	1.112	4.77E-02	1.45E-01
225	Q7Z4H3|HDDC2	2	-2.13	-3.27	-1.14	-2.27	-0.01	-2.78	-2.32	0.047772	1.45E-01	-4.52	1	2.18E+07	NA	8.69E+06	5.85E+06	9.69E+06	1.08E+07	1.13E+07	7.61E+06	-1.194	NA	-2.652	-2.533	-3.742	-3.475	-3.457	-2.406	-2.126	-3.270	-1.144	4.78E-02	1.45E-01
226	Q9UPY7|PHF24	4	-0.54	-1.53	-0.99	-1.97	-0.01	-1.04	-2.28	0.047969	1.45E-01	-4.63	0	2.40E+07	2.99E+07	2.99E+07	2.76E+07	3.52E+07	2.76E+07	3.35E+07	2.87E+07	-1.056	0.189	-0.862	-0.441	-1.818	-2.022	-1.814	-0.479	-0.543	-1.533	-0.990	4.80E-02	1.45E-01
227	P07741|APT	2	-3.51	-2.08	1.44	0.01	2.86	-2.44	2.55	0.048548	1.46E-01	-3.98	4	4.07E+06	NA	NA	NA	2.56E+07	NA	2.63E+07	1.19E+07	-3.513	NA	NA	NA	-2.294	NA	-2.181	-1.756	-3.513	-2.077	1.436	4.85E-02	1.46E-01
228	Q8WVW12|PCNP	2	-0.55	-1.55	-1.00	-2.00	0.00	-1.12	-2.29	0.0503	1.51E-01	-4.57	1	2.47E+07	NA	2.73E+07	4.99E+07	3.47E+07	3.55E+07	3.62E+07	1.94E+07	-1.020	NA	-0.996	0.355	-1.840	-1.629	-1.696	-1.043	-0.554	-1.552	-0.998	5.03E-02	1.51E-01
229	Q8IWJ2|GCC2	3	2.89	1.35	-1.55	-3.10	0.01	2.01	-2.28	0.051157	1.53E-01	-4.58	1	3.50E+08	2.30E+08	4.42E+08	NA	4.09E+08	8.99E+07	1.89E+08	2.98E+08	2.650	2.992	3.034	NA	1.836	-0.186	0.809	2.924	2.892	1.346	-1.546	5.12E-02	1.53E-01
230	Q96KP4|CNDP2	5	-0.85	0.10	0.95	-0.01	1.90	-0.31	2.27	0.05183	1.54E-01	-4.60	1	2.89E+07	1.62E+07	2.55E+07	NA	1.42E+08	6.23E+07	1.91E+08	4.17E+07	-0.799	-0.652	-1.096	NA	0.261	-0.755	0.823	0.066	-0.849	0.099	0.948	5.18E-02	1.54E-01
231	P61758|PFD3	2	-3.36	-2.49	0.87	-0.01	1.75	-2.86	2.26	0.0523	1.55E-01	-4.61	1	5.15E+06	2.06E+06	5.17E+06	NA	1.38E+07	1.83E+07	2.83E+07	9.95E+06	-3.188	-3.487	-3.405	NA	-3.216	-2.658	-2.070	-2.017	-3.360	-2.490	0.870	5.23E-02	1.55E-01
232	zz|Y-FGC2Cont00093|	3	-0.09	-0.73	-0.64	-1.29	0.01	-0.41	-2.22	0.052539	1.55E-01	-4.72	0	5.77E+07	1.94E+07	5.43E+07	3.56E+07	6.57E+07	6.10E+07	5.86E+07	3.29E+07	0.155	-0.406	-0.001	-0.098	-0.888	-0.787	-0.965	-0.277	-0.088	-0.729	-0.642	5.25E-02	1.55E-01
233	P15104|GLNA	4	1.88	3.02	1.15	-0.02	2.31	2.45	2.21	0.05336	1.56E-01	-4.73	0	2.77E+08	1.09E+08	3.89E+08	5.06E+07	1.13E+09	7.05E+08	9.46E+08	2.18E+08	2.326	1.960	2.850	0.375	3.356	3.017	3.254	2.466	1.878	3.023	1.145	5.34E-02	1.56E-01
234	Q16799|RTN1	2	1.89	0.93	-0.96	-1.94	0.02	1.41	-2.21	0.053328	1.56E-01	-4.73	0	2.47E+08	5.77E+07	2.20E+08	2.08E+08	1.64E+08	1.39E+08	1.86E+08	1.55E+08	2.168	1.093	2.026	2.280	0.476	0.492	0.788	1.976	1.892	0.933	-0.959	5.33E-02	1.56E-01
235	Q96I99|SUCB2	5	-2.16	-0.82	1.34	-0.04	2.72	-1.27	2.29	0.054781	1.59E-01	-4.49	2	5.74E+06	NA	2.24E+07	NA	1.06E+08	6.16E+07	5.88E+07	1.56E+07	-3.039	NA	-1.284	NA	-0.175	-0.773	-0.960	-1.361	-2.162	-0.817	1.345	5.48E-02	1.59E-01
236	O95670|VATG2	2	-1.89	-1.00	0.89	-0.03	1.81	-1.45	2.18	0.055821	1.62E-01	-4.78	0	1.27E+07	9.89E+06	1.13E+07	8.50E+06	3.13E+07	5.69E+07	6.56E+07	3.20E+07	-1.935	-1.330	-2.269	-2.031	-1.996	-0.895	-0.794	-0.319	-1.891	-1.001	0.890	5.58E-02	1.62E-01

1	ProteinName	# Peptides	Ctrl	Group1	log2FC	CI.L	CI.R	Ave Expr	t	P.Value	adj.P.Val	B	nrNAs	M.3_Control.raw	M.2_Control.raw	M.4_Control.raw	M.1_Control.raw	E4.2_Group_1.raw	E4.4_Group_1.raw	E4.3_Group_1.raw	E4.1_Group_1.raw	M.3_Control.transf	M.2_Control.transf	M.4_Control.transf	M.1_Control.transf	E4.2_Group_1.transf	E4.4_Group_1.transf	E4.3_Group_1.transf	E4.1_Group_1.transf	pseudo.Ctrl	pseudo.Group1	pseudo.log2FC	pseudo.P.Value	pseudo.adj.P.Val
237	P21281|VATB2	9	0.14	1.14	1.01	-0.03	2.05	0.64	2.18	0.056336	1.62E-01	-4.79	0	6.61E+07	1.75E+07	1.42E+08	2.38E+07	2.59E+08	1.68E+08	2.74E+08	9.47E+07	0.343	-0.547	1.391	-0.642	1.156	0.790	1.375	1.257	0.136	1.144	1.008	5.63E-02	1.62E-01
238	Q9UPQ0|LIMC1	2	-2.02	-3.43	-1.41	-2.88	0.06	-2.37	-2.43	0.05658	1.62E-01	-4.14	4	1.06E+07	5.07E+06	1.78E+07	NA	1.20E+07	NA	NA	NA	-2.189	-2.248	-1.617	NA	-3.430	NA	NA	NA	-2.018	-3.430	-1.412	5.66E-02	1.62E-01
239	P07205|PGK2	6	-2.42	-1.67	0.75	-0.03	1.53	-2.05	2.25	0.057436	1.64E-01	-4.59	2	7.59E+06	4.74E+06	1.13E+07	NA	3.92E+07	3.75E+07	3.36E+07	NA	-2.651	-2.341	-2.272	NA	-1.660	-1.546	-1.810	NA	-2.422	-1.672	0.750	5.74E-02	1.64E-01
240	P18669|PGAM1	10	3.43	4.44	1.01	-0.04	2.06	3.94	2.16	0.058077	1.65E-01	-4.81	0	4.92E+08	3.04E+08	1.49E+09	2.35E+08	2.35E+09	1.90E+09	2.05E+09	7.89E+08	3.123	3.376	4.789	2.441	4.441	4.558	4.423	4.338	3.432	4.440	1.008	5.81E-02	1.65E-01
241	Q13409|DC1I2	2	-0.93	-1.94	-1.01	-2.07	0.05	-1.60	-2.23	0.059213	1.68E-01	-4.57	2	NA	1.16E+07	NA	2.21E+07	3.32E+07	2.66E+07	2.11E+07	1.69E+07	NA	-1.113	NA	-0.743	-1.909	-2.078	-2.511	-1.250	-0.928	-1.937	-1.009	5.92E-02	1.68E-01
242	P60174|TPIS	15	6.88	7.93	1.05	-0.05	2.16	7.40	2.14	0.059779	1.69E-01	-4.84	0	9.69E+09	2.95E+09	1.14E+10	3.34E+09	2.76E+10	2.67E+10	2.20E+10	4.61E+09	7.246	6.495	7.739	6.020	8.119	8.666	8.028	6.904	6.875	7.929	1.054	5.98E-02	1.69E-01
243	P04156|PRIO	2	-1.04	-2.12	-1.07	-2.21	0.06	-1.69	-2.29	0.060298	1.69E-01	-4.48	3	2.49E+07	NA	NA	1.72E+07	4.05E+07	2.68E+07	1.90E+07	NA	-1.006	NA	NA	-1.078	-1.609	-2.066	-2.670	NA	-1.042	-2.115	-1.073	6.03E-02	1.69E-01
244	Q9Y4L1|HYOU1	5	-1.50	-0.41	1.09	-0.07	2.24	-0.88	2.16	0.061523	1.72E-01	-4.76	1	1.84E+07	8.90E+06	1.80E+07	NA	1.27E+08	1.14E+08	1.00E+08	1.19E+07	-1.427	-1.475	-1.595	NA	0.094	0.177	-0.155	-1.761	-1.499	-0.411	1.088	6.15E-02	1.72E-01
245	zz|Y-FGC2Cont00487|	15	0.94	1.87	0.92	-0.06	1.91	1.40	2.20	0.062053	1.73E-01	-4.67	2	1.01E+08	3.46E+07	1.54E+08	NA	4.51E+08	2.67E+08	4.45E+08	NA	0.924	0.390	1.513	NA	1.982	1.509	2.108	NA	0.942	1.866	0.924	6.21E-02	1.73E-01
246	Q14847|LASP1	6	0.74	1.62	0.89	-0.07	1.85	1.18	2.09	0.065025	1.80E-01	-4.92	0	8.70E+07	5.25E+07	1.43E+08	3.44E+07	2.65E+08	2.56E+08	2.78E+08	2.18E+08	0.724	0.962	1.403	-0.146	1.192	1.444	1.394	2.470	0.736	1.625	0.889	6.50E-02	1.80E-01
247	O60687|SRPX2	2	0.53	-1.51	-2.04	-4.27	0.20	-0.29	-2.21	0.067531	1.86E-01	-4.59	3	9.47E+07	2.30E+07	1.02E+08	NA	1.56E+07	NA	1.11E+08	NA	0.841	-0.168	0.906	NA	-3.029	NA	0.008	NA	0.526	-1.511	-2.037	6.75E-02	1.86E-01
248	Q16555|DPYL2	21	5.61	6.73	1.12	-0.10	2.33	6.17	2.07	0.067781	1.86E-01	-4.96	0	3.79E+09	1.70E+09	5.15E+09	8.54E+08	1.30E+10	9.21E+09	1.22E+10	2.14E+09	5.948	5.739	6.588	4.183	6.990	7.009	7.129	5.790	5.614	6.729	1.115	6.78E-02	1.86E-01
249	zz|Y-FGC2Cont00099|	9	4.88	5.49	0.61	-0.05	1.27	5.18	2.07	0.067718	1.86E-01	-4.96	0	1.68E+09	8.17E+08	2.33E+09	1.10E+09	4.44E+09	3.90E+09	4.12E+09	1.64E+09	4.822	4.733	5.440	4.525	5.393	5.676	5.483	5.403	4.880	5.489	0.609	6.77E-02	1.86E-01
250	zz|Y-FGC2Cont00192|	6	5.91	5.26	-0.65	-1.36	0.06	5.59	-2.06	0.068354	1.87E-01	-4.97	0	3.59E+09	2.40E+09	3.96E+09	2.04E+09	3.27E+09	2.86E+09	3.52E+09	1.98E+09	5.874	6.214	6.207	5.359	4.937	5.193	5.244	5.672	5.914	5.262	-0.652	6.84E-02	1.87E-01
251	O60869|EDF1	2	-1.15	-2.00	-0.84	-1.77	0.08	-1.58	-2.05	0.069632	1.89E-01	-4.99	0	1.53E+07	7.00E+06	2.62E+07	3.62E+07	2.65E+07	3.41E+07	2.95E+07	9.78E+06	-1.685	-1.805	-1.054	-0.076	-2.245	-1.691	-2.008	-2.042	-1.155	-1.997	-0.842	6.96E-02	1.89E-01
252	P32004|L1CAM	3	-1.04	-1.69	-0.65	-1.36	0.06	-1.36	-2.05	0.069961	1.89E-01	-4.99	0	2.03E+07	9.61E+06	3.30E+07	2.16E+07	4.12E+07	2.43E+07	3.88E+07	1.58E+07	-1.288	-1.370	-0.720	-0.774	-1.585	-2.221	-1.590	-1.345	-1.038	-1.685	-0.648	7.00E-02	1.89E-01
253	Q9UMX5|NENF	2	-1.65	-2.32	-0.67	-1.42	0.07	-1.98	-2.05	0.070023	1.89E-01	-4.99	0	1.12E+07	9.35E+06	1.41E+07	1.67E+07	2.00E+07	2.05E+07	2.77E+07	9.86E+06	-2.110	-1.407	-1.947	-1.118	-2.664	-2.483	-2.099	-2.030	-1.645	-2.319	-0.674	7.00E-02	1.89E-01
254	Q08174|PCDH1	7	0.25	-0.40	-0.66	-1.38	0.07	-0.07	-2.03	0.072096	1.94E-01	-5.02	0	5.28E+07	2.94E+07	7.24E+07	5.16E+07	9.92E+07	5.38E+07	7.68E+07	4.59E+07	0.034	0.166	0.416	0.402	-0.275	-0.983	-0.554	0.205	0.254	-0.402	-0.656	7.21E-02	1.94E-01
255	Q9HD15|SRA1	3	-1.78	-2.56	-0.78	-1.66	0.10	-2.30	-2.09	0.073207	1.95E-01	-4.77	2	1.34E+07	NA	NA	1.69E+07	NA	1.64E+07	2.34E+07	2.01E+07	7.54E+06	-1.864	NA	-1.688	NA	-2.955	-2.277	-2.590	-2.419	-1.776	-2.561	-0.784	7.32E-02	1.95E-01
256	Q9UDY4|DNJB4	2	0.52	-0.35	-0.87	-1.84	0.10	0.02	-2.05	0.07318	1.95E-01	-4.93	1	NA	6.47E+07	7.75E+07	3.31E+07	9.11E+07	9.23E+07	1.11E+08	2.23E+07	NA	1.251	0.515	-0.199	-0.402	-0.144	-0.001	-0.845	0.522	-0.348	-0.870	7.32E-02	1.95E-01
257	Q8IV50|LYSM2	2	-2.56	-3.88	-1.32	-2.83	0.19	-3.22	-2.21	0.074858	1.97E-01	-4.54	4	5.16E+06	NA	NA	9.15E+06	NA	NA	8.74E+06	2.71E+06	-3.186	NA	NA	-1.932	NA	NA	-3.852	-3.907	-2.559	-3.880	-1.321	7.49E-02	1.97E-01
258	Q9BW30|TPPP3	8	2.48	1.83	-0.65	-1.38	0.08	2.16	-2.01	0.07463	1.97E-01	-5.05	0	2.56E+08	1.20E+08	3.29E+08	3.59E+08	3.04E+08	3.36E+08	3.86E+08	1.79E+08	2.216	2.094	2.605	3.016	1.393	1.866	1.895	2.184	2.483	1.834	-0.648	7.46E-02	1.97E-01
259	Q9HAV7|GRPE1	2	-2.68	-3.70	-1.02	-2.17	0.13	-3.29	-2.14	0.074033	1.97E-01	-4.68	3	8.87E+06	3.10E+06	NA	NA	6.98E+06	1.26E+07	1.02E+07	NA	-2.437	-2.922	NA	NA	-4.232	-3.244	-3.618	NA	-2.679	-3.698	-1.019	7.40E-02	1.97E-01
260	zz|Y-FGC2Cont00116|	3	2.20	1.56	-0.64	-1.37	0.08	1.88	-2.01	0.074384	1.97E-01	-5.05	0	2.73E+08	8.84E+07	2.34E+08	2.85E+08	3.00E+08	3.01E+08	2.53E+08	1.48E+08	2.307	1.679	2.114	2.706	1.376	1.691	1.251	1.911	2.201	1.557	-0.644	7.44E-02	1.97E-01
261	O95394|AGM1	2	-1.68	-3.01	-1.32	-2.84	0.19	-2.67	-2.21	0.0752	1.97E-01	-4.42	4	NA	NA	1.70E+07	NA	1.16E+07	1.69E+07	1.79E+07	NA	NA	NA	-1.683	NA	-3.472	-2.784	-2.760	NA	-1.683	-3.005	-1.323	7.52E-02	1.97E-01
262	Q15181|IPYR	8	2.72	3.53	0.82	-0.11	1.74	3.18	2.03	0.075978	1.98E-01	-4.96	1	4.25E+08	1.43E+08	4.01E+08	NA	1.70E+09	1.21E+09	1.21E+09	2.55E+08	2.920	2.339	2.895	NA	3.960	3.857	3.627	2.695	2.718	3.535	0.817	7.60E-02	1.98E-01
263	zz|Y-FGC2Cont00463|	9	3.09	3.98	0.90	-0.12	1.91	3.54	1.99	0.076584	1.99E-01	-5.08	0	5.01E+08	3.38E+08	7.80E+08	1.49E+08	2.23E+09	1.24E+09	1.63E+09	4.77E+08	3.147	3.522	3.856	1.833	4.363	3.893	4.075	3.608	3.089	3.985	0.895	7.66E-02	1.99E-01
264	P46108|CRK	7	-0.53	1.01	1.53	-0.21	3.28	0.24	1.98	0.077823	2.01E-01	-5.09	0	7.78E+07	2.85E+06	9.29E+07	2.81E+07	3.10E+08	2.27E+08	2.27E+08	4.74E+07	0.570	-3.038	0.777	-0.419	1.425	1.258	1.092	0.252	-0.528	1.007	1.534	7.78E-02	2.01E-01
265	Q9BY67|CADM1	3	0.76	0.04	-0.72	-1.54	0.10	0.40	-1.98	0.078077	2.01E-01	-5.09	0	1.43E+08	3.67E+07	9.16E+07	5.17E+07	1.13E+08	6.91E+07	1.40E+08	5.57E+07	1.413	0.471	0.756	0.404	-0.080	-0.593	0.358	0.486	0.761	0.043	-0.718	7.81E-02	2.01E-01
266	O95757|HS74L	2	-0.79	-1.55	-0.76	-1.62	0.11	-1.17	-1.98	0.078408	2.01E-01	-5.10	0	2.79E+07	1.15E+07	4.42E+07	1.96E+07	4.82E+07	6.33E+07	3.09E+07	8.80E+06	-0.848	-1.126	-0.299	-0.902	-1.352	-0.731	-1.934	-2.196	-0.794	-1.553	-0.759	7.84E-02	2.01E-01
267	P31937|HIDH	4	-1.35	-0.58	0.78	-0.12	1.67	-0.84	2.03	0.079957	2.04E-01	-4.86	2	NA	NA	2.10E+07	1.42E+07	7.92E+07	6.66E+07	6.04E+07	3.64E+07	NA	NA	-1.373	-1.335	-0.610	-0.651	-0.919	-0.132	-1.354	-0.578	0.776	8.00E-02	2.04E-01
268	Q01484|ANK2	10	1.22	0.39	-0.82	-1.77	0.12	0.80	-1.96	0.080556	2.05E-01	-5.12	0	1.46E+08	3.50E+07	2.49E+08	7.02E+07	1.62E+08	1.40E+08	1.76E+08	3.76E+07	1.438	0.407	2.202	0.816	0.458	0.500	0.700	-0.086	1.216	0.393	-0.823	8.06E-02	2.05E-01
269	P52799|EFNB2	3	-2.47	-1.11	1.35	-0.21	2.92	-1.79	1.95	0.082122	2.08E-01	-5.14	0	1.78E+07	3.08E+06	2.22E+07	1.74E+06	7.61E+07	5.97E+07	7.83E+07	7.42E+06	-1.475	-2.934	-1.295	-4.172	-0.669	-0.820	-0.526	-2.442	-2.469	-1.114	1.355	8.21E-02	2.08E-01
270	O43505|B4GA1	3	-1.92	-1.03	0.89	-0.15	1.94	-1.41	1.97	0.083672	2.12E-01	-5.06	1	1.19E+07	4.35E+06	2.25E+07	NA	9.30E+07	3.09E+07	6.27E+07	1.96E+07	-2.030	-2.458	-1.275	NA	-0.371	-1.845	-0.862	-1.029	-1.921	-1.027	0.894	8.37E-02	2.12E-01
271	O75390|CISY	4	0.00	1.23	1.23	-0.21	2.67	0.70	1.95	0.085301	2.15E-01	-5.07	1	1.82E+07	2.97E+07	1.29E+08	NA	3.00E+08	1.60E+08	3.90E+08	7.46E+07	-1.444	0.181	1.252	NA	1.373	0.713	1.908	0.910	-0.004	1.226	1.230	8.53E-02	2.15E-01
272	P02452|CO1A1	36	9.31	8.71	-0.61	-1.32	0.10	9.01	-1.92	0.086075	2.16E-01	-5.19	0	3.52E+10	2.24E+10	4.14E+10	3.91E+10	2.89E+10	2.95E+10	3.19E+10	2.31E+10	9.030	9.283	9.603	9.339	8.184	8.818	8.587	9.243	9.313	8.708	-0.605	8.61E-02	2.16E-01
273	P47736|RPGP1	3	-3.23	-4.36	-1.13	-2.46	0.20	-3.79	-1.92	0.086466	2.16E-01	-5.19	0	7.77E+06	2.12E+06	8.80E+06	1.68E+06	9.58E+06	2.72E+06	4.44E+06	4.48E+06	-2.619	-3.448	-2.634	-4.213	-3.759	-5.623	-4.877	-3.177	-3.228	-4.359	-1.131	8.65E-02	2.16E-01
274	Q07021|C1QBP	4	-0.72	0.38	1.10	-0.19	2.38	-0.17	1.92	0.08656	2.16E-01	-5.19	0	5.79E+07	2.30E+07	4.09E+07	6.27E+06	1.57E+08	1.84E+08	1.56E+08	3.14E+07	0.160	-0.173	-0.410	-2.441	0.411	0.931	0.523	-0.345	-0.716	0.380	1.096	8.66E-02	2.16E-01
275	Q12860|CNTN1	10	0.94	1.87	0.93	-0.17	2.03	1.41	1.90	0.088674	2.20E-01	-5.21	0	5.33E+07	5.68E+07	2.08E+08	6.49E+07	4.63E+08	5.33E+08	4.09E+08	7.43E+07	0.046	1.071	1.943	0.709	2.023	2.580	1.980	0.904	0.942	1.872	0.930	8.87E-02	2.20E-01
276	REV__Q8W242|TITIN	3	0.55	-0.97	-1.53	-3.36	0.30	-0.32	-1.91	0.090869	2.21E-01	-5.13	1	7.99E+07	3.39E+07	8.77E+07	NA	2.01E+08	7.52E+07	5.39E+07	4.69E+06	0.605	0.364	0.694	NA	0.776	-0.464	-1.094	-3.111	0.554	-0.973	-1.527	9.09E-02	2.21E-01
277	P61981|1433G	10	2.63	3.27	0.64	-0.12	1.41	2.95	1.89	0.090372	2.21E-01	-5.23	0	3.29E+08	1.60E+08	4.87E+08	2.10E+08	9.81E+08	1.29E+09	8.04E+08	3.13E+08	2.563	2.491	3.174	2.295	3.142	3.955	3.007	2.994	2.631	3.275	0.644	9.04E-02	2.21E-01
278	Q08257|QOR	2	-1.93	-0.78	1.15	-0.22	2.52	-1.36	1.90	0.089472	2.21E-01	-5.22	0	6.51E+06	1.42E+07	3.27E+07	3.32E+06	7.31E+07	4.84E+07	8.99E+07	2.11E+07	-2.865	-0.832	-0.733	-3.297	-0.731	-1.149	-0.317	-0.924	-1.932	-0.780	1.151	8.95E-02	2.21E-01
279	Q8N6G6|ATL1	3	-4.29	-2.39	1.91	-0.40	4.22	-2.77	2.00	0.090691	2.21E-01	-4.70	3	NA	NA	2.79E+06	NA	4.56E+07	3.82E+07	1.53E+07	3.37E+06	NA	NA	-4.295	NA	-1.432	-1.516	-3.003	-3.592	-4.295	-2.386	1.909	9.07E-02	2.21E-01
280	Q93045|STMN2	2	1.26	0.59	-0.68	-1.48	0.13	0.92	-1.89	0.090252	2.21E-01	-5.23	0	1.39E+08	4.50E+07	1.78E+08	9.39E+07	1.29E+08	1.92E+08	1.24E+08	8.29E+07	1.372	0.750	1.717	1.207	0.114	0.997	0.171	1.064	1.262	0.586	-0.675	9.03E-02	2.21E-01
281	zz|Y-FGC2Cont00305|	3	-1.00	-0.35	0.65	-0.12	1.42	-0.68	1.89	0.090429	2.21E-01	-5.23	0	3.28E+07	9.86E+06	3.44E+07	1.38E+07	1.01E+08	5.39E+07	1.15E+08	3.37E+07	-0.628	-1.334	-0.663	-1.378	-0.241	-0.981	0.054	-0.243	-1.001	-0.353	0.648	9.04E-02	2.21E-01
282	P41567|EIF1	4	0.44	1.38	0.95	-0.19	2.08	0.91	1.88	0.091689	2.22E-01	-5.24	0	1.32E+08	3.10E+07	1.22E+08	1.88E+07	3.52E+08	2.68E+08	3.05E+08	7.28E+07	1.300	0.241	1.166	-0.962	1.613	1.514	1.535	0.874	0.436	1.384	0.948	9.17E-02	2.22E-01
283	O94903|PLPHP	3	-0.85	0.19	1.05	-0.24	2.33	-0.22	1.97	0.094683	2.23E-01	-4.92	3	NA	9.26E+06	4.47E+07	NA	1.44E+08	1.48E+08	9.18E+07	NA	NA	-1.420	-0.283	NA	0.277	0.591	-0.285	NA	-0.851	0.194	1.046	9.47E-02	2.23E-01

	ProteinName	# Peptides	Ctrl	Group1	log2FC	CI.L	CI.R	Ave Expr	t	P.Value	adj.P.Val	B	nrNAs	M.3_Control.raw	M.2_Control.raw	M.4_Control.raw	M.1_Control.raw	E4.2_Group1.raw	E4.4_Group1.raw	E4.3_Group1.raw	E4.1_Group1.raw	M.3_Control.transf	M.2_Control.transf	M.4_Control.transf	M.1_Control.transf	E4.2_Group_1.transf	E4.4_Group_1.transf	E4.3_Group_1.transf	E4.1_Group_1.transf	pseudo.Ctrl	pseudo.Group1	pseudo.log2FC	pseudo.P.Value	pseudo.adj.P.Val
284	P07954|FUMH	9	0.39	1.80	1.42	-0.30	3.14	1.09	1.86	0.094823	2.23E-01	-5.27	0	9.16E+07	3.81E+07	2.21E+08	1.00E+07	4.59E+08	3.97E+08	5.66E+08	6.07E+07	0.796	0.522	2.030	-1.807	2.009	2.121	2.473	0.612	0.385	1.804	1.419	9.48E-02	2.23E-01
285	Q01469|FABP5	4	1.58	2.45	0.86	-0.18	1.90	2.02	1.86	0.095136	2.23E-01	-5.28	0	1.66E+08	3.12E+07	2.63E+08	1.95E+08	7.59E+08	5.01E+08	5.69E+08	1.64E+08	1.621	0.247	2.282	2.189	2.760	2.485	2.482	2.056	1.585	2.446	0.861	9.51E-02	2.23E-01
286	Q13813|SPTN1	55	2.86	4.10	1.25	-0.26	2.75	3.48	1.87	0.093445	2.23E-01	-5.26	0	5.76E+08	1.78E+08	9.90E+08	9.64E+07	2.22E+09	2.11E+09	2.27E+09	2.66E+08	3.340	2.643	4.201	1.243	4.362	4.718	4.580	2.757	2.857	4.104	1.247	9.34E-02	2.23E-01
287	Q16186|ADRM1	2	0.93	0.34	-0.59	-1.30	0.12	0.64	-1.87	0.093115	2.23E-01	-5.26	0	8.83E+07	5.07E+07	1.04E+08	8.86E+07	1.26E+08	1.21E+08	1.09E+08	8.10E+07	0.745	0.914	0.942	1.129	0.088	0.274	-0.018	1.031	0.933	0.344	-0.589	9.31E-02	2.23E-01
288	Q99962|SH3G2	4	-1.18	-0.24	0.95	-0.20	2.09	-0.71	1.86	0.094811	2.23E-01	-5.27	0	4.09E+07	1.23E+07	2.67E+07	6.73E+06	5.50E+07	1.32E+08	1.32E+08	2.90E+07	-0.320	-1.030	-1.029	-2.345	-1.154	0.406	0.267	-0.462	-1.181	-0.236	0.945	9.48E-02	2.23E-01
289	Q9UMX0|UBQL1	10	3.14	2.49	-0.65	-1.45	0.14	2.81	-1.86	0.094879	2.23E-01	-5.28	0	6.14E+08	3.58E+08	5.26E+08	2.03E+08	5.45E+08	4.91E+08	5.86E+08	2.55E+08	3.429	3.598	3.286	2.249	2.266	2.453	2.526	2.700	3.140	2.486	-0.654	9.49E-02	2.23E-01
290	Q9Y4J8|DTNA	6	-2.25	-2.96	-0.71	-1.57	0.14	-2.61	-1.87	0.093127	2.23E-01	-5.26	0	1.38E+07	4.01E+06	1.31E+07	5.72E+06	9.07E+06	1.66E+07	1.71E+07	7.82E+06	-1.822	-2.569	-2.061	-2.564	-3.841	-2.814	-2.836	-2.366	-2.254	-2.964	-0.710	9.31E-02	2.23E-01
291	Q9Y5X3|SNX5	5	1.07	0.44	-0.63	-1.38	0.13	0.76	-1.86	0.09456	2.23E-01	-5.27	0	1.39E+08	4.63E+07	1.19E+08	8.00E+07	1.81E+08	2.03E+08	1.27E+08	3.63E+07	1.373	0.792	1.130	0.992	0.621	1.084	0.209	-0.136	1.072	0.445	-0.627	9.46E-02	2.23E-01
292	O95865|DDAH2	8	0.92	1.47	0.55	-0.12	1.23	1.19	1.85	0.095778	2.24E-01	-5.28	0	1.11E+08	3.56E+07	1.27E+08	7.70E+07	3.68E+08	2.96E+08	2.32E+08	1.05E+08	1.062	0.428	1.234	0.940	1.682	1.667	1.122	1.412	0.916	1.471	0.555	9.58E-02	2.24E-01
293	Q13228|SBP1	5	-2.69	-1.23	1.46	-0.32	3.24	-1.96	1.84	0.097457	2.27E-01	-5.30	0	2.88E+06	6.77E+06	3.13E+07	1.81E+06	8.25E+07	4.51E+07	7.55E+07	7.01E+06	-3.991	-1.850	-0.799	-4.112	-0.549	-1.257	-0.581	-2.525	-2.688	-1.228	1.460	9.75E-02	2.27E-01
294	Q9HBL0|TENS1	3	1.75	1.14	-0.61	-1.37	0.15	1.44	-1.81	0.103085	2.38E-01	-5.35	0	1.90E+08	8.16E+07	2.56E+08	1.06E+08	2.25E+08	1.54E+08	2.56E+08	1.28E+08	1.803	1.569	2.246	1.375	0.945	0.653	1.269	1.690	1.748	1.139	-0.609	1.03E-01	2.38E-01
295	Q9Y281|COF2	6	0.32	1.72	1.40	-0.34	3.14	1.02	1.81	0.10277	2.38E-01	-5.35	0	1.13E+08	2.36E+07	1.67E+08	1.46E+07	5.11E+08	5.27E+08	5.14E+08	3.51E+07	1.090	-0.135	1.622	-1.300	2.170	2.563	2.329	-0.183	0.319	1.720	1.401	1.03E-01	2.38E-01
296	C9JLW8|MCRI1	3	-3.62	-4.55	-0.92	-2.11	0.26	-3.99	-1.88	0.106522	2.46E-01	-5.04	3	3.46E+06	2.16E+06	4.17E+06	NA	NA	7.86E+06	NA	1.17E+06	-3.739	-3.417	-3.713	NA	NA	-3.973	NA	-5.121	-3.623	-4.547	-0.924	1.07E-01	2.46E-01
297	P17174|AATC	3	0.52	-0.56	-1.08	-2.46	0.30	-0.20	-1.84	0.106995	2.46E-01	-5.13	2	NA	NA	5.36E+07	8.41E+07	7.56E+07	4.50E+07	6.52E+07	5.62E+07	NA	NA	-0.019	1.059	-0.680	-1.260	-0.805	0.500	0.520	-0.561	-1.081	1.07E-01	2.46E-01
298	Q32CW2|LEGL	4	2.90	2.36	-0.55	-1.24	0.15	2.63	-1.78	0.107858	2.46E-01	-5.39	0	4.14E+08	2.86E+08	4.85E+08	2.07E+08	5.98E+08	4.84E+08	5.48E+08	1.77E+08	2.883	3.289	3.168	2.275	2.403	2.431	2.424	2.169	2.904	2.357	-0.547	1.08E-01	2.46E-01
299	Q96D15|RICN3	5	-2.82	-1.31	1.51	-0.42	3.44	-1.95	1.80	0.108454	2.46E-01	-5.30	1	1.13E+07	2.28E+06	6.80E+06	NA	4.16E+07	6.77E+07	1.47E+08	3.71E+06	-2.103	-3.347	-3.007	NA	-1.570	-0.627	0.427	-3.452	-2.819	-1.305	1.514	1.08E-01	2.46E-01
300	Q96Q27|MAGI1	3	-0.97	-1.66	-0.69	-1.59	0.20	-1.31	-1.83	0.108468	2.46E-01	-5.20	2	3.28E+07	9.96E+06	2.82E+07	NA	3.38E+07	4.51E+07	3.29E+07	NA	-0.627	-1.320	-0.948	NA	-1.879	-1.258	-1.843	NA	-0.965	-1.660	-0.695	1.08E-01	2.46E-01
301	Q9H4G0|E41L1	3	-2.36	-3.36	-1.00	-2.28	0.27	-2.79	-1.80	0.107665	2.46E-01	-5.29	1	1.19E+07	2.20E+06	2.02E+07	5.66E+06	7.94E+06	1.04E+07	2.11E+07	NA	-2.034	-3.397	-1.432	-2.578	-4.040	-3.536	-2.514	NA	-2.360	-3.363	-1.003	1.08E-01	2.46E-01
302	P08631|HCK	2	0.48	-1.06	-1.54	-3.52	0.44	-0.29	-1.82	0.109107	2.46E-01	-5.21	2	6.53E+07	NA	6.45E+07	7.34E+07	2.35E+08	2.39E+07	3.08E+07	NA	0.326	NA	0.248	0.876	1.011	-2.244	-1.943	NA	0.483	-1.059	-1.542	1.09E-01	2.46E-01
303	P09104|ENOG	16	6.57	7.94	1.37	-0.37	3.11	7.25	1.77	0.109225	2.46E-01	-5.40	0	9.22E+09	4.14E+09	1.27E+10	8.90E+08	3.09E+10	2.61E+10	2.43E+10	3.91E+09	7.178	6.961	7.899	4.239	8.287	8.626	8.174	6.665	6.569	7.938	1.369	1.09E-01	2.46E-01
304	zz|Y-FGC2Cont00478|	3	-1.78	-2.79	-1.01	-2.33	0.30	-2.29	-1.81	0.111032	2.49E-01	-5.22	2	1.11E+07	8.36E+06	1.73E+07	NA	2.92E+07	7.80E+06	2.43E+07	NA	-2.123	-1.561	-1.653	NA	-2.098	-3.985	-2.299	NA	-1.779	-2.794	-1.015	1.11E-01	2.49E-01
305	P49189|AL9A1	3	-2.03	-1.09	0.95	-0.27	2.17	-1.49	1.78	0.111684	2.50E-01	-5.33	1	7.90E+06	3.70E+06	3.08E+07	NA	6.10E+07	6.43E+07	6.35E+07	1.16E+07	-2.597	-2.682	-0.819	NA	-1.000	-0.706	-0.845	-1.793	-2.032	-1.086	0.946	1.12E-01	2.50E-01
306	P60880|SNP25	9	1.28	0.65	-0.63	-1.45	0.18	0.96	-1.75	0.11236	2.51E-01	-5.43	0	1.87E+08	5.70E+07	1.18E+08	8.92E+07	1.41E+08	1.34E+08	1.44E+08	1.12E+08	1.779	1.077	1.128	1.138	0.252	0.433	0.402	1.503	1.281	0.647	-0.633	1.12E-01	2.51E-01
307	P13645|K1C10	18	4.62	2.91	-1.71	-3.93	0.51	3.76	-1.74	0.115169	2.54E-01	-5.45	0	3.49E+08	1.00E+09	1.92E+09	2.55E+09	3.76E+08	1.71E+08	1.80E+09	1.15E+09	2.645	5.014	5.161	5.658	1.712	0.811	4.230	4.882	4.620	2.908	-1.711	1.15E-01	2.54E-01
308	P31946|1433B	10	3.47	4.12	0.65	-0.19	1.50	3.80	1.74	0.115615	2.54E-01	-5.46	0	5.88E+08	2.94E+08	1.13E+09	3.07E+08	1.77E+09	1.85E+09	1.54E+09	6.11E+08	3.369	3.329	4.390	2.803	4.023	4.511	3.995	3.968	3.473	4.124	0.651	1.16E-01	2.54E-01
309	P35030|TRY3	2	-0.90	-1.83	-0.93	-2.15	0.28	-1.30	-1.76	0.115356	2.54E-01	-5.35	1	1.92E+07	1.68E+07	3.57E+07	1.81E+07	2.07E+07	NA	2.39E+07	2.72E+07	-1.367	-0.605	-0.609	-1.014	-2.609	NA	-2.328	-0.553	-0.899	-1.830	-0.931	1.15E-01	2.54E-01
310	Q5JSH3|WDR44	5	-0.36	-1.03	-0.67	-1.54	0.20	-0.69	-1.74	0.114768	2.54E-01	-5.45	0	4.53E+07	9.99E+06	5.24E+07	4.19E+07	5.75E+07	3.90E+07	6.08E+07	2.59E+07	-0.180	-1.316	-0.053	0.121	-1.087	-1.483	-0.910	-0.626	-0.357	-1.027	-0.670	1.15E-01	2.54E-01
311	zz|Y-FGC2Cont00309|	4	-0.33	-1.20	-0.87	-2.00	0.27	-0.82	-1.75	0.116532	2.56E-01	-5.36	1	6.37E+07	8.52E+06	6.50E+07	NA	4.75E+07	4.16E+07	5.00E+07	2.27E+07	0.292	-1.534	0.261	NA	-1.371	-1.383	-1.207	-0.820	-0.327	-1.195	-0.868	1.17E-01	2.56E-01
312	P30086|PEBP1	6	7.46	8.01	0.54	-0.17	1.26	7.74	1.72	0.118732	2.60E-01	-5.48	0	1.20E+10	4.67E+09	1.37E+10	7.95E+09	2.05E+10	2.20E+10	1.95E+10	1.09E+10	7.537	7.128	8.002	7.189	7.674	8.360	7.840	8.159	7.464	8.008	0.544	1.19E-01	2.60E-01
313	P46379|BAG6	2	-4.45	-3.44	1.01	-0.38	2.40	-3.69	1.84	0.121331	2.62E-01	-4.89	4	NA	NA	2.51E+06	NA	1.42E+07	1.05E+07	1.02E+07	NA	NA	NA	-4.450	NA	-3.176	-3.521	-3.611	NA	-4.450	-3.436	1.014	1.21E-01	2.62E-01
314	P55287|CAD11	7	-1.88	0.03	1.91	-0.64	4.46	-0.61	1.75	0.121061	2.62E-01	-5.25	2	4.04E+07	NA	5.07E+06	NA	1.83E+08	1.72E+08	1.72E+08	9.88E+06	-0.339	NA	-3.431	NA	0.641	0.821	0.667	-2.027	-1.885	0.025	1.910	1.21E-01	2.62E-01
315	Q9BPU6|DPYL5	4	0.08	-1.45	-1.53	-3.57	0.51	-0.94	-1.76	0.12102	2.62E-01	-5.25	2	2.72E+07	NA	1.11E+08	NA	1.50E+07	5.80E+07	9.23E+07	1.34E+07	-0.888	NA	1.040	NA	-3.089	-0.865	-0.276	-1.582	0.076	-1.453	-1.529	1.21E-01	2.62E-01
316	Q9H098|F107B	4	-3.24	-1.42	1.82	-0.58	4.22	-2.33	1.71	0.120619	2.62E-01	-5.49	0	4.23E+06	4.64E+06	6.54E+06	1.87E+06	3.14E+08	1.41E+07	9.85E+07	2.77E+06	-3.462	-2.370	-3.063	-4.070	1.444	-3.067	-0.178	-3.876	-3.241	-1.419	1.822	1.21E-01	2.62E-01
317	Q13449|LSAMP	5	1.60	1.07	-0.53	-1.23	0.17	1.34	-1.70	0.121907	2.62E-01	-5.50	0	2.05E+08	5.74E+07	1.75E+08	1.38E+08	2.02E+08	1.99E+08	2.02E+08	1.15E+08	1.910	1.085	1.697	1.727	0.785	1.052	0.913	1.544	1.605	1.073	-0.531	1.22E-01	2.62E-01
318	zz|Y-FGC2Cont00310|	2	0.94	2.97	2.03	-0.66	4.71	1.95	1.70	0.122593	2.63E-01	-5.51	0	3.73E+08	6.16E+06	4.80E+08	3.44E+07	1.37E+09	1.48E+09	1.05E+09	6.22E+07	2.737	-1.981	3.153	-0.146	3.637	4.172	3.410	0.647	0.941	2.967	2.026	1.23E-01	2.63E-01
319	P00568|KAD1	9	2.10	2.73	0.63	-0.21	1.48	2.41	1.69	0.125082	2.65E-01	-5.53	0	2.50E+08	7.77E+07	2.99E+08	2.02E+08	8.11E+08	9.10E+08	6.37E+08	1.58E+08	2.183	1.502	2.469	2.238	2.859	3.412	2.653	2.004	2.098	2.732	0.634	1.25E-01	2.65E-01
320	P36871|PGM1	4	-4.25	-2.50	1.75	-0.60	4.11	-3.25	1.71	0.124473	2.65E-01	-5.42	1	NA	1.63E+06	2.97E+06	1.13E+06	4.35E+06	1.03E+07	5.32E+07	3.04E+07	NA	-3.808	-4.207	-4.748	-4.938	-3.556	-1.111	-0.395	-4.254	-2.500	1.754	1.24E-01	2.65E-01
321	Q8N8E3|CE112	2	-3.21	-4.15	-0.94	-2.25	0.36	-3.68	-1.83	0.123985	2.65E-01	-5.04	4	NA	1.96E+06	7.51E+06	NA	6.43E+06	7.97E+06	NA	NA	NA	-3.552	-2.863	NA	-4.353	-3.951	NA	NA	-3.207	-4.152	-0.945	1.24E-01	2.65E-01
322	Q8WTS6|SETD7	2	-1.22	-2.07	-0.84	-1.98	0.29	-1.70	-1.71	0.124837	2.65E-01	-5.43	1	2.25E+07	9.83E+06	2.40E+07	NA	3.28E+07	3.92E+07	4.11E+07	3.95E+06	-1.146	-1.338	-1.182	NA	-1.926	-1.475	-1.504	-3.358	-1.222	-2.066	-0.844	1.25E-01	2.65E-01
323	P84074|HPCA	3	-1.78	-0.77	1.01	-0.34	2.36	-1.28	1.68	0.125572	2.65E-01	-5.53	0	2.19E+07	1.49E+07	1.27E+07	3.91E+06	9.02E+07	9.03E+07	8.51E+07	9.36E+06	-1.187	-0.766	-2.101	-3.079	-0.417	-0.178	-0.399	-2.106	-1.783	-0.775	1.008	1.26E-01	2.65E-01
324	Q9HC38|GLOD4	2	-0.18	0.56	0.75	-0.25	1.74	0.19	1.68	0.126681	2.67E-01	-5.54	0	3.47E+07	3.75E+07	7.24E+07	1.69E+07	2.46E+08	9.87E+07	1.40E+08	7.20E+07	-0.547	0.501	0.417	-1.102	1.079	-0.041	0.351	0.860	-0.183	0.562	0.745	1.27E-01	2.67E-01
325	P14136|GFAP	14	2.73	2.25	-0.48	-1.13	0.17	2.49	-1.67	0.127575	2.67E-01	-5.54	0	4.08E+08	1.82E+08	3.99E+08	2.46E+08	4.06E+08	3.96E+08	6.11E+08	2.16E+08	2.862	2.672	2.885	2.506	1.827	2.121	2.590	2.458	2.731	2.249	-0.482	1.28E-01	2.67E-01
326	P62258|1433E	14	5.40	6.39	0.99	-0.34	2.32	5.90	1.67	0.128002	2.67E-01	-5.55	0	3.00E+09	1.66E+09	5.25E+09	5.85E+08	8.35E+09	8.84E+09	8.42E+09	2.04E+09	5.626	5.704	6.614	3.672	6.335	6.945	6.568	5.718	5.404	6.392	0.988	1.28E-01	2.67E-01
327	P78559|MAP1A	9	3.42	2.80	-0.61	-1.44	0.21	3.11	-1.67	0.127719	2.67E-01	-5.55	0	7.61E+08	2.82E+08	7.53E+08	3.19E+08	5.53E+08	7.18E+08	5.60E+08	4.19E+08	3.726	3.274	3.804	2.856	2.287	3.045	2.457	3.419	3.415	2.802	-0.613	1.28E-01	2.67E-01
328	O00533|NCHL1	5	-0.14	1.01	1.16	-0.43	2.74	0.43	1.64	0.133651	2.78E-01	-5.59	0	2.28E+07	4.83E+07	1.60E+08	9.63E+06	1.82E+08	2.02E+08	2.14E+08	1.00E+08	-1.129	0.849	1.566	-1.862	0.634	1.071	1.000	1.340	-0.144	1.011	1.155	1.34E-01	2.78E-01
329	O76070|SYUG	4	1.73	1.22	-0.51	-1.21	0.19	1.48	-1.64	0.135332	2.79E-01	-5.60	0	1.84E+08	6.73E+07	1.59E+08	2.12E+08	2.19E+08	2.60E+08	2.40E+08	1.00E+08	1.759	1.304	1.558	2.303	0.906	1.463	1.172	1.341	1.731	1.221	-0.510	1.35E-01	2.79E-01
330	P54289|CA2D1	17	2.09	2.69	0.60	-0.22	1.42	2.39	1.64	0.134961	2.79E-01	-5.59	0	2.94E+08	1.63E+08	2.41E+08	9.80E+07	8.68E+08	5.93E+08	7.46E+08	1.74E+08	2.407	2.522	2.154	1.264	2.959	2.746	2.893	2.143	2.087	2.686	0.599	1.35E-01	2.79E-01

1	ProteinName	# Peptides	Ctrl	Group1	log2FC	CI.L	CI.R	AveExpr	t	P.Value	adj.P.Val	B	nrNAs	M.3_Control.raw	M.2_Control.raw	M.4_Control.raw	M.1_Control.raw	E4.2_Group_1.raw	E4.4_Group_1.raw	E4.3_Group_1.raw	E4.1_Group_1.raw	M.3_Control.transf	M.2_Control.transf	M.4_Control.transf	M.1_Control.transf	E4.2_Group_1.transf	E4.4_Group_1.transf	E4.3_Group_1.transf	E4.1_Group_1.transf	pseudo.Ctrl	pseudo.Group1	pseudo.log2FC	pseudo.P.Value	pseudo.adj.P.Val
331	Q9Y5P6|GMPPB	2	-3.04	-1.83	1.22	-0.50	2.93	-2.07	1.72	0.134554	2.79E-01	-5.07	3	NA	2.84E+06	NA	NA	5.23E+07	2.75E+07	4.61E+07	6.15E+06	NA	-3.043	NA	NA	-1.229	-2.029	-1.330	-2.716	-3.043	-1.826	1.218	1.35E-01	2.79E-01
332	P30041|PRDX6	16	4.30	5.13	0.84	-0.32	1.99	4.72	1.63	0.136617	2.80E-01	-5.61	0	1.81E+09	1.90E+08	1.80E+09	1.06E+09	4.07E+09	3.27E+09	3.44E+09	9.88E+08	4.924	2.727	5.069	4.473	5.262	5.400	5.210	4.665	4.298	5.134	0.836	1.37E-01	2.80E-01
333	Q9H299|SH3L3	3	2.42	2.93	0.51	-0.19	1.21	2.67	1.63	0.13691	2.80E-01	-5.61	0	3.87E+08	1.02E+08	2.96E+08	2.54E+08	8.37E+08	8.66E+08	6.26E+08	2.80E+08	2.790	1.874	2.453	2.550	2.906	3.335	2.627	2.834	2.417	2.925	0.508	1.37E-01	2.80E-01
334	Q9NVG8|TBC13	3	-3.05	-2.56	0.49	-0.19	1.17	-2.81	1.62	0.137846	2.81E-01	-5.61	0	8.33E+06	2.39E+06	7.33E+06	2.84E+06	2.30E+07	2.06E+07	1.83E+07	6.72E+06	-2.523	-3.282	-2.899	-3.507	-2.453	-2.477	-2.728	-2.587	-3.053	-2.561	0.492	1.38E-01	2.81E-01
335	P27348|1433T	9	3.35	3.87	0.51	-0.20	1.23	3.61	1.61	0.140264	2.86E-01	-5.63	0	4.37E+08	3.37E+08	7.61E+08	3.87E+08	1.45E+09	1.30E+09	1.12E+09	7.55E+08	2.957	3.517	3.821	3.118	3.725	3.961	3.504	4.274	3.353	3.866	0.513	1.40E-01	2.86E-01
336	P54725|RD23A	8	0.60	-0.20	-0.80	-1.93	0.32	0.20	-1.61	0.141202	2.87E-01	-5.63	0	1.37E+08	1.51E+07	9.73E+07	7.81E+07	1.13E+08	8.76E+07	5.95E+07	5.41E+07	1.356	-0.745	0.843	0.958	-0.077	-0.226	-0.943	0.443	0.603	-0.201	-0.804	1.41E-01	2.87E-01
337	Q9NVT9|ARMC1	2	-2.78	-3.38	-0.59	-1.45	0.26	-3.08	-1.63	0.145864	2.95E-01	-5.48	2	6.47E+06	4.23E+06	6.91E+06	NA	1.61E+07	1.01E+07	1.05E+07	NA	-2.872	-2.496	-2.984	NA	-2.984	-3.580	-3.572	NA	-2.784	-3.378	-0.595	1.46E-01	2.95E-01
338	P23381|SYWC	2	-3.32	-2.12	1.20	-0.59	2.98	-2.42	1.70	0.146876	2.96E-01	-5.08	4	NA	NA	5.48E+06	NA	1.73E+07	NA	3.78E+07	1.11E+07	NA	NA	-3.320	NA	-2.875	NA	-1.631	-1.859	-3.320	-2.122	1.198	1.47E-01	2.96E-01
339	P63104|1433Z	11	6.17	6.65	0.48	-0.21	1.17	6.41	1.58	0.147416	2.96E-01	-5.67	0	4.80E+09	1.83E+09	5.43E+09	3.04E+09	1.03E+10	9.19E+09	8.40E+09	3.24E+09	6.274	5.839	6.664	5.896	6.646	7.006	6.565	6.390	6.168	6.652	0.483	1.47E-01	2.96E-01
340	Q9ULL5|PRR12	2	2.09	1.21	-0.88	-2.14	0.38	1.59	-1.60	0.147649	2.96E-01	-5.58	1	2.84E+08	1.57E+08	1.47E+08	NA	1.13E+08	2.53E+08	2.73E+08	1.72E+08	2.362	2.468	1.438	NA	-0.082	1.422	1.368	2.128	2.090	1.209	-0.881	1.48E-01	2.96E-01
341	P30153|2AAA	12	-0.66	0.92	1.58	-0.71	3.88	0.13	1.56	0.152957	3.06E-01	-5.70	0	1.35E+07	7.50E+07	9.88E+07	3.78E+06	4.46E+08	6.79E+07	1.88E+08	1.14E+08	-1.855	1.452	0.866	-3.123	1.966	-0.622	0.802	1.531	-0.665	0.920	1.585	1.53E-01	3.06E-01
342	P22676|CALB2	10	5.68	5.23	-0.45	-1.10	0.20	5.46	-1.55	0.154065	3.07E-01	-5.71	0	3.19E+09	1.69E+09	2.72E+09	2.50E+09	2.72E+09	3.20E+09	3.80E+09	1.80E+09	5.708	5.730	5.661	5.630	4.660	5.368	5.364	5.540	5.682	5.233	-0.449	1.54E-01	3.07E-01
343	P09497|CLCB	5	-2.48	-1.20	1.29	-0.62	3.19	-1.62	1.59	0.154985	3.08E-01	-5.48	2	3.12E+06	NA	2.57E+07	NA	3.50E+07	3.52E+07	5.84E+07	3.15E+07	-3.881	NA	-1.083	NA	-1.829	-1.642	-0.969	-0.344	-2.482	-1.196	1.286	1.55E-01	3.08E-01
344	P42167|LAP2B	2	-2.35	-3.46	-1.10	-2.74	0.53	-3.09	-1.58	0.155953	3.08E-01	-5.48	2	NA	1.90E+06	NA	1.68E+07	8.29E+06	1.56E+07	1.10E+07	3.71E+06	NA	-3.592	NA	-1.114	-3.975	-2.908	-3.499	-3.449	-2.353	-3.458	-1.105	1.56E-01	3.08E-01
345	P62993|GRB2	3	-2.88	-1.97	0.90	-0.43	2.24	-2.42	1.58	0.155756	3.08E-01	-5.54	2	8.38E+06	NA	1.37E+07	1.81E+06	3.09E+07	3.03E+07	2.90E+07	NA	-2.514	NA	-1.998	-4.114	-2.012	-1.875	-2.034	NA	-2.875	-1.974	0.902	1.56E-01	3.08E-01
346	P11388|TOP2A	2	1.13	-1.06	-2.20	-5.51	1.11	-0.18	-1.61	0.156738	3.09E-01	-5.40	3	NA	6.52E+07	NA	8.10E+07	8.15E+06	1.21E+08	NA	5.75E+07	NA	1.260	NA	1.009	-4.000	0.278	NA	0.532	1.135	-1.063	-2.198	1.57E-01	3.09E-01
347	REV__Q5T9S5|CCD18	2	-0.21	-0.85	-0.64	-1.58	0.30	-0.57	-1.55	0.158379	3.10E-01	-5.64	1	NA	1.52E+07	6.23E+07	3.60E+07	6.61E+07	9.52E+07	4.76E+07	1.83E+07	NA	-0.743	0.198	-0.086	-0.880	-0.096	-1.280	-1.130	-0.210	-0.847	-0.636	1.58E-01	3.10E-01
348	P00492|HPRT	6	1.65	2.59	0.94	-0.44	2.31	2.12	1.54	0.157591	3.10E-01	-5.73	0	1.66E+08	1.11E+08	4.38E+08	3.81E+07	1.00E+09	4.85E+08	7.69E+08	1.40E+08	1.614	1.992	3.021	-0.008	3.176	2.433	2.938	1.823	1.655	2.593	0.938	1.58E-01	3.10E-01
349	Q9BWD1|THIC	2	-2.53	-1.65	0.88	-0.48	2.24	-1.87	1.64	0.15842	3.10E-01	-5.15	4	NA	NA	9.47E+06	NA	3.97E+07	3.87E+07	3.37E+07	NA	NA	NA	-2.527	NA	-1.640	-1.495	-1.805	NA	-2.527	-1.647	0.881	1.58E-01	3.10E-01
350	Q9NRR5|UBQL4	4	-2.86	-3.44	-0.58	-1.44	0.29	-3.15	-1.57	0.159379	3.11E-01	-5.56	2	6.21E+06	4.47E+06	5.86E+06	NA	1.09E+07	1.27E+07	NA	3.55E+06	-2.929	-2.422	-3.222	NA	-3.561	-3.232	NA	-3.514	-2.858	-3.435	-0.578	1.59E-01	3.11E-01
351	P40926|MDHM	6	2.84	3.88	1.04	-0.50	2.58	3.36	1.52	0.161206	3.12E-01	-5.75	0	6.15E+08	2.96E+08	7.31E+08	7.05E+07	1.71E+09	1.93E+09	1.85E+09	2.55E+08	3.431	3.339	3.762	0.821	3.968	4.578	4.268	2.698	2.838	3.878	1.040	1.61E-01	3.12E-01
352	Q15714|T22D1	4	0.56	-0.40	-0.96	-2.39	0.47	0.01	-1.54	0.160707	3.12E-01	-5.65	1	1.64E+08	NA	9.47E+07	2.25E+07	1.35E+08	3.89E+07	9.90E+07	3.66E+07	1.598	NA	0.804	-0.718	0.185	-1.487	-0.170	-0.124	0.561	-0.399	-0.960	1.61E-01	3.12E-01
353	zz|Y-FGC2Cont00374|	7	0.00	-0.56	-0.56	-1.39	0.27	-0.28	-1.52	0.16147	3.12E-01	-5.75	0	4.58E+07	3.05E+07	4.07E+07	4.97E+07	6.35E+07	7.27E+07	5.51E+07	4.76E+07	-0.164	0.217	-0.417	0.350	-0.940	-0.516	-1.060	0.257	-0.004	-0.565	-0.561	1.61E-01	3.12E-01
354	P52565|GDIR1	4	-0.45	-1.36	-0.92	-2.31	0.48	-1.06	-1.54	0.164961	3.18E-01	-5.53	2	NA	NA	5.29E+07	2.04E+07	2.87E+07	3.00E+07	5.28E+07	3.20E+07	NA	NA	-0.039	-0.853	-2.123	-1.891	-1.124	-0.317	-0.446	-1.364	-0.917	1.65E-01	3.18E-01
355	P05937|CALB1	13	6.36	5.80	-0.56	-1.40	0.28	6.08	-1.50	0.166434	3.19E-01	-5.78	0	5.85E+09	2.81E+09	6.40E+09	2.34E+09	6.12E+09	4.73E+09	6.30E+09	1.44E+09	6.548	6.431	6.901	5.543	5.872	5.972	6.128	5.209	6.355	5.795	-0.560	1.66E-01	3.19E-01
356	P15924|DESP	3	-3.83	-2.71	1.12	-0.65	2.90	-3.55	1.60	0.167791	3.19E-01	-5.20	4	NA	2.68E+06	2.56E+06	2.07E+06	NA	NA	NA	6.19E+06	NA	-3.123	-4.421	-3.937	NA	NA	NA	-2.705	-3.827	-2.705	1.122	1.68E-01	3.19E-01
357	P19404|NDUV2	2	-0.49	-0.05	0.44	-0.22	1.10	-0.27	1.49	0.168204	3.19E-01	-5.79	0	4.79E+07	1.77E+07	2.72E+07	2.99E+07	1.20E+08	1.09E+08	9.46E+07	3.74E+07	-0.103	-0.531	-1.001	-0.334	0.006	0.110	-0.239	-0.093	-0.492	-0.054	0.438	1.68E-01	3.19E-01
358	P20916|MAG	4	2.25	1.78	-0.47	-1.18	0.24	2.01	-1.50	0.16693	3.19E-01	-5.78	0	2.56E+08	1.31E+08	2.58E+08	2.12E+08	3.95E+08	3.06E+08	2.45E+08	2.08E+08	2.217	2.218	2.253	2.303	1.785	1.718	1.202	2.404	2.248	1.777	-0.470	1.67E-01	3.19E-01
359	Q01995|TAGL	11	3.01	3.48	0.47	-0.24	1.18	3.24	1.50	0.16804	3.19E-01	-5.79	0	3.84E+08	2.31E+08	6.65E+08	2.68E+08	1.24E+09	1.13E+09	8.93E+08	4.43E+08	2.780	2.999	3.625	2.621	3.496	3.753	3.166	3.498	3.006	3.478	0.472	1.68E-01	3.19E-01
360	Q8N3V7|SYNPO	3	-2.69	-3.52	-0.83	-2.10	0.44	-3.24	-1.53	0.169105	3.20E-01	-5.55	2	8.33E+06	3.26E+06	NA	NA	6.14E+06	8.52E+06	1.65E+07	5.38E+06	-2.523	-2.856	NA	NA	-4.422	-3.847	-2.883	-2.910	-2.689	-3.516	-0.826	1.69E-01	3.20E-01
361	Q92823|NRCAM	12	3.27	3.70	0.43	-0.22	1.07	3.49	1.49	0.169225	3.20E-01	-5.79	0	5.29E+08	3.74E+08	5.23E+08	3.39E+08	1.39E+09	1.32E+09	1.32E+09	4.16E+08	3.223	3.660	3.277	2.937	3.661	3.985	3.756	3.407	3.274	3.702	0.428	1.69E-01	3.20E-01
362	P63267|ACTH	12	1.06	2.78	1.72	-0.92	4.36	2.04	1.49	0.173119	3.26E-01	-5.72	1	2.14E+08	5.78E+07	5.83E+07	NA	1.64E+09	1.20E+09	1.60E+09	2.47E+07	1.971	1.095	0.104	NA	3.910	3.840	4.048	-0.692	1.057	2.776	1.720	1.73E-01	3.26E-01
363	Q15404|RSU1	2	-3.76	-2.62	1.14	-0.72	3.00	-2.91	1.55	0.178012	3.34E-01	-5.26	4	3.40E+06	NA	NA	NA	1.27E+07	2.98E+07	1.96E+07	NA	-3.763	NA	NA	NA	-3.342	-1.900	-2.628	NA	-3.763	-2.623	1.139	1.78E-01	3.34E-01
364	Q08209|PP2BA	6	-0.21	-1.22	-1.02	-2.60	0.57	-0.71	-1.44	0.181786	3.41E-01	-5.85	0	3.84E+07	1.04E+08	3.13E+07	1.24E+07	2.90E+07	4.97E+07	4.69E+07	3.08E+07	-0.410	1.904	-0.799	-1.521	-2.107	-1.107	-1.302	-0.373	-0.207	-1.222	-1.016	1.82E-01	3.41E-01
365	zz|Y-FGC2Cont00314|	6	0.98	2.52	1.54	-0.89	3.97	1.75	1.43	0.18654	3.48E-01	-5.88	0	1.49E+08	1.31E+08	3.93E+08	5.47E+06	8.27E+08	5.68E+08	9.49E+08	9.57E+07	1.468	2.223	2.865	-2.624	2.887	2.679	3.257	1.273	0.983	2.524	1.541	1.87E-01	3.48E-01
366	P62745|RHOB	2	-1.71	-0.72	0.99	-0.58	2.57	-1.21	1.42	0.188921	3.50E-01	-5.89	0	3.77E+06	1.51E+07	3.10E+07	1.12E+07	9.73E+07	8.83E+07	9.50E+07	9.28E+06	-3.621	-0.749	-0.810	-1.657	-0.303	-0.213	-0.233	-2.117	-1.709	-0.716	0.993	1.89E-01	3.50E-01
367	Q16881|TRXR1	2	-2.15	-3.58	-1.43	-3.77	0.92	-3.29	-1.47	0.188796	3.50E-01	-5.38	3	NA	NA	1.23E+07	NA	5.08E+06	9.74E+06	2.81E+07	2.76E+06	NA	NA	-2.150	NA	-4.705	-3.639	-2.079	-3.881	-2.150	-3.576	-1.426	1.89E-01	3.50E-01
368	Q72406|MYH14	2	1.45	0.20	-1.25	-3.30	0.80	0.70	-1.48	0.188179	3.50E-01	-5.57	3	1.26E+08	8.69E+07	NA	NA	1.62E+08	NA	4.48E+07	1.12E+08	1.238	1.655	NA	NA	0.457	NA	-1.373	1.502	1.446	0.195	-1.251	1.88E-01	3.50E-01
369	P20336|RAB3A	3	-3.41	-2.74	0.67	-0.42	1.76	-2.97	1.44	0.190531	3.52E-01	-5.66	2	NA	1.50E+06	7.28E+06	NA	1.44E+07	1.51E+07	2.54E+07	6.53E+06	NA	-3.920	-2.908	NA	-3.157	-2.957	-2.235	-2.628	-3.414	-2.744	0.670	1.91E-01	3.52E-01
370	P17600|SYN1	4	-2.27	-3.08	-0.81	-2.17	0.54	-2.60	-1.46	0.192521	3.55E-01	-5.59	3	1.65E+07	4.13E+06	8.38E+06	NA	2.12E+07	1.00E+07	NA	NA	-1.575	-2.528	-2.705	NA	-2.575	-3.594	NA	NA	-2.269	-3.084	-0.815	1.93E-01	3.55E-01
371	P12277|KCRB	13	6.17	7.01	0.84	-0.51	2.19	6.59	1.40	0.194253	3.57E-01	-5.91	0	6.31E+09	2.43E+09	8.43E+09	1.09E+09	1.61E+10	1.19E+10	1.38E+10	2.51E+09	6.652	6.230	7.300	4.510	7.309	7.403	7.321	6.019	6.173	7.013	0.840	1.94E-01	3.57E-01
372	Q05397|FAK1	3	-2.42	-1.86	0.56	-0.35	1.47	-2.14	1.39	0.198124	3.63E-01	-5.93	0	7.65E+06	9.17E+06	6.46E+06	5.89E+06	2.78E+07	4.02E+07	2.57E+07	1.31E+07	-2.642	-1.433	-3.081	-2.525	-2.171	-1.437	-2.215	-1.622	-2.420	-1.861	0.559	1.98E-01	3.63E-01
373	Q9UK76|JUPI1	5	2.78	2.38	-0.40	-1.04	0.25	2.58	-1.38	0.199007	3.64E-01	-5.93	0	3.79E+08	2.45E+08	3.15E+08	2.90E+08	5.09E+08	4.12E+08	5.20E+08	2.79E+08	2.759	3.079	2.542	2.727	2.164	2.180	2.346	2.829	2.777	2.380	-0.397	1.99E-01	3.64E-01
374	zz|Y-FGC2Cont00373|	20	4.86	5.40	0.53	-0.34	1.41	5.13	1.38	0.200938	3.66E-01	-5.94	0	2.17E+09	6.23E+08	2.47E+09	1.00E+09	3.93E+09	5.08E+09	3.76E+09	1.21E+09	5.175	4.360	5.524	4.397	5.211	6.086	5.344	4.955	4.864	5.399	0.535	2.01E-01	3.66E-01
375	zz|Y-FGC2Cont00327|	2	0.42	0.00	-0.41	-1.09	0.27	0.21	-1.37	0.20265	3.68E-01	-5.95	0	7.67E+07	4.23E+07	5.44E+07	5.32E+07	1.04E+08	8.32E+07	1.16E+08	5.41E+07	0.550	0.668	0.002	0.442	-0.200	-0.306	0.074	0.443	0.415	0.003	-0.413	2.03E-01	3.68E-01
376	Q04917|1433F	8	2.13	3.30	1.17	-0.76	3.10	2.71	1.37	0.204249	3.70E-01	-5.95	0	4.12E+08	1.71E+08	7.27E+08	2.27E+07	1.46E+09	1.13E+09	9.72E+08	2.12E+08	2.878	2.582	3.753	-0.704	3.730	3.746	3.294	2.426	2.127	3.299	1.172	2.04E-01	3.70E-01
377	REV__Q15326|2MY11	2	-1.66	-0.64	1.02	-0.73	2.77	-1.05	1.41	0.206463	3.73E-01	-5.65	3	NA	6.29E+06	2.10E+07	NA	1.62E+08	7.23E+07	3.25E+07	NA	NA	-1.952	-1.376	NA	0.453	-0.525	-1.860	NA	-1.664	-0.644	1.020	2.06E-01	3.73E-01

1	ProteinName	# Peptides	Ctrl	Group1	log2FC	CI.L	CI.R	Ave Expr	t	P.Value	adj.P.Val	B	nrNAs	M.3_Control.raw	M.2_Control.raw	M.4_Control.raw	M.1_Control.raw	E4.2_Group_1.raw	E4.4_Group_1.raw	E4.3_Group_1.raw	E4.1_Group_1.raw	M.3_Control.transf	M.2_Control.transf	M.4_Control.transf	M.1_Control.transf	E4.2_Group_1.transf	E4.4_Group_1.transf	E4.3_Group_1.transf	E4.1_Group_1.transf	pseudo.Ctrl	pseudo.Group1	pseudo.log2FC	pseudo.P.Value	pseudo.adj.P.Val
378	O43175|SERA	4	0.78	1.29	0.51	-0.34	1.35	1.03	1.35	0.207699	3.75E-01	-5.97	0	9.65E+07	2.61E+07	1.70E+08	5.96E+07	2.56E+08	2.25E+08	3.08E+08	9.18E+07	0.867	0.004	1.651	0.594	1.140	1.238	1.551	1.212	0.779	1.285	0.506	2.08E-01	3.75E-01
379	P29218|IMPA1	2	-1.42	-3.20	-1.78	-4.94	1.37	-2.75	-1.43	0.208779	3.75E-01	-5.40	4	NA	NA	2.04E+07	NA	NA	4.77E+06	3.93E+07	4.18E+06	NA	NA	-1.415	NA	NA	-4.750	-1.570	-3.277	-1.415	-3.199	-1.784	2.09E-01	3.75E-01
380	Q9NV23|NECP2	2	-5.17	-3.53	1.64	-1.19	4.47	-3.86	1.40	0.208301	3.75E-01	-5.47	3	NA	NA	1.52E+06	NA	3.02E+07	3.81E+06	1.82E+07	2.16E+06	NA	NA	-5.171	NA	-2.047	-5.099	-2.739	-4.238	-5.171	-3.531	1.640	2.08E-01	3.75E-01
381	O95777|LSM8	3	-3.03	-2.26	0.77	-0.53	2.07	-2.59	1.35	0.211352	3.78E-01	-5.89	1	1.41E+07	1.40E+06	5.57E+06	NA	3.14E+07	3.22E+07	2.54E+07	4.88E+06	-1.793	-4.012	-3.296	NA	-1.990	-1.779	-2.235	-3.050	-3.034	-2.264	0.770	2.11E-01	3.78E-01
382	P16949|STMN1	7	3.43	3.09	-0.34	-0.93	0.24	3.26	-1.33	0.215134	3.84E-01	-6.00	0	6.69E+08	2.85E+08	6.32E+08	4.56E+08	8.23E+08	8.21E+08	9.25E+08	3.12E+08	3.547	3.285	3.551	3.337	2.881	3.251	3.219	2.990	3.430	3.085	-0.345	2.15E-01	3.84E-01
383	P08238|HS90B	12	-1.83	-0.51	1.32	-0.94	3.58	-1.08	1.34	0.216278	3.84E-01	-5.91	1	6.66E+07	1.85E+06	1.17E+07	NA	1.65E+08	1.33E+08	2.71E+07	2.28E+07	0.354	-3.629	-2.217	NA	0.485	0.422	-2.134	-0.810	-1.831	-0.510	1.321	2.16E-01	3.84E-01
384	P08559|ODPA	2	-2.71	-1.50	1.21	-0.92	3.34	-1.74	1.37	0.216455	3.84E-01	-5.50	3	NA	NA	8.36E+06	NA	2.03E+07	5.73E+07	3.08E+07	2.77E+07	NA	NA	-2.708	NA	-2.637	-0.886	-1.940	-0.529	-2.708	-1.498	1.210	2.16E-01	3.84E-01
385	P29762|RABP1	2	-3.05	-2.42	0.63	-0.48	1.74	-2.68	1.37	0.217472	3.85E-01	-5.70	3	6.35E+06	NA	5.92E+06	NA	1.64E+07	2.35E+07	2.88E+07	NA	-2.898	NA	-3.209	NA	-2.958	-2.268	-2.044	NA	-3.054	-2.423	0.630	2.17E-01	3.85E-01
386	Q4VC31|CCD58	3	0.65	-0.11	-0.75	-2.03	0.53	0.27	-1.32	0.218288	3.86E-01	-6.01	0	1.25E+08	4.17E+07	1.30E+08	2.54E+07	1.45E+08	1.52E+08	1.24E+08	1.41E+07	1.226	0.646	1.268	-0.558	0.288	0.631	0.167	-1.507	0.645	-0.105	-0.751	2.18E-01	3.86E-01
387	P27816|MAP4	17	1.80	2.17	0.37	-0.26	1.00	1.99	1.31	0.22095	3.87E-01	-6.02	0	1.97E+08	9.79E+07	1.61E+08	1.64E+08	5.30E+08	4.07E+08	3.56E+08	2.26E+08	1.856	1.819	1.563	1.961	2.224	2.162	1.772	2.519	1.801	2.169	0.368	2.21E-01	3.87E-01
388	Q9HC56|PCDH9	2	-3.83	-4.45	-0.62	-1.71	0.47	-4.14	-1.34	0.220962	3.87E-01	-5.84	2	2.93E+06	1.00E+06	6.60E+06	NA	6.99E+06	6.42E+06	4.56E+06	NA	-3.967	-4.473	-3.049	NA	-4.230	-4.288	-4.836	NA	-3.830	-4.451	-0.622	2.21E-01	3.87E-01
389	Q9Y2H0|DLGP4	3	-1.37	-1.88	-0.52	-1.40	0.37	-1.63	-1.31	0.220448	3.87E-01	-6.02	0	2.83E+07	1.14E+07	2.28E+07	7.22E+06	3.95E+07	2.60E+07	4.49E+07	7.60E+06	-0.829	-1.133	-1.256	-2.251	-1.649	-2.115	-1.368	-2.408	-1.367	-1.885	-0.517	2.20E-01	3.87E-01
390	O75368|SH3L1	5	2.38	3.17	0.79	-0.59	2.17	2.77	1.29	0.228701	3.95E-01	-6.05	0	5.54E+08	1.37E+08	5.49E+08	5.93E+07	9.68E+08	1.20E+09	9.16E+08	2.22E+08	3.285	2.285	3.347	0.588	3.123	3.844	3.204	2.495	2.376	3.166	0.790	2.29E-01	3.95E-01
391	P0C221|CC175	2	1.97	1.18	-0.80	-2.20	0.60	1.63	-1.30	0.227662	3.95E-01	-5.95	1	2.82E+08	4.66E+07	1.63E+08	3.98E+08	1.54E+08	3.39E+08	NA	9.65E+07	2.352	0.799	1.594	3.155	0.377	1.876	NA	1.285	1.975	1.179	-0.796	2.28E-01	3.95E-01
392	P60983|GMFB	4	-2.18	-1.30	0.88	-0.69	2.45	-1.74	1.32	0.227298	3.95E-01	-5.87	2	1.16E+07	NA	2.97E+07	2.70E+06	NA	3.73E+07	5.52E+07	1.65E+07	-2.080	NA	-0.875	-3.575	NA	-1.552	-1.056	-1.280	-2.177	-1.296	0.881	2.27E-01	3.95E-01
393	Q05682|CALD1	6	0.32	0.77	0.45	-0.33	1.23	0.54	1.29	0.227256	3.95E-01	-6.04	0	6.53E+07	2.86E+07	5.05E+07	7.59E+07	1.71E+08	1.46E+08	1.59E+08	1.06E+08	0.326	0.129	-0.105	0.920	0.539	0.565	0.544	1.416	0.318	0.766	0.448	2.27E-01	3.95E-01
394	Q14982|OPCM	4	0.08	-0.37	-0.45	-1.22	0.33	-0.15	-1.29	0.227153	3.95E-01	-6.04	0	6.10E+07	2.92E+07	6.55E+07	2.97E+07	1.22E+08	8.15E+07	1.09E+08	1.82E+07	0.232	0.155	0.270	-0.345	0.032	-0.338	-0.027	-1.141	0.078	-0.369	-0.447	2.27E-01	3.95E-01
395	Q8NCW5|NNRE	4	-0.21	0.51	0.71	-0.56	1.98	0.27	1.31	0.228761	3.95E-01	-5.82	2	3.05E+07	NA	6.76E+07	NA	2.19E+08	1.47E+08	2.08E+08	3.00E+07	-0.727	NA	0.316	NA	0.903	0.581	0.954	-0.415	-0.206	0.506	0.711	2.29E-01	3.95E-01
396	Q9P0L0|VAPA	4	1.11	-0.74	-1.85	-5.11	1.40	0.18	-1.28	0.230696	3.97E-01	-6.05	0	1.24E+08	5.02E+07	3.29E+08	3.11E+07	2.05E+08	1.30E+08	3.05E+08	7.89E+05	1.217	0.901	2.609	-0.284	0.805	0.388	1.536	-5.700	1.111	-0.743	-1.854	2.31E-01	3.97E-01
397	P09493|TPM1	5	-5.03	-3.66	1.36	-1.19	3.92	-4.01	1.35	0.232226	3.97E-01	-5.50	4	NA	NA	NA	9.19E+05	NA	1.63E+07	3.94E+06	4.74E+06	NA	NA	NA	-5.028	NA	-2.839	-5.060	-3.095	-5.028	-3.665	1.363	2.32E-01	3.97E-01
398	P24666|PPAC	2	2.78	2.46	-0.32	-0.88	0.24	2.62	-1.28	0.231813	3.97E-01	-6.06	0	3.60E+08	2.15E+08	3.76E+08	2.95E+08	5.76E+08	4.88E+08	5.52E+08	2.44E+08	2.688	2.898	2.801	2.750	2.349	2.444	2.436	2.630	2.784	2.465	-0.320	2.32E-01	3.97E-01
399	Q15149|PLEC	15	0.96	0.28	-0.68	-1.91	0.55	0.51	-1.30	0.232468	3.97E-01	-5.83	2	NA	2.94E+07	NA	1.41E+08	1.48E+08	1.04E+08	1.76E+08	4.14E+07	NA	0.165	NA	1.758	0.325	0.043	0.702	0.056	0.962	0.281	-0.680	2.32E-01	3.97E-01
400	Q14651|PLSI	3	-4.32	-3.21	1.11	-0.98	3.19	-3.49	1.34	0.234019	3.99E-01	-5.51	4	NA	1.12E+06	NA	NA	7.96E+06	NA	1.22E+07	8.41E+06	NA	-4.321	NA	NA	-4.036	NA	-3.345	-2.261	-4.321	-3.214	1.107	2.34E-01	3.99E-01
401	Q9BV19|CA050	2	-3.01	-3.53	-0.52	-1.47	0.44	-3.32	-1.31	0.235463	4.00E-01	-5.77	3	5.76E+06	NA	6.89E+06	NA	1.29E+07	9.61E+06	1.03E+07	NA	-3.034	NA	-2.989	NA	-3.315	-3.661	-3.604	NA	-3.011	-3.526	-0.515	2.35E-01	4.00E-01
402	Q15691|MARE1	2	-2.86	-2.04	0.82	-0.73	2.37	-2.24	1.34	0.236081	4.00E-01	-5.52	4	NA	NA	7.54E+06	NA	3.36E+07	3.41E+07	2.08E+07	NA	NA	NA	-2.857	NA	-1.889	-1.691	-2.537	NA	-2.857	-2.039	0.818	2.36E-01	4.00E-01
403	Q15493|RGN	2	-2.34	-2.00	0.34	-0.27	0.95	-2.17	1.24	0.243985	4.13E-01	-6.10	0	1.08E+07	3.80E+06	1.25E+07	6.37E+06	2.95E+07	2.58E+07	2.86E+07	1.20E+07	-2.163	-2.643	-2.126	-2.419	-2.082	-2.125	-2.054	-1.745	-2.338	-2.001	0.336	2.44E-01	4.13E-01
404	O95502|NPTXR	5	0.54	0.11	-0.44	-1.23	0.36	0.32	-1.23	0.248141	4.19E-01	-6.11	0	9.10E+07	5.16E+07	9.56E+07	2.90E+07	1.18E+08	1.16E+08	1.07E+08	4.87E+07	0.787	0.938	0.818	-0.377	-0.020	0.209	-0.056	0.292	0.542	0.106	-0.435	2.48E-01	4.19E-01
405	P07900|HS90A	12	2.62	3.27	0.65	-0.54	1.83	2.94	1.23	0.250013	4.21E-01	-6.12	0	1.33E+08	2.52E+08	7.33E+08	2.08E+08	7.85E+08	6.57E+08	1.19E+09	5.22E+08	1.310	3.117	3.765	2.280	2.808	2.906	3.607	3.738	2.618	3.265	0.647	2.50E-01	4.21E-01
406	Q15819|UB2V2	6	0.92	1.47	0.55	-0.46	1.56	1.19	1.22	0.252441	4.24E-01	-6.13	0	1.02E+08	6.93E+07	1.83E+08	2.93E+07	3.05E+08	3.12E+08	2.78E+08	9.92E+07	0.940	1.344	1.758	-0.362	1.400	1.746	1.395	1.325	0.920	1.466	0.547	2.52E-01	4.24E-01
407	O94856|NFASC	11	1.50	1.87	0.37	-0.32	1.06	1.68	1.22	0.253685	4.25E-01	-6.13	0	1.41E+08	5.43E+07	2.29E+08	1.17E+08	3.75E+08	3.39E+08	3.88E+08	1.56E+08	1.392	1.009	2.084	1.502	1.709	1.878	1.901	1.982	1.497	1.868	0.371	2.54E-01	4.25E-01
408	Q9UQB8|BAIP2	6	0.70	0.23	-0.48	-1.37	0.42	0.50	-1.22	0.254831	4.26E-01	-6.05	1	1.10E+08	2.70E+07	1.31E+08	5.27E+07	1.57E+08	1.23E+08	NA	3.88E+07	1.053	0.050	1.276	0.429	0.414	0.301	NA	-0.039	0.702	0.225	-0.477	2.55E-01	4.26E-01
409	Q9NP97|DLRB1	3	0.83	-0.09	-0.91	-2.67	0.84	0.37	-1.22	0.259343	4.32E-01	-5.98	2	7.93E+07	4.04E+07	1.32E+08	NA	3.63E+07	1.22E+08	2.48E+08	NA	0.596	0.602	1.280	NA	-1.774	0.286	1.224	NA	0.826	-0.088	-0.914	2.59E-01	4.32E-01
410	P51452|DUS3	4	0.26	0.80	0.54	-0.48	1.55	0.53	1.19	0.263988	4.38E-01	-6.16	0	8.89E+07	1.34E+07	5.98E+07	8.51E+07	1.65E+08	2.32E+08	1.62E+08	7.15E+07	0.753	-0.916	0.139	1.075	0.488	1.288	0.573	0.850	0.263	0.800	0.537	2.64E-01	4.38E-01
411	P55786|PSA	7	-2.84	-1.11	1.73	-1.69	5.15	-1.80	1.22	0.264614	4.38E-01	-5.87	3	NA	6.33E+05	3.67E+07	NA	NA	1.84E+07	7.57E+07	3.73E+07	NA	-5.107	-0.569	NA	NA	-2.647	-0.578	-0.095	-2.838	-1.107	1.731	2.65E-01	4.38E-01
412	Q02252|MMSA	5	-1.60	-1.08	0.52	-0.47	1.51	-1.30	1.20	0.264335	4.38E-01	-6.08	1	1.18E+07	6.73E+06	2.92E+07	NA	6.51E+07	7.71E+07	4.29E+07	1.37E+07	-2.040	-1.859	-0.896	NA	-0.903	-0.423	-1.439	-1.554	-1.598	-1.080	0.519	2.64E-01	4.38E-01
413	P04632|CPNS1	4	0.63	1.04	0.41	-0.37	1.19	0.83	1.18	0.268345	4.43E-01	-6.18	0	7.99E+07	3.98E+07	1.25E+08	4.18E+07	1.91E+08	1.80E+08	3.31E+08	7.34E+07	0.607	0.581	1.203	0.118	0.702	0.891	1.659	0.888	0.627	1.035	0.408	2.68E-01	4.43E-01
414	P31150|GDIA	12	0.29	1.52	1.24	-1.14	3.61	0.91	1.17	0.270336	4.45E-01	-6.18	0	3.96E+07	3.07E+07	5.50E+08	8.38E+06	1.98E+08	1.22E+08	6.97E+08	1.89E+08	-0.366	0.225	3.349	-2.049	0.758	0.289	2.789	2.264	0.290	1.525	1.235	2.70E-01	4.45E-01
415	O95202|LETM1	3	-3.09	-3.98	-0.89	-2.67	0.90	-3.62	-1.21	0.27144	4.46E-01	-5.89	3	NA	2.26E+06	7.73E+06	NA	3.41E+06	1.49E+07	9.95E+06	NA	NA	-3.356	-2.821	NA	-5.301	-2.975	-3.655	NA	-3.088	-3.977	-0.889	2.71E-01	4.46E-01
416	P17677|NEUM	4	4.74	4.24	-0.51	-1.49	0.48	4.49	-1.16	0.274809	4.50E-01	-6.19	0	1.86E+09	3.45E+08	1.61E+09	2.37E+09	1.75E+09	1.89E+09	1.51E+09	8.48E+08	4.960	3.549	4.903	5.556	4.000	4.545	3.957	4.444	4.742	4.237	-0.506	2.75E-01	4.50E-01
417	P61956|SUMO2	2	2.69	2.25	-0.44	-1.29	0.41	2.47	-1.16	0.275085	4.50E-01	-6.20	0	3.28E+08	1.74E+08	2.97E+08	3.87E+08	4.41E+08	5.64E+08	2.90E+08	2.94E+08	2.561	2.605	2.459	3.118	1.949	2.670	1.462	2.903	2.686	2.246	-0.440	2.75E-01	4.50E-01
418	Q9UIK7|CDV3	3	1.43	0.95	-0.49	-1.43	0.46	1.19	-1.16	0.276073	4.50E-01	-6.20	0	2.36E+08	3.11E+07	1.93E+08	1.21E+08	2.48E+08	2.11E+08	1.74E+08	7.27E+07	2.106	0.243	1.831	1.552	1.092	1.137	0.688	0.874	1.433	0.948	-0.485	2.76E-01	4.50E-01
419	Q12959|DLG1	5	-1.80	-2.85	-1.05	-3.10	1.00	-2.32	-1.15	0.278565	4.51E-01	-6.21	0	7.87E+06	9.35E+06	2.39E+07	8.68E+06	3.65E+07	2.21E+06	2.47E+07	1.51E+07	-2.601	-1.407	-1.189	-2.003	-1.764	-5.943	-2.278	-1.412	-1.800	-2.849	-1.050	2.79E-01	4.51E-01
420	Q6FI81|CPIN1	3	-2.39	-3.19	-0.80	-2.42	0.83	-3.03	-1.19	0.278129	4.51E-01	-5.72	3	9.15E+06	NA	NA	NA	1.17E+07	1.39E+07	8.82E+06	7.79E+06	-2.393	NA	NA	NA	-3.467	-3.086	-3.837	-2.372	-2.393	-3.191	-0.797	2.78E-01	4.51E-01
421	zz|Y-FGC2Cont00370|	6	0.03	-0.69	-0.71	-2.11	0.69	-0.38	-1.16	0.277689	4.51E-01	-6.12	1	8.75E+07	1.21E+07	7.16E+07	NA	1.43E+08	5.73E+07	9.08E+07	1.13E+07	0.731	-1.056	0.401	NA	0.274	-0.884	-0.302	-1.829	0.025	-0.685	-0.711	2.78E-01	4.51E-01
422	P30044|PRDX5	4	1.77	2.24	0.46	-0.48	1.40	2.08	1.15	0.284842	4.59E-01	-6.00	2	2.06E+08	NA	1.68E+08	NA	6.19E+08	5.24E+08	4.79E+08	1.30E+08	1.914	NA	1.636	NA	2.455	2.555	2.221	1.715	1.775	2.236	0.462	2.85E-01	4.59E-01
423	zz|Y-FGC2Cont00180|	5	7.50	7.03	-0.47	-1.41	0.46	7.27	-1.14	0.284775	4.59E-01	-6.22	0	8.64E+09	8.52E+09	1.01E+10	9.41E+09	8.73E+09	8.64E+09	9.13E+09	1.07E+10	7.088	7.955	7.555	7.418	6.401	6.911	6.691	8.126	7.504	7.032	-0.472	2.85E-01	4.59E-01
424	P25686|DNJB2	3	-2.81	-3.31	-0.50	-1.54	0.54	-3.11	-1.16	0.288956	4.65E-01	-5.94	3	NA	4.12E+06	6.43E+06	NA	1.06E+07	1.28E+07	1.44E+07	NA	NA	-2.533	-3.087	NA	-3.610	-3.214	-3.098	NA	-2.810	-3.307	-0.497	2.89E-01	4.65E-01

1	ProteinName	# Peptides	Ctrl	Group1	log2FC	CI.L	CI.R	Ave Expr	t	P.Value	adj.P.Val	B	nrNAs	M.3_Control.raw	M.2_Control.raw	M.4_Control.raw	M.1_Control.raw	E4.2_Group_1.raw	E4.4_Group_1.raw	E4.3_Group_1.raw	E4.1_Group_1.raw	M.3_Control.transf	M.2_Control.transf	M.4_Control.transf	M.1_Control.transf	E4.2_Group_1.transf	E4.4_Group_1.transf	E4.3_Group_1.transf	E4.1_Group_1.transf	pseudo.Ctrl	pseudo.Group1	pseudo.log2FC	pseudo.P.Value	pseudo.adj.P.Val
425	P21589|5NTD	2	-2.73	-3.94	-1.21	-3.84	1.41	-3.64	-1.17	0.291582	4.65E-01	-5.70	4	NA	NA	8.24E+06	NA	1.68E+07	3.24E+06	1.06E+07	NA	NA	NA	-2.729	NA	-2.919	-5.347	-3.562	NA	-2.729	-3.943	-1.214	2.92E-01	4.65E-01
426	P28066|PSA5	5	-0.17	0.93	1.10	-1.11	3.31	0.38	1.12	0.291449	4.65E-01	-6.24	0	9.06E+07	4.14E+07	1.24E+08	3.35E+06	3.73E+08	2.76E+08	2.41E+08	2.45E+07	0.781	0.635	1.199	-3.286	1.700	1.558	1.180	-0.708	-0.168	0.932	1.100	2.91E-01	4.65E-01
427	Q92752|TENR	2	-1.03	-1.40	-0.36	-1.10	0.37	-1.19	-1.13	0.290654	4.65E-01	-6.15	1	2.00E+07	1.46E+07	3.32E+07	1.44E+07	5.00E+07	3.62E+07	4.70E+07	NA	-1.309	-0.796	-0.711	-1.322	-1.296	-1.600	-1.299	NA	-1.035	-1.398	-0.364	2.91E-01	4.65E-01
428	Q92905|CSN5	2	-4.47	-5.03	-0.56	-1.74	0.62	-4.81	-1.15	0.292618	4.66E-01	-5.95	3	NA	1.06E+06	2.36E+06	NA	2.75E+06	5.80E+06	4.04E+06	NA	NA	-4.401	-4.538	NA	-5.622	-4.444	-5.023	NA	-4.469	-5.030	-0.560	2.93E-01	4.66E-01
429	P23588|IF4B	2	-2.59	-3.49	-0.90	-2.86	1.06	-3.26	-1.16	0.294386	4.68E-01	-5.71	4	7.95E+06	NA	NA	NA	2.11E+07	7.27E+06	9.06E+06	NA	-2.588	NA	NA	NA	-2.579	-4.094	-3.796	NA	-2.588	-3.490	-0.902	2.94E-01	4.68E-01
430	P07237|PDIA1	5	-3.55	-2.57	0.98	-1.16	3.13	-2.81	1.16	0.295203	4.68E-01	-5.71	4	NA	NA	4.67E+06	NA	NA	1.27E+07	4.12E+07	5.13E+06	NA	NA	-3.551	NA	NA	-3.228	-1.498	-2.978	-3.551	-2.568	0.983	2.95E-01	4.68E-01
431	P32119|PRDX2	5	1.74	2.41	0.67	-0.70	2.04	2.07	1.11	0.296808	4.69E-01	-6.25	0	2.72E+08	1.25E+08	3.52E+08	3.29E+07	5.06E+08	4.69E+08	4.34E+08	3.22E+08	2.301	2.152	2.706	-0.207	2.154	2.382	2.070	3.036	1.738	2.410	0.673	2.97E-01	4.69E-01
432	Q16630|CPSF6	2	4.08	0.96	-3.12	-9.84	3.60	1.58	-1.12	0.301939	4.74E-01	-5.78	3	9.85E+08	NA	NA	NA	6.61E+08	5.46E+08	8.08E+08	2.01E+06	4.082	NA	NA	NA	2.552	2.619	3.015	-4.344	4.082	0.961	-3.121	3.02E-01	4.74E-01
433	Q969T9|WBP2	2	-0.53	0.06	0.59	-0.63	1.81	-0.24	1.09	0.302502	4.74E-01	-6.27	0	2.40E+07	1.69E+07	4.03E+07	3.71E+07	1.98E+08	1.36E+08	3.80E+07	6.16E+07	-1.060	-0.596	-0.430	-0.045	0.758	0.459	-1.621	0.632	-0.533	0.057	0.590	3.03E-01	4.74E-01
434	Q96C19|EFHD2	7	3.05	2.63	-0.43	-1.31	0.46	2.84	-1.09	0.30228	4.74E-01	-6.27	0	4.16E+08	1.45E+08	5.50E+08	5.61E+08	5.80E+08	4.23E+08	5.83E+08	4.15E+08	2.890	2.358	3.351	3.617	2.357	2.222	2.519	3.403	3.054	2.625	-0.429	3.02E-01	4.74E-01
435	zz|Y-FGC2Cont00461|	8	2.53	1.97	-0.56	-1.72	0.59	2.25	-1.09	0.301283	4.74E-01	-6.27	0	4.05E+08	2.58E+08	4.95E+08	7.65E+07	4.28E+08	4.90E+08	3.56E+08	1.33E+08	2.854	3.150	3.198	0.931	1.905	2.449	1.771	1.756	2.533	1.971	-0.563	3.01E-01	4.74E-01
436	O15067|PUR4	3	-2.89	-2.32	0.57	-0.65	1.78	-2.51	1.09	0.310176	4.85E-01	-6.07	2	3.58E+06	NA	1.28E+07	NA	3.28E+07	1.98E+07	2.18E+07	7.81E+06	-3.693	NA	-2.087	NA	-1.925	-2.535	-2.468	-2.369	-2.890	-2.324	0.565	3.10E-01	4.85E-01
437	O75914|PAK3	13	-1.37	-0.90	0.47	-0.53	1.47	-1.14	1.07	0.313105	4.85E-01	-6.30	0	8.91E+06	8.21E+06	2.89E+07	2.52E+07	8.03E+07	7.27E+07	4.37E+07	1.89E+07	-2.430	-1.586	-0.914	-0.564	-0.590	-0.515	-1.410	-1.095	-1.373	-0.900	0.473	3.13E-01	4.85E-01
438	Q09666|AHNK	110	3.47	4.89	1.42	-1.58	4.43	4.18	1.07	0.312404	4.85E-01	-6.29	0	8.14E+07	2.05E+09	5.06E+09	6.34E+07	2.82E+09	2.44E+09	2.55E+09	1.38E+09	0.632	5.998	6.562	0.677	4.715	4.944	4.755	5.151	3.467	4.892	1.425	3.12E-01	4.85E-01
439	Q13907|IDI1	3	-3.19	-2.63	0.56	-0.68	1.80	-2.86	1.10	0.313171	4.85E-01	-6.01	3	4.55E+06	NA	6.71E+06	NA	2.59E+07	1.16E+07	NA	8.50E+06	-3.359	NA	-3.025	NA	-2.278	-3.371	NA	-2.246	-3.192	-2.632	0.560	3.13E-01	4.85E-01
440	Q86UJ8|ISCA2	3	-0.80	-1.28	-0.48	-1.51	0.54	-1.04	-1.06	0.31379	4.85E-01	-6.30	0	3.51E+07	1.98E+07	4.06E+07	9.71E+06	5.99E+07	4.80E+07	6.87E+07	8.69E+06	-0.531	-0.379	-0.423	-1.850	-1.027	-1.159	-0.723	-2.213	-0.796	-1.281	-0.485	3.14E-01	4.85E-01
441	Q96D71|REPS1	2	-3.09	-2.59	0.49	-0.55	1.53	-2.84	1.07	0.312981	4.85E-01	-6.30	0	4.86E+06	4.61E+06	5.84E+06	2.92E+06	2.74E+07	1.88E+07	9.26E+06	1.15E+07	-3.268	-2.378	-3.227	-3.471	-2.196	-2.613	-3.763	-1.805	-3.086	-2.594	0.492	3.13E-01	4.85E-01
442	Q02246|CNTN2	3	-3.89	-4.47	-0.58	-1.84	0.68	-4.22	-1.05	0.322617	4.97E-01	-6.23	1	2.95E+06	1.02E+06	5.67E+06	NA	7.70E+06	2.45E+06	9.73E+06	2.02E+06	-3.960	-4.452	-3.269	NA	-4.085	-5.785	-3.689	-4.332	-3.894	-4.473	-0.579	3.23E-01	4.97E-01
443	Q8NF28|CADM4	5	-1.15	-1.77	-0.62	-1.99	0.74	-1.41	-1.05	0.325038	5.00E-01	-6.24	1	1.42E+07	1.08E+07	4.29E+07	1.51E+07	7.53E+07	3.70E+07	1.48E+07	NA	-1.785	-1.203	-0.341	-1.256	-0.687	-1.565	-3.056	NA	-1.146	-1.769	-0.623	3.25E-01	5.00E-01
444	Q9UNZ2|NSF1C	3	-1.27	-0.91	0.36	-0.42	1.13	-1.09	1.04	0.325984	5.00E-01	-6.33	0	2.46E+07	1.07E+07	1.41E+07	2.01E+07	5.64E+07	5.40E+07	5.07E+07	3.09E+07	-1.025	-1.223	-1.953	-0.871	-1.117	-0.976	-1.184	-0.369	-1.268	-0.911	0.357	3.26E-01	5.00E-01
445	O60884|DNJA2	2	-1.33	-2.19	-0.86	-2.77	1.06	-1.62	-1.05	0.328929	5.03E-01	-6.11	2	1.92E+07	2.32E+07	3.02E+07	4.29E+06	NA	NA	4.32E+07	5.24E+06	-1.369	-0.159	-0.849	-2.953	NA	NA	-1.426	-2.949	-1.333	-2.188	-0.855	3.29E-01	5.03E-01
446	O75688|PPM1B	3	-3.93	-4.74	-0.81	-2.59	0.98	-4.39	-1.04	0.328397	5.03E-01	-6.25	1	2.72E+06	1.83E+06	3.27E+06	NA	1.32E+07	6.37E+06	6.11E+06	3.30E+05	-4.071	-3.647	-4.066	NA	-3.286	-4.298	-4.394	-6.965	-3.928	-4.736	-0.808	3.28E-01	5.03E-01
447	P13929|ENOB	6	2.85	3.91	1.06	-1.27	3.40	3.38	1.02	0.331694	5.06E-01	-6.34	0	7.43E+08	3.71E+08	1.36E+09	2.43E+07	1.98E+09	1.81E+09	1.95E+09	2.41E+08	3.692	3.647	4.658	-0.613	4.191	4.480	4.346	2.616	2.846	3.908	1.062	3.32E-01	5.06E-01
448	zz|Y-FGC2Cont00182|	9	6.07	5.74	-0.33	-1.04	0.39	5.91	-1.02	0.333681	5.08E-01	-6.34	0	4.34E+09	1.95E+09	5.36E+09	2.38E+09	4.47E+09	4.02E+09	5.64E+09	2.29E+09	6.135	5.930	6.645	5.564	5.403	5.722	5.960	5.888	6.069	5.743	-0.325	3.34E-01	5.08E-01
449	P50395|GDIB	7	-0.48	-1.45	-0.97	-3.16	1.22	-1.03	-1.02	0.338174	5.12E-01	-6.27	1	1.46E+07	1.06E+07	1.58E+08	NA	2.54E+07	2.82E+07	1.63E+08	9.43E+06	-1.749	-1.234	1.542	NA	-2.305	-1.985	0.584	-2.095	-0.480	-1.450	-0.970	3.38E-01	5.12E-01
450	P63241|IF5A1	4	1.73	2.04	0.30	-0.37	0.98	1.89	1.01	0.338292	5.12E-01	-6.35	0	2.33E+08	6.45E+07	1.98E+08	1.39E+08	5.01E+08	4.44E+08	4.28E+08	1.26E+08	2.087	1.246	1.869	1.736	2.138	2.297	2.049	1.671	1.735	2.039	0.304	3.38E-01	5.12E-01
451	O00330|IDPX	2	-2.45	-2.10	0.35	-0.46	1.15	-2.22	1.01	0.343776	5.18E-01	-6.15	2	NA	4.80E+06	9.19E+06	NA	2.75E+07	2.65E+07	2.74E+07	9.98E+06	NA	-2.322	-2.572	NA	-2.188	-2.081	-2.120	-2.012	-2.447	-2.100	0.347	3.44E-01	5.18E-01
452	O00584|RNT2	2	-0.28	-1.66	-1.38	-4.65	1.89	-1.11	-1.02	0.345726	5.18E-01	-6.08	3	NA	2.60E+07	NA	2.53E+07	8.60E+07	5.48E+06	1.14E+08	NA	NA	0.000	NA	-0.559	-0.487	-4.532	0.047	NA	-0.279	-1.657	-1.378	3.46E-01	5.18E-01
453	O43491|E41L2	2	-2.99	-4.19	-1.20	-4.14	1.73	-3.89	-1.04	0.344163	5.18E-01	-5.84	4	NA	2.96E+06	NA	NA	4.05E+06	4.01E+06	2.12E+07	NA	NA	-2.987	NA	NA	-5.043	-5.019	-2.511	NA	-2.987	-4.191	-1.204	3.44E-01	5.18E-01
454	P61086|UBE2K	5	-0.84	0.05	0.89	-1.15	2.93	-0.33	1.00	0.346844	5.18E-01	-6.29	1	1.34E+07	NA	1.32E+08	9.15E+06	1.71E+08	2.06E+08	1.07E+08	1.55E+07	-1.868	NA	1.290	-1.932	0.536	1.105	-0.058	-1.375	-0.837	0.052	0.888	3.47E-01	5.18E-01
455	P61457|PHS	5	2.26	2.57	0.31	-0.39	1.00	2.41	0.99	0.34634	5.18E-01	-6.37	0	3.22E+08	9.05E+07	3.41E+08	1.88E+08	7.15E+08	6.10E+08	5.48E+08	2.05E+08	2.533	1.711	2.660	2.144	2.670	2.791	2.426	2.382	2.262	2.567	0.305	3.46E-01	5.18E-01
456	Q99729|ROAA	2	-2.45	-1.91	0.54	-0.68	1.75	-2.18	0.99	0.345556	5.18E-01	-6.37	0	6.11E+06	7.25E+06	1.99E+07	2.60E+06	4.74E+07	2.96E+07	3.95E+07	5.82E+06	-2.952	-1.756	-1.455	-3.628	-1.377	-1.909	-1.564	-2.797	-2.448	-1.912	0.536	3.46E-01	5.18E-01
457	zz|Y-FGC2Cont00369|	6	0.68	1.10	0.42	-0.53	1.36	0.89	0.99	0.348579	5.20E-01	-6.38	0	9.39E+07	2.84E+07	1.29E+08	5.68E+07	2.95E+08	3.11E+08	2.46E+08	4.24E+07	0.829	0.119	1.256	0.531	1.351	1.746	1.211	0.090	0.684	1.100	0.416	3.49E-01	5.20E-01
458	Q9UHV9|PFD2	5	1.52	1.94	0.42	-0.54	1.37	1.73	0.98	0.349986	5.21E-01	-6.38	0	1.46E+08	7.45E+07	2.90E+08	6.88E+07	4.47E+08	5.38E+08	3.97E+08	9.51E+07	1.438	1.444	2.424	0.788	1.971	2.596	1.936	1.263	1.524	1.942	0.418	3.50E-01	5.21E-01
459	Q9HD42|CHM1A	4	-0.81	-1.23	-0.43	-1.41	0.55	-1.02	-0.98	0.350807	5.21E-01	-6.38	0	2.02E+07	1.11E+07	2.97E+07	4.18E+07	5.18E+07	4.76E+07	2.91E+07	2.84E+07	-1.299	-1.174	-0.873	0.115	-1.244	-1.175	-2.028	-0.492	-0.808	-1.235	-0.427	3.51E-01	5.21E-01
460	P15586|GNS	4	-2.86	-1.64	1.21	-1.58	4.01	-2.25	0.98	0.353	5.23E-01	-6.38	0	1.27E+08	1.16E+06	2.84E+06	1.78E+06	3.43E+07	1.12E+08	1.59E+07	1.06E+07	1.250	-4.273	-4.271	-4.140	-1.857	0.156	-2.943	-1.930	-2.858	-1.644	1.215	3.53E-01	5.23E-01
461	P23471|PTPR2	6	1.57	2.05	0.48	-0.63	1.58	1.81	0.97	0.355489	5.23E-01	-6.39	0	3.03E+08	1.11E+08	1.59E+08	4.74E+07	5.80E+08	4.95E+08	4.21E+08	1.00E+08	2.450	1.995	1.553	0.285	2.358	2.467	2.026	1.341	1.571	2.048	0.477	3.55E-01	5.23E-01
462	P23528|COF1	11	5.29	5.62	0.33	-0.44	1.11	5.45	0.97	0.354632	5.23E-01	-6.39	0	2.39E+09	1.24E+09	2.79E+09	1.38E+09	5.21E+09	5.48E+09	4.56E+09	1.25E+09	5.311	5.307	5.698	4.826	5.632	6.202	5.638	5.008	5.285	5.620	0.335	3.55E-01	5.23E-01
463	zz|Y-FGC2Cont00492|	10	-1.15	-0.11	1.04	-1.37	3.46	-0.63	0.97	0.355308	5.23E-01	-6.39	0	1.77E+07	6.56E+06	2.21E+08	3.40E+06	5.37E+07	4.50E+07	2.35E+08	7.28E+07	-1.482	-1.895	2.033	-3.267	-1.189	-1.262	1.142	0.875	-1.153	-0.108	1.044	3.55E-01	5.23E-01
464	zz|Y-FGC2Cont00362|	18	9.91	10.28	0.38	-0.51	1.26	10.09	0.96	0.359582	5.28E-01	-6.40	0	7.38E+10	4.48E+10	7.73E+10	2.67E+10	1.07E+11	8.92E+10	8.93E+10	4.79E+10	10.057	10.234	10.507	8.823	10.139	10.538	10.151	10.307	9.905	10.284	0.378	3.60E-01	5.28E-01
465	zz|Y-FGC2Cont00304|	4	-2.24	-2.77	-0.53	-1.87	0.81	-2.63	-1.00	0.361076	5.29E-01	-5.87	4	1.02E+07	NA	NA	NA	1.96E+07	1.59E+07	1.83E+07	NA	-2.237	NA	NA	NA	-2.696	-2.874	-2.729	NA	-2.237	-2.766	-0.529	3.61E-01	5.29E-01
466	P12532|KCRU	4	-3.59	-2.86	0.72	-1.07	2.51	-3.01	0.98	0.364487	5.33E-01	-5.93	3	NA	1.91E+06	NA	NA	3.57E+07	1.26E+07	1.11E+07	5.28E+06	NA	-3.586	NA	NA	-1.799	-3.233	-3.483	-2.938	-3.586	-2.863	0.723	3.64E-01	5.33E-01
467	O15212|PFD6	5	3.01	2.62	-0.40	-1.34	0.55	2.81	-0.95	0.368413	5.38E-01	-6.42	0	4.66E+08	2.86E+08	6.92E+08	1.72E+08	8.31E+08	6.50E+08	6.83E+08	1.50E+08	3.046	3.293	3.683	2.026	2.895	2.890	2.759	1.922	3.012	2.616	-0.395	3.68E-01	5.38E-01
468	P13611|CSPG2	2	-1.33	-1.65	-0.32	-1.11	0.47	-1.49	-0.95	0.371868	5.40E-01	-6.26	2	2.22E+07	9.32E+06	2.05E+07	NA	4.61E+07	3.45E+07	3.26E+07	NA	-1.165	-1.411	-1.408	NA	-1.416	-1.672	-1.854	NA	-1.328	-1.647	-0.319	3.72E-01	5.40E-01
469	zz|Y-FGC2Cont00151|	3	-2.94	-3.36	-0.42	-1.43	0.59	-3.15	-0.94	0.371708	5.40E-01	-6.42	0	9.03E+06	1.47E+06	1.12E+07	3.77E+06	7.81E+06	1.09E+07	1.48E+07	5.60E+06	-2.411	-3.945	-2.280	-3.127	-4.065	-3.469	-3.057	-2.851	-2.941	-3.361	-0.420	3.72E-01	5.40E-01
470	Q94888|UBXN7	2	-1.91	-2.54	-0.63	-2.28	1.02	-2.38	-0.96	0.376901	5.45E-01	-5.91	4	NA	NA	NA	9.27E+06	1.44E+07	2.20E+07	2.76E+07	NA	NA	NA	NA	-1.913	-3.149	-2.370	-2.105	NA	-1.913	-2.541	-0.628	3.77E-01	5.45E-01
471	Q9Y2V2|CHSP1	2	0.25	-0.56	-0.81	-2.79	1.16	-0.16	-0.93	0.376892	5.45E-01	-6.43	0	9.97E+07	4.31E+07	1.15E+08	1.09E+07	8.85E+07	1.34E+08	1.72E+08	5.34E+06	0.913	0.691	1.090	-1.695	-0.445	0.439	0.667	-2.921	0.250	-0.565	-0.815	3.77E-01	5.45E-01

1	ProteinName	# Peptides	Ctrl	Group1	log2FC	CI.L	CI.R	Ave Expr	t	P.Value	adj.P.Val	B	nrNAs	M.3_Control.raw	M.2_Control.raw	M.4_Control.raw	M.1_Control.raw	E4.2_Group1.raw	E4.4_Group1.raw	E4.3_Group1.raw	E4.1_Group1.raw	M.3_Control.transf	M.2_Control.transf	M.4_Control.transf	M.1_Control.transf	E4.2_Group_1.transf	E4.4_Group_1.transf	E4.3_Group_1.transf	E4.1_Group_1.transf	pseudo.Ctrl	pseudo.Group1	pseudo.log2FC	pseudo.P.Value	pseudo.adj.P.Val
472	O14562|UBFD1	3	-0.31	-1.07	-0.76	-2.67	1.15	-0.75	-0.92	0.385778	5.57E-01	-6.37	1	7.79E+07	NA	3.19E+07	2.23E+07	1.22E+07	1.16E+08	7.94E+07	2.65E+07	0.571	NA	-0.771	-0.729	-3.403	0.206	-0.504	-0.591	-0.310	-1.073	-0.763	3.86E-01	5.57E-01
473	P09936|UCHL1	11	6.36	5.92	-0.44	-1.54	0.66	6.14	-0.91	0.3883	5.59E-01	-6.45	0	4.60E+09	3.27E+09	2.99E+09	5.87E+09	3.41E+09	5.38E+09	3.80E+09	5.43E+09	6.217	6.637	5.802	6.780	4.999	6.173	5.360	7.142	6.359	5.918	-0.440	3.88E-01	5.59E-01
474	O95881|TXD12	2	-0.64	-1.06	-0.42	-1.46	0.63	-0.85	-0.90	0.390713	5.62E-01	-6.46	0	3.34E+07	2.10E+07	4.67E+07	1.32E+07	6.54E+07	6.80E+07	8.09E+07	8.55E+06	-0.600	-0.299	-0.220	-1.441	-0.896	-0.618	-0.476	-2.236	-0.640	-1.057	-0.417	3.91E-01	5.62E-01
475	O75347|TBCA	3	2.13	1.83	-0.30	-1.07	0.46	1.98	-0.89	0.393513	5.65E-01	-6.46	0	2.22E+08	8.82E+07	2.80E+08	2.37E+08	3.07E+08	4.65E+08	2.90E+08	1.66E+08	2.018	1.675	2.373	2.454	1.408	2.367	1.460	2.070	2.130	1.826	-0.304	3.94E-01	5.65E-01
476	P30419|NMT1	2	-0.66	-1.00	-0.34	-1.21	0.53	-0.83	-0.89	0.397593	5.68E-01	-6.47	0	2.09E+07	1.06E+07	4.37E+07	4.26E+07	7.73E+07	4.75E+07	5.97E+07	1.68E+07	-1.247	-1.233	-0.314	0.141	-0.647	-1.176	-0.938	-1.256	-0.663	-1.005	-0.341	3.98E-01	5.68E-01
477	Q9H1K1|ISCU	3	-1.72	-1.25	0.47	-0.72	1.66	-1.48	0.89	0.397205	5.68E-01	-6.47	0	8.76E+06	1.34E+07	1.43E+07	1.19E+07	5.92E+07	7.27E+07	1.89E+07	2.38E+07	-2.454	-0.917	-1.929	-1.572	-1.044	-0.515	-2.680	-0.752	-1.718	-1.248	0.470	3.97E-01	5.68E-01
478	zz|Y-FGC2Cont00361|	7	1.18	0.76	-0.43	-1.52	0.66	0.97	-0.88	0.398993	5.69E-01	-6.47	0	1.32E+08	5.14E+07	1.63E+08	7.55E+07	2.91E+08	1.84E+08	2.89E+08	2.48E+07	1.302	0.933	1.586	0.914	1.328	0.929	1.457	-0.689	1.184	0.756	-0.427	3.99E-01	5.69E-01
479	Q13526|PIN1	3	-1.64	-2.08	-0.44	-1.60	0.72	-1.86	-0.89	0.401734	5.72E-01	-6.32	2	2.57E+07	4.39E+06	1.91E+07	NA	4.17E+07	2.53E+07	2.10E+07	NA	-0.964	-2.446	-1.513	NA	-1.568	-2.158	-2.519	NA	-1.641	-2.082	-0.441	4.02E-01	5.72E-01
480	P20774|MIME	2	-3.20	-2.87	0.32	-0.51	1.15	-3.03	0.88	0.40294	5.72E-01	-6.48	0	5.21E+06	2.66E+06	6.36E+06	3.15E+06	1.55E+07	1.20E+07	1.29E+07	1.10E+07	-3.173	-3.136	-3.105	-3.368	-3.040	-3.318	-3.260	-1.876	-3.195	-2.874	0.322	4.03E-01	5.72E-01
481	O43504|LTOR5	2	-2.46	-1.55	0.91	-1.51	3.34	-1.85	0.88	0.405254	5.74E-01	-6.27	2	3.04E+06	NA	2.71E+07	NA	4.08E+07	6.85E+07	7.33E+07	3.93E+06	-3.917	NA	-1.007	NA	-1.599	-0.608	-0.627	-3.365	-2.462	-1.550	0.912	4.05E-01	5.74E-01
482	zz|Y-FGC2Cont00326|	7	1.58	1.86	0.28	-0.44	1.00	1.72	0.87	0.407526	5.76E-01	-6.49	0	1.77E+08	1.03E+08	2.05E+08	6.99E+07	4.04E+08	3.39E+08	3.78E+08	1.45E+08	1.705	1.885	1.922	0.809	1.817	1.880	1.863	1.876	1.580	1.859	0.279	4.08E-01	5.76E-01
483	Q8NC96|NECP1	3	-1.04	-1.38	-0.34	-1.25	0.56	-1.24	-0.87	0.41136	5.80E-01	-6.41	1	1.94E+07	NA	2.24E+07	2.65E+07	4.52E+07	3.77E+07	3.30E+07	2.42E+07	-1.350	NA	-1.282	-0.499	-1.446	-1.534	-1.837	-0.722	-1.044	-1.385	-0.341	4.11E-01	5.80E-01
484	P13693|TCTP	5	3.16	3.64	0.48	-0.78	1.73	3.40	0.85	0.415513	5.85E-01	-6.50	0	6.75E+08	3.26E+08	8.84E+08	1.25E+08	1.69E+09	1.35E+09	1.43E+09	2.55E+08	3.559	3.470	4.037	1.590	3.956	4.021	3.880	2.699	3.164	3.639	0.475	4.16E-01	5.85E-01
485	Q86Y82|STX12	8	2.76	2.48	-0.29	-1.06	0.48	2.62	-0.84	0.419769	5.90E-01	-6.51	0	5.88E+08	1.19E+08	4.52E+08	2.52E+08	5.46E+08	5.80E+08	5.51E+08	2.21E+08	3.369	2.084	3.066	2.540	2.269	2.712	2.434	2.491	2.765	2.477	-0.288	4.20E-01	5.90E-01
486	O95782|AP2A1	2	-4.04	-3.53	0.51	-0.96	1.97	-3.66	0.87	0.420909	5.90E-01	-5.99	4	2.79E+06	NA	NA	NA	9.52E+06	9.40E+06	1.40E+07	NA	-4.038	NA	NA	NA	-3.768	-3.695	-3.134	NA	-4.038	-3.532	0.506	4.21E-01	5.90E-01
487	P36957|DDO2	5	1.23	1.53	0.30	-0.52	1.12	1.40	0.84	0.426646	5.97E-01	-6.44	1	NA	6.80E+07	1.58E+08	7.12E+07	3.10E+08	2.20E+08	2.78E+08	1.68E+08	NA	1.319	1.546	0.834	1.425	1.209	1.398	2.092	1.233	1.531	0.298	4.27E-01	5.97E-01
488	Q9NP79|VTA1	2	-1.62	-2.16	-0.54	-2.07	0.98	-1.98	-0.84	0.428868	5.99E-01	-6.31	2	NA	6.77E+06	2.08E+07	NA	2.55E+07	1.24E+07	6.24E+07	8.61E+06	NA	-1.850	-1.390	NA	-2.299	-3.265	-0.869	-2.227	-1.620	-2.165	-0.545	4.29E-01	5.99E-01
489	P60953|CDC42	4	0.03	-0.38	-0.41	-1.56	0.74	-0.20	-0.83	0.431784	6.02E-01	-6.44	1	6.76E+07	1.39E+07	8.16E+07	NA	8.02E+07	1.23E+08	1.07E+08	1.77E+07	0.375	-0.861	0.589	NA	-0.591	0.302	-0.053	-1.180	0.034	-0.380	-0.415	4.32E-01	6.02E-01
490	Q15365|PCBP1	6	0.18	0.52	0.34	-0.60	1.28	0.37	0.82	0.432874	6.02E-01	-6.45	1	5.68E+07	NA	5.45E+07	5.17E+07	1.92E+08	2.08E+08	1.68E+08	3.06E+07	0.135	NA	0.004	0.402	0.708	1.118	0.635	-0.384	0.180	0.519	0.339	4.33E-01	6.02E-01
491	Q9UBB6|NCDN	4	-1.33	-1.00	0.33	-0.60	1.27	-1.14	0.82	0.43397	6.02E-01	-6.45	1	1.03E+07	1.52E+07	2.67E+07	NA	6.01E+07	5.10E+07	6.18E+07	1.99E+07	-2.226	-0.737	-1.030	NA	-1.023	-1.066	-0.884	-1.011	-1.331	-0.996	0.335	4.34E-01	6.02E-01
492	O43295|SRGP3	2	-3.37	-3.93	-0.57	-2.22	1.09	-3.48	-0.83	0.438325	6.06E-01	-6.07	3	5.03E+06	4.18E+06	3.59E+06	2.28E+06	NA	NA	NA	2.66E+06	-3.221	-2.511	-3.932	-3.807	NA	NA	NA	-3.934	-3.368	-3.934	-0.567	4.38E-01	6.06E-01
493	Q5T013|HY1	4	-1.14	-0.55	0.59	-1.08	2.27	-0.80	0.81	0.4385	6.06E-01	-6.45	1	2.26E+07	1.09E+07	2.57E+07	NA	1.53E+08	1.47E+08	7.89E+07	6.52E+06	-1.139	-1.202	-1.084	NA	0.375	0.579	-0.515	-2.631	-1.142	-0.548	0.594	4.39E-01	6.06E-01
494	Q16143|SYUB	6	6.65	6.33	-0.32	-1.24	0.59	6.49	-0.80	0.44423	6.13E-01	-6.55	0	8.94E+09	1.96E+09	3.59E+09	9.78E+09	6.40E+09	5.98E+09	7.95E+09	3.60E+09	7.134	5.935	6.067	7.469	5.939	6.340	6.482	6.545	6.651	6.326	-0.325	4.44E-01	6.13E-01
495	P46109|CRKL	5	0.29	0.66	0.37	-0.69	1.43	0.47	0.79	0.447582	6.16E-01	-6.55	0	5.43E+07	5.28E+07	9.30E+07	2.32E+07	2.13E+08	2.49E+08	1.62E+08	3.46E+07	0.070	0.972	0.778	-0.677	0.864	1.399	0.580	-0.205	0.286	0.660	0.374	4.48E-01	6.16E-01
496	P50991|TCPD	2	-3.08	-2.67	0.41	-0.85	1.67	-2.75	0.79	0.459113	6.31E-01	-6.10	3	NA	2.77E+06	NA	NA	2.14E+07	1.93E+07	1.43E+07	7.51E+06	NA	-3.076	NA	NA	-2.562	-2.575	-3.102	-2.425	-3.076	-2.666	0.410	4.59E-01	6.31E-01
497	O43765|SGTA	4	-0.49	-0.11	0.38	-0.76	1.52	-0.27	0.77	0.465349	6.37E-01	-6.49	1	1.88E+07	2.71E+07	NA	3.49E+07	1.05E+08	5.50E+07	1.29E+08	5.50E+07	-1.397	0.056	NA	-0.126	-0.188	-0.950	0.235	0.469	-0.489	-0.109	0.380	4.65E-01	6.37E-01
498	zz|Y-FGC2Cont00261|	11	8.07	7.67	-0.39	-1.55	0.77	7.87	-0.76	0.464672	6.37E-01	-6.57	0	1.71E+10	1.82E+10	2.10E+10	5.21E+09	1.70E+10	2.11E+10	1.69E+10	6.39E+09	8.030	8.995	8.622	6.620	7.393	8.296	7.630	7.378	8.067	7.674	-0.392	4.65E-01	6.37E-01
499	P62072|TIM10	2	-3.15	-3.54	-0.39	-1.59	0.81	-3.35	-0.77	0.467036	6.38E-01	-6.42	2	6.11E+06	2.33E+06	6.01E+06	NA	7.30E+06	7.87E+06	2.15E+07	NA	-2.951	-3.314	-3.185	NA	-4.165	-3.971	-2.488	NA	-3.150	-3.541	-0.391	4.67E-01	6.38E-01
500	O94811|TPPP	3	-1.22	-0.93	0.28	-0.56	1.13	-1.08	0.76	0.468557	6.38E-01	-6.58	0	1.65E+07	9.04E+06	2.10E+07	2.73E+07	6.70E+07	4.44E+07	4.61E+07	3.32E+07	-1.577	-1.453	-1.378	-0.460	-0.859	-1.283	-1.328	-0.265	-1.217	-0.934	0.283	4.69E-01	6.38E-01
501	P45381|ACY2	2	-2.84	-2.51	0.33	-0.65	1.30	-2.67	0.75	0.469191	6.38E-01	-6.58	0	6.69E+06	6.16E+06	7.17E+06	2.63E+06	2.06E+07	2.15E+07	1.33E+07	1.15E+07	-2.827	-1.980	-2.930	-3.613	-2.618	-2.411	-3.214	-1.806	-2.837	-2.512	0.325	4.69E-01	6.38E-01
502	Q92783|STAM1	9	2.03	1.74	-0.29	-1.15	0.57	1.88	-0.75	0.47138	6.40E-01	-6.58	0	3.05E+08	1.85E+08	1.98E+08	8.54E+07	4.09E+08	3.25E+08	3.04E+08	1.35E+08	2.461	2.690	1.870	1.079	1.837	1.811	1.530	1.777	2.025	1.739	-0.286	4.71E-01	6.40E-01
503	P04264|K2C1	25	5.14	4.44	-0.71	-2.84	1.43	4.79	-0.74	0.476339	6.44E-01	-6.59	0	5.97E+08	1.07E+09	3.10E+09	3.93E+09	6.76E+08	8.00E+08	3.44E+09	4.15E+09	3.390	5.098	5.851	6.241	2.586	3.212	5.210	6.752	5.145	4.440	-0.705	4.76E-01	6.44E-01
504	Q9Y224|RTRAF	5	-3.26	-2.89	0.37	-0.78	1.52	-3.01	0.75	0.476014	6.44E-01	-6.38	2	NA	1.53E+06	8.89E+06	NA	1.44E+07	1.26E+07	2.23E+07	6.10E+06	NA	-3.893	-2.619	NA	-3.152	-3.240	-2.433	-2.727	-3.256	-2.888	0.368	4.76E-01	6.44E-01
505	Q8WZA0|LZIC	2	-2.34	-2.85	-0.52	-2.14	1.11	-2.68	-0.74	0.48078	6.49E-01	-6.39	2	NA	NA	1.14E+07	6.41E+06	2.29E+07	2.05E+07	5.85E+06	9.96E+06	NA	NA	-2.263	-2.411	-2.458	-2.480	-4.459	-2.015	-2.337	-2.853	-0.516	4.81E-01	6.49E-01
506	P31947|1433S	3	2.89	3.14	0.24	-0.50	0.99	3.01	0.73	0.483575	6.51E-01	-6.60	0	3.79E+08	2.28E+08	6.22E+08	2.12E+08	1.06E+09	8.61E+08	6.93E+08	3.56E+08	2.760	2.979	3.528	2.308	3.250	3.327	2.782	3.184	2.894	3.136	0.242	4.84E-01	6.51E-01
507	P48444|COPD	5	-1.40	-1.75	-0.35	-1.48	0.79	-1.68	-0.74	0.486248	6.53E-01	-6.14	3	NA	NA	2.06E+07	NA	3.76E+07	3.32E+07	3.53E+07	1.14E+07	NA	NA	-1.405	NA	-1.719	-1.732	-1.732	-1.819	-1.405	-1.751	-0.346	4.86E-01	6.53E-01
508	Q96PU8|QKI	4	-1.78	-1.30	0.48	-1.10	2.06	-1.62	0.72	0.496695	6.66E-01	-6.41	2	1.31E+07	1.44E+07	2.20E+07	3.88E+06	NA	3.26E+07	NA	2.25E+07	-1.899	-0.818	-1.308	-3.087	NA	-1.763	NA	-0.829	-1.778	-1.296	0.481	4.97E-01	6.66E-01
509	Q9UI15|TAGL3	10	3.85	4.15	0.30	-0.66	1.26	4.00	0.70	0.49976	6.69E-01	-6.62	0	1.10E+09	4.42E+08	1.29E+09	2.81E+08	1.91E+09	1.72E+09	1.90E+09	5.30E+08	4.234	3.891	4.589	2.685	4.132	4.398	4.310	3.759	3.850	4.150	0.300	5.00E-01	6.69E-01
510	zz|Y-FGC2Cont00288|	10	-0.94	-1.86	-0.92	-3.90	2.07	-1.46	-0.70	0.500658	6.69E-01	-6.54	1	NA	1.61E+07	1.31E+07	3.55E+07	9.22E+06	9.12E+06	3.65E+07	1.39E+08	NA	-0.658	-2.057	-0.104	-3.817	-3.741	-1.683	1.817	-0.940	-1.856	-0.916	5.01E-01	6.69E-01
511	Q8N0Y7|PGAM4	5	1.35	0.59	-0.76	-3.44	1.92	0.78	-0.72	0.502368	6.70E-01	-6.12	4	NA	NA	1.38E+08	NA	1.65E+08	6.64E+07	3.94E+08	NA	NA	NA	1.347	NA	0.487	-0.657	1.926	NA	1.347	0.585	-0.762	5.02E-01	6.70E-01
512	P49006|MRP	2	0.41	0.15	-0.27	-1.14	0.60	0.28	-0.69	0.509356	6.77E-01	-6.63	0	7.73E+07	2.14E+07	8.13E+07	6.81E+07	7.88E+07	1.19E+08	1.22E+08	6.97E+07	0.561	-0.267	0.584	0.773	-0.617	0.250	0.145	0.812	0.413	0.148	-0.265	5.09E-01	6.77E-01
513	Q9Y3C8|UFC1	2	-3.02	-1.99	1.03	-2.64	4.69	-2.25	0.71	0.509381	6.77E-01	-6.13	4	NA	2.90E+06	NA	NA	5.96E+07	6.87E+06	6.73E+07	NA	NA	-3.017	NA	NA	-1.034	-4.182	-0.756	NA	-3.017	-1.991	1.026	5.09E-01	6.77E-01
514	P13591|NCAM1	5	-0.12	0.17	0.28	-0.66	1.23	0.02	0.68	0.513517	6.81E-01	-6.64	0	4.78E+07	1.10E+07	5.47E+07	7.01E+07	1.09E+08	1.24E+08	1.37E+08	4.46E+07	-0.105	-1.187	0.009	0.812	-0.138	0.319	0.323	0.164	-0.117	0.167	0.285	5.14E-01	6.81E-01
515	Q04760|LGUL	2	1.66	1.37	-0.30	-1.29	0.69	1.51	-0.67	0.516465	6.83E-01	-6.64	0	1.47E+08	9.39E+07	1.49E+08	1.66E+08	1.50E+08	2.09E+08	3.06E+08	2.15E+08	1.452	1.761	1.463	1.973	0.343	1.124	1.543	2.452	1.662	1.365	-0.297	5.16E-01	6.83E-01
516	O60641|AP180	7	1.95	2.36	0.41	-0.98	1.79	2.15	0.66	0.52435	6.92E-01	-6.65	0	1.30E+08	1.41E+08	4.34E+08	8.11E+07	7.25E+08	1.80E+08	7.69E+08	2.93E+08	1.278	2.320	3.194	1.009	2.690	0.895	2.940	2.900	1.950	2.356	0.406	5.24E-01	6.92E-01
517	Q86YM7|HOME1	3	-1.55	-1.82	-0.27	-1.20	0.66	-1.69	-0.66	0.526911	6.94E-01	-6.65	0	2.31E+07	4.64E+06	3.15E+07	9.21E+06	3.78E+07	2.62E+07	2.61E+07	1.65E+07	-1.113	-2.371	-0.791	-1.923	-1.714	-2.099	-2.189	-1.284	-1.549	-1.822	-0.272	5.27E-01	6.94E-01
518	Q96EQ0|SGTB	2	-0.81	-1.19	-0.38	-1.68	0.92	-1.00	-0.66	0.52731	6.94E-01	-6.65	0	3.02E+07	4.54E+06	3.40E+07	5.89E+07	4.91E+07	3.36E+07	5.28E+07	2.64E+07	-0.739	-2.399	-0.680	0.579	-1.324	-1.715	-1.123	-0.598	-0.810	-1.190	-0.380	5.27E-01	6.94E-01

1	ProteinName	# Peptides	Ctrl	Group1	log2FC	CI.L	CI.R	Ave Expr	t	P.Value	adj.P.Val	B	nrNAs	M.3_Control.raw	M.2_Control.raw	M.4_Control.raw	M.1_Control.raw	E4.2_Group_1.raw	E4.4_Group_1.raw	E4.3_Group_1.raw	E4.1_Group_1.raw	M.3_Control.transf	M.2_Control.transf	M.4_Control.transf	M.1_Control.transf	E4.2_Group_1.transf	E4.4_Group_1.transf	E4.3_Group_1.transf	E4.1_Group_1.transf	pseudo.Ctrl	pseudo.Group1	pseudo.log2FC	pseudo.P.Value	pseudo.adj.P.Val
519	P62253|UB2G1	2	-2.12	-2.61	-0.49	-2.21	1.23	-2.40	-0.65	0.53375	7.01E-01	-6.58	1	1.22E+07	5.02E+06	1.27E+07	NA	4.25E+07	2.63E+07	3.07E+07	1.42E+06	-1.993	-2.262	-2.106	NA	-1.539	-2.096	-1.945	-4.851	-2.120	-2.608	-0.487	5.34E-01	7.01E-01
520	P52815|RM12	2	0.47	0.26	-0.21	-0.95	0.53	0.37	-0.64	0.538394	7.05E-01	-6.66	0	6.61E+07	3.28E+07	6.74E+07	7.55E+07	1.46E+08	8.49E+07	1.24E+08	7.16E+07	0.344	0.317	0.313	0.914	0.306	-0.274	0.167	0.851	0.472	0.262	-0.210	5.38E-01	7.05E-01
521	zz|Y-FGC2Cont00148|	3	5.00	4.79	-0.22	-0.99	0.56	4.89	-0.63	0.545817	7.12E-01	-6.67	0	1.69E+09	5.98E+08	2.15E+09	2.35E+09	2.36E+09	2.24E+09	2.63E+09	1.31E+09	4.833	4.304	5.325	5.545	4.448	4.809	4.806	5.080	5.002	4.785	-0.216	5.46E-01	7.12E-01
522	zz|Y-FGC2Cont00455|	9	2.76	2.96	0.20	-0.52	0.93	2.86	0.63	0.545745	7.12E-01	-6.67	0	4.77E+08	1.66E+08	5.00E+08	1.94E+08	9.41E+08	7.52E+08	8.08E+08	2.43E+08	3.080	2.546	3.212	2.187	3.080	3.115	3.013	2.625	2.756	2.958	0.202	5.46E-01	7.12E-01
523	P00491|PNPH	2	-1.91	-2.20	-0.28	-1.36	0.80	-2.08	-0.63	0.548467	7.14E-01	-6.41	3	1.23E+07	6.78E+06	NA	NA	2.25E+07	2.13E+07	3.65E+07	NA	-1.978	-1.849	NA	NA	-2.485	-2.420	-1.684	NA	-1.914	-2.196	-0.282	5.48E-01	7.14E-01
524	P00338|LDHA	3	0.86	1.14	0.27	-0.73	1.27	1.00	0.61	0.55573	7.23E-01	-6.68	0	6.74E+07	3.79E+07	1.75E+08	7.35E+07	1.71E+08	1.44E+08	2.93E+08	1.56E+08	0.370	0.514	1.692	0.878	0.538	0.548	1.476	1.980	0.864	1.136	0.272	5.56E-01	7.23E-01
525	P13798|ACPH	3	-3.14	-2.61	0.53	-1.54	2.60	-2.72	0.62	0.557967	7.23E-01	-6.22	3	NA	NA	6.21E+06	NA	1.38E+07	1.87E+07	1.26E+07	1.64E+07	NA	NA	-3.139	NA	-3.219	-2.625	-3.302	-1.291	-3.139	-2.609	0.529	5.58E-01	7.23E-01
526	P55290|CAD13	11	1.53	1.73	0.19	-0.52	0.91	1.63	0.61	0.557774	7.23E-01	-6.68	0	1.00E+08	1.12E+08	1.74E+08	1.18E+08	3.84E+08	2.47E+08	3.81E+08	1.48E+08	0.923	2.007	1.681	1.517	1.742	1.383	1.874	1.904	1.532	1.726	0.194	5.58E-01	7.23E-01
527	Q95292|VAPB	5	3.30	3.12	-0.18	-0.86	0.50	3.21	-0.60	0.565237	7.27E-01	-6.69	0	4.90E+08	3.33E+08	6.44E+08	3.61E+08	8.54E+08	6.99E+08	7.49E+08	4.94E+08	3.116	3.502	3.578	3.022	2.936	3.002	2.898	3.659	3.305	3.124	-0.181	5.65E-01	7.27E-01
528	P17050|NAGAB	3	-1.97	-1.74	0.23	-0.65	1.11	-1.84	0.60	0.5665	7.27E-01	-6.61	1	1.15E+07	4.18E+06	2.20E+07	NA	3.42E+07	2.98E+07	3.20E+07	1.62E+07	-2.081	-2.512	-1.309	NA	-1.863	-1.903	-1.882	-1.307	-1.967	-1.739	0.229	5.66E-01	7.27E-01
529	P22061|PIMT	8	3.89	4.10	0.22	-0.61	1.04	4.00	0.60	0.565861	7.27E-01	-6.69	0	1.24E+09	3.27E+08	1.16E+09	4.24E+08	2.18E+09	1.68E+09	1.51E+09	5.29E+08	4.404	3.476	4.426	3.239	4.329	4.365	3.965	3.758	3.886	4.104	0.218	5.66E-01	7.27E-01
530	Q99576|T22D3	2	-2.32	-2.66	-0.34	-1.74	1.06	-2.41	-0.61	0.56527	7.27E-01	-6.19	4	9.58E+06	NA	9.24E+06	8.21E+06	NA	NA	NA	6.38E+06	-2.330	NA	-2.564	-2.077	NA	NA	NA	-2.663	-2.324	-2.663	-0.339	5.65E-01	7.27E-01
531	zz|Y-FGC2Cont00295|	6	-0.53	-0.21	0.32	-0.91	1.55	-0.35	0.60	0.564141	7.27E-01	-6.61	1	1.50E+07	2.67E+07	5.77E+07	NA	1.46E+08	6.16E+07	1.26E+08	2.70E+07	-1.712	0.032	0.088	NA	0.305	-0.773	0.198	-0.568	-0.531	-0.209	0.321	5.64E-01	7.27E-01
532	P0DPI2|GAL3A	2	-1.54	-1.28	0.26	-0.75	1.26	-1.39	0.59	0.573707	7.35E-01	-6.62	1	1.45E+07	NA	1.73E+07	1.56E+07	7.62E+07	3.45E+07	6.88E+07	9.56E+06	-1.755	NA	-1.653	-1.215	-0.668	-1.673	-0.723	-2.074	-1.541	-1.284	0.257	5.74E-01	7.35E-01
533	P52788|SPSY	3	-1.86	-1.18	0.69	-2.09	3.46	-1.40	0.58	0.578362	7.38E-01	-6.50	2	7.17E+06	NA	2.73E+07	NA	4.89E+07	3.00E+07	1.54E+07	1.12E+08	-2.730	NA	-0.997	NA	-1.328	-1.889	-2.988	1.503	-1.864	-1.176	0.688	5.78E-01	7.38E-01
534	Q15369|ELOC	4	0.64	0.80	0.16	-0.47	0.79	0.72	0.58	0.577728	7.38E-01	-6.70	0	7.94E+07	4.72E+07	9.21E+07	5.10E+07	1.99E+08	1.33E+08	2.19E+08	7.81E+07	0.597	0.816	0.765	0.385	0.763	0.428	1.036	0.977	0.641	0.801	0.160	5.78E-01	7.38E-01
535	P61158|ARP3	4	-2.06	-2.54	-0.47	-2.48	1.53	-2.44	-0.57	0.587284	7.47E-01	-6.25	3	NA	NA	1.31E+07	NA	4.36E+07	1.20E+07	2.78E+07	4.30E+06	NA	NA	-2.063	NA	-1.500	-3.319	-2.095	-3.235	-2.063	-2.537	-0.474	5.87E-01	7.47E-01
536	zz|Y-FGC2Cont00356|	9	1.16	0.79	-0.36	-1.84	1.12	0.95	-0.56	0.587628	7.47E-01	-6.63	1	4.08E+07	6.55E+07	3.11E+08	NA	1.82E+08	1.34E+08	3.05E+08	5.87E+07	-0.323	1.267	2.525	NA	0.631	0.439	1.536	0.562	1.156	0.792	-0.364	5.88E-01	7.47E-01
537	O15540|FABP7	3	3.14	2.95	-0.19	-0.98	0.59	3.04	-0.56	0.591118	7.50E-01	-6.72	0	4.26E+08	1.78E+08	4.17E+08	7.72E+08	8.76E+08	7.39E+08	7.35E+08	2.83E+08	2.921	2.644	2.949	4.046	2.973	3.089	2.869	2.849	3.140	2.945	-0.195	5.91E-01	7.50E-01
538	Q16851|UGPA	5	-1.18	-0.81	0.38	-1.24	1.99	-0.96	0.56	0.592073	7.50E-01	-6.45	3	NA	1.35E+07	1.97E+07	NA	9.72E+07	2.82E+07	1.02E+08	NA	NA	-0.899	-1.470	NA	-0.304	-1.989	-0.129	NA	-1.184	-0.807	0.377	5.92E-01	7.50E-01
539	O60784|TOM1	4	-0.19	-0.38	-0.18	-0.92	0.56	-0.28	-0.55	0.595749	7.53E-01	-6.72	0	5.16E+07	1.68E+07	4.23E+07	4.39E+07	6.13E+07	9.80E+07	1.01E+08	3.20E+07	0.000	-0.599	-0.361	0.182	-0.992	-0.052	-0.138	-0.320	-0.195	-0.375	-0.181	5.96E-01	7.53E-01
540	P07197|NFM	5	-0.97	-0.70	0.27	-0.84	1.38	-0.84	0.55	0.59696	7.53E-01	-6.72	0	1.41E+07	7.94E+06	2.97E+07	5.23E+07	6.07E+07	7.76E+07	5.68E+07	3.08E+07	-1.798	-1.631	-0.875	0.419	-1.006	-0.413	-1.012	-0.373	-0.971	-0.701	0.271	5.97E-01	7.53E-01
541	zz|Y-FGC2Cont00382|	5	0.62	0.34	-0.28	-1.45	0.89	0.48	-0.54	0.598604	7.54E-01	-6.72	0	8.40E+07	5.11E+07	1.35E+08	2.77E+07	1.42E+08	2.42E+08	1.52E+08	2.39E+07	0.675	0.926	1.313	-0.437	0.256	1.351	0.481	-0.745	0.619	0.336	-0.283	5.99E-01	7.54E-01
542	P26440|IVD	2	-2.46	-2.82	-0.36	-1.92	1.19	-2.70	-0.55	0.601109	7.56E-01	-6.52	2	NA	1.01E+07	4.44E+06	NA	1.46E+07	1.29E+07	2.29E+07	6.76E+06	NA	-1.300	-3.622	NA	-3.127	-3.199	-2.391	-2.578	-2.461	-2.824	-0.362	6.01E-01	7.56E-01
543	Q16595|FRDA	2	-1.18	-0.89	0.29	-0.94	1.52	-1.01	0.54	0.604847	7.59E-01	-6.65	1	NA	9.14E+06	4.79E+07	9.24E+06	9.02E+07	6.11E+07	8.05E+07	1.09E+07	NA	-1.438	-0.182	-1.919	-0.416	-0.784	-0.485	-1.880	-1.180	-0.891	0.288	6.05E-01	7.59E-01
544	P13473|LAMP2	2	-1.77	-1.49	0.28	-0.91	1.46	-1.63	0.53	0.609331	7.60E-01	-6.73	0	1.92E+07	9.22E+06	2.24E+07	4.12E+06	7.11E+07	5.43E+07	3.73E+07	6.76E+06	-1.368	-1.426	-1.279	-3.006	-0.770	-0.969	-1.649	-2.578	-1.770	-1.492	0.278	6.09E-01	7.60E-01
545	P30048|PRDX3	6	-1.16	-0.97	0.19	-0.61	0.99	-1.06	0.53	0.609466	7.60E-01	-6.73	0	2.38E+07	6.53E+06	3.00E+07	2.13E+07	7.66E+07	5.39E+07	7.00E+07	1.39E+07	-1.070	-1.901	-0.858	-0.795	-0.659	-0.981	-0.696	-1.533	-1.156	-0.967	0.189	6.09E-01	7.60E-01
546	Q9NP74|PALMD	4	-2.85	-2.52	0.33	-1.11	1.76	-2.68	0.54	0.608129	7.60E-01	-6.58	2	1.27E+07	1.56E+06	8.17E+06	NA	2.98E+07	2.61E+07	1.19E+07	NA	-1.935	-3.863	-2.741	NA	-2.070	-2.106	-3.382	NA	-2.847	-2.519	0.328	6.08E-01	7.60E-01
547	Q96K17|IBT3L4	3	-2.07	-2.49	-0.42	-2.26	1.43	-2.35	-0.53	0.611484	7.62E-01	-6.53	2	9.68E+06	NA	1.53E+07	NA	3.18E+07	3.21E+07	3.33E+07	1.96E+06	-2.315	NA	-1.831	NA	-1.971	-1.784	-1.824	-4.379	-2.073	-2.489	-0.417	6.11E-01	7.62E-01
548	P53999|TCP4	3	-2.65	-1.91	0.74	-2.57	4.06	-2.16	0.53	0.615058	7.63E-01	-6.53	2	8.94E+05	NA	NA	4.81E+07	3.42E+07	2.84E+07	2.08E+07	1.67E+07	-5.613	NA	NA	0.306	-1.865	-1.974	-2.538	-1.267	-2.653	-1.911	0.743	6.15E-01	7.63E-01
549	Q9P121|NTRI	4	0.76	0.46	-0.30	-1.60	1.00	0.61	-0.52	0.613959	7.63E-01	-6.74	0	7.21E+07	6.60E+07	6.69E+07	7.96E+07	2.39E+08	2.36E+08	1.91E+08	1.57E+07	0.464	1.277	0.301	0.985	1.036	1.315	0.823	-1.354	0.757	0.455	-0.302	6.14E-01	7.63E-01
550	zz|Y-FGC2Cont00191|	3	0.68	0.96	0.28	-0.93	1.49	0.82	0.52	0.617998	7.65E-01	-6.74	0	1.34E+08	3.12E+07	1.90E+08	2.34E+07	1.46E+08	2.15E+08	2.48E+08	8.67E+07	1.324	0.246	1.812	-0.666	0.306	1.168	1.222	1.130	0.679	0.956	0.277	6.18E-01	7.65E-01
551	Q15417|CNN3	4	-0.37	-0.16	0.21	-0.73	1.16	-0.27	0.51	0.622445	7.70E-01	-6.74	0	2.27E+07	1.89E+07	7.76E+07	2.79E+07	1.44E+08	5.82E+07	1.24E+08	3.43E+07	-1.135	-0.443	0.517	-0.429	0.277	-0.861	0.167	-0.220	-0.373	-0.159	0.214	6.22E-01	7.70E-01
552	P15121|ALDR	2	-0.24	-0.49	-0.24	-1.37	0.88	-0.41	-0.51	0.626393	7.72E-01	-6.54	2	2.69E+07	NA	7.23E+07	NA	9.22E+07	7.14E+07	1.01E+08	2.18E+07	-0.899	NA	0.414	NA	-0.384	-0.543	-0.145	-0.874	-0.243	-0.486	-0.244	6.26E-01	7.72E-01
553	P60981|DEST	3	1.31	1.03	-0.28	-1.50	0.95	1.17	-0.50	0.625666	7.72E-01	-6.75	0	8.27E+07	4.76E+07	1.93E+08	1.59E+08	4.03E+08	2.01E+08	3.33E+08	2.98E+07	0.654	0.829	1.833	1.914	1.817	1.065	1.669	-0.422	1.307	1.032	-0.275	6.26E-01	7.72E-01
554	Q92734|TFG	6	0.17	0.32	0.15	-0.55	0.85	0.25	0.48	0.64134	7.89E-01	-6.76	0	5.58E+07	2.88E+07	7.04E+07	4.05E+07	1.07E+08	1.43E+08	1.14E+08	7.29E+07	0.110	0.137	0.376	0.075	-0.156	0.534	0.044	0.876	0.174	0.324	0.150	6.41E-01	7.89E-01
555	Q96PX8|SLIK1	2	-3.27	-3.60	-0.33	-2.04	1.38	-3.52	-0.49	0.643601	7.89E-01	-6.27	4	NA	NA	NA	3.38E+06	8.00E+06	NA	1.62E+07	2.78E+06	NA	NA	NA	-3.272	-4.028	NA	-2.917	-3.868	-3.272	-3.604	-0.332	6.44E-01	7.89E-01
556	Q99471|PFD5	3	1.08	1.32	0.24	-0.88	1.35	1.20	0.48	0.642813	7.89E-01	-6.76	0	1.37E+08	8.55E+07	4.25E+07	1.36E+08	2.74E+08	1.61E+08	2.98E+08	1.39E+08	1.352	1.634	-0.355	1.705	1.241	0.725	1.502	1.818	1.084	1.322	0.238	6.43E-01	7.89E-01
557	Q62VM7|TM1L2	4	1.20	1.51	0.30	-1.15	1.76	1.35	0.47	0.647161	7.91E-01	-6.76	0	2.87E+08	1.69E+07	2.59E+08	6.78E+07	2.99E+08	2.79E+08	4.47E+08	7.72E+07	2.375	-0.597	2.261	0.769	1.370	1.577	2.118	0.961	1.202	1.507	0.305	6.47E-01	7.91E-01
558	P40925|MDHC	3	2.30	2.07	-0.23	-1.34	0.88	2.19	-0.47	0.650856	7.93E-01	-6.76	0	2.69E+08	1.20E+08	6.61E+08	9.44E+07	4.51E+08	2.80E+08	5.62E+08	1.89E+08	2.288	2.093	3.615	1.214	1.982	1.583	2.464	2.263	2.303	2.073	-0.230	6.51E-01	7.93E-01
559	Q9H910|JUPI2	4	-1.34	-1.68	-0.35	-2.12	1.42	-1.61	-0.47	0.651564	7.93E-01	-6.31	3	NA	NA	NA	1.42E+07	2.30E+07	2.87E+07	3.87E+07	2.42E+07	NA	NA	NA	-1.336	-2.453	-1.960	-1.595	-0.722	-1.336	-1.682	-0.347	6.52E-01	7.93E-01
560	zz|Y-FGC2Cont00317|	9	2.87	3.03	0.16	-0.62	0.95	2.95	0.47	0.649941	7.93E-01	-6.76	0	5.43E+08	1.18E+08	4.98E+08	3.36E+08	9.72E+08	5.46E+08	8.20E+08	3.95E+08	3.258	2.071	3.206	2.926	3.128	2.618	3.037	3.334	2.865	3.029	0.164	6.50E-01	7.93E-01
561	P50213|IDH3A	4	0.61	0.78	0.17	-0.68	1.03	0.70	0.45	0.660267	7.96E-01	-6.77	0	9.73E+07	2.40E+07	1.29E+08	5.24E+07	1.60E+08	2.35E+08	2.07E+08	5.36E+07	0.878	-0.112	1.256	0.422	0.441	1.311	0.952	0.431	0.611	0.784	0.173	6.60E-01	7.96E-01
562	Q5SW79|CE170	5	-0.36	-0.69	-0.33	-2.00	1.34	-0.58	-0.46	0.6596	7.96E-01	-6.57	2	6.11E+07	NA	2.81E+07	NA	9.49E+07	1.13E+08	8.51E+07	8.97E+06	0.236	NA	-0.953	NA	-0.341	0.166	-0.400	-2.167	-0.359	-0.685	-0.327	6.60E-01	7.96E-01
563	Q9Y2J2|E41L3	8	1.31	1.10	-0.20	-1.21	0.80	1.20	-0.46	0.656898	7.96E-01	-6.77	0	1.75E+08	4.22E+07	1.19E+08	1.38E+08	3.82E+08	2.56E+08	2.53E+08	3.90E+07	1.691	0.663	1.137	1.730	1.736	1.444	1.254	-0.030	1.305	1.101	-0.204	6.57E-01	7.96E-01
564	zz|Y-FGC2Cont00169|	2	-3.64	-2.91	0.72	-3.18	4.62	-3.28	0.47	0.657693	7.96E-01	-6.42	4	NA	1.76E+06	4.58E+06	NA	3.39E+06	7.24E+07	NA	NA	NA	-3.698	-3.578	NA	-5.308	-0.522	NA	NA	-3.638	-2.915	0.723	6.58E-01	7.96E-01
565	zz|Y-FGC2Cont00367|	4	0.57	1.18	0.61	-2.40	3.62	0.87	0.46	0.658171	7.96E-01	-6.77	0	5.05E+06	9.02E+07	2.50E+08	1.23E+08	4.81E+08	2.98E+07	4.29E+08	2.20E+08	-3.215	1.706	2.208	1.567	2.080	-1.903	2.054	2.479	0.567	1.177	0.611	6.58E-01	7.96E-01

1	ProteinName	# Peptides	Ctrl	Group1	log2FC	CI.L	CI.R	Ave Expr	t	P.Value	adj.P.Val	B	nrNAs	M.3_Control.raw	M.2_Control.raw	M.4_Control.raw	M.1_Control.raw	E4.2_Group_1.raw	E4.4_Group_1.raw	E4.3_Group_1.raw	E4.1_Group_1.raw	M.3_Control.transf	M.2_Control.transf	M.4_Control.transf	M.1_Control.transf	E4.2_Group_1.transf	E4.4_Group_1.transf	E4.3_Group_1.transf	E4.1_Group_1.transf	pseudo.Ctrl	pseudo.Group1	pseudo.log2FC	pseudo.P.Value	pseudo.adj.P.Val
566	P54727|RD23B	11	4.33	4.21	-0.12	-0.74	0.50	4.27	-0.45	0.664671	7.97E-01	-6.77	0	1.13E+09	5.00E+08	1.19E+09	1.12E+09	1.86E+09	1.46E+09	1.59E+09	9.25E+08	4.270	4.060	4.463	4.545	4.094	4.146	4.037	4.569	4.335	4.212	-0.123	6.65E-01	7.97E-01
567	Q96AT9|RPE	2	-0.68	-1.07	-0.39	-2.42	1.64	-0.94	-0.45	0.664071	7.97E-01	-6.57	2	NA	6.65E+06	7.80E+07	NA	7.20E+07	2.85E+07	1.33E+08	1.14E+07	NA	-1.875	0.523	NA	-0.753	-1.972	0.278	-1.821	-0.676	-1.067	-0.391	6.64E-01	7.97E-01
568	Q9C005|DPY30	2	-0.28	0.11	0.38	-1.56	2.32	-0.06	0.45	0.663145	7.97E-01	-6.70	1	NA	4.11E+06	7.22E+07	1.00E+08	8.81E+07	8.05E+07	1.65E+08	6.13E+07	NA	-2.538	0.411	1.296	-0.451	-0.357	0.605	0.626	-0.277	0.106	0.383	6.63E-01	7.97E-01
569	Q39757|THIOM	3	1.50	0.97	-0.53	-3.19	2.14	1.24	-0.45	0.666049	7.97E-01	-6.78	0	3.02E+08	8.79E+07	4.50E+08	1.61E+07	3.78E+08	5.28E+08	3.81E+08	8.36E+06	2.444	1.672	3.061	-1.172	1.721	2.568	1.875	-2.269	1.501	0.974	-0.528	6.66E-01	7.97E-01
570	O15116|LSM1	2	-2.06	-1.89	0.18	-0.78	1.14	-1.96	0.45	0.670449	8.00E-01	-6.52	3	1.06E+07	NA	1.42E+07	NA	3.27E+07	3.40E+07	2.88E+07	NA	-2.186	NA	-1.944	NA	-1.928	-1.696	-2.041	NA	-2.065	-1.888	0.177	6.70E-01	8.00E-01
571	Q9H446|RWDD1	2	-5.03	-4.78	0.25	-1.15	1.66	-4.91	0.45	0.669524	8.00E-01	-6.43	4	NA	NA	1.31E+06	1.19E+06	3.74E+06	NA	NA	1.92E+06	NA	NA	-5.389	-4.678	-5.161	NA	NA	-4.404	-5.033	-4.783	0.251	6.70E-01	8.00E-01
572	O00499|BIN1	10	4.19	4.39	0.20	-0.85	1.26	4.29	0.43	0.673688	8.02E-01	-6.78	0	1.70E+09	4.38E+08	1.75E+09	3.59E+08	2.07E+09	1.82E+09	2.66E+09	6.27E+08	4.840	3.878	5.028	3.016	4.257	4.492	4.820	4.005	4.190	4.393	0.203	6.74E-01	8.02E-01
573	P51858|HDGF	2	-2.49	-2.65	-0.16	-1.05	0.72	-2.60	-0.43	0.677906	8.06E-01	-6.58	2	NA	3.73E+06	1.10E+07	NA	2.00E+07	1.90E+07	1.53E+07	7.91E+06	NA	-2.670	-2.315	NA	-2.665	-2.598	-3.006	-2.350	-2.492	-2.655	-0.163	6.78E-01	8.06E-01
574	zz|Y-FGCZCont00100|	17	3.02	2.56	-0.46	-2.89	1.97	2.79	-0.43	0.678949	8.06E-01	-6.78	0	1.65E+08	2.79E+08	6.10E+08	6.03E+08	1.06E+08	3.05E+08	8.58E+08	1.87E+09	1.606	3.260	3.500	3.715	-0.171	1.712	3.105	5.594	3.020	2.560	-0.460	6.79E-01	8.06E-01
575	Q15700|DLG2	6	-0.83	-1.43	-0.59	-3.79	2.61	-1.09	-0.42	0.682162	8.08E-01	-6.71	1	7.97E+06	4.43E+06	6.30E+08	9.58E+06	4.04E+07	6.14E+07	3.19E+07	NA	-2.584	-2.432	3.547	-1.870	-1.612	-0.778	-1.890	NA	-0.835	-1.427	-0.592	6.82E-01	8.08E-01
576	O60888|CUTA	3	3.82	3.55	-0.27	-1.75	1.21	3.69	-0.41	0.68798	8.14E-01	-6.79	0	1.18E+09	7.17E+08	1.27E+09	1.51E+08	1.56E+09	1.28E+09	1.54E+09	2.12E+08	4.330	4.554	4.567	1.846	3.837	3.946	3.992	2.431	3.824	3.552	-0.273	6.88E-01	8.14E-01
577	zz|Y-FGCZCont00359|	10	1.58	1.42	-0.17	-1.10	0.77	1.49	-0.41	0.691342	8.16E-01	-6.71	1	1.09E+08	7.02E+07	2.77E+08	NA	3.76E+08	2.01E+08	3.35E+08	9.15E+07	1.032	1.363	2.358	NA	1.710	1.067	1.681	1.208	1.584	1.416	-0.168	6.91E-01	8.16E-01
578	O60925|PFD1	4	0.40	0.25	-0.15	-0.97	0.67	0.32	-0.41	0.692649	8.16E-01	-6.79	0	9.93E+07	3.69E+07	3.87E+07	6.42E+07	1.63E+08	1.18E+08	1.01E+08	5.40E+07	0.906	0.479	-0.492	0.694	0.462	0.232	-0.143	0.441	0.397	0.248	-0.149	6.93E-01	8.16E-01
579	P43487|RANG	2	-1.34	-1.47	-0.13	-0.88	0.62	-1.41	-0.39	0.702825	8.27E-01	-6.72	1	2.04E+07	NA	1.66E+07	1.81E+07	3.75E+07	4.09E+07	3.90E+07	1.81E+07	-1.284	NA	-1.715	-1.010	-1.724	-1.411	-1.585	-1.144	-1.336	-1.466	-0.130	7.03E-01	8.27E-01
580	P28070|PSB4	2	-3.76	-3.52	0.24	-1.17	1.64	-3.64	0.39	0.705151	8.28E-01	-6.66	2	1.97E+06	1.67E+06	NA	4.22E+06	8.29E+06	7.22E+06	2.15E+07	NA	-4.516	-3.777	NA	-2.976	-3.975	-4.104	-2.483	NA	-3.756	-3.521	0.235	7.05E-01	8.28E-01
581	Q726G3|NECA2	2	-2.43	-2.72	-0.29	-2.01	1.43	-2.62	-0.39	0.706282	8.28E-01	-6.60	2	NA	NA	4.48E+06	1.52E+07	1.52E+07	1.25E+07	1.77E+07	1.19E+07	NA	NA	-3.612	-1.245	-3.069	-3.254	-2.780	-1.762	-2.429	-2.716	-0.287	7.06E-01	8.28E-01
582	P24752|THIL	3	-3.66	-3.95	-0.29	-2.01	1.44	-3.86	-0.39	0.707533	8.28E-01	-6.60	2	3.98E+06	1.66E+06	NA	NA	6.86E+06	3.29E+06	2.12E+07	3.10E+06	-3.546	-3.783	NA	NA	-4.257	-5.327	-2.507	-3.713	-3.664	-3.951	-0.287	7.08E-01	8.28E-01
583	Q9HCJ6|VAT1L	4	-1.38	-1.76	-0.38	-2.66	1.91	-1.63	-0.39	0.709125	8.29E-01	-6.60	2	NA	NA	3.23E+07	8.63E+06	7.84E+06	4.37E+07	7.60E+07	1.87E+07	NA	NA	-0.752	-2.010	-4.059	-1.307	-0.571	-1.100	-1.381	-1.759	-0.378	7.09E-01	8.29E-01
584	P52306|GDS1	4	-3.30	-2.91	0.39	-2.04	2.82	-3.07	0.39	0.712665	8.30E-01	-6.55	3	1.40E+06	NA	1.79E+07	NA	1.35E+07	NA	2.63E+07	4.08E+06	-4.991	NA	-1.610	NA	-3.247	NA	-2.181	-3.312	-3.301	-2.913	0.387	7.13E-01	8.30E-01
585	Q15818|NPTX1	3	-0.11	-0.39	-0.29	-1.98	1.41	-0.25	-0.38	0.713819	8.30E-01	-6.81	0	5.71E+07	3.00E+07	6.26E+07	1.86E+07	1.96E+08	1.19E+08	1.38E+08	5.45E+06	0.140	0.193	0.205	-0.972	0.741	0.250	0.328	-2.892	-0.108	-0.393	-0.285	7.14E-01	8.30E-01
586	Q9H0E2|TOLIP	2	-0.20	-0.44	-0.23	-1.63	1.16	-0.34	-0.38	0.713659	8.30E-01	-6.73	1	4.42E+07	2.22E+07	4.79E+07	NA	1.21E+08	1.26E+08	1.18E+08	8.81E+06	-0.213	-0.218	-0.183	NA	0.016	0.335	0.099	-2.194	-0.204	-0.436	-0.231	7.14E-01	8.30E-01
587	Q8N573|OXR1	5	0.69	0.84	0.15	-0.73	1.02	0.76	0.38	0.715826	8.31E-01	-6.81	0	9.79E+07	2.02E+07	1.25E+08	8.17E+07	2.10E+08	2.18E+08	1.59E+08	6.77E+07	0.887	-0.348	1.206	1.020	0.841	1.190	0.546	0.770	0.691	0.837	0.146	7.16E-01	8.31E-01
588	P09471|GNAO	2	-3.07	-3.24	-0.17	-1.25	0.91	-3.17	-0.37	0.721057	8.32E-01	-6.73	1	4.83E+06	NA	7.99E+06	3.67E+06	6.79E+06	1.18E+07	1.51E+07	7.93E+06	-3.276	NA	-2.773	-3.161	-4.273	-3.336	-3.023	-2.346	-3.070	-3.244	-0.174	7.21E-01	8.32E-01
589	P35658|NU214	2	-4.56	-4.05	0.51	-2.64	3.67	-4.27	0.37	0.719727	8.32E-01	-6.73	1	1.42E+06	1.12E+06	NA	1.47E+06	3.07E+06	2.76E+06	2.99E+06	4.99E+07	-4.968	-4.323	NA	-4.396	-5.455	-5.599	-5.477	0.326	-4.562	-4.051	0.511	7.20E-01	8.32E-01
590	P41236|IPP2	2	-0.93	-0.42	0.51	-2.64	3.66	-0.63	0.37	0.719494	8.32E-01	-6.73	1	8.84E+07	NA	1.08E+08	1.34E+06	1.34E+08	1.47E+08	1.22E+08	6.84E+06	0.745	NA	1.000	-4.524	0.175	0.581	0.143	-2.562	-0.926	-0.416	0.511	7.19E-01	8.32E-01
591	P80723|BASP1	8	1.93	2.07	0.14	-0.74	1.02	2.00	0.37	0.721617	8.32E-01	-6.81	0	1.68E+08	1.28E+08	1.29E+08	2.71E+08	3.48E+08	4.15E+08	3.74E+08	2.48E+08	1.635	2.187	1.250	2.637	1.595	2.191	1.845	2.654	1.927	2.071	0.144	7.22E-01	8.32E-01
592	zz|Y-FGCZCont00342|	6	-3.36	-3.51	-0.15	-1.16	0.85	-3.43	-0.35	0.73492	8.46E-01	-6.67	2	3.29E+06	2.87E+06	5.82E+06	NA	1.63E+07	7.47E+06	1.10E+07	NA	-3.807	-3.030	-3.233	NA	-2.968	-4.052	-3.501	NA	-3.356	-3.507	-0.151	7.35E-01	8.46E-01
593	Q95336|6PGL	5	-0.02	0.13	0.16	-0.89	1.20	0.07	0.34	0.740722	8.49E-01	-6.74	1	NA	2.11E+07	9.13E+07	2.59E+07	1.48E+08	1.28E+08	1.57E+08	2.49E+07	NA	-0.290	0.751	-0.527	0.320	0.367	0.531	-0.684	-0.022	0.133	0.156	7.41E-01	8.49E-01
594	P30085|KCY	3	-1.34	-1.45	-0.12	-0.89	0.65	-1.40	-0.34	0.740645	8.49E-01	-6.82	0	1.89E+07	8.01E+06	3.08E+07	1.24E+07	4.32E+07	5.41E+07	2.78E+07	1.71E+07	-1.387	-1.620	-0.822	-1.522	-1.515	-0.974	-2.097	-1.231	-1.338	-1.454	-0.117	7.41E-01	8.49E-01
595	Q9BW91|NUDT9	2	-3.63	-3.37	0.27	-1.62	2.15	-3.45	0.33	0.74981	8.58E-01	-6.62	2	NA	NA	2.33E+06	5.15E+06	1.97E+07	1.82E+07	4.26E+06	4.50E+06	NA	NA	-4.558	-2.705	-2.683	-2.669	-4.940	-3.169	-3.632	-3.365	0.266	7.50E-01	8.58E-01
596	Q9NR46|SHLB2	7	0.44	0.54	0.09	-0.55	0.73	0.49	0.32	0.752514	8.60E-01	-6.83	0	7.47E+07	3.78E+07	6.27E+07	5.74E+07	2.15E+08	1.63E+08	1.24E+08	5.08E+07	0.512	0.511	0.207	0.544	0.876	0.742	0.172	0.353	0.444	0.536	0.092	7.53E-01	8.60E-01
597	zz|Y-FGCZCont00251|	4	3.67	3.83	0.16	-0.97	1.30	3.75	0.32	0.754528	8.61E-01	-6.83	0	1.01E+09	4.88E+08	2.40E+08	9.87E+08	1.62E+09	1.46E+09	1.59E+09	3.74E+08	4.123	4.024	2.152	4.378	3.888	4.144	4.041	3.255	3.669	3.832	0.162	7.55E-01	8.61E-01
598	P34932|HSP74	8	2.12	2.26	0.14	-0.87	1.16	2.19	0.32	0.755874	8.61E-01	-6.83	0	3.05E+08	5.09E+07	3.50E+08	2.26E+08	6.61E+08	6.05E+08	4.26E+08	1.26E+08	2.458	0.922	2.695	2.392	2.554	2.777	2.043	1.672	2.117	2.262	0.145	7.56E-01	8.61E-01
599	Q86X76|NIT1	2	-3.64	-3.87	-0.22	-1.98	1.53	-3.81	-0.32	0.758475	8.62E-01	-6.34	4	NA	NA	4.39E+06	NA	8.21E+06	5.86E+06	1.36E+07	NA	NA	NA	-3.641	NA	-3.991	-4.429	-3.176	NA	-3.641	-3.865	-0.224	7.58E-01	8.62E-01
600	zz|Y-FGCZCont00477|	4	-1.98	-2.25	-0.27	-2.26	1.73	-2.16	-0.32	0.760501	8.63E-01	-6.63	2	NA	NA	2.95E+07	3.91E+06	1.39E+07	1.79E+07	2.28E+07	2.46E+07	NA	NA	-0.885	-3.076	-3.207	-2.693	-2.395	-0.703	-1.980	-2.249	-0.269	7.61E-01	8.63E-01
601	Q93034|CUL5	2	1.47	1.60	0.13	-0.88	1.14	1.52	0.32	0.762312	8.64E-01	-6.58	3	1.68E+08	7.74E+07	1.31E+08	NA	4.20E+08	NA	2.65E+08	NA	1.634	1.496	1.272	NA	1.876	NA	1.322	NA	1.467	1.599	0.132	7.62E-01	8.64E-01
602	zz|Y-FGCZCont00113|	25	5.00	4.87	-0.13	-1.17	0.91	4.94	-0.29	0.779882	8.82E-01	-6.84	0	2.82E+09	1.14E+09	2.80E+09	5.43E+08	2.95E+09	2.45E+09	2.68E+09	1.17E+09	5.538	5.189	5.707	3.572	4.784	4.951	4.832	4.908	5.002	4.869	-0.133	7.80E-01	8.82E-01
603	Q9UN36|NDRG2	2	1.00	0.88	-0.12	-1.07	0.83	0.94	-0.28	0.782471	8.84E-01	-6.84	0	1.30E+08	7.13E+07	1.30E+08	3.99E+07	1.59E+08	1.53E+08	1.75E+08	1.32E+08	1.283	1.383	1.266	0.053	0.429	0.638	0.697	1.740	0.996	0.876	-0.120	7.82E-01	8.84E-01
604	P49757|NUMB	2	1.69	1.98	0.28	-2.05	2.62	1.82	0.28	0.787572	8.88E-01	-6.76	1	3.23E+08	1.74E+08	3.65E+08	1.67E+07	8.09E+08	NA	5.84E+08	5.85E+07	2.540	2.606	2.756	-1.123	2.855	NA	2.523	0.559	1.695	1.979	0.284	7.88E-01	8.88E-01
605	Q96CX2|KCD12	2	-1.95	-1.84	0.11	-0.83	1.05	-1.89	0.27	0.793449	8.93E-01	-6.70	2	1.33E+07	4.90E+06	1.70E+07	NA	3.27E+07	4.34E+07	2.47E+07	NA	-1.876	-2.294	-1.677	NA	-1.930	-1.317	-2.274	NA	-1.949	-1.840	0.109	7.93E-01	8.93E-01
606	P63098|CANB1	8	2.84	2.74	-0.10	-1.00	0.79	2.79	-0.26	0.797052	8.95E-01	-6.85	0	4.16E+08	3.46E+08	4.34E+08	1.58E+08	7.43E+08	6.29E+08	8.71E+08	1.87E+08	2.889	3.555	3.008	1.909	2.727	2.838	3.128	2.248	2.840	2.735	-0.105	7.97E-01	8.95E-01
607	zz|Y-FGCZCont00060|	12	-1.98	-1.43	0.55	-4.61	5.71	-1.71	0.27	0.797683	8.95E-01	-6.50	4	NA	NA	1.06E+07	1.17E+07	NA	NA	5.19E+06	1.36E+08	NA	NA	-2.364	-1.598	NA	NA	-4.642	1.780	-1.981	-1.431	0.550	7.98E-01	8.95E-01
608	P51610|HCFC1	3	-2.95	-2.83	0.13	-1.03	1.28	-2.85	0.26	0.800536	8.97E-01	-6.39	3	NA	NA	7.05E+06	NA	2.02E+07	1.66E+07	1.65E+07	5.18E+06	NA	NA	-2.954	NA	-2.645	-2.811	-2.892	-2.966	-2.954	-2.828	0.126	8.01E-01	8.97E-01
609	Q9NUP9|LIN7C	3	-3.44	-3.57	-0.13	-1.31	1.05	-3.52	-0.26	0.804768	8.99E-01	-6.59	3	NA	1.50E+06	NA	4.25E+06	9.29E+06	1.32E+07	9.46E+06	NA	NA	-3.921	NA	-2.965	-3.806	-3.169	-3.732	NA	-3.443	-3.569	-0.126	8.05E-01	8.99E-01
610	Q9UIJ7|KAD3	2	-3.92	-3.74	0.18	-1.51	1.87	-3.78	0.26	0.803483	8.99E-01	-6.40	3	3.03E+06	NA	NA	NA	5.80E+06	7.99E+06	1.63E+07	3.33E+06	-3.923	NA	NA	NA	-4.509	-3.947	-2.906	-3.606	-3.923	-3.742	0.181	8.03E-01	8.99E-01
611	P09622|DLDH	4	-0.70	-0.83	-0.13	-1.37	1.10	-0.77	-0.25	0.808203	9.01E-01	-6.71	2	2.06E+07	1.51E+07	5.13E+07	NA	1.19E+08	3.73E+07	5.93E+07	NA	-1.272	-0.744	-0.083	NA	0.001	-1.551	-0.948	NA	-0.700	-0.832	-0.133	8.08E-01	9.01E-01
612	P26885|FKBP2	3	1.49	1.42	-0.08	-0.80	0.65	1.45	-0.24	0.813289	9.04E-01	-6.85	0	1.10E+08	7.12E+07	1.48E+08	1.82E+08	3.03E+08	3.21E+08	2.27E+08	1.04E+08	1.044	1.381	1.451	2.100	1.390	1.794	1.088	1.390	1.494	1.416	-0.078	8.13E-01	9.04E-01

1	ProteinName	# Peptides	Ctrl	Group1	log2FC	CI.L	CI.R	Ave Expr	t	P.Value	adj.P.Val	B	nrNAs	M.3_Control.raw	M.2_Control.raw	M.4_Control.raw	M.1_Control.raw	E4.2_Group_1.raw	E4.4_Group_1.raw	E4.3_Group_1.raw	E4.1_Group_1.raw	M.3_Control.transf	M.2_Control.transf	M.4_Control.transf	M.1_Control.transf	E4.2_Group_1.transf	E4.4_Group_1.transf	E4.3_Group_1.transf	E4.1_Group_1.transf	pseudo.Ctrl	pseudo.Group1	pseudo.log2FC	pseudo.P.Value	pseudo.adj.P.Val
613	Q15233|NONO	4	-4.87	-5.06	-0.19	-2.13	1.75	-5.02	-0.25	0.813533	9.04E-01	-6.37	4	NA	NA	NA	1.03E+06	5.55E+06	2.18E+06	NA	1.63E+06	NA	NA	NA	-4.873	-4.573	-5.966	NA	-4.649	-4.873	-5.063	-0.190	8.14E-01	9.04E-01
614	zz|Y-FGC2Cont00276|	8	-2.96	-2.46	0.50	-4.46	5.46	-2.56	0.24	0.815071	9.04E-01	-6.40	3	NA	NA	NA	4.27E+06	6.31E+06	7.76E+06	1.83E+07	9.57E+07	NA	NA	NA	-2.959	-4.382	-3.992	-2.733	1.273	-2.959	-2.459	0.500	8.15E-01	9.04E-01
615	P55036|PSMD4	3	-1.13	-1.24	-0.11	-1.14	0.92	-1.21	-0.24	0.816639	9.04E-01	-6.65	2	1.60E+07	NA	NA	2.37E+07	4.56E+07	5.42E+07	5.85E+07	1.33E+07	-1.621	NA	NA	-0.649	-1.433	-0.970	-0.968	-1.590	-1.135	-1.240	-0.106	8.17E-01	9.04E-01
616	Q9UJU6|DBNL	6	0.26	0.18	-0.08	-0.80	0.65	0.22	-0.24	0.818906	9.05E-01	-6.85	0	7.04E+07	2.41E+07	6.24E+07	5.60E+07	1.20E+08	1.75E+08	1.04E+08	3.86E+07	0.430	-0.108	0.201	0.510	0.013	0.852	-0.089	-0.047	0.258	0.182	-0.076	8.19E-01	9.05E-01
617	P23515|OMGP	4	-0.21	-0.15	0.07	-0.58	0.71	-0.18	0.23	0.821077	9.06E-01	-6.85	0	4.01E+07	1.92E+07	4.45E+07	4.42E+07	9.89E+07	8.71E+07	9.05E+07	4.66E+07	-0.349	-0.415	-0.288	0.193	-0.279	-0.234	-0.307	0.226	-0.215	-0.148	0.066	8.21E-01	9.06E-01
618	Q8N3J6|CADM2	4	-1.14	-1.00	0.14	-1.24	1.51	-1.07	0.22	0.827225	9.11E-01	-6.86	0	2.57E+07	4.56E+06	2.43E+07	3.75E+07	8.99E+07	2.03E+07	7.71E+07	2.76E+07	-0.962	-2.394	-1.162	-0.029	-0.421	-2.497	-0.550	-0.532	-1.137	-1.000	0.137	8.27E-01	9.11E-01
619	Q9UM22|EPDR1	3	-0.46	-0.55	-0.09	-1.07	0.88	-0.50	-0.23	0.827782	9.11E-01	-6.71	2	3.91E+07	1.92E+07	3.67E+07	NA	5.75E+07	1.11E+08	6.98E+07	NA	-0.382	-0.420	-0.568	NA	-1.088	0.136	-0.699	NA	-0.457	-0.550	-0.094	8.28E-01	9.11E-01
620	P61960|UFM1	2	3.29	3.40	0.10	-0.97	1.18	3.34	0.22	0.831696	9.12E-01	-6.86	0	9.23E+08	3.05E+08	7.47E+08	1.70E+08	1.07E+09	1.30E+09	1.17E+09	2.69E+08	3.993	3.378	3.792	2.006	3.270	3.966	3.578	2.773	3.292	3.397	0.105	8.32E-01	9.12E-01
621	Q9Y6I3|EPN1	4	1.76	1.57	-0.19	-2.14	1.77	1.66	-0.22	0.831782	9.12E-01	-6.86	0	1.69E+08	3.35E+08	3.53E+08	2.07E+07	4.26E+08	4.01E+08	3.99E+08	4.85E+07	1.644	3.508	2.707	-0.831	1.897	2.140	1.945	0.286	1.757	1.567	-0.190	8.32E-01	9.12E-01
622	zz|Y-FGC2Cont00142|	6	1.93	1.66	-0.27	-3.05	2.52	1.80	-0.22	0.834033	9.13E-01	-6.86	0	5.33E+08	8.23E+07	6.61E+08	2.26E+07	7.00E+08	7.11E+08	6.75E+08	1.19E+07	3.232	1.581	3.617	-0.710	2.639	3.028	2.741	-1.753	1.930	1.664	-0.266	8.34E-01	9.13E-01
623	Q02952|AKA12	7	0.71	0.60	-0.11	-1.23	1.02	0.65	-0.21	0.835869	9.13E-01	-6.86	0	6.79E+07	2.71E+07	7.13E+07	1.69E+08	1.08E+08	1.38E+08	1.70E+08	1.06E+08	0.380	0.056	0.394	1.996	-0.149	0.482	0.652	1.416	0.707	0.600	-0.106	8.36E-01	9.13E-01
624	Q15102|PA1B3	4	1.99	1.92	-0.07	-0.82	0.68	1.95	-0.21	0.836897	9.13E-01	-6.86	0	3.16E+08	1.05E+08	2.56E+08	9.92E+07	4.31E+08	3.53E+08	3.35E+08	1.72E+08	2.507	1.910	2.242	1.281	1.914	1.940	1.679	2.127	1.985	1.915	-0.070	8.37E-01	9.13E-01
625	zz|Y-FGC2Cont00464|	2	0.75	0.66	-0.10	-1.15	0.96	0.70	-0.21	0.840915	9.16E-01	-6.78	1	7.55E+07	2.74E+07	NA	1.32E+08	1.68E+08	1.97E+08	1.20E+08	7.82E+07	0.528	0.067	NA	1.667	0.509	1.031	0.116	0.980	0.754	0.659	-0.095	8.41E-01	9.16E-01
626	Q9UMF0|ICAM5	4	-0.44	-0.32	0.12	-1.24	1.48	-0.38	0.20	0.845655	9.19E-01	-6.86	0	5.85E+07	1.87E+07	7.52E+07	8.98E+06	1.33E+08	1.13E+08	1.08E+08	1.34E+07	0.174	-0.457	0.470	-1.957	0.158	0.175	-0.032	-1.587	-0.442	-0.321	0.121	8.46E-01	9.19E-01
627	zz|Y-FGC2Cont00347|	15	9.76	9.67	-0.09	-1.12	0.93	9.71	-0.20	0.846465	9.19E-01	-6.86	0	9.50E+10	4.39E+10	5.74E+10	1.88E+10	8.60E+10	5.45E+10	6.08E+10	2.80E+10	10.405	10.207	10.076	8.353	9.811	9.774	9.567	9.527	9.760	9.670	-0.091	8.46E-01	9.19E-01
628	Q9C040|TRIM2	2	-3.79	-3.67	0.13	-1.40	1.65	-3.74	0.20	0.847953	9.20E-01	-6.61	3	3.68E+06	9.19E+05	6.24E+06	NA	NA	1.44E+07	6.49E+06	NA	-3.655	-4.594	-3.130	NA	NA	-3.031	-4.303	NA	-3.793	-3.667	0.126	8.48E-01	9.20E-01
629	P15374|UCHL3	7	3.08	3.14	0.06	-0.64	0.76	3.11	0.19	0.850258	9.21E-01	-6.86	0	5.23E+08	2.82E+08	5.87E+08	2.29E+08	1.01E+09	8.51E+08	8.61E+08	3.08E+08	3.207	3.271	3.444	2.406	3.178	3.309	3.111	2.971	3.082	3.142	0.060	8.50E-01	9.21E-01
630	Q9UH65|SWP70	3	-3.01	-3.16	-0.14	-1.96	1.67	-3.13	-0.19	0.853616	9.23E-01	-6.41	3	NA	NA	6.77E+06	NA	1.82E+07	1.64E+07	6.54E+06	6.20E+06	NA	NA	-3.013	NA	-2.800	-2.832	-4.292	-2.705	-3.013	-3.157	-0.144	8.54E-01	9.23E-01
631	P04179|SODM	3	2.41	2.20	-0.20	-2.71	2.30	2.30	-0.18	0.858792	9.24E-01	-6.87	0	4.31E+08	2.02E+08	4.66E+08	6.74E+07	1.11E+09	1.08E+09	9.73E+08	1.43E+07	2.938	2.813	3.110	0.760	3.324	3.678	3.295	-1.491	2.405	2.202	-0.204	8.59E-01	9.24E-01
632	P33240|CSTF2	4	-1.38	-1.47	-0.09	-1.22	1.03	-1.43	-0.19	0.856963	9.24E-01	-6.86	0	3.47E+07	1.76E+07	1.58E+07	5.32E+06	5.61E+07	3.74E+07	3.17E+07	1.60E+07	-0.548	-0.535	-1.783	-2.662	-1.125	-1.547	-1.900	-1.328	-1.382	-1.475	-0.093	8.57E-01	9.24E-01
633	P58546|MTPN	5	3.85	3.79	-0.06	-0.75	0.64	3.82	-0.18	0.858084	9.24E-01	-6.86	0	9.16E+08	4.94E+08	6.01E+08	6.86E+08	1.17E+09	1.10E+09	1.27E+09	7.32E+08	3.981	4.043	3.479	3.887	3.403	3.713	3.703	4.344	3.848	3.791	-0.057	8.58E-01	9.24E-01
634	Q15599|NHRF2	3	-3.53	-3.43	0.11	-1.33	1.54	-3.45	0.18	0.861716	9.26E-01	-6.41	3	NA	1.99E+06	NA	NA	1.39E+07	1.52E+07	7.63E+06	3.61E+06	NA	-3.533	NA	NA	-3.205	-2.950	-4.057	-3.489	-3.533	-3.426	0.108	8.62E-01	9.26E-01
635	Q6F5E8|CARL2	4	-1.82	-1.90	-0.08	-1.12	0.96	-1.86	-0.18	0.864019	9.27E-01	-6.87	0	2.40E+07	4.33E+06	1.85E+07	7.50E+06	1.97E+07	4.17E+07	2.31E+07	1.78E+07	-1.058	-2.466	-1.557	-2.199	-2.682	-1.380	-2.375	-1.169	-1.820	-1.901	-0.081	8.64E-01	9.27E-01
636	Q9H7C9|AAMDC	2	-0.46	-0.51	-0.06	-0.81	0.69	-0.48	-0.17	0.869504	9.31E-01	-6.87	0	3.62E+07	1.83E+07	3.01E+07	3.85E+07	8.35E+07	6.99E+07	5.70E+07	4.18E+07	-0.492	-0.481	-0.854	0.005	-0.532	-0.577	-1.008	0.070	-0.456	-0.512	-0.056	8.70E-01	9.31E-01
637	P01111|RASN	3	-3.44	-3.31	0.14	-2.05	2.32	-3.34	0.16	0.881706	9.38E-01	-6.39	4	NA	NA	5.04E+06	NA	1.98E+07	1.65E+07	6.01E+06	NA	NA	NA	-3.441	NA	-2.676	-2.821	-4.421	NA	-3.441	-3.306	0.135	8.82E-01	9.38E-01
638	P68402|PA1B2	8	2.89	2.75	-0.13	-2.03	1.76	2.82	-0.16	0.878025	9.38E-01	-6.87	0	7.51E+08	3.59E+08	8.80E+08	4.47E+07	1.10E+09	7.72E+08	8.70E+08	1.06E+08	3.707	3.605	4.031	0.207	3.312	3.156	3.127	1.424	2.888	2.755	-0.133	8.78E-01	9.38E-01
639	Q9UMS0|NFU1	3	0.35	0.25	-0.11	-1.66	1.45	0.30	-0.15	0.881831	9.38E-01	-6.87	0	1.08E+08	5.12E+07	1.20E+08	1.10E+07	1.95E+08	1.65E+08	1.58E+08	1.95E+07	1.023	0.929	1.150	-1.686	0.734	0.757	0.538	-1.037	0.354	0.248	-0.106	8.82E-01	9.38E-01
640	zz|Y-FGC2Cont00284|	14	0.59	0.80	0.22	-3.13	3.56	0.68	0.16	0.880991	9.38E-01	-6.62	3	NA	1.18E+07	8.92E+07	1.87E+08	NA	NA	5.01E+07	2.76E+08	NA	-1.084	0.718	2.133	NA	NA	-1.205	2.813	0.589	0.804	0.215	8.81E-01	9.38E-01
641	Q8NFH3|NUP43	2	-0.47	-0.26	0.21	-3.01	3.44	-0.35	0.15	0.884244	9.40E-01	-6.79	1	NA	5.42E+07	1.42E+08	2.29E+06	2.12E+08	1.45E+08	1.62E+08	4.96E+06	NA	1.006	1.390	-3.799	0.861	0.561	0.581	-3.028	-0.468	-0.256	0.211	8.84E-01	9.40E-01
642	P49773|HINT1	3	-0.60	-0.73	-0.13	-2.21	1.95	-0.67	-0.15	0.885971	9.40E-01	-6.73	2	1.36E+08	9.27E+06	1.64E+07	NA	1.27E+08	7.08E+07	3.51E+07	NA	1.347	-1.419	-1.733	NA	0.099	-0.557	-1.743	NA	-0.602	-0.734	-0.132	8.86E-01	9.40E-01
643	P24821|TENA	3	-3.97	-3.89	0.07	-1.21	1.36	-3.92	0.14	0.892745	9.43E-01	-6.62	3	2.80E+06	NA	3.65E+06	NA	7.03E+06	5.99E+06	NA	4.82E+06	-4.031	NA	-3.908	NA	-4.220	-4.394	NA	-3.070	-3.969	-3.895	0.075	8.93E-01	9.43E-01
644	P55327|TPD52	4	2.66	2.72	0.06	-0.84	0.95	2.69	0.14	0.890396	9.43E-01	-6.87	0	6.88E+08	1.03E+08	3.27E+08	2.58E+08	5.83E+08	7.11E+08	8.08E+08	2.17E+08	3.585	1.895	2.599	2.567	2.365	3.028	3.014	2.464	2.661	2.718	0.056	8.90E-01	9.43E-01
645	Q7Z2D5|PLPR4	2	-3.16	-3.07	0.09	-1.40	1.58	-3.11	0.14	0.891639	9.43E-01	-6.80	1	4.16E+06	NA	6.52E+06	4.36E+06	6.79E+06	3.08E+07	2.73E+07	2.49E+06	-3.484	NA	-3.067	-2.932	-4.273	-1.851	-2.123	-4.031	-3.161	-3.069	0.091	8.92E-01	9.43E-01
646	Q92890|UFD1	3	-2.01	-1.88	0.13	-2.13	2.39	-1.92	0.14	0.894559	9.43E-01	-6.67	2	NA	6.24E+06	NA	8.31E+06	7.01E+06	5.63E+07	3.61E+07	2.50E+07	NA	-1.963	NA	-2.061	-4.226	-0.914	-1.700	-0.679	-2.012	-1.880	0.132	8.95E-01	9.43E-01
647	zz|Y-FGC2Cont00313|	10	3.24	3.17	-0.07	-1.32	1.17	3.20	-0.13	0.901476	9.49E-01	-6.87	0	7.14E+08	3.16E+08	8.42E+08	1.59E+08	1.14E+09	1.08E+09	1.26E+09	1.50E+08	3.638	3.427	3.966	1.913	3.368	3.673	3.693	1.929	3.236	3.166	-0.070	9.01E-01	9.49E-01
648	P23297|S10A1	2	3.85	3.69	-0.16	-3.12	2.80	3.77	-0.12	0.90698	9.51E-01	-6.88	0	1.46E+09	1.13E+09	2.45E+09	4.04E+07	2.72E+09	1.81E+09	2.72E+09	6.70E+07	4.628	5.176	5.512	0.070	4.661	4.484	4.855	0.755	3.847	3.689	-0.158	9.07E-01	9.51E-01
649	P61020|RAB5B	3	-1.63	-1.71	-0.08	-1.64	1.48	-1.69	-0.12	0.905778	9.51E-01	-6.42	3	NA	NA	1.77E+07	NA	2.47E+07	2.84E+07	5.58E+07	1.47E+07	NA	NA	-1.626	NA	-2.349	-1.977	-1.041	-1.454	-1.626	-1.705	-0.079	9.06E-01	9.51E-01
650	zz|Y-FGC2Cont00355|	6	-0.43	-0.47	-0.04	-0.87	0.78	-0.45	-0.12	0.907581	9.51E-01	-6.88	0	2.68E+07	3.19E+07	2.90E+07	3.34E+07	9.51E+07	5.48E+07	1.02E+08	2.87E+07	-0.904	0.277	-0.909	-0.185	-0.338	-0.954	-0.125	-0.479	-0.430	-0.474	-0.044	9.08E-01	9.51E-01
651	REV__Q9BT92|TCHP	2	4.33	4.28	-0.05	-1.03	0.93	4.30	-0.12	0.909111	9.51E-01	-6.80	1	NA	4.69E+08	7.71E+08	1.77E+09	1.58E+09	1.45E+09	1.93E+09	1.06E+09	NA	3.972	3.839	5.167	3.854	4.138	4.338	4.771	4.326	4.275	-0.050	9.09E-01	9.51E-01
652	Q14444|CAPR1	6	1.28	1.31	0.03	-0.68	0.75	1.29	0.10	0.919045	9.60E-01	-6.88	0	1.32E+08	8.06E+07	1.62E+08	6.31E+07	3.64E+08	2.04E+08	2.83E+08	8.28E+07	1.304	1.552	1.578	0.671	1.662	1.091	1.422	1.063	1.276	1.309	0.033	9.19E-01	9.60E-01
653	P05091|ALDH2	8	0.58	0.66	0.07	-1.65	1.79	0.63	0.10	0.923089	9.62E-01	-6.80	1	6.49E+07	2.57E+07	1.48E+08	NA	2.38E+08	2.29E+08	3.41E+08	1.55E+07	0.318	-0.017	1.451	NA	1.030	1.270	1.705	-1.369	0.584	0.659	0.075	9.23E-01	9.62E-01
654	P23470|PTPRG	3	-2.64	-2.61	0.03	-0.63	0.69	-2.63	0.10	0.923404	9.62E-01	-6.88	0	7.66E+06	4.12E+06	6.78E+06	6.50E+06	2.37E+07	1.63E+07	2.43E+07	5.39E+06	-2.639	-2.532	-3.011	-2.393	-2.409	-2.843	-2.301	-2.907	-2.644	-2.615	0.029	9.23E-01	9.62E-01
655	zz|Y-FGC2Cont00363|	3	1.56	1.52	-0.05	-1.19	1.10	1.54	-0.09	0.930938	9.68E-01	-6.88	0	2.29E+08	1.70E+08	1.58E+08	4.02E+07	3.14E+08	2.99E+08	3.46E+08	9.22E+07	2.065	2.576	1.544	0.064	1.441	1.682	1.727	1.218	1.562	1.517	-0.045	9.31E-01	9.68E-01
656	O15145|ARPC3	3	-1.46	-1.44	0.03	-0.70	0.75	-1.45	0.09	0.93342	9.68E-01	-6.88	0	1.64E+07	1.34E+07	1.57E+07	1.20E+07	3.50E+07	5.52E+07	4.27E+07	1.39E+07	-1.588	-0.918	-1.792	-1.562	-1.826	-0.944	-1.445	-1.533	-1.465	-1.437	0.028	9.33E-01	9.68E-01
657	zz|Y-FGC2Cont00296|	5	-0.33	-0.36	-0.03	-0.87	0.81	-0.35	-0.09	0.934084	9.68E-01	-6.80	1	4.26E+07	1.90E+07	4.45E+07	NA	1.21E+08	1.08E+08	7.49E+07	2.04E+07	-0.265	-0.436	-0.288	NA	0.024	0.097	-0.593	-0.971	-0.330	-0.361	-0.031	9.34E-01	9.68E-01
658	P61088|UBE2N	7	5.41	5.44	0.03	-0.90	0.96	5.43	0.07	0.942655	9.76E-01	-6.88	0	2.87E+09	1.01E+09	3.45E+09	1.61E+09	4.97E+09	4.81E+09	4.91E+09	8.52E+08	5.565	5.025	6.008	5.041	5.561	5.999	5.751	4.450	5.410	5.440	0.031	9.43E-01	9.76E-01
659	P51911|CNN1	3	-2.48	-2.51	-0.03	-1.17	1.11	-2.50	-0.07	0.94786	9.77E-01	-6.68	2	5.93E+06	NA	1.40E+07	NA	2.73E+07	1.47E+07	1.73E+07	9.91E+06	-2.993	NA	-1.960	NA	-2.201	-2.997	-2.817	-2.022	-2.476	-2.509	-0.033	9.48E-01	9.77E-01

1	ProteinName	# Peptides	Ctrl	Group1	log2FC	CI.L	CI.R	Ave Expr	t	P.Value	adj.P.Val	B	nrNAs	M.3_Control.raw	M.2_Control.raw	M.4_Control.raw	M.1_Control.raw	E4.2_Group_1.raw	E4.4_Group_1.raw	E4.3_Group_1.raw	E4.1_Group_1.raw	M.3_Control.transf	M.2_Control.transf	M.4_Control.transf	M.1_Control.transf	E4.2_Group_1.transf	E4.4_Group_1.transf	E4.3_Group_1.transf	E4.1_Group_1.transf	pseudo.Ctrl	pseudo.Group1	pseudo.log2FC	pseudo.P.Value	pseudo.adj.P.Val
660	P56537|IF6	2	-0.95	-0.90	0.05	-1.93	2.03	-0.91	0.06	0.952155	9.77E-01	-6.40	4	2.59E+07	NA	NA	NA	8.63E+07	7.93E+07	3.28E+07	NA	-0.951	NA	NA	NA	-0.482	-0.381	-1.844	NA	-0.951	-0.902	0.049	9.52E-01	9.77E-01
661	Q9BX68|HINT2	3	1.48	1.52	0.04	-1.46	1.55	1.50	0.07	0.948456	9.77E-01	-6.88	0	1.79E+08	9.65E+07	3.01E+08	3.59E+07	4.87E+08	3.98E+08	4.08E+08	3.68E+07	1.720	1.800	2.478	-0.090	2.096	2.126	1.977	-0.115	1.477	1.521	0.044	9.48E-01	9.77E-01
662	Q9NQR4|NIT2	2	-3.55	-3.58	-0.03	-1.02	0.97	-3.57	-0.06	0.952247	9.77E-01	-6.63	3	NA	1.67E+06	5.46E+06	NA	9.39E+06	1.08E+07	1.13E+07	NA	NA	-3.775	-3.325	NA	-3.790	-3.474	-3.463	NA	-3.550	-3.576	-0.026	9.52E-01	9.77E-01
663	Q9UBC2|EP15R	10	0.92	0.95	0.02	-0.74	0.78	0.94	0.07	0.94769	9.77E-01	-6.88	0	1.10E+08	6.13E+07	1.40E+08	4.13E+07	2.05E+08	1.80E+08	2.08E+08	8.70E+07	1.053	1.175	1.367	0.101	0.805	0.894	0.954	1.135	0.924	0.947	0.023	9.48E-01	9.77E-01
664	zz|Y-FGCZCont00349|	8	2.86	2.84	-0.03	-1.05	0.99	2.85	-0.06	0.949841	9.77E-01	-6.88	0	5.87E+08	1.60E+08	7.49E+08	1.45E+08	6.39E+08	6.38E+08	6.64E+08	3.76E+08	3.367	2.497	3.797	1.796	2.503	2.861	2.716	3.260	2.864	2.835	-0.029	9.50E-01	9.77E-01
665	Q12765|SCRN1	3	3.60	3.63	0.03	-1.13	1.19	3.61	0.06	0.955263	9.78E-01	-6.88	0	8.22E+08	5.20E+08	1.02E+09	1.94E+08	1.68E+09	1.31E+09	1.42E+09	2.58E+08	3.832	4.113	4.251	2.186	3.944	3.974	3.871	2.713	3.596	3.625	0.030	9.55E-01	9.78E-01
666	Q13522|PPR1A	2	0.10	0.18	0.08	-3.32	3.48	0.14	0.06	0.956539	9.78E-01	-6.63	3	1.46E+08	3.11E+06	1.88E+08	NA	NA	1.09E+08	1.31E+08	NA	1.441	-2.921	1.794	NA	NA	0.108	0.260	NA	0.104	0.184	0.080	9.57E-01	9.78E-01
667	O95747|OXSR1	6	0.01	0.00	-0.02	-0.78	0.74	0.01	-0.05	0.958635	9.79E-01	-6.88	0	3.56E+07	3.63E+07	7.37E+07	3.01E+07	1.58E+08	8.87E+07	1.11E+08	3.41E+07	-0.514	0.455	0.442	-0.325	0.416	-0.205	0.001	-0.226	0.014	-0.004	-0.018	9.59E-01	9.79E-01
668	Q13404|UB2V1	5	-0.77	-0.74	0.03	-1.22	1.27	-0.75	0.05	0.960702	9.79E-01	-6.43	3	NA	NA	3.20E+07	NA	6.32E+07	5.73E+07	6.51E+07	3.18E+07	NA	NA	-0.768	NA	-0.946	-0.884	-0.805	-0.330	-0.768	-0.741	0.026	9.61E-01	9.79E-01
669	P10515|ODP2	2	0.27	0.30	0.02	-1.03	1.08	0.29	0.05	0.963516	9.80E-01	-6.88	0	3.64E+07	1.77E+07	1.03E+08	9.19E+07	1.25E+08	1.10E+08	1.15E+08	7.55E+07	-0.481	-0.527	0.927	1.178	0.064	0.130	0.063	0.928	0.274	0.296	0.022	9.64E-01	9.80E-01
670	Q99426|TBCB	2	-0.25	-0.28	-0.03	-1.62	1.56	-0.27	-0.05	0.964741	9.80E-01	-6.68	2	3.30E+07	NA	NA	4.20E+07	1.47E+08	3.18E+07	1.27E+08	4.47E+07	-0.616	NA	NA	0.123	0.312	-1.799	0.212	0.166	-0.246	-0.277	-0.031	9.65E-01	9.80E-01
671	Q9NUQ9|FA49B	8	0.65	0.62	-0.03	-1.51	1.45	0.63	-0.04	0.965796	9.80E-01	-6.88	0	1.02E+08	9.03E+07	1.47E+08	1.26E+07	2.41E+08	1.74E+08	1.48E+08	4.43E+07	0.946	1.707	1.437	-1.495	1.048	0.837	0.443	0.153	0.649	0.620	-0.029	9.66E-01	9.80E-01
672	P11940|PABP1	4	2.29	2.31	0.02	-1.00	1.03	2.30	0.03	0.9739	9.83E-01	-6.88	0	5.32E+08	1.71E+08	2.68E+08	8.28E+07	6.77E+08	4.28E+08	4.68E+08	1.82E+08	3.231	2.587	2.308	1.038	2.588	2.241	2.196	2.210	2.291	2.306	0.015	9.74E-01	9.83E-01
673	Q13765|NACA	2	-1.28	-1.26	0.02	-1.08	1.12	-1.27	0.04	0.971524	9.83E-01	-6.81	1	3.60E+07	NA	1.72E+07	1.10E+07	3.29E+07	4.57E+07	4.11E+07	3.03E+07	-0.497	NA	-1.662	-1.687	-1.922	-1.235	-1.504	-0.397	-1.282	-1.264	0.018	9.72E-01	9.83E-01
674	Q9BY11|PACN1	3	-0.81	-0.83	-0.02	-1.51	1.47	-0.82	-0.03	0.974662	9.83E-01	-6.54	4	2.48E+07	NA	3.55E+07	NA	1.01E+08	NA	4.36E+07	NA	-1.011	NA	-0.617	NA	-0.253	NA	-1.414	NA	-0.814	-0.834	-0.020	9.75E-01	9.83E-01
675	zz|Y-FGCZCont00248|	5	3.46	3.45	-0.01	-0.85	0.83	3.45	-0.03	0.974806	9.83E-01	-6.88	0	6.63E+08	2.94E+08	7.79E+08	3.87E+08	9.36E+08	1.67E+09	1.04E+09	3.07E+08	3.533	3.328	3.854	3.117	3.072	4.352	3.392	2.968	3.458	3.446	-0.012	9.75E-01	9.83E-01
676	P30043|BLVRB	2	2.07	2.09	0.02	-2.34	2.39	2.08	0.02	0.983432	9.88E-01	-6.88	0	5.19E+08	2.68E+08	5.71E+08	1.24E+07	5.28E+08	5.47E+08	6.40E+08	7.23E+07	3.195	3.203	3.404	-1.526	2.219	2.621	2.660	0.865	2.069	2.091	0.022	9.83E-01	9.88E-01
677	zz|Y-FGCZCont00193|	4	-1.21	-1.22	-0.01	-1.00	0.98	-1.22	-0.02	0.983043	9.88E-01	-6.81	1	1.54E+07	1.08E+07	3.21E+07	NA	4.00E+07	3.10E+07	7.84E+07	2.15E+07	-1.676	-1.204	-0.759	NA	-1.628	-1.840	-0.524	-0.898	-1.213	-1.222	-0.009	9.83E-01	9.88E-01
678	zz|Y-FGCZCont00332|	3	-0.53	-0.54	-0.01	-0.92	0.90	-0.53	-0.02	0.980861	9.88E-01	-6.88	0	4.01E+07	2.09E+07	5.55E+07	1.26E+07	1.19E+08	7.90E+07	6.77E+07	1.97E+07	-0.349	-0.304	0.030	-1.497	0.000	-0.385	-0.747	-1.027	-0.530	-0.540	-0.010	9.81E-01	9.88E-01
679	zz|Y-FGCZCont00319|	12	4.62	4.61	-0.01	-0.66	0.65	4.62	-0.02	0.985122	9.88E-01	-6.88	0	1.66E+09	6.61E+08	1.62E+09	9.41E+08	2.75E+09	2.22E+09	2.55E+09	7.28E+08	4.803	4.443	4.917	4.313	4.680	4.799	4.755	4.221	4.619	4.614	-0.006	9.85E-01	9.88E-01
680	P61604|CH10	6	4.93	4.93	0.00	-0.76	0.77	4.93	0.01	0.989914	9.91E-01	-6.88	0	1.74E+09	6.31E+08	2.04E+09	1.84E+09	2.79E+09	3.66E+09	2.46E+09	1.05E+09	4.871	4.378	5.244	5.218	4.698	5.577	4.705	4.749	4.928	4.932	0.004	9.90E-01	9.91E-01
681	Q04637|IF4G1	3	-2.74	-2.74	-0.01	-1.36	1.35	-2.74	-0.01	0.993025	9.93E-01	-6.81	1	1.18E+07	2.90E+06	6.12E+06	NA	1.72E+07	4.18E+07	1.66E+07	2.85E+06	-2.040	-3.013	-3.160	NA	-2.886	-1.376	-2.877	-3.834	-2.738	-2.743	-0.005	9.93E-01	9.93E-01
682	REV__Q8IWB9|TEX2	2	NA	-2.23	NA	NA	NA	-2.23	NA	NA	NA	NA	4	NA	NA	NA	NA	2.04E+07	2.24E+07	4.17E+07	7.41E+06	NA	NA	NA	NA	-2.632	-2.347	-1.480	-2.444	-4.066	-2.226	1.840	0.00E+00	0.00E+00
683	O00267|SPT5H	2	NA	-3.08	NA	NA	NA	-3.08	NA	NA	NA	NA	4	NA	NA	NA	NA	1.74E+07	5.80E+06	2.28E+07	6.62E+06	NA	NA	NA	NA	-2.870	-4.444	-2.395	-2.609	-4.066	-3.080	0.986	0.00E+00	0.00E+00
684	O00299|CLIC1	6	NA	-0.06	NA	NA	NA	-0.06	NA	NA	NA	NA	4	NA	NA	NA	NA	1.40E+08	9.59E+07	1.13E+08	3.00E+07	NA	NA	NA	NA	0.240	-0.085	0.036	-0.415	-4.066	-0.056	4.010	0.00E+00	0.00E+00
685	O00391|QSOX1	7	NA	-0.51	NA	NA	NA	-0.51	NA	NA	NA	NA	4	NA	NA	NA	NA	8.76E+07	2.62E+07	1.78E+08	3.47E+07	NA	NA	NA	NA	-0.460	-2.103	0.718	-0.201	-4.066	-0.512	3.555	0.00E+00	0.00E+00
686	O00622|CCN1	3	NA	0.65	NA	NA	NA	0.65	NA	NA	NA	NA	4	NA	NA	NA	NA	2.02E+08	1.67E+08	9.96E+07	9.02E+07	NA	NA	NA	NA	0.786	0.778	-0.161	1.187	-4.066	0.647	4.714	0.00E+00	0.00E+00
687	O14672|ADA10	3	NA	0.60	NA	NA	NA	0.60	NA	NA	NA	NA	4	NA	NA	NA	NA	1.42E+08	1.51E+08	2.66E+08	4.54E+07	NA	NA	NA	NA	0.265	0.617	1.327	0.188	-4.066	0.599	4.665	0.00E+00	0.00E+00
688	O43237|DC1L2	2	NA	-1.97	NA	NA	NA	-1.97	NA	NA	NA	NA	4	NA	NA	NA	NA	4.00E+07	1.28E+07	2.85E+07	2.01E+07	NA	NA	NA	NA	-1.629	-3.214	-2.058	-0.993	-4.066	-1.973	2.093	0.00E+00	0.00E+00
689	O43390|HNRPR	3	NA	-2.95	NA	NA	NA	-2.95	NA	NA	NA	NA	4	NA	NA	NA	NA	1.93E+07	8.82E+06	1.78E+07	7.10E+06	NA	NA	NA	NA	-2.713	-3.794	-2.773	-2.506	-4.066	-2.947	1.119	0.00E+00	0.00E+00
690	O43707|ACTN4	10	NA	0.75	NA	NA	NA	0.75	NA	NA	NA	NA	4	NA	NA	NA	NA	1.78E+08	1.74E+08	1.82E+08	6.96E+07	NA	NA	NA	NA	0.599	0.841	0.754	0.811	-4.066	0.751	4.817	0.00E+00	0.00E+00
691	O60749|SNX2	2	NA	-3.82	NA	NA	NA	-3.82	NA	NA	NA	NA	4	NA	NA	NA	NA	8.60E+06	6.56E+06	8.93E+06	4.19E+06	NA	NA	NA	NA	-3.920	-4.252	-3.818	-3.275	-4.066	-3.816	0.250	0.00E+00	0.00E+00
692	O75533|SF3B1	2	NA	-2.88	NA	NA	NA	-2.88	NA	NA	NA	NA	4	NA	NA	NA	NA	2.80E+07	1.55E+07	1.57E+07	3.59E+06	NA	NA	NA	NA	-2.159	-2.914	-2.965	-3.498	-4.066	-2.884	1.182	0.00E+00	0.00E+00
693	O75787|RENR	5	NA	-0.51	NA	NA	NA	-0.51	NA	NA	NA	NA	4	NA	NA	NA	NA	7.12E+07	7.35E+07	1.59E+08	1.60E+07	NA	NA	NA	NA	-0.769	-0.498	0.551	-1.324	-4.066	-0.510	3.556	0.00E+00	0.00E+00
694	O95084|PRS23	7	NA	3.76	NA	NA	NA	3.76	NA	NA	NA	NA	4	NA	NA	NA	NA	1.51E+09	1.86E+09	1.14E+09	3.56E+08	NA	NA	NA	NA	3.780	4.525	3.536	3.181	-4.066	3.756	7.822	0.00E+00	0.00E+00
695	O95150|TNF15	2	NA	-2.63	NA	NA	NA	-2.63	NA	NA	NA	NA	4	NA	NA	NA	NA	1.99E+07	1.66E+07	1.81E+07	8.17E+06	NA	NA	NA	NA	-2.672	-2.813	-2.749	-2.304	-4.066	-2.634	1.432	0.00E+00	0.00E+00
696	O95810|CAVN2	4	NA	-4.31	NA	NA	NA	-4.31	NA	NA	NA	NA	4	NA	NA	NA	NA	4.70E+06	1.15E+07	4.31E+06	2.34E+06	NA	NA	NA	NA	-4.822	-3.384	-4.922	-4.119	-4.066	-4.312	-0.246	0.00E+00	0.00E+00
697	P00749|UROK	3	NA	-1.37	NA	NA	NA	-1.37	NA	NA	NA	NA	4	NA	NA	NA	NA	5.76E+07	3.65E+07	6.05E+07	1.09E+07	NA	NA	NA	NA	-1.086	-1.586	-0.918	-1.879	-4.066	-1.367	2.699	0.00E+00	0.00E+00
698	P01033|TIMP1	2	NA	0.51	NA	NA	NA	0.51	NA	NA	NA	NA	4	NA	NA	NA	NA	1.47E+08	1.44E+08	1.62E+08	6.10E+07	NA	NA	NA	NA	0.314	0.543	0.573	0.618	-4.066	0.512	4.578	0.00E+00	0.00E+00
699	P01034|CYTC	3	NA	1.78	NA	NA	NA	1.78	NA	NA	NA	NA	4	NA	NA	NA	NA	3.81E+08	2.41E+08	3.58E+08	1.92E+08	NA	NA	NA	NA	1.730	1.347	1.779	2.281	-4.066	1.784	5.850	0.00E+00	0.00E+00
700	P01892|1A02	5	NA	1.08	NA	NA	NA	1.08	NA	NA	NA	NA	4	NA	NA	NA	NA	2.33E+08	1.92E+08	2.57E+08	8.28E+07	NA	NA	NA	NA	1.001	0.996	1.278	1.063	-4.066	1.085	5.151	0.00E+00	0.00E+00
701	P04080|CYTB	4	NA	0.10	NA	NA	NA	0.10	NA	NA	NA	NA	4	NA	NA	NA	NA	1.43E+08	1.27E+08	1.03E+08	3.68E+07	NA	NA	NA	NA	0.272	0.352	-0.111	-0.118	-4.066	0.099	4.165	0.00E+00	0.00E+00
702	P04792|HSPB1	10	NA	3.10	NA	NA	NA	3.10	NA	NA	NA	NA	4	NA	NA	NA	NA	1.00E+09	1.09E+09	7.58E+08	2.42E+08	NA	NA	NA	NA	3.175	3.687	2.918	2.623	-4.066	3.101	7.167	0.00E+00	0.00E+00
703	P05067|A4	3	NA	-1.69	NA	NA	NA	-1.69	NA	NA	NA	NA	4	NA	NA	NA	NA	3.81E+07	2.30E+07	5.63E+07	1.22E+07	NA	NA	NA	NA	-1.703	-2.301	-1.025	-1.722	-4.066	-1.688	2.378	0.00E+00	0.00E+00
704	P05362|ICAM1	5	NA	-1.62	NA	NA	NA	-1.62	NA	NA	NA	NA	4	NA	NA	NA	NA	3.43E+07	3.94E+07	3.32E+07	1.59E+07	NA	NA	NA	NA	-1.859	-1.468	-1.829	-1.333	-4.066	-1.622	2.444	0.00E+00	0.00E+00
705	P05556|ITB1	4	NA	0.40	NA	NA	NA	0.40	NA	NA	NA	NA	4	NA	NA	NA	NA	1.94E+08	1.50E+08	1.67E+08	3.15E+07	NA	NA	NA	NA	0.726	0.612	0.618	-0.342	-4.066	0.404	4.470	0.00E+00	0.00E+00
706	P06703|S10A6	4	NA	2.95	NA	NA	NA	2.95	NA	NA	NA	NA	4	NA	NA	NA	NA	8.52E+08	5.43E+08	6.70E+08	4.52E+08	NA	NA	NA	NA	2.932	2.611	2.730	3.528	-4.066	2.950	7.016	0.00E+00	0.00E+00

1	ProteinName	# Peptides	Ctrl	Group1	log2FC	CI.L	CI.R	Ave Expr	t	P.Value	adj.P.Val	B	nrNAs	M.3_Control.raw	M.2_Control.raw	M.4_Control.raw	M.1_Control.raw	E4.2_Group_1.raw	E4.4_Group_1.raw	E4.3_Group_1.raw	E4.1_Group_1.raw	M.3_Control.transf	M.2_Control.transf	M.4_Control.transf	M.1_Control.transf	E4.2_Group_1.transf	E4.4_Group_1.transf	E4.3_Group_1.transf	E4.1_Group_1.transf	pseudo.Ctrl	pseudo.Group1	pseudo.log2FC	pseudo.P.Value	pseudo.adj.P.Val
707	P06748|NPM	2	NA	-1.41	NA	NA	NA	-1.41	NA	NA	NA	NA	4	NA	NA	NA	NA	3.61E+07	4.43E+07	6.40E+07	1.21E+07	NA	NA	NA	NA	-1.782	-1.286	-0.832	-1.732	-4.066	-1.408	2.658	0.00E+00	0.00E+00
708	P06753|TPM3	3	NA	-4.28	NA	NA	NA	-4.28	NA	NA	NA	NA	4	NA	NA	NA	NA	4.74E+06	8.54E+06	7.16E+06	2.06E+06	NA	NA	NA	NA	-4.807	-3.844	-4.153	-4.303	-4.066	-4.277	-0.211	0.00E+00	0.00E+00
709	P06756|ITAV	5	NA	-1.41	NA	NA	NA	-1.41	NA	NA	NA	NA	4	NA	NA	NA	NA	5.80E+07	4.51E+07	4.12E+07	1.16E+07	NA	NA	NA	NA	-1.074	-1.257	-1.501	-1.792	-4.066	-1.406	2.660	0.00E+00	0.00E+00
710	P07858|CATB	3	NA	0.09	NA	NA	NA	0.09	NA	NA	NA	NA	4	NA	NA	NA	NA	1.58E+08	1.36E+08	1.16E+08	2.67E+07	NA	NA	NA	NA	0.415	0.454	0.074	-0.582	-4.066	0.090	4.156	0.00E+00	0.00E+00
711	P07942|LAMB1	19	NA	1.94	NA	NA	NA	1.94	NA	NA	NA	NA	4	NA	NA	NA	NA	5.55E+08	2.09E+08	4.74E+08	1.73E+08	NA	NA	NA	NA	2.293	1.130	2.204	2.134	-4.066	1.940	6.006	0.00E+00	0.00E+00
712	P07996|TSP1	20	NA	5.01	NA	NA	NA	5.01	NA	NA	NA	NA	4	NA	NA	NA	NA	2.24E+09	2.13E+09	4.20E+09	1.66E+09	NA	NA	NA	NA	4.370	4.736	5.514	5.416	-4.066	5.009	9.075	0.00E+00	0.00E+00
713	P08253|MMP2	8	NA	2.53	NA	NA	NA	2.53	NA	NA	NA	NA	4	NA	NA	NA	NA	7.39E+08	3.76E+08	8.35E+08	1.96E+08	NA	NA	NA	NA	2.718	2.039	3.063	2.313	-4.066	2.533	6.599	0.00E+00	0.00E+00
714	P08572|CD4A2	12	NA	1.40	NA	NA	NA	1.40	NA	NA	NA	NA	4	NA	NA	NA	NA	2.00E+08	3.03E+08	2.70E+08	1.36E+08	NA	NA	NA	NA	0.767	1.702	1.354	1.778	-4.066	1.401	5.467	0.00E+00	0.00E+00
715	P08648|ITA5	7	NA	0.47	NA	NA	NA	0.47	NA	NA	NA	NA	4	NA	NA	NA	NA	1.69E+08	1.41E+08	1.43E+08	5.37E+07	NA	NA	NA	NA	0.519	0.519	0.389	0.434	-4.066	0.465	4.531	0.00E+00	0.00E+00
716	P08865|RSSA	2	NA	-2.92	NA	NA	NA	-2.92	NA	NA	NA	NA	4	NA	NA	NA	NA	1.39E+07	8.54E+06	2.91E+07	6.65E+06	NA	NA	NA	NA	-3.202	-3.844	-2.027	-2.601	-4.066	-2.918	1.148	0.00E+00	0.00E+00
717	P10321|1C07	5	NA	-0.23	NA	NA	NA	-0.23	NA	NA	NA	NA	4	NA	NA	NA	NA	1.03E+08	6.16E+07	1.15E+08	4.05E+07	NA	NA	NA	NA	-0.224	-0.773	0.056	0.022	-4.066	-0.230	3.836	0.00E+00	0.00E+00
718	P10644|KAP0	2	NA	-3.31	NA	NA	NA	-3.31	NA	NA	NA	NA	4	NA	NA	NA	NA	1.52E+07	5.19E+06	1.36E+07	7.86E+06	NA	NA	NA	NA	-3.069	-4.618	-3.184	-2.359	-4.066	-3.308	0.759	0.00E+00	0.00E+00
719	P11047|LAMC1	23	NA	4.30	NA	NA	NA	4.30	NA	NA	NA	NA	4	NA	NA	NA	NA	2.28E+09	1.58E+09	2.00E+09	6.96E+08	NA	NA	NA	NA	4.401	4.272	4.391	4.156	-4.066	4.305	8.371	0.00E+00	0.00E+00
720	P12643|BMP2	2	NA	-3.41	NA	NA	NA	-3.41	NA	NA	NA	NA	4	NA	NA	NA	NA	1.68E+07	1.72E+07	7.60E+06	2.74E+06	NA	NA	NA	NA	-2.923	-2.753	-4.064	-3.893	-4.066	-3.408	0.658	0.00E+00	0.00E+00
721	P13489|RINI	3	NA	0.08	NA	NA	NA	0.08	NA	NA	NA	NA	4	NA	NA	NA	NA	9.68E+07	9.39E+07	1.19E+08	6.15E+07	NA	NA	NA	NA	-0.311	-0.117	0.115	0.630	-4.066	0.079	4.146	0.00E+00	0.00E+00
722	P13639|EF2	5	NA	-0.85	NA	NA	NA	-0.85	NA	NA	NA	NA	4	NA	NA	NA	NA	5.78E+07	5.71E+07	7.53E+07	2.22E+07	NA	NA	NA	NA	-1.079	-0.890	-0.585	-0.851	-4.066	-0.851	3.215	0.00E+00	0.00E+00
723	P14209|CD99	2	NA	-1.38	NA	NA	NA	-1.38	NA	NA	NA	NA	4	NA	NA	NA	NA	3.80E+07	2.84E+07	4.83E+07	2.66E+07	NA	NA	NA	NA	-1.705	-1.976	-1.258	-0.590	-4.066	-1.382	2.684	0.00E+00	0.00E+00
724	P14543|NID1	16	NA	2.16	NA	NA	NA	2.16	NA	NA	NA	NA	4	NA	NA	NA	NA	6.88E+08	3.08E+08	4.97E+08	1.61E+08	NA	NA	NA	NA	2.612	1.729	2.277	2.025	-4.066	2.161	6.227	0.00E+00	0.00E+00
725	P14625|ENPL	4	NA	-3.40	NA	NA	NA	-3.40	NA	NA	NA	NA	4	NA	NA	NA	NA	1.46E+07	5.09E+06	1.25E+07	7.05E+06	NA	NA	NA	NA	-3.130	-4.647	-3.308	-2.518	-4.066	-3.401	0.665	0.00E+00	0.00E+00
726	P14866|HNRPL	5	NA	-1.27	NA	NA	NA	-1.27	NA	NA	NA	NA	4	NA	NA	NA	NA	7.80E+07	7.92E+07	3.14E+07	9.01E+06	NA	NA	NA	NA	-0.633	-0.381	-1.913	-2.162	-4.066	-1.272	2.794	0.00E+00	0.00E+00
727	P15144|AMPN	3	NA	-2.40	NA	NA	NA	-2.40	NA	NA	NA	NA	4	NA	NA	NA	NA	4.84E+07	1.76E+07	2.78E+07	3.76E+06	NA	NA	NA	NA	-1.346	-2.720	-2.094	-3.432	-4.066	-2.398	1.668	0.00E+00	0.00E+00
728	P15311|EZRI	6	NA	-2.41	NA	NA	NA	-2.41	NA	NA	NA	NA	4	NA	NA	NA	NA	3.20E+07	2.84E+07	1.55E+07	6.14E+06	NA	NA	NA	NA	-1.960	-1.975	-2.981	-2.719	-4.066	-2.409	1.657	0.00E+00	0.00E+00
729	P16870|CBPE	7	NA	-1.17	NA	NA	NA	-1.17	NA	NA	NA	NA	4	NA	NA	NA	NA	1.04E+08	5.44E+07	5.03E+07	8.10E+06	NA	NA	NA	NA	-0.201	-0.966	-1.198	-2.315	-4.066	-1.170	2.896	0.00E+00	0.00E+00
730	P17813|EGLN	5	NA	1.90	NA	NA	NA	1.90	NA	NA	NA	NA	4	NA	NA	NA	NA	5.11E+08	3.83E+08	5.08E+08	8.18E+07	NA	NA	NA	NA	2.169	2.069	2.310	1.045	-4.066	1.898	5.964	0.00E+00	0.00E+00
731	P19105|ML12A	7	NA	-1.18	NA	NA	NA	-1.18	NA	NA	NA	NA	4	NA	NA	NA	NA	8.80E+07	4.98E+07	4.71E+07	1.11E+07	NA	NA	NA	NA	-0.453	-1.102	-1.296	-1.855	-4.066	-1.176	2.890	0.00E+00	0.00E+00
732	P20700|LMNB1	7	NA	-1.86	NA	NA	NA	-1.86	NA	NA	NA	NA	4	NA	NA	NA	NA	6.18E+07	2.22E+07	3.21E+07	8.54E+06	NA	NA	NA	NA	-0.980	-2.361	-1.877	-2.239	-4.066	-1.865	2.202	0.00E+00	0.00E+00
733	P21980|TGM2	5	NA	0.48	NA	NA	NA	0.48	NA	NA	NA	NA	4	NA	NA	NA	NA	1.87E+08	1.76E+08	2.26E+08	2.46E+07	NA	NA	NA	NA	0.669	0.860	1.079	-0.699	-4.066	0.477	4.543	0.00E+00	0.00E+00
734	P22392|NDKB	2	NA	-1.36	NA	NA	NA	-1.36	NA	NA	NA	NA	4	NA	NA	NA	NA	5.00E+07	3.09E+07	3.33E+07	2.90E+07	NA	NA	NA	NA	-1.296	-1.845	-1.823	-0.462	-4.066	-1.356	2.710	0.00E+00	0.00E+00
735	P26038|MOES	13	NA	1.11	NA	NA	NA	1.11	NA	NA	NA	NA	4	NA	NA	NA	NA	2.34E+08	2.38E+08	1.75E+08	1.04E+08	NA	NA	NA	NA	1.007	1.327	0.693	1.397	-4.066	1.106	5.172	0.00E+00	0.00E+00
736	P27658|CO8A1	3	NA	0.89	NA	NA	NA	0.89	NA	NA	NA	NA	4	NA	NA	NA	NA	1.90E+08	1.65E+08	1.86E+08	9.94E+07	NA	NA	NA	NA	0.691	0.759	0.790	1.327	-4.066	0.892	4.958	0.00E+00	0.00E+00
737	P28799|GRN	2	NA	-0.37	NA	NA	NA	-0.37	NA	NA	NA	NA	4	NA	NA	NA	NA	8.04E+07	7.14E+07	8.21E+07	4.34E+07	NA	NA	NA	NA	-0.588	-0.542	-0.453	0.123	-4.066	-0.365	3.701	0.00E+00	0.00E+00
738	P29279|CCN2	3	NA	4.51	NA	NA	NA	4.51	NA	NA	NA	NA	4	NA	NA	NA	NA	2.29E+09	2.78E+09	2.09E+09	6.38E+08	NA	NA	NA	NA	4.405	5.146	4.455	4.029	-4.066	4.509	8.575	0.00E+00	0.00E+00
739	P29692|EF1D	6	NA	-1.07	NA	NA	NA	-1.07	NA	NA	NA	NA	4	NA	NA	NA	NA	5.31E+07	5.48E+07	8.99E+07	1.15E+07	NA	NA	NA	NA	-1.206	-0.954	-0.316	-1.811	-4.066	-1.072	2.995	0.00E+00	0.00E+00
740	P29966|MARCS	8	NA	0.57	NA	NA	NA	0.57	NA	NA	NA	NA	4	NA	NA	NA	NA	8.01E+07	1.54E+08	1.82E+08	1.10E+08	NA	NA	NA	NA	-0.594	0.647	0.752	1.475	-4.066	0.570	4.636	0.00E+00	0.00E+00
741	P30626|SORCN	4	NA	-0.15	NA	NA	NA	-0.15	NA	NA	NA	NA	4	NA	NA	NA	NA	1.10E+08	7.99E+07	9.07E+07	4.51E+07	NA	NA	NA	NA	-0.121	-0.368	-0.303	0.178	-4.066	-0.153	3.913	0.00E+00	0.00E+00
742	P31949|S10AB	2	NA	0.86	NA	NA	NA	0.86	NA	NA	NA	NA	4	NA	NA	NA	NA	3.15E+08	3.09E+08	5.83E+07	9.24E+07	NA	NA	NA	NA	1.447	1.732	-0.973	1.222	-4.066	0.857	4.923	0.00E+00	0.00E+00
743	P33316|DUT	2	NA	-3.08	NA	NA	NA	-3.08	NA	NA	NA	NA	4	NA	NA	NA	NA	1.81E+07	1.66E+07	1.26E+07	3.78E+06	NA	NA	NA	NA	-2.808	-2.814	-3.293	-3.424	-4.066	-3.085	0.981	0.00E+00	0.00E+00
744	P35052|GPC1	3	NA	-2.27	NA	NA	NA	-2.27	NA	NA	NA	NA	4	NA	NA	NA	NA	4.99E+07	5.10E+07	4.20E+07	1.07E+06	NA	NA	NA	NA	-1.301	-1.068	-1.471	-5.257	-4.066	-2.274	1.792	0.00E+00	0.00E+00
745	P35555|FBN1	5	NA	-1.71	NA	NA	NA	-1.71	NA	NA	NA	NA	4	NA	NA	NA	NA	4.48E+07	3.71E+07	3.92E+07	8.46E+06	NA	NA	NA	NA	-1.460	-1.563	-1.577	-2.253	-4.066	-1.713	2.353	0.00E+00	0.00E+00
746	P35556|FBN2	6	NA	0.95	NA	NA	NA	0.95	NA	NA	NA	NA	4	NA	NA	NA	NA	1.89E+08	1.39E+08	2.36E+08	1.08E+08	NA	NA	NA	NA	0.685	0.496	1.147	1.453	-4.066	0.945	5.011	0.00E+00	0.00E+00
747	P35579|MYH9	12	NA	-0.85	NA	NA	NA	-0.85	NA	NA	NA	NA	4	NA	NA	NA	NA	5.74E+07	7.20E+07	8.97E+07	1.47E+07	NA	NA	NA	NA	-1.089	-0.530	-0.320	-1.445	-4.066	-0.846	3.220	0.00E+00	0.00E+00
748	P35590|TIE1	4	NA	-0.23	NA	NA	NA	-0.23	NA	NA	NA	NA	4	NA	NA	NA	NA	1.53E+08	8.04E+07	1.12E+08	2.10E+07	NA	NA	NA	NA	0.374	-0.358	0.011	-0.931	-4.066	-0.226	3.840	0.00E+00	0.00E+00
749	P39019|RS19	2	NA	-2.31	NA	NA	NA	-2.31	NA	NA	NA	NA	4	NA	NA	NA	NA	2.20E+07	2.38E+07	1.90E+07	1.16E+07	NA	NA	NA	NA	-2.519	-2.251	-2.675	-1.789	-4.066	-2.309	1.757	0.00E+00	0.00E+00
750	P39060|COIA1	10	NA	1.90	NA	NA	NA	1.90	NA	NA	NA	NA	4	NA	NA	NA	NA	5.32E+08	3.65E+08	4.97E+08	8.56E+07	NA	NA	NA	NA	2.230	1.992	2.277	1.110	-4.066	1.902	5.968	0.00E+00	0.00E+00
751	P41250|GARS	2	NA	-1.33	NA	NA	NA	-1.33	NA	NA	NA	NA	4	NA	NA	NA	NA	3.95E+07	4.02E+07	4.53E+07	2.21E+07	NA	NA	NA	NA	-1.649	-1.438	-1.357	-0.858	-4.066	-1.325	2.741	0.00E+00	0.00E+00
752	P43121|MUC18	11	NA	2.64	NA	NA	NA	2.64	NA	NA	NA	NA	4	NA	NA	NA	NA	5.50E+08	6.92E+08	5.29E+08	2.95E+08	NA	NA	NA	NA	2.278	2.986	2.372	2.909	-4.066	2.636	6.702	0.00E+00	0.00E+00
753	P46940|IQGA1	5	NA	-2.27	NA	NA	NA	-2.27	NA	NA	NA	NA	4	NA	NA	NA	NA	2.32E+07	3.26E+07	3.84E+07	4.16E+06	NA	NA	NA	NA	-2.439	-1.760	-1.605	-3.284	-4.066	-2.272	1.794	0.00E+00	0.00E+00

1	ProteinName	# Peptides	Ctrl	Group1	log2FC	CI.L	CI.R	Ave Expr	t	P.Value	adj.P.Val	B	nrNAs	M.3_Control.raw	M.2_Control.raw	M.4_Control.raw	M.1_Control.raw	E4.2_Group_1.raw	E4.4_Group_1.raw	E4.3_Group_1.raw	E4.1_Group_1.raw	M.3_Control.transf	M.2_Control.transf	M.4_Control.transf	M.1_Control.transf	E4.2_Group_1.transf	E4.4_Group_1.transf	E4.3_Group_1.transf	E4.1_Group_1.transf	pseudo.Ctrl	pseudo.Group1	pseudo.log2FC	pseudo.P.Value	pseudo.adj.P.Val
754	P49802|RGS7	2	NA	-3.72	NA	NA	NA	-3.72	NA	NA	NA	NA	4	NA	NA	NA	NA	8.93E+06	7.30E+06	9.62E+06	4.35E+06	NA	NA	NA	NA	-3.864	-4.088	-3.706	-3.219	-4.066	-3.719	0.347	0.00E+00	0.00E+00
755	P50281|MMP14	2	NA	-0.73	NA	NA	NA	-0.73	NA	NA	NA	NA	4	NA	NA	NA	NA	6.52E+07	6.58E+07	6.56E+07	2.72E+07	NA	NA	NA	NA	-0.899	-0.669	-0.795	-0.554	-4.066	-0.730	3.337	0.00E+00	0.00E+00
756	P52272|HNRPM	2	NA	-2.99	NA	NA	NA	-2.99	NA	NA	NA	NA	4	NA	NA	NA	NA	7.23E+06	6.06E+06	2.89E+07	1.54E+07	NA	NA	NA	NA	-4.179	-4.375	-2.036	-1.387	-4.066	-2.994	1.072	0.00E+00	0.00E+00
757	P55011|S12A2	2	-1.38	NA	NA	NA	NA	-1.38	NA	NA	NA	NA	4	2.66E+07	9.41E+06	2.43E+07	8.53E+06	NA	NA	NA	NA	-0.914	-1.398	-1.164	-2.026	NA	NA	NA	NA	-1.376	-3.762	-2.387	0.00E+00	0.00E+00
758	P62714|PP2AB	4	NA	-3.18	NA	NA	NA	-3.18	NA	NA	NA	NA	4	NA	NA	NA	NA	2.11E+07	1.19E+07	1.69E+07	2.63E+06	NA	NA	NA	NA	-2.584	-3.331	-2.847	-3.951	-4.066	-3.178	0.888	0.00E+00	0.00E+00
759	P62826|RAN	2	NA	-3.76	NA	NA	NA	-3.76	NA	NA	NA	NA	4	NA	NA	NA	NA	6.26E+06	6.88E+06	1.43E+07	3.98E+06	NA	NA	NA	NA	-4.393	-4.179	-3.109	-3.346	-4.066	-3.757	0.309	0.00E+00	0.00E+00
760	P62873|GBB1	3	NA	-2.85	NA	NA	NA	-2.85	NA	NA	NA	NA	4	NA	NA	NA	NA	2.03E+07	1.57E+07	2.60E+07	3.24E+06	NA	NA	NA	NA	-2.639	-2.901	-2.198	-3.645	-4.066	-2.846	1.220	0.00E+00	0.00E+00
761	P67809|YBOX1	5	NA	-2.55	NA	NA	NA	-2.55	NA	NA	NA	NA	4	NA	NA	NA	NA	2.10E+07	1.42E+07	1.46E+07	1.42E+07	NA	NA	NA	NA	-2.593	-3.051	-3.074	-1.496	-4.066	-2.554	1.513	0.00E+00	0.00E+00
762	P78417|GSTO1	2	NA	-3.52	NA	NA	NA	-3.52	NA	NA	NA	NA	4	NA	NA	NA	NA	3.04E+07	5.93E+06	7.61E+06	3.41E+06	NA	NA	NA	NA	-2.038	-4.411	-4.060	-3.573	-4.066	-3.521	0.546	0.00E+00	0.00E+00
763	P84090|ERH	2	NA	-1.75	NA	NA	NA	-1.75	NA	NA	NA	NA	4	NA	NA	NA	NA	1.06E+07	3.19E+07	4.82E+07	3.15E+07	NA	NA	NA	NA	-3.615	-1.797	-1.261	-0.342	-4.066	-1.754	2.312	0.00E+00	0.00E+00
764	P98082|DAB2	5	NA	-2.51	NA	NA	NA	-2.51	NA	NA	NA	NA	4	NA	NA	NA	NA	2.87E+07	1.18E+07	2.42E+07	8.38E+06	NA	NA	NA	NA	-2.125	-3.345	-2.308	-2.267	-4.066	-2.511	1.555	0.00E+00	0.00E+00
765	P98179|RBM3	2	NA	-1.46	NA	NA	NA	-1.46	NA	NA	NA	NA	4	NA	NA	NA	NA	6.55E+07	4.40E+07	2.63E+07	1.45E+07	NA	NA	NA	NA	-0.894	-1.297	-2.183	-1.471	-4.066	-1.461	2.605	0.00E+00	0.00E+00
766	Q01638|ILRL1	3	NA	1.55	NA	NA	NA	1.55	NA	NA	NA	NA	4	NA	NA	NA	NA	3.38E+08	2.81E+08	3.33E+08	1.05E+08	NA	NA	NA	NA	1.552	1.588	1.669	1.411	-4.066	1.555	5.621	0.00E+00	0.00E+00
767	Q03252|LMNB2	4	NA	-2.59	NA	NA	NA	-2.59	NA	NA	NA	NA	4	NA	NA	NA	NA	1.96E+07	1.94E+07	1.53E+07	9.41E+06	NA	NA	NA	NA	-2.692	-2.568	-2.937	-2.098	-4.066	-2.589	1.477	0.00E+00	0.00E+00
768	Q08629|TICN1	5	NA	-0.50	NA	NA	NA	-0.50	NA	NA	NA	NA	4	NA	NA	NA	NA	7.70E+07	1.16E+08	4.64E+07	3.38E+07	NA	NA	NA	NA	-0.653	0.204	-1.321	-0.240	-4.066	-0.502	3.564	0.00E+00	0.00E+00
769	Q08752|PPID	3	NA	-2.10	NA	NA	NA	-2.10	NA	NA	NA	NA	4	NA	NA	NA	NA	4.64E+07	3.99E+07	1.38E+07	7.77E+06	NA	NA	NA	NA	-1.409	-1.447	-3.160	-2.376	-4.066	-2.098	1.968	0.00E+00	0.00E+00
770	Q12805|FBLN3	3	NA	-0.98	NA	NA	NA	-0.98	NA	NA	NA	NA	4	NA	NA	NA	NA	5.17E+07	3.51E+07	7.62E+07	2.90E+07	NA	NA	NA	NA	-1.248	-1.646	-0.566	-0.465	-4.066	-0.981	3.085	0.00E+00	0.00E+00
771	Q12906|ILF3	4	NA	-1.53	NA	NA	NA	-1.53	NA	NA	NA	NA	4	NA	NA	NA	NA	3.07E+07	2.85E+07	3.29E+07	3.32E+07	NA	NA	NA	NA	-2.023	-1.973	-1.842	-0.267	-4.066	-1.526	2.540	0.00E+00	0.00E+00
772	Q13263|TIF1B	5	NA	-0.01	NA	NA	NA	-0.01	NA	NA	NA	NA	4	NA	NA	NA	NA	9.02E+07	9.38E+07	1.18E+08	5.19E+07	NA	NA	NA	NA	-0.416	-0.118	0.092	0.384	-4.066	-0.015	4.051	0.00E+00	0.00E+00
773	Q13435|SF3B2	4	NA	-2.20	NA	NA	NA	-2.20	NA	NA	NA	NA	4	NA	NA	NA	NA	3.71E+07	2.04E+07	3.25E+07	6.27E+06	NA	NA	NA	NA	-1.742	-2.492	-1.860	-2.688	-4.066	-2.196	1.871	0.00E+00	0.00E+00
774	Q13444|ADA15	6	NA	1.11	NA	NA	NA	1.11	NA	NA	NA	NA	4	NA	NA	NA	NA	2.73E+08	2.04E+08	2.07E+08	8.98E+07	NA	NA	NA	NA	1.234	1.086	0.947	1.181	-4.066	1.112	5.178	0.00E+00	0.00E+00
775	Q13740|CD166	6	NA	-0.21	NA	NA	NA	-0.21	NA	NA	NA	NA	4	NA	NA	NA	NA	1.57E+08	1.75E+08	9.76E+07	1.07E+07	NA	NA	NA	NA	0.412	0.847	-0.191	-1.906	-4.066	-0.210	3.856	0.00E+00	0.00E+00
776	Q13753|LAMC2	18	NA	1.28	NA	NA	NA	1.28	NA	NA	NA	NA	4	NA	NA	NA	NA	3.31E+08	2.55E+08	2.50E+08	7.46E+07	NA	NA	NA	NA	1.522	1.437	1.237	0.912	-4.066	1.277	5.343	0.00E+00	0.00E+00
777	Q14767|LTBP2	9	NA	3.31	NA	NA	NA	3.31	NA	NA	NA	NA	4	NA	NA	NA	NA	1.08E+09	7.84E+08	8.24E+08	5.13E+08	NA	NA	NA	NA	3.291	3.181	3.044	3.712	-4.066	3.307	7.373	0.00E+00	0.00E+00
778	Q15075|EEA1	2	NA	-3.12	NA	NA	NA	-3.12	NA	NA	NA	NA	4	NA	NA	NA	NA	7.54E+06	2.84E+07	2.67E+07	2.17E+06	NA	NA	NA	NA	-4.117	-1.977	-2.155	-4.229	-4.066	-3.119	0.947	0.00E+00	0.00E+00
779	Q15942|ZYX	9	NA	1.48	NA	NA	NA	1.48	NA	NA	NA	NA	4	NA	NA	NA	NA	2.58E+08	2.55E+08	3.02E+08	1.40E+08	NA	NA	NA	NA	1.153	1.437	1.523	1.824	-4.066	1.484	5.551	0.00E+00	0.00E+00
780	Q16363|LAMA4	2	NA	-2.82	NA	NA	NA	-2.82	NA	NA	NA	NA	4	NA	NA	NA	NA	1.37E+07	3.30E+07	2.78E+07	2.16E+06	NA	NA	NA	NA	-3.222	-1.741	-2.099	-4.233	-4.066	-2.824	1.242	0.00E+00	0.00E+00
781	Q16543|CDC37	2	NA	-2.48	NA	NA	NA	-2.48	NA	NA	NA	NA	4	NA	NA	NA	NA	1.81E+07	2.20E+07	1.60E+07	1.14E+07	NA	NA	NA	NA	-2.813	-2.375	-2.932	-1.813	-4.066	-2.483	1.583	0.00E+00	0.00E+00
782	Q16610|ECM1	8	NA	-1.00	NA	NA	NA	-1.00	NA	NA	NA	NA	4	NA	NA	NA	NA	3.61E+07	3.56E+07	8.45E+07	3.53E+07	NA	NA	NA	NA	-1.781	-1.624	-0.411	-0.177	-4.066	-0.998	3.068	0.00E+00	0.00E+00
783	Q16658|FSCN1	6	NA	-0.12	NA	NA	NA	-0.12	NA	NA	NA	NA	4	NA	NA	NA	NA	7.02E+07	8.34E+07	1.21E+08	5.60E+07	NA	NA	NA	NA	-0.790	-0.301	0.134	0.494	-4.066	-0.116	3.950	0.00E+00	0.00E+00
784	Q6N212|CAVN1	4	NA	1.51	NA	NA	NA	1.51	NA	NA	NA	NA	4	NA	NA	NA	NA	3.51E+08	3.91E+08	3.34E+08	6.22E+07	NA	NA	NA	NA	1.609	2.101	1.674	0.646	-4.066	1.508	5.574	0.00E+00	0.00E+00
785	Q727G0|TARSH	8	NA	0.62	NA	NA	NA	0.62	NA	NA	NA	NA	4	NA	NA	NA	NA	1.64E+08	1.51E+08	1.48E+08	7.67E+07	NA	NA	NA	NA	0.473	0.617	0.438	0.951	-4.066	0.620	4.686	0.00E+00	0.00E+00
786	Q86UD1|DAF	3	NA	-1.16	NA	NA	NA	-1.16	NA	NA	NA	NA	4	NA	NA	NA	NA	6.77E+07	3.76E+07	3.44E+07	2.89E+07	NA	NA	NA	NA	-0.845	-1.540	-1.774	-0.468	-4.066	-1.157	2.909	0.00E+00	0.00E+00
787	Q8IVF2|AHNK2	5	NA	-2.79	NA	NA	NA	-2.79	NA	NA	NA	NA	4	NA	NA	NA	NA	1.76E+07	1.61E+07	1.06E+07	1.08E+07	NA	NA	NA	NA	-2.849	-2.862	-3.557	-1.904	-4.066	-2.793	1.273	0.00E+00	0.00E+00
788	Q8IWU6|SULF1	3	NA	-3.38	NA	NA	NA	-3.38	NA	NA	NA	NA	4	NA	NA	NA	NA	1.13E+07	2.16E+07	3.89E+06	7.02E+06	NA	NA	NA	NA	-3.515	-2.399	-5.077	-2.524	-4.066	-3.379	0.687	0.00E+00	0.00E+00
789	Q8N0X7|SPART	2	NA	-1.60	NA	NA	NA	-1.60	NA	NA	NA	NA	4	NA	NA	NA	NA	2.76E+07	4.52E+07	3.04E+07	1.97E+07	NA	NA	NA	NA	-2.180	-1.253	-1.963	-1.023	-4.066	-1.605	2.461	0.00E+00	0.00E+00
790	Q8NBJ4|GOLM1	5	NA	-0.41	NA	NA	NA	-0.41	NA	NA	NA	NA	4	NA	NA	NA	NA	4.06E+07	7.81E+07	1.15E+08	4.94E+07	NA	NA	NA	NA	-1.607	-0.404	0.061	0.313	-4.066	-0.409	3.657	0.00E+00	0.00E+00
791	Q8WZ75|ROBO4	7	NA	1.98	NA	NA	NA	1.98	NA	NA	NA	NA	4	NA	NA	NA	NA	5.09E+08	4.04E+08	2.85E+08	1.78E+08	NA	NA	NA	NA	2.163	2.151	1.435	2.174	-4.066	1.981	6.047	0.00E+00	0.00E+00
792	Q92520|FAM3C	3	NA	-1.97	NA	NA	NA	-1.97	NA	NA	NA	NA	4	NA	NA	NA	NA	4.12E+07	1.85E+07	4.57E+07	8.02E+06	NA	NA	NA	NA	-1.585	-2.642	-1.341	-2.330	-4.066	-1.974	2.092	0.00E+00	0.00E+00
793	Q92626|PXDN	6	NA	0.88	NA	NA	NA	0.88	NA	NA	NA	NA	4	NA	NA	NA	NA	1.54E+08	1.39E+08	1.99E+08	1.32E+08	NA	NA	NA	NA	0.380	0.488	0.892	1.742	-4.066	0.875	4.942	0.00E+00	0.00E+00
794	Q92743|HTRA1	3	NA	-2.76	NA	NA	NA	-2.76	NA	NA	NA	NA	4	NA	NA	NA	NA	1.25E+07	7.99E+06	2.93E+07	1.22E+07	NA	NA	NA	NA	-3.368	-3.947	-2.019	-1.715	-4.066	-2.762	1.304	0.00E+00	0.00E+00
795	Q96AP7|ESAM	2	NA	-1.72	NA	NA	NA	-1.72	NA	NA	NA	NA	4	NA	NA	NA	NA	3.42E+07	3.78E+07	4.01E+07	1.04E+07	NA	NA	NA	NA	-1.861	-1.530	-1.541	-1.957	-4.066	-1.722	2.344	0.00E+00	0.00E+00
796	Q96FQ6|S10AG	2	NA	0.12	NA	NA	NA	0.12	NA	NA	NA	NA	4	NA	NA	NA	NA	1.47E+08	8.89E+07	1.06E+08	5.46E+07	NA	NA	NA	NA	0.310	-0.202	-0.068	0.458	-4.066	0.125	4.191	0.00E+00	0.00E+00
797	Q96JQ0|PCD16	4	NA	-3.02	NA	NA	NA	-3.02	NA	NA	NA	NA	4	NA	NA	NA	NA	1.00E+07	7.29E+06	3.31E+07	7.27E+06	NA	NA	NA	NA	-3.688	-4.090	-1.830	-2.473	-4.066	-3.020	1.046	0.00E+00	0.00E+00
798	Q99880|H2B1L	4	NA	0.79	NA	NA	NA	0.79	NA	NA	NA	NA	4	NA	NA	NA	NA	3.42E+08	5.02E+08	6.61E+07	3.64E+07	NA	NA	NA	NA	1.570	2.488	-0.783	-0.131	-4.066	0.786	4.852	0.00E+00	0.00E+00
799	Q99988|GDF15	7	NA	1.55	NA	NA	NA	1.55	NA	NA	NA	NA	4	NA	NA	NA	NA	3.19E+08	3.09E+08	3.56E+08	9.22E+07	NA	NA	NA	NA	1.466	1.736	1.769	1.219	-4.066	1.547	5.614	0.00E+00	0.00E+00
800	Q9BQT9|CSTN3	2	NA	-3.93	NA	NA	NA	-3.93	NA	NA	NA	NA	4	NA	NA	NA	NA	3.82E+06	3.70E+06	2.44E+07	4.51E+06	NA	NA	NA	NA	-5.129	-5.141	-2.296	-3.166	-4.066	-3.933	0.133	0.00E+00	0.00E+00

1	ProteinName	# Peptides	Ctrl	Group1	log2FC	CI.L	CI.R	Average Expr	t	P.Value	adj.P.Val	B	nrNAs	M.3_Control.raw	M.2_Control.raw	M.4_Control.raw	M.1_Control.raw	E4.2_Group_1.raw	E4.4_Group_1.raw	E4.3_Group_1.raw	E4.1_Group_1.raw	M.3_Control.transf	M.2_Control.transf	M.4_Control.transf	M.1_Control.transf	E4.2_Group_1.transf	E4.4_Group_1.transf	E4.3_Group_1.transf	E4.1_Group_1.transf	pseudo.Ctrl	pseudo.Group1	pseudo.log2FC	pseudo.P.Value	pseudo.adj.P.Val
801	Q9H4M9|EHD1	2	NA	-2.05	NA	NA	NA	-2.05	NA	NA	NA	NA	4	NA	NA	NA	NA	3.32E+07	3.84E+07	3.39E+07	5.02E+06	NA	NA	NA	NA	-1.905	-1.507	-1.794	-3.011	-4.066	-2.054	2.012	0.00E+00	0.00E+00
802	Q9H8L6|MMRN2	7	NA	-0.24	NA	NA	NA	-0.24	NA	NA	NA	NA	4	NA	NA	NA	NA	1.64E+08	6.92E+07	1.84E+08	1.31E+07	NA	NA	NA	NA	0.476	-0.592	0.774	-1.613	-4.066	-0.239	3.827	0.00E+00	0.00E+00
803	Q9HB63|NET4	2	NA	-3.10	NA	NA	NA	-3.10	NA	NA	NA	NA	4	NA	NA	NA	NA	2.30E+07	1.35E+07	8.51E+06	5.40E+06	NA	NA	NA	NA	-2.456	-3.135	-3.892	-2.904	-4.066	-3.097	0.970	0.00E+00	0.00E+00
804	Q9P2E7|PCD10	4	NA	-3.17	NA	NA	NA	-3.17	NA	NA	NA	NA	4	NA	NA	NA	NA	1.11E+07	1.27E+07	1.28E+07	6.38E+06	NA	NA	NA	NA	-3.541	-3.224	-3.271	-2.662	-4.066	-3.175	0.892	0.00E+00	0.00E+00
805	Q9P2E9|RRBP1	13	NA	-0.72	NA	NA	NA	-0.72	NA	NA	NA	NA	4	NA	NA	NA	NA	5.93E+07	5.71E+07	1.36E+08	1.67E+07	NA	NA	NA	NA	-1.041	-0.889	0.313	-1.266	-4.066	-0.721	3.345	0.00E+00	0.00E+00
806	Q9UBR2|CAT2	2	NA	-2.26	NA	NA	NA	-2.26	NA	NA	NA	NA	4	NA	NA	NA	NA	3.17E+07	2.67E+07	2.36E+07	6.43E+06	NA	NA	NA	NA	-1.978	-2.072	-2.346	-2.652	-4.066	-2.262	1.804	0.00E+00	0.00E+00
807	Q9UJJ9|GNPTG	3	NA	-1.86	NA	NA	NA	-1.86	NA	NA	NA	NA	4	NA	NA	NA	NA	3.78E+07	3.57E+07	3.96E+07	6.95E+06	NA	NA	NA	NA	-1.714	-1.619	-1.558	-2.539	-4.066	-1.858	2.209	0.00E+00	0.00E+00
808	Q9UMY4|SNX12	2	NA	-0.72	NA	NA	NA	-0.72	NA	NA	NA	NA	4	NA	NA	NA	NA	5.77E+07	5.25E+07	6.77E+07	3.86E+07	NA	NA	NA	NA	-1.082	-1.020	-0.746	-0.046	-4.066	-0.723	3.343	0.00E+00	0.00E+00
809	Q9UNN8|EPCR	4	NA	2.35	NA	NA	NA	2.35	NA	NA	NA	NA	4	NA	NA	NA	NA	7.18E+08	5.35E+08	4.38E+08	1.63E+08	NA	NA	NA	NA	2.677	2.587	2.087	2.049	-4.066	2.350	6.416	0.00E+00	0.00E+00
810	Q9UPN3|MACF1	7	NA	-2.17	NA	NA	NA	-2.17	NA	NA	NA	NA	4	NA	NA	NA	NA	3.17E+07	1.31E+07	2.59E+07	1.62E+07	NA	NA	NA	NA	-1.976	-3.177	-2.201	-1.312	-4.066	-2.166	1.900	0.00E+00	0.00E+00
811	Q9UQ80|PA2G4	5	NA	-2.44	NA	NA	NA	-2.44	NA	NA	NA	NA	4	NA	NA	NA	NA	2.65E+07	3.86E+07	1.48E+07	5.22E+06	NA	NA	NA	NA	-2.242	-1.499	-3.050	-2.954	-4.066	-2.436	1.630	0.00E+00	0.00E+00
812	Q9Y4K0|LOXL2	10	NA	3.67	NA	NA	NA	3.67	NA	NA	NA	NA	4	NA	NA	NA	NA	1.37E+09	1.13E+09	1.20E+09	4.97E+08	NA	NA	NA	NA	3.635	3.754	3.613	3.667	-4.066	3.667	7.733	0.00E+00	0.00E+00
813	Q9Y624|JAM1	2	NA	-1.55	NA	NA	NA	-1.55	NA	NA	NA	NA	4	NA	NA	NA	NA	5.46E+07	3.68E+07	3.66E+07	1.18E+07	NA	NA	NA	NA	-1.166	-1.574	-1.681	-1.768	-4.066	-1.547	2.519	0.00E+00	0.00E+00
814	zz|Y-FGC2Cont00027|	2	NA	4.42	NA	NA	NA	4.42	NA	NA	NA	NA	4	NA	NA	NA	NA	1.80E+09	2.05E+09	1.36E+09	1.37E+09	NA	NA	NA	NA	4.044	4.673	3.804	5.139	-4.066	4.415	8.481	0.00E+00	0.00E+00
815	zz|Y-FGC2Cont00222|	7	NA	-1.89	NA	NA	NA	-1.89	NA	NA	NA	NA	4	NA	NA	NA	NA	4.23E+07	1.68E+07	3.73E+07	1.35E+07	NA	NA	NA	NA	-1.546	-2.792	-1.650	-1.576	-4.066	-1.891	2.175	0.00E+00	0.00E+00
816	zz|Y-FGC2Cont00230|	6	NA	-3.08	NA	NA	NA	-3.08	NA	NA	NA	NA	4	NA	NA	NA	NA	1.51E+07	1.19E+07	1.56E+07	5.33E+06	NA	NA	NA	NA	-3.079	-3.326	-2.976	-2.924	-4.066	-3.076	0.990	0.00E+00	0.00E+00
817	zz|Y-FGC2Cont00333|	4	NA	-3.98	NA	NA	NA	-3.98	NA	NA	NA	NA	4	NA	NA	NA	NA	5.66E+06	1.27E+07	6.85E+06	2.72E+06	NA	NA	NA	NA	-4.544	-3.233	-4.222	-3.902	-4.066	-3.975	0.091	0.00E+00	0.00E+00
818	zz|Y-FGC2Cont00454|	2	NA	0.77	NA	NA	NA	0.77	NA	NA	NA	NA	4	NA	NA	NA	NA	1.59E+08	1.27E+08	1.86E+08	1.15E+08	NA	NA	NA	NA	0.432	0.349	0.785	1.534	-4.066	0.775	4.841	0.00E+00	0.00E+00

References

Adams, R. H. and K. Alitalo (2007). "Molecular regulation of angiogenesis and lymphangiogenesis." Nature reviews Molecular cell biology **8**(6): 464-478.

Alpert, E., A. Gruzman, Y. Riahi, R. Blejter, P. Aharoni, G. Weisinger, J. Eckel, N. Kaiser and S. Sasson (2005). "Delayed autoregulation of glucose transport in vascular endothelial cells." Diabetologia **48**(4): 752-755.

Andresen, J., Shafi NI, Bryan RM Jr (2006). "Endothelial influences on cerebrovascular tone." J Appl Physiol **100**: 318-327.

Antohe, F., D. Popov, L. Rădulescu, N. Simionescu, T. Börchers, F. Spener and M. Simionescu (1998). "Heart microvessels and aortic endothelial cells express the 15 kDa heart-type fatty acid-binding proteins." European journal of cell biology **76**(2): 102-109.

Arsic, N., S. Zacchigna, L. Zentilin, G. Ramirez-Correa, L. Pattarini, A. Salvi, G. Sinagra and M. Giacca (2004). "Vascular endothelial growth factor stimulates skeletal muscle regeneration in vivo." Molecular Therapy **10**(5): 844-854.

Banks, A. S., J. Y. Kim-Muller, T. L. Mastracci, N. M. Kofler, L. Qiang, R. A. Haeusler, M. J. Jurczak, D. Laznik, G. Heinrich and V. T. Samuel (2011). "Dissociation of the glucose and lipid regulatory functions of FoxO1 by targeted knockin of acetylation-defective alleles in mice." Cell metabolism **14**(5): 587-597.

Barbato, D. L., G. Tatulli, K. Aquilano and M. Ciriolo (2013). "FoxO1 controls lysosomal acid lipase in adipocytes: implication of lipophagy during nutrient restriction and metformin treatment." Cell death & disease **4**(10): e861-e861.

Basse, A. L., E. Dalbram, L. Larsson, Z. Gerhart-Hines, J. R. Zierath and J. T. Treebak (2018). "Skeletal muscle insulin sensitivity show circadian rhythmicity which is independent of exercise training status." Frontiers in physiology **9**: 1198.

Bazzoni, G. and E. Dejana (2004). "Endothelial cell-to-cell junctions: molecular organization and role in vascular homeostasis." Physiological reviews **84**(3): 869-901.

Blanco, R. and H. Gerhardt (2013). "VEGF and Notch in tip and stalk cell selection." Cold Spring Harbor perspectives in medicine **3**(1): a006569.

BonDurant, L. D., M. Ameka, M. C. Naber, K. R. Markan, S. O. Idiga, M. R. Acevedo, S. A. Walsh, D. M. Ornitz and M. J. Potthoff (2017). "FGF21 regulates metabolism through adipose-dependent and-independent mechanisms." Cell metabolism **25**(4): 935-944. e934.

Bonnefoy, A., K. Daenens, H. B. Feys, R. De Vos, P. Vandervoort, J. Vermylen, J. Lawler and M. F. Hoylaerts (2006). "Thrombospondin-1 controls vascular platelet recruitment and thrombus adherence in mice by protecting (sub)endothelial VWF from cleavage by ADAMTS13." Blood **107**(3): 955-964.

Bootcov, M. R., A. R. Bauskin, S. M. Valenzuela, A. G. Moore, M. Bansal, X. Y. He, H. P. Zhang, M. Donnellan, S. Mahler, K. Pryor, B. J. Walsh, R. C. Nicholson, W. D. Fairlie, S. B. Por, J. M. Robbins and S. N. Breit (1997). "MIC-1, a novel macrophage inhibitory cytokine, is a divergent member of the TGF-beta superfamily." Proc Natl Acad Sci U S A **94**(21): 11514-11519.

Borselli, C., H. Storrie, F. Benesch-Lee, D. Shvartsman, C. Cezar, J. W. Lichtman, H. H. Vandenburgh and D. J. Mooney (2010). "Functional muscle regeneration with combined delivery of angiogenesis and myogenesis factors." Proceedings of the National Academy of Sciences **107**(8): 3287-3292.

Braet, F. and E. Wisse (2002). "Structural and functional aspects of liver sinusoidal endothelial cell fenestrae: a review." Comparative hepatology **1**(1): 1-17.
Bryan, B. A., T. E. Walshe, D. C. Mitchell, J. S. Havumaki, M. Saint-Geniez, A. S. Maharaj, A. E. Maldonado and P. A. D'Amore (2008). "Coordinated vascular endothelial growth factor expression and signaling during skeletal myogenic differentiation." Molecular biology of the cell **19**(3): 994-1006.
Buckley, P., S. Dickson and W. Walker (1985). "Human splenic sinusoidal lining cells express antigens associated with monocytes, macrophages, endothelial cells, and T lymphocytes." The Journal of Immunology **134**(4): 2310-2315.
Burghoff, S. and J. Schrader (2011). "Secretome of human endothelial cells under shear stress." J Proteome Res **10**(3): 1160-1169.
Butler, J. M., D. J. Nolan, E. L. Vertes, B. Varnum-Finney, H. Kobayashi, A. T. Hooper, M. Seandel, K. Shido, I. A. White and M. Kobayashi (2010). "Endothelial cells are essential for the self-renewal and repopulation of Notch-dependent hematopoietic stem cells." Cell stem cell **6**(3): 251-264.
Cantelmo, A. R., L.-C. Conradi, A. Brajic, J. Goveia, J. Kalucka, A. Pircher, P. Chaturvedi, J. Hol, B. Thienpont and L.-A. Teuwen (2016). "Inhibition of the glycolytic activator PFKFB3 in endothelium induces tumor vessel normalization, impairs metastasis, and improves chemotherapy." Cancer cell **30**(6): 968-985.
Carmeliet, P. and R. K. Jain (2011). "Molecular mechanisms and clinical applications of angiogenesis." Nature **473**(7347): 298-307.
Ceddia, R., R. Somwar, A. Maida, X. Fang, G. Bikopoulos and G. Sweeney (2005). "Globular adiponectin increases GLUT4 translocation and glucose uptake but reduces glycogen synthesis in rat skeletal muscle cells." Diabetologia **48**(1): 132-139.
Chen, D., Y. Gong, L. Xu, M. Zhou, J. Li and J. Song (2019). "Bidirectional regulation of osteogenic differentiation by the FOXO subfamily of Forkhead transcription factors in mammalian MSCs." Cell proliferation **52**(2): e12540.
Christov, C., F. Chrétien, R. Abou-Khalil, G. Bassez, G. Vallet, F.-J. Authier, Y. Bassaglia, V. Shinin, S. Tajbakhsh and B. Chazaud (2007). "Muscle satellite cells and endothelial cells: close neighbors and privileged partners." Molecular biology of the cell **18**(4): 1397-1409.
Chrysovergis, K., X. Wang, J. Kosak, S.-H. Lee, J. S. Kim, J. F. Foley, G. Travlos, S. Singh, S. J. Baek and T. E. Eling (2014). "NAG-1/GDF-15 prevents obesity by increasing thermogenesis, lipolysis and oxidative metabolism." International journal of obesity **38**(12): 1555-1564.
Chung, H. K., D. Ryu, K. S. Kim, J. Y. Chang, Y. K. Kim, H.-S. Yi, S. G. Kang, M. J. Choi, S. E. Lee and S.-B. Jung (2017). "Growth differentiation factor 15 is a myomitokine governing systemic energy homeostasis." Journal of Cell Biology **216**(1): 149-165.
Claxton, S., V. Kostourou, S. Jadeja, P. Chambon, K. Hodivala-Dilke and M. Fruttiger (2008). "Efficient, inducible Cre-recombinase activation in vascular endothelium." Genesis **46**(2): 74-80.
Clem, B., S. Telang, A. Clem, A. Yalcin, J. Meier, A. Simmons, M. A. Rasku, S. Arumugam, W. L. Dean and J. Eaton (2008). "Small-molecule inhibition of 6-phosphofructo-2-kinase activity suppresses glycolytic flux and tumor growth." Molecular cancer therapeutics **7**(1): 110-120.
Coll, A. P., M. Chen, P. Taskar, D. Rimmington, S. Patel, J. A. Tadross, I. Cimino, M. Yang, P. Welsh, S. Virtue, D. A. Goldspink, E. L. Miedzybrodzka, A. R. Konopka, R. R. Esponda, J. T. Huang, Y. C. L. Tung, S. Rodriguez-Cuenca, R. A. Tomaz, H. P. Harding, A. Melvin, G. S. H. Yeo, D. Preiss, A. Vidal-Puig, L. Vallier, K. S. Nair, N. J. Wareham, D. Ron, F. M. Gribble, F. Reimann, N. Sattar, D. B. Savage, B. B. Allan and

S. O'Rahilly (2020). "GDF15 mediates the effects of metformin on body weight and energy balance." Nature **578**(7795): 444-448.
Cox, J. and M. Mann (2008). "MaxQuant enables high peptide identification rates, individualized p.p.b.-range mass accuracies and proteome-wide protein quantification." Nat Biotechnol **26**(12): 1367-1372.
Cox, J. and M. Mann (2011). "Quantitative, high-resolution proteomics for data-driven systems biology." Annu Rev Biochem **80**: 273-299.
Cox, J., N. Neuhauser, A. Michalski, R. A. Scheltema, J. V. Olsen and M. Mann (2011). "Andromeda: a peptide search engine integrated into the MaxQuant environment." J Proteome Res **10**(4): 1794-1805.
Davis, M. B., Z. Arany, D. M. McNamara, S. Goland and U. Elkayam (2020). "Peripartum cardiomyopathy: JACC state-of-the-art review." Journal of the American College of Cardiology **75**(2): 207-221.
Davis, M. E., I. M. Grumbach, T. Fukai, A. Cutchins and D. G. Harrison (2004). "Shear stress regulates endothelial nitric-oxide synthase promoter activity through nuclear factor κB binding." Journal of Biological Chemistry **279**(1): 163-168.
Day, E. A., R. J. Ford, B. K. Smith, P. Mohammadi-Shemirani, M. R. Morrow, R. M. Gutgesell, R. Lu, A. R. Raphenya, M. Kabiri, A. G. McArthur, N. McInnes, S. Hess, G. Pare, H. C. Gerstein and G. R. Steinberg (2019). "Metformin-induced increases in GDF15 are important for suppressing appetite and promoting weight loss." Nat Metab **1**(12): 1202-1208.
De Bock, K., M. Georgiadou and P. Carmeliet (2013). "Role of endothelial cell metabolism in vessel sprouting." Cell metabolism **18**(5): 634-647.
De Bock, K., M. Georgiadou, S. Schoors, A. Kuchnio, B. W. Wong, A. R. Cantelmo, A. Quaegebeur, B. Ghesquiere, S. Cauwenberghs and G. Eelen (2013). "Role of PFKFB3-driven glycolysis in vessel sprouting." Cell **154**(3): 651-663.
Ding, B.-S., D. J. Nolan, P. Guo, A. O. Babazadeh, Z. Cao, Z. Rosenwaks, R. G. Crystal, M. Simons, T. N. Sato and S. Worgall (2011). "Endothelial-derived angiocrine signals induce and sustain regenerative lung alveolarization." Cell **147**(3): 539-553.
Doddaballapur, A., K. M. Michalik, Y. Manavski, T. Lucas, R. H. Houtkooper, X. You, W. Chen, A. M. Zeiher, M. Potente and S. Dimmeler (2015). "Laminar shear stress inhibits endothelial cell metabolism via KLF2-mediated repression of PFKFB3." Arteriosclerosis, thrombosis, and vascular biology **35**(1): 137-145.
Dong, X. C., K. D. Copps, S. Guo, Y. Li, R. Kollipara, R. A. DePinho and M. F. White (2008). "Inactivation of hepatic Foxo1 by insulin signaling is required for adaptive nutrient homeostasis and endocrine growth regulation." Cell metabolism **8**(1): 65-76.
Drynan, L., P. A. Quant and V. A. ZAMMIT (1996). "Flux control exerted by mitochondrial outer membrane carnitine palmitoyltransferase over β-oxidation, ketogenesis and tricarboxylic acid cycle activity in hepatocytes isolated from rats in different metabolic states." Biochemical Journal **317**(3): 791-795.
Durante, W., X. m. Liu, B. Yates, Y. Yu and K. J. Peyton (2017). "Glutaminase 1 promotes the proliferation of endothelial cells via the induction of cyclin a." The FASEB Journal **31**: 1065.1064-1065.1064.
Duvillié, B. (2013). "Vascularization of the pancreas: an evolving role from embryogenesis to adulthood." Diabetes **62**(12): 4004-4005.
Eelen, G., P. de Zeeuw, L. Treps, U. Harjes, B. W. Wong and P. Carmeliet (2018). "Endothelial cell metabolism." Physiological reviews **98**(1): 3-58.
Egginton, S. (2011). "Physiological factors influencing capillary growth." Acta physiologica **202**(3): 225-239.
El-Gohary, Y. and G. Gittes (2018). "Structure of islets and vascular relationship to the exocrine pancreas." Pancreapedia: The Exocrine Pancreas Knowledge Base.

Elmasri, H., C. Karaaslan, Y. Teper, E. Ghelfi, M. Weng, T. A. Ince, H. Kozakewich, J. Bischoff and S. Cataltepe (2009). "Fatty acid binding protein 4 is a target of VEGF and a regulator of cell proliferation in endothelial cells." The FASEB Journal **23**(11): 3865-3873.
Emmerson, P. J., K. L. Duffin, S. Chintharlapalli and X. Wu (2018). "GDF15 and growth control." Frontiers in physiology **9**: 1712.
Emmerson, P. J., F. Wang, Y. Du, Q. Liu, R. T. Pickard, M. D. Gonciarz, T. Coskun, M. J. Hamang, D. K. Sindelar, K. K. Ballman, L. A. Foltz, A. Muppidi, J. Alsina-Fernandez, G. C. Barnard, J. X. Tang, X. Liu, X. Mao, R. Siegel, J. H. Sloan, P. J. Mitchell, B. B. Zhang, R. E. Gimeno, B. Shan and X. Wu (2017). "The metabolic effects of GDF15 are mediated by the orphan receptor GFRAL." Nat Med **23**(10): 1215-1219.
Fairlie, W. D., A. G. Moore, A. R. Bauskin, P. K. Russell, H. P. Zhang and S. N. Breit (1999). "MIC-1 is a novel TGF-beta superfamily cytokine associated with macrophage activation." J Leukoc Biol **65**(1): 2-5.
Fruebis, J., T.-S. Tsao, S. Javorschi, D. Ebbets-Reed, M. R. S. Erickson, F. T. Yen, B. E. Bihain and H. F. Lodish (2001). "Proteolytic cleavage product of 30-kDa adipocyte complement-related protein increases fatty acid oxidation in muscle and causes weight loss in mice." Proceedings of the National Academy of Sciences **98**(4): 2005-2010.
Graupera, M. and M. Claret (2018). "Endothelial Cells: New Players in Obesity and Related Metabolic Disorders." Trends Endocrinol Metab **29**(11): 781-794.
Greenwalt, D. E., K. Watt, T. Hasler, R. Howard and S. Patel (1990). "Structural, functional, and antigenic differences between bovine heart endothelial CD36 and human platelet CD36." Journal of Biological Chemistry **265**(27): 16296-16299.
Grumbach, I. M., W. Chen, S. A. Mertens and D. G. Harrison (2005). "A negative feedback mechanism involving nitric oxide and nuclear factor kappa-B modulates endothelial nitric oxide synthase transcription." Journal of molecular and cellular cardiology **39**(4): 595-603.
Gupte, A. A., G. L. Bomhoff and P. C. Geiger (2008). "Age-related differences in skeletal muscle insulin signaling: the role of stress kinases and heat shock proteins." Journal of Applied Physiology **105**(3): 839-848.
Ha, G., F. De Torres, N. Arouche, N. Benzoubir, S. Ferratge, E. Hatem, A. Anginot and G. Uzan (2019). "GDF15 secreted by senescent endothelial cells improves vascular progenitor cell functions." PLoS One **14**(5): e0216602.
Hagberg, C. E., A. Falkevall, X. Wang, E. Larsson, J. Huusko, I. Nilsson, L. A. van Meeteren, E. Samen, L. Lu and M. Vanwildemeersch (2010). "Vascular endothelial growth factor B controls endothelial fatty acid uptake." Nature **464**(7290): 917-921.
Halkein, J., S. P. Tabruyn, M. Ricke-Hoch, A. Haghikia, M. Scherr, K. Castermans, L. Malvaux, V. Lambert, M. Thiry and K. Sliwa (2013). "MicroRNA-146a is a therapeutic target and biomarker for peripartum cardiomyopathy." The Journal of clinical investigation **123**(5): 2143-2154.
Hannoun, Z., J. Fletcher, S. Greenhough, C. Medine, K. Samuel, R. Sharma, A. Pryde, J. R. Black, J. A. Ross and I. Wilmut (2010). The comparison between conditioned media and serum-free media in human embryonic stem cell culture and differentiation, Mary Ann Liebert, Inc. 140 Huguenot Street, 3rd Floor New Rochelle, NY 10801 USA.
Hasan, S. S. and A. Fischer (2021). "The Endothelium: An Active Regulator of Lipid and Glucose Homeostasis." Trends Cell Biol **31**(1): 37-49.
Hasan, S. S., M. Jabs, J. Taylor, L. Wiedmann, T. Leibing, V. Nordstrom, G. Federico, L. P. Roma, C. Carlein, G. Wolff, B. Ekim-Ustunel, M. Brune, I. Moll, F. Tetzlaff, H. J. Grone, T. Fleming, C. Geraud, S. Herzig, P. P. Nawroth and A. Fischer (2020). "Endothelial Notch signaling controls insulin transport in muscle." EMBO Mol Med **12**(4): e09271.

Hogan, B. L., C. E. Barkauskas, H. A. Chapman, J. A. Epstein, R. Jain, C. C. Hsia, L. Niklason, E. Calle, A. Le and S. H. Randell (2014). "Repair and regeneration of the respiratory system: complexity, plasticity, and mechanisms of lung stem cell function." Cell stem cell **15**(2): 123-138.
Hsu, J. Y., S. Crawley, M. Chen, D. A. Ayupova, D. A. Lindhout, J. Higbee, A. Kutach, W. Joo, Z. Gao, D. Fu, C. To, K. Mondal, B. Li, A. Kekatpure, M. Wang, T. Laird, G. Horner, J. Chan, M. McEntee, M. Lopez, D. Lakshminarasimhan, A. White, S. P. Wang, J. Yao, J. Yie, H. Matern, M. Solloway, R. Haldankar, T. Parsons, J. Tang, W. D. Shen, Y. Alice Chen, H. Tian and B. B. Allan (2017). "Non-homeostatic body weight regulation through a brainstem-restricted receptor for GDF15." Nature **550**(7675): 255-259.
Huang, H., S. Vandekeere, J. Kalucka, L. Bierhansl, A. Zecchin, U. Brüning, A. Visnagri, N. Yuldasheva, J. Goveia and B. Cruys (2017). "Role of glutamine and interlinked asparagine metabolism in vessel formation." The EMBO journal **36**(16): 2334-2352.
Huang, Y., L. Lei, D. Liu, I. Jovin, R. Russell, R. S. Johnson, A. Di Lorenzo and F. J. Giordano (2012). "Normal glucose uptake in the brain and heart requires an endothelial cell-specific HIF-1α–dependent function." Proceedings of the National Academy of Sciences **109**(43): 17478-17483.
Iadecola, C. (2004). "Neurovascular regulation in the normal brain and in Alzheimer's disease." Nature Reviews Neuroscience **5**(5): 347-360.
Jabs, M., A. J. Rose, L. H. Lehmann, J. Taylor, I. Moll, T. P. Sijmonsma, S. E. Herberich, S. W. Sauer, G. Poschet, G. Federico, C. Mogler, E. M. Weis, H. G. Augustin, M. Yan, N. Gretz, R. M. Schmid, R. H. Adams, H. J. Grone, R. Hell, J. G. Okun, J. Backs, P. P. Nawroth, S. Herzig and A. Fischer (2018). "Inhibition of Endothelial Notch Signaling Impairs Fatty Acid Transport and Leads to Metabolic and Vascular Remodeling of the Adult Heart." Circulation **137**(24): 2592-2608.
Jaffe, E. A., L. W. Hoyer and R. L. Nachman (1974). "Synthesis of von Willebrand factor by cultured human endothelial cells." Proc Natl Acad Sci U S A **71**(5): 1906-1909.
Jambusaria, A., Z. Hong, L. Zhang, S. Srivastava, A. Jana, P. T. Toth, Y. Dai, A. B. Malik and J. Rehman (2020). "Endothelial heterogeneity across distinct vascular beds during homeostasis and inflammation." Elife **9**: e51413.
Jang, C., S. F. Oh, S. Wada, G. C. Rowe, L. Liu, M. C. Chan, J. Rhee, A. Hoshino, B. Kim, A. Ibrahim, L. G. Baca, E. Kim, C. C. Ghosh, S. M. Parikh, A. Jiang, Q. Chu, D. E. Forman, S. H. Lecker, S. Krishnaiah, J. D. Rabinowitz, A. M. Weljie, J. A. Baur, D. L. Kasper and Z. Arany (2016). "A branched-chain amino acid metabolite drives vascular fatty acid transport and causes insulin resistance." Nat Med **22**(4): 421-426.
Jansen, F., X. Yang, K. Baumann, D. Przybilla, T. Schmitz, A. Flender, K. Paul, A. Alhusseiny, G. Nickenig and N. Werner (2015). "Endothelial microparticles reduce ICAM-1 expression in a micro RNA-222-dependent mechanism." Journal of cellular and molecular medicine **19**(9): 2202-2214.
Jeon, M. K., J.-B. Lim and G. M. Lee (2010). "Development of a serum-free medium for in vitro expansion of human cytotoxic T lymphocytes using a statistical design." BMC biotechnology **10**(1): 1-9.
Jung, S.-B., M. J. Choi, D. Ryu, H.-S. Yi, S. E. Lee, J. Y. Chang, H. K. Chung, Y. K. Kim, S. G. Kang and J. H. Lee (2018). "Reduced oxidative capacity in macrophages results in systemic insulin resistance." Nature communications **9**(1): 1-15.
Kadl, A. and N. Leitinger (2005). "The role of endothelial cells in the resolution of acute inflammation." Antioxidants & redox signaling **7**(11-12): 1744-1754.
Kaiser, N., S. Sasson, E. P. Feener, N. Boukobza-Vardi, S. Higashi, D. E. Moller, S. Davidheiser, R. J. Przybylski and G. L. King (1993). "Differential regulation of glucose

transport and transporters by glucose in vascular endothelial and smooth muscle cells." Diabetes **42**(1): 80-89.
Kalra, H., R. J. Simpson, H. Ji, E. Aikawa, P. Altevogt, P. Askenase, V. C. Bond, F. E. Borras, X. Breakefield, V. Budnik, E. Buzas, G. Camussi, A. Clayton, E. Cocucci, J. M. Falcon-Perez, S. Gabrielsson, Y. S. Gho, D. Gupta, H. C. Harsha, A. Hendrix, A. F. Hill, J. M. Inal, G. Jenster, E. M. Kramer-Albers, S. K. Lim, A. Llorente, J. Lotvall, A. Marcilla, L. Mincheva-Nilsson, I. Nazarenko, R. Nieuwland, E. N. Nolte-'t Hoen, A. Pandey, T. Patel, M. G. Piper, S. Pluchino, T. S. Prasad, L. Rajendran, G. Raposo, M. Record, G. E. Reid, F. Sanchez-Madrid, R. M. Schiffelers, P. Siljander, A. Stensballe, W. Stoorvogel, D. Taylor, C. Thery, H. Valadi, B. W. van Balkom, J. Vazquez, M. Vidal, M. H. Wauben, M. Yanez-Mo, M. Zoeller and S. Mathivanan (2012). "Vesiclepedia: a compendium for extracellular vesicles with continuous community annotation." PLoS Biol **10**(12): e1001450.
Kalucka, J., L. Bierhansl, N. V. Conchinha, R. Missiaen, I. Elia, U. Bruning, S. Scheinok, L. Treps, A. R. Cantelmo, C. Dubois, P. de Zeeuw, J. Goveia, A. Zecchin, F. Taverna, F. Morales-Rodriguez, A. Brajic, L. C. Conradi, S. Schoors, U. Harjes, K. Vriens, G. A. Pilz, R. Chen, R. Cubbon, B. Thienpont, B. Cruys, B. W. Wong, B. Ghesquiere, M. Dewerchin, K. De Bock, X. Sagaert, S. Jessberger, E. A. V. Jones, B. Gallez, D. Lambrechts, M. Mazzone, G. Eelen, X. Li, S. M. Fendt and P. Carmeliet (2018). "Quiescent Endothelial Cells Upregulate Fatty Acid beta-Oxidation for Vasculoprotection via Redox Homeostasis." Cell Metab **28**(6): 881-894 e813.
Karki, S., M. G. Farb, D. T. Ngo, S. Myers, V. Puri, N. M. Hamburg, B. Carmine, D. T. Hess and N. Gokce (2015). "Forkhead box O-1 modulation improves endothelial insulin resistance in human obesity." Arterioscler Thromb Vasc Biol **35**(6): 1498-1506.
Karnieli, O., O. M. Friedner, J. G. Allickson, N. Zhang, S. Jung, D. Fiorentini, E. Abraham, S. S. Eaker, A. Chan and S. Griffiths (2017). "A consensus introduction to serum replacements and serum-free media for cellular therapies." Cytotherapy **19**(2): 155-169.
Keerthikumar, S., D. Chisanga, D. Ariyaratne, H. Al Saffar, S. Anand, K. Zhao, M. Samuel, M. Pathan, M. Jois, N. Chilamkurti, L. Gangoda and S. Mathivanan (2016). "ExoCarta: A Web-Based Compendium of Exosomal Cargo." J Mol Biol **428**(4): 688-692.
Kharitonenkov, A., V. J. Wroblewski, A. Koester, Y.-F. Chen, C. K. Clutinger, X. T. Tigno, B. C. Hansen, A. B. Shanafelt and G. J. Etgen (2007). "The metabolic state of diabetic monkeys is regulated by fibroblast growth factor-21." Endocrinology **148**(2): 774-781.
Kim, B., J. Li, C. Jang and Z. Arany (2017). "Glutamine fuels proliferation but not migration of endothelial cells." The EMBO journal **36**(16): 2321-2333.
Kim, G. and J. H. Kim (2020). "Impact of skeletal muscle mass on metabolic health." Endocrinology and Metabolism **35**(1): 1.
Kim, K. H., S. H. Kim, Y. S. Jo, Y.-h. Lee and M.-S. Lee (2018). "Growth differentiation factor 15 ameliorates nonalcoholic steatohepatitis and related metabolic disorders in mice." Scientific reports **8**(1): 1-14.
King, H., R. E. Aubert and W. H. Herman (1998). "Global burden of diabetes, 1995-2025: prevalence, numerical estimates, and projections." Diabetes Care **21**(9): 1414-1431.
Klein, A. B., T. S. Nicolaisen, N. Ortenblad, K. D. Gejl, R. Jensen, A. M. Fritzen, E. L. Larsen, K. Karstoft, H. E. Poulsen, T. Morville, R. E. Sahl, J. W. Helge, J. Lund, S. Falk, M. Lyngbaek, H. Ellingsgaard, B. K. Pedersen, W. Lu, B. Finan, S. B. Jorgensen, R. J. Seeley, M. Kleinert, B. Kiens, E. A. Richter and C. Clemmensen (2021).

"Pharmacological but not physiological GDF15 suppresses feeding and the motivation to exercise." Nat Commun **12**(1): 1041.
Kler, R. S., H. Sherratt and D. Turnbull (1992). "The measurement of mitochondrial β-oxidation by release of 3H2O from [9, 10-3H] hexadecanoate: application to skeletal muscle and the use of inhibitors as models of metabolic disease." Biochemical medicine and metabolic biology **47**(2): 145-156.
Kode, A., I. Mosialou, B. C. Silva, S. Joshi, M. Ferron, M. T. Rached and S. Kousteni (2012). "FoxO1 protein cooperates with ATF4 protein in osteoblasts to control glucose homeostasis." Journal of Biological Chemistry **287**(12): 8757-8768.
Kode, A., I. Mosialou, B. C. Silva, M.-T. Rached, B. Zhou, J. Wang, T. M. Townes, R. Hen, R. A. DePinho and X. E. Guo (2012). "FOXO1 orchestrates the bone-suppressing function of gut-derived serotonin." The Journal of clinical investigation **122**(10): 3490-3503.
Kubota, T., N. Kubota, H. Kumagai, S. Yamaguchi, H. Kozono, T. Takahashi, M. Inoue, S. Itoh, I. Takamoto and T. Sasako (2011). "Impaired insulin signaling in endothelial cells reduces insulin-induced glucose uptake by skeletal muscle." Cell metabolism **13**(3): 294-307.
Langlet, F., R. A. Haeusler, D. Lindén, E. Ericson, T. Norris, A. Johansson, J. R. Cook, K. Aizawa, L. Wang and C. Buettner (2017). "Selective inhibition of FOXO1 activator/repressor balance modulates hepatic glucose handling." Cell **171**(4): 824-835. e818.
Lawler, P. R. and J. Lawler (2012). "Molecular basis for the regulation of angiogenesis by thrombospondin-1 and -2." Cold Spring Harb Perspect Med **2**(5): a006627.
Lee, Y.-J., I.-J. Kang, R. Bünger and Y.-H. Kang (2003). "Mechanisms of pyruvate inhibition of oxidant-induced apoptosis in human endothelial cells." Microvascular research **66**(2): 91-101.
Leighton, B., R. Curi, A. Hussein and E. A. Newsholme (1987). "Maximum activities of some key enzymes of glycolysis, glutaminolysis, Krebs cycle and fatty acid utilization in bovine pulmonary endothelial cells." FEBS letters **225**(1-2): 93-96.
Leopold, J. A., A. Dam, B. A. Maron, A. W. Scribner, R. Liao, D. E. Handy, R. C. Stanton, B. Pitt and J. Loscalzo (2007). "Aldosterone impairs vascular reactivity by decreasing glucose-6-phosphate dehydrogenase activity." Nature medicine **13**(2): 189-197.
Leopold, J. A., J. Walker, A. W. Scribner, B. Voetsch, Y.-Y. Zhang, A. J. Loscalzo, R. C. Stanton and J. Loscalzo (2003). "Glucose-6-phosphate dehydrogenase modulates vascular endothelial growth factor-mediated angiogenesis." Journal of Biological Chemistry **278**(34): 32100-32106.
Li, J., L. Yang, W. Qin, G. Zhang, J. Yuan and F. Wang (2013). "Adaptive induction of growth differentiation factor 15 attenuates endothelial cell apoptosis in response to high glucose stimulus." PLoS One **8**(6): e65549.
Li, Z., B. Wang, X. Wu, S. Y. Cheng, L. Paraoan and J. Zhou (2005). "Identification, expression and functional characterization of the GRAL gene." Journal of neurochemistry **95**(2): 361-376.
Lin, Z., V. Natesan, H. Shi, F. Dong, D. Kawanami, G. H. Mahabeleshwar, G. B. Atkins, L. Nayak, Y. Cui and J. H. Finigan (2010). "Kruppel-like factor 2 regulates endothelial barrier function." Arteriosclerosis, thrombosis, and vascular biology **30**(10): 1952-1959.
Luan, H. H., A. Wang, B. K. Hilliard, F. Carvalho, C. E. Rosen, A. M. Ahasic, E. L. Herzog, I. Kang, M. A. Pisani, S. Yu, C. Zhang, A. M. Ring, L. H. Young and R. Medzhitov (2019). "GDF15 Is an Inflammation-Induced Central Mediator of Tissue Tolerance." Cell **178**(5): 1231-1244 e1211.

Ma, X., P. Su, C. Yin, X. Lin, X. Wang, Y. Gao, S. Patil, A. R. War, A. Qadir and Y. Tian (2020). "The roles of FoxO transcription factors in regulation of bone cells function." International journal of molecular sciences **21**(3): 692.
Maaser, C., J. Heidemann, W. Domschke and T. Kucharzik (2006). "Intestinal Microvascular Endothelium and." Infect. Immun **74**(10): 5425.
Miloudi, K., M. Oubaha, C. Menard, A. Dejda, V. Guber, G. Cagnone, A. M. Wilson, N. Tetreault, G. Mawambo, F. Binet, R. Chidiac, C. Delisle, M. Buscarlet, A. Cerani, S. Crespo-Garcia, K. Bentley, F. Rezende, J. S. Joyal, F. A. Mallette, J. P. Gratton, B. Larrivee and P. Sapieha (2019). "NOTCH1 signaling induces pathological vascular permeability in diabetic retinopathy." Proc Natl Acad Sci U S A **116**(10): 4538-4547.
Mullican, S. E., X. Lin-Schmidt, C. N. Chin, J. A. Chavez, J. L. Furman, A. A. Armstrong, S. C. Beck, V. J. South, T. Q. Dinh, T. D. Cash-Mason, C. R. Cavanaugh, S. Nelson, C. Huang, M. J. Hunter and S. M. Rangwala (2017). "GFRAL is the receptor for GDF15 and the ligand promotes weight loss in mice and nonhuman primates." Nat Med **23**(10): 1150-1157.
Nagashima, T., N. Shigematsu, R. Maruki, Y. Urano, H. Tanaka, A. Shimaya, T. Shimokawa and M. Shibasaki (2010). "Discovery of novel forkhead box O1 inhibitors for treating type 2 diabetes: improvement of fasting glycemia in diabetic db/db mice." Mol Pharmacol **78**(5): 961-970.
Nakae, J., Y. Cao, F. Hakuno, H. Takemori, Y. Kawano, R. Sekioka, T. Abe, H. Kiyonari, T. Tanaka and J. Sakai (2012). "Novel repressor regulates insulin sensitivity through interaction with Foxo1." The EMBO journal **31**(10): 2275-2295.
Nakayasu, E. S., F. Syed, S. A. Tersey, M. A. Gritsenko, H. D. Mitchell, C. Y. Chan, E. Dirice, J.-V. Turatsinze, Y. Cui and R. N. Kulkarni (2020). "Comprehensive proteomics analysis of stressed human islets identifies GDF15 as a target for type 1 diabetes intervention." Cell metabolism **31**(2): 363-374. e366.
Nikolova, G., N. Jabs, I. Konstantinova, A. Domogatskaya, K. Tryggvason, L. Sorokin, R. Fassler, G. Gu, H. P. Gerber, N. Ferrara, D. A. Melton and E. Lammert (2006). "The vascular basement membrane: a niche for insulin gene expression and Beta cell proliferation." Dev Cell **10**(3): 397-405.
Nolan, D. J., M. Ginsberg, E. Israely, B. Palikuqi, M. G. Poulos, D. James, B.-S. Ding, W. Schachterle, Y. Liu and Z. Rosenwaks (2013). "Molecular signatures of tissue-specific microvascular endothelial cell heterogeneity in organ maintenance and regeneration." Developmental cell **26**(2): 204-219.
Nwadozi, E., E. Roudier, E. Rullman, S. Tharmalingam, H. Y. Liu, T. Gustafsson and T. L. Haas (2016). "Endothelial FoxO proteins impair insulin sensitivity and restrain muscle angiogenesis in response to a high-fat diet." FASEB J **30**(9): 3039-3052.
Obata, A., T. Kimura, Y. Obata, M. Shimoda, T. Kinoshita, K. Kohara, S. Okauchi, H. Hirukawa, S. Kamei and S. Nakanishi (2019). "Vascular endothelial PDPK1 plays a pivotal role in the maintenance of pancreatic beta cell mass and function in adult male mice." Diabetologia **62**(7): 1225-1236.
Olfert, I. M. and O. Birot (2011). "Importance of anti-angiogenic factors in the regulation of skeletal muscle angiogenesis." Microcirculation **18**(4): 316-330.
Ong, S.-G., W. H. Lee, M. Huang, D. Dey, K. Kodo, V. Sanchez-Freire, J. D. Gold and J. C. Wu (2014). "Cross talk of combined gene and cell therapy in ischemic heart disease: role of exosomal microRNA transfer." Circulation **130**(11_suppl_1): S60-S69.
Osaki, T., V. Sivathanu and R. D. Kamm (2018). "Crosstalk between developing vasculature and optogenetically engineered skeletal muscle improves muscle contraction and angiogenesis." Biomaterials **156**: 65-76.

Paik, J.-H., R. Kollipara, G. Chu, H. Ji, Y. Xiao, Z. Ding, L. Miao, Z. Tothova, J. W. Horner and D. R. Carrasco (2007). "FoxOs are lineage-restricted redundant tumor suppressors and regulate endothelial cell homeostasis." Cell **128**(2): 309-323.
Paik, J. H., R. Kollipara, G. Chu, H. Ji, Y. Xiao, Z. Ding, L. Miao, Z. Tothova, J. W. Horner, D. R. Carrasco, S. Jiang, D. G. Gilliland, L. Chin, W. H. Wong, D. H. Castrillon and R. A. DePinho (2007). "FoxOs are lineage-restricted redundant tumor suppressors and regulate endothelial cell homeostasis." Cell **128**(2): 309-323.
Pandolfi, P., F. Sonati, R. Rivi, P. Mason, F. Grosveld and L. Luzzatto (1995). "Targeted disruption of the housekeeping gene encoding glucose 6-phosphate dehydrogenase (G6PD): G6PD is dispensable for pentose synthesis but essential for defense against oxidative stress." The EMBO journal **14**(21): 5209-5215.
Paneni, F., S. Costantino and F. Cosentino (2015). "Role of oxidative stress in endothelial insulin resistance." World journal of diabetes **6**(2): 326.
Patel, S., A. Alvarez-Guaita, A. Melvin, D. Rimmington, A. Dattilo, E. L. Miedzybrodzka, I. Cimino, A. C. Maurin, G. P. Roberts, C. L. Meek, S. Virtue, L. M. Sparks, S. A. Parsons, L. M. Redman, G. A. Bray, A. P. Liou, R. M. Woods, S. A. Parry, P. B. Jeppesen, A. J. Kolnes, H. P. Harding, D. Ron, A. Vidal-Puig, F. Reimann, F. M. Gribble, C. J. Hulston, I. S. Farooqi, P. Fafournoux, S. R. Smith, J. Jensen, D. Breen, Z. Wu, B. B. Zhang, A. P. Coll, D. B. Savage and S. O'Rahilly (2019). "GDF15 Provides an Endocrine Signal of Nutritional Stress in Mice and Humans." Cell Metab **29**(3): 707-718 e708.
Pavelka, M. and J. Roth (2010). Fenestrated Capillary. Functional Ultrastructure, Springer**:** 258-259.
Pi, X., L. Xie and C. Patterson (2018). "Emerging Roles of Vascular Endothelium in Metabolic Homeostasis." Circ Res **123**(4): 477-494.
Pober, J. S. and W. C. Sessa (2007). "Evolving functions of endothelial cells in inflammation." Nature Reviews Immunology **7**(10): 803-815.
Potente, M. and T. Mäkinen (2017). "Vascular heterogeneity and specialization in development and disease." Nature Reviews Molecular Cell Biology **18**(8): 477.
Potente, M., C. Urbich, K. Sasaki, W. K. Hofmann, C. Heeschen, A. Aicher, R. Kollipara, R. A. DePinho, A. M. Zeiher and S. Dimmeler (2005). "Involvement of Foxo transcription factors in angiogenesis and postnatal neovascularization." J Clin Invest **115**(9): 2382-2392.
Prior, S. J., A. P. Goldberg, H. K. Ortmeyer, E. R. Chin, D. Chen, J. B. Blumenthal and A. S. Ryan (2015). "Increased skeletal muscle capillarization independently enhances insulin sensitivity in older adults after exercise training and detraining." Diabetes **64**(10): 3386-3395.
Rached, M.-T., A. Kode, L. Xu, Y. Yoshikawa, J.-H. Paik, R. A. DePinho and S. Kousteni (2010). "FoxO1 is a positive regulator of bone formation by favoring protein synthesis and resistance to oxidative stress in osteoblasts." Cell metabolism **11**(2): 147-160.
Rafii, S., J. M. Butler and B.-S. Ding (2016). "Angiocrine functions of organ-specific endothelial cells." Nature **529**(7586): 316-325.
Rajah, T. T., A. L. Olson and P. Grammas (2001). "Differential glucose uptake in retina- and brain-derived endothelial cells." Microvascular research **62**(3): 236-242.
Randi, A. M., K. E. Smith and G. Castaman (2018). "von Willebrand factor regulation of blood vessel formation." Blood **132**(2): 132-140.
Reynolds IV, T. H., J. T. Brozinick Jr, L. M. Larkin and S. W. Cushman (2000). "Transient enhancement of GLUT-4 levels in rat epitrochlearis muscle after exercise training." Journal of Applied Physiology **88**(6): 2240-2245.

Ricard, N., S. Bailly, C. Guignabert and M. Simons (2021). "The quiescent endothelium: signalling pathways regulating organ-specific endothelial normalcy." Nature Reviews Cardiology: 1-16.
Richter, E. A., L. P. Garetto, M. N. Goodman and N. B. Ruderman (1982). "Muscle glucose metabolism following exercise in the rat: increased sensitivity to insulin." The Journal of clinical investigation **69**(4): 785-793.
Richter, E. A. and M. Hargreaves (2013). "Exercise, GLUT4, and skeletal muscle glucose uptake." Physiological reviews.
Ritchie, I. R. and D. J. Dyck (2012). "Rapid loss of adiponectin-stimulated fatty acid oxidation in skeletal muscle of rats fed a high fat diet is not due to altered muscle redox state." PLoS One **7**(12): e52193.
Robciuc, M. R., R. Kivelä, I. M. Williams, J. F. de Boer, T. H. van Dijk, H. Elamaa, F. Tigistu-Sahle, D. Molotkov, V.-M. Leppänen and R. Käkelä (2016). "VEGFB/VEGFR1-induced expansion of adipose vasculature counteracts obesity and related metabolic complications." Cell metabolism **23**(4): 712-724.
Rocha, A. S., V. Vidal, M. Mertz, T. J. Kendall, A. Charlet, H. Okamoto and A. Schedl (2015). "The angiocrine factor Rspondin3 is a key determinant of liver zonation." Cell reports **13**(9): 1757-1764.
Rodrigues, M. L., L. Nimrichter, D. L. Oliveira, J. D. Nosanchuk and A. Casadevall (2008). "Vesicular trans-cell wall transport in fungi: a mechanism for the delivery of virulence-associated macromolecules?" Lipid insights **2**: LPI. S1000.
Rohlenova, K., K. Veys, I. Miranda-Santos, K. De Bock and P. Carmeliet (2018). "Endothelial cell metabolism in health and disease." Trends in cell biology **28**(3): 224-236.
Roudier, E., M. Milkiewicz, O. Birot, D. Slopack, A. Montelius, T. Gustafsson, J. H. Paik, R. A. DePinho, G. P. Casale and I. I. Pipinos (2013). "Endothelial FoxO1 is an intrinsic regulator of thrombospondin 1 expression that restrains angiogenesis in ischemic muscle." Angiogenesis **16**(4): 759-772.
Rudnicki, M., G. Abdifarkosh, E. Nwadozi, S. V. Ramos, A. Makki, D. M. Sepa-Kishi, R. B. Ceddia, C. G. Perry, E. Roudier and T. L. Haas (2018). "Endothelial-specific FoxO1 depletion prevents obesity-related disorders by increasing vascular metabolism and growth." Elife **7**.
Sanchez, E. L., P. A. Carroll, A. B. Thalhofer and M. Lagunoff (2015). "Latent KSHV infected endothelial cells are glutamine addicted and require glutaminolysis for survival." PLoS pathogens **11**(7): e1005052.
Sansbury, B. E. and B. G. Hill (2014). "Regulation of obesity and insulin resistance by nitric oxide." Free radical biology and medicine **73**: 383-399.
Sarruf, D. A., J. P. Thaler, G. J. Morton, J. German, J. D. Fischer, K. Ogimoto and M. W. Schwartz (2010). "Fibroblast growth factor 21 action in the brain increases energy expenditure and insulin sensitivity in obese rats." Diabetes **59**(7): 1817-1824.
Sawada, N. and Z. Arany (2017). "Metabolic regulation of angiogenesis in diabetes and aging." Physiology **32**(4): 290-307.
Schoors, S., U. Bruning, R. Missiaen, K. C. Queiroz, G. Borgers, I. Elia, A. Zecchin, A. R. Cantelmo, S. Christen and J. Goveia (2015). "Fatty acid carbon is essential for dNTP synthesis in endothelial cells." Nature **520**(7546): 192-197.
Schoors, S., K. De Bock, A. R. Cantelmo, M. Georgiadou, B. Ghesquière, S. Cauwenberghs, A. Kuchnio, B. W. Wong, A. Quaegebeur and J. Goveia (2014). "Partial and transient reduction of glycolysis by PFKFB3 blockade reduces pathological angiogenesis." Cell metabolism **19**(1): 37-48.

Schubert, W., P. G. Frank, B. Razani, D. S. Park, C.-W. Chow and M. P. Lisanti (2001). "Caveolae-deficient endothelial cells show defects in the uptake and transport of albumin in vivo." Journal of Biological Chemistry **276**(52): 48619-48622.
Schwartsburd, P. (2019). "Cancer-induced reprogramming of host glucose metabolism:“vicious cycle” supporting cancer progression." Frontiers in oncology **9**: 218.
Seandel, M., J. M. Butler, H. Kobayashi, A. T. Hooper, I. A. White, F. Zhang, E. L. Vertes, M. Kobayashi, Y. Zhang, S. V. Shmelkov, N. R. Hackett, S. Rabbany, J. L. Boyer and S. Rafii (2008). "Generation of a functional and durable vascular niche by the adenoviral E4ORF1 gene." Proc Natl Acad Sci U S A **105**(49): 19288-19293.
Shetty, S., P. F. Lalor and D. H. Adams (2018). "Liver sinusoidal endothelial cells—gatekeepers of hepatic immunity." Nature Reviews Gastroenterology & Hepatology **15**(9): 555-567.
Shi, Y., S. Fan, D. Wang, T. Huyan, J. Chen, J. Chen, J. Su, X. Li, Z. Wang, S. Xie, C. Yun, X. Li and L. Tie (2018). "FOXO1 inhibition potentiates endothelial angiogenic functions in diabetes via suppression of ROCK1/Drp1-mediated mitochondrial fission." Biochim Biophys Acta Mol Basis Dis **1864**(7): 2481-2494.
Spargo, E., O. Pratt and P. Daniel (1979). "Metabolic functions of skeletal muscles of man, mammals, birds and fishes: a review." Journal of the Royal Society of Medicine **72**(12): 921-925.
Swarts, D. C., K. Makarova, Y. Wang, K. Nakanishi, R. F. Ketting, E. V. Koonin, D. J. Patel and J. Van Der Oost (2014). "The evolutionary journey of Argonaute proteins." Nature structural & molecular biology **21**(9): 743.
Taraboletti, G., S. D'Ascenzo, P. Borsotti, R. Giavazzi, A. Pavan and V. Dolo (2002). "Shedding of the matrix metalloproteinases MMP-2, MMP-9, and MT1-MMP as membrane vesicle-associated components by endothelial cells." Am J Pathol **160**(2): 673-680.
Thiebaud, D., E. Jacot, R. A. Defronzo, E. Maeder, E. Jequier and J.-P. Felber (1982). "The effect of graded doses of insulin on total glucose uptake, glucose oxidation, and glucose storage in man." Diabetes **31**(11): 957-963.
Tsai, V. W. W., Y. Husaini, A. Sainsbury, D. A. Brown and S. N. Breit (2018). "The MIC-1/GDF15-GFRAL Pathway in Energy Homeostasis: Implications for Obesity, Cachexia, and Other Associated Diseases." Cell Metab **28**(3): 353-368.
Tsuchiya, K. and D. Accili (2013). "Liver sinusoidal endothelial cells link hyperinsulinemia to hepatic insulin resistance." Diabetes **62**(5): 1478-1489.
Türker, C., F. Akal, D. Joho, C. Panse, S. Barkow-Oesterreicher, H. Rehrauer and R. Schlapbach (2010). B-Fabric: the Swiss Army Knife for life sciences. Proceedings of the 13th International Conference on Extending Database Technology.
Uebelhoer, M. and M. L. Iruela-Arispe (2016). "Cross-talk between signaling and metabolism in the vasculature." Vascular pharmacology **83**: 4-9.
Vallejo-Gracia, A., I. P. Chen, R. Perrone, E. Besnard, D. Boehm, E. Battivelli, T. Tezil, K. Krey, K. A. Raymond and P. A. Hull (2020). "FOXO1 promotes HIV latency by suppressing ER stress in T cells." Nature microbiology **5**(9): 1144-1157.
Vénéreau, E., C. Ceriotti and M. E. Bianchi (2015). "DAMPs from cell death to new life." Frontiers in immunology **6**: 422.
Verma, M., Y. Asakura, B. S. R. Murakonda, T. Pengo, C. Latroche, B. Chazaud, L. K. McLoon and A. Asakura (2018). "Muscle satellite cell cross-talk with a vascular niche maintains quiescence via VEGF and notch signaling." Cell stem cell **23**(4): 530-543. e539.

Veys, K., A. Alvarado-Diaz and K. De Bock (2019). Measuring glycolytic and mitochondrial fluxes in endothelial cells using radioactive tracers. Metabolic Signaling, Springer**:** 121-136.
Veys, K., Z. Fan, M. Ghobrial, A. Bouché, M. García-Caballero, K. Vriens, N. V. Conchinha, A. Seuwen, F. Schlegel and T. Gorski (2020). "Role of the GLUT1 glucose transporter in postnatal CNS angiogenesis and blood-brain barrier integrity." Circulation research **127**(4): 466-482.
Videm, V. and M. Albrigtsen (2008). "Soluble ICAM-1 and VCAM-1 as markers of endothelial activation." Scand J Immunol **67**(5): 523-531.
Wang, B., L. Zhao, M. Fish, C. Y. Logan and R. Nusse (2015). "Self-renewing diploid Axin2+ cells fuel homeostatic renewal of the liver." Nature **524**(7564): 180-185.
Wang, H., Z. Liu, G. Li and E. J. Barrett (2006). "The vascular endothelial cell mediates insulin transport into skeletal muscle." American Journal of Physiology-Endocrinology and Metabolism **291**(2): 5P

-E332.
Wang, Y., Y. Zhou and D. T. Graves (2014). "FOXO transcription factors: their clinical significance and regulation." BioMed research international **2014**.
Wang Y., Z. S. (2010). Vascular Biology of the Placenta.. Chapter 7, Angiogenic Factors. M. C. L. Sciences.
Waters, R. E., S. Rotevatn, P. Li, B. H. Annex and Z. Yan (2004). "Voluntary running induces fiber type-specific angiogenesis in mouse skeletal muscle." American Journal of Physiology-Cell Physiology **287**(5): C1342-C1348.
Watt, N. T., M. C. Gage, P. A. Patel, H. Viswambharan, P. Sukumar, S. Galloway, N. Y. Yuldasheva, H. Imrie, A. M. Walker and K. J. Griffin (2017). "Endothelial SHIP2 Suppresses Nox2 NADPH Oxidase–Dependent Vascular Oxidative Stress, Endothelial Dysfunction, and Systemic Insulin Resistance." Diabetes **66**(11): 2808-2821.
Wessel, D. and U. I. Flugge (1984). "A method for the quantitative recovery of protein in dilute solution in the presence of detergents and lipids." Anal Biochem **138**(1): 141-143.
Wilhelm, K., K. Happel, G. Eelen, S. Schoors, M. F. Oellerich, R. Lim, B. Zimmermann, I. M. Aspalter, C. A. Franco and T. Boettger (2016). "FOXO1 couples metabolic activity and growth state in the vascular endothelium." Nature **529**(7585): 216-220.
Wilhelm, K., K. Happel, G. Eelen, S. Schoors, M. F. Oellerich, R. Lim, B. Zimmermann, I. M. Aspalter, C. A. Franco, T. Boettger, T. Braun, M. Fruttiger, K. Rajewsky, C. Keller, J. C. Bruning, H. Gerhardt, P. Carmeliet and M. Potente (2016). "FOXO1 couples metabolic activity and growth state in the vascular endothelium." Nature **529**(7585): 216-220.
Wolski, W., J. Grossmann and C. Panse (2018). SRMService-R-Package to Report Quantitative Mass Spectrometry Data.
Wong, B. W., X. Wang, A. Zecchin, B. Thienpont, I. Cornelissen, J. Kalucka, M. García-Caballero, R. Missiaen, H. Huang and U. Brüning (2017). "The role of fatty acid β-oxidation in lymphangiogenesis." Nature **542**(7639): 49-54.
Wu, H. and C. M. Ballantyne (2017). "Skeletal muscle inflammation and insulin resistance in obesity." The Journal of clinical investigation **127**(1): 43-54.
Xiong, Y., K. Walker, X. Min, C. Hale, T. Tran, R. Komorowski, J. Yang, J. Davda, N. Nuanmanee, D. Kemp, X. Wang, H. Liu, S. Miller, K. J. Lee, Z. Wang and M. M. Veniant (2017). "Long-acting MIC-1/GDF15 molecules to treat obesity: Evidence from mice to monkeys." Sci Transl Med **9**(412).

Yamauchi, T., J. Kamon, Y. a. Minokoshi, Y. Ito, H. Waki, S. Uchida, S. Yamashita, M. Noda, S. Kita and K. Ueki (2002). "Adiponectin stimulates glucose utilization and fatty-acid oxidation by activating AMP-activated protein kinase." Nature medicine **8**(11): 1288-1295.
Yang, L., C. C. Chang, Z. Sun, D. Madsen, H. Zhu, S. B. Padkjaer, X. Wu, T. Huang, K. Hultman, S. J. Paulsen, J. Wang, A. Bugge, J. B. Frantzen, P. Norgaard, J. F. Jeppesen, Z. Yang, A. Secher, H. Chen, X. Li, L. M. John, B. Shan, Z. He, X. Gao, J. Su, K. T. Hansen, W. Yang and S. B. Jorgensen (2017). "GFRAL is the receptor for GDF15 and is required for the anti-obesity effects of the ligand." Nat Med **23**(10): 1158-1166.
Yoon, M. J., G. Y. Lee, J.-J. Chung, Y. H. Ahn, S. H. Hong and J. B. Kim (2006). "Adiponectin increases fatty acid oxidation in skeletal muscle cells by sequential activation of AMP-activated protein kinase, p38 mitogen-activated protein kinase, and peroxisome proliferator–activated receptor α." Diabetes **55**(9): 2562-2570.
Yu, P., K. Wilhelm, A. Dubrac, J. K. Tung, T. C. Alves, J. S. Fang, Y. Xie, J. Zhu, Z. Chen and F. De Smet (2017). "FGF-dependent metabolic control of vascular development." Nature **545**(7653): 224-228.
Zecchin, A., J. Kalucka, C. Dubois and P. Carmeliet (2017). "How endothelial cells adapt their metabolism to form vessels in tumors." Frontiers in immunology **8**: 1750.
Zhang, J., J. Muri, G. Fitzgerald, T. Gorski, R. Gianni-Barrera, E. Masschelein, G. D'Hulst, P. Gilardoni, G. Turiel and Z. Fan (2020). "Endothelial lactate controls muscle regeneration from ischemia by inducing M2-like macrophage polarization." Cell metabolism **31**(6): 1136-1153. e1137.
Zheng, B., B. Cao, M. Crisan, B. Sun, G. Li, A. Logar, S. Yap, J. B. Pollett, L. Drowley and T. Cassino (2007). "Prospective identification of myogenic endothelial cells in human skeletal muscle." Nature biotechnology **25**(9): 1025-1034.